University of Strathclyde
Department of Pure and Applied Chemistry

DNA Diagnostic Assays using Surface Enhanced Raman Scattering (SERS)

by
Mhairi Harper

A thesis submitted to the Department of Pure and Applied Chemistry, University of Strathclyde, in fulfilment of the requirements for the degree of Doctor of Philosophy

July 2013

Acknowledgements

First and foremost, I would like to thank my supervisors Dr Karen Faulds and Professor Duncan Graham for giving me the opportunity to work within their research group. I have gained vast experience from this opportunity and greatly appreciate their help and assistance throughout the project.

In terms of funding and sponsorship, I would like to acknowledge Dstl as they provided financial support and advice throughout the studentship. In particular I would like to thank Neil Shand, Nicola Chatwell, Terry Clark and Michael Hill.

Thank you to the members of the Raman group for providing invaluable SERS advice, beneficial DNA knowledge and non-work related conversations. A special thanks to Dr Eleanore Irvine and Dr Lee Barrett for advice throughout my study and suggestions in writing my thesis. A special mention to Derek Craig, Alan Hutton and Sarah McAughtrie for some much needed office banter and always keeping me smiling. I would also like to acknowledge the contribution to this work by final year students Barry Robertson and Kerry O'Hare.

I would especially like to thank my family and friends for their ongoing encouragement and support. My biggest thanks is to Paul for putting up with me through all my PhD highs and lows and always believing in me.

Abstract

DNA is the prerequisite for all biological life and its discovery has revolutionised the understanding of biomolecular interactions and disease expression. This has enabled significant improvements in patient diagnosis and medical treatment to be carried out. The advancements in technology and instrumentation have continually progressed this knowledge and continue to push the boundaries of diagnostic and clinical advancements. One effective way to achieve this is through application of dye labelled DNA sequences and metallic nanoparticle suspensions. This research details an understanding of the interaction between dye labelled oligonucleotides and silver nanoparticle surfaces, which generate strong surface enhanced Raman scattering (SERS) responses through specific hybridisation events which correlate to the presence of targeted sequences.

During this study, the attraction of oligonucleotides onto metal nanoparticles was shown to be driven through the DNA nucleobases. Therefore, the increased exposure of the base groups within single stranded DNA sequences generated a higher affinity for metal surfaces which in turn produced stronger SERS responses when compared to double stranded DNA. This principle was utilised within a DNA detection assay to successfully demonstrate the presence of target DNA sequences.

Two novel DNA detection assays were also investigated which utilised SERS to determine the presence of sequences relating to the methicillin resistant *Staphylococcus aureus* (MRSA) strain. A solution based detection method was developed through coupling a TaqMan assay with SERS. This combination enabled highly specific detection of clinically relevant sequences of MRSA to be obtained with 7 fM limits of detection achievable. The multiple detection of different genomic *S. aureus* strains was achieved through the molecularly specific and narrow emission spectral profiles obtained. A contrasting DNA detection strategy which relies upon the hybridisation of complementary sequences on a solid substrate surface was shown. Silver nanoparticles were functionalised with specific DNA sequences and a variety of SERS active molecules, enabling the selective detection of target sequences from nitrocellulose membranes.

This thesis has exploited SERS to enable the specific identification of DNA sequences to be achieved *via* utilisation of silver nanoparticles. Through SERS, an insight into the interactions of DNA and silver nanoparticles surfaces has been gained as well as enhancing the sensitivity and specificity achievable within SERS detection assays.

Abbreviations

μ_{ep}	Electrophilic Mobility
λ_{max}	Absorption Maxima
3D	Three Dimensional
A	Adenine
ARMS	Amplification Refractory Mutation System
BT	Benzotriazole
C	Cytosine
CCD	Charge Coupled Device
CFTR	Cystic Fibrosis Transmembrane Regulator
dATP	Adenosine-5'-Triphosphate
dCTP	Cytidine Triphosphate
DEPC	Diethylpyrocarbonate
dGTP	Guanosine-5'- Triphosphate
dNTP	Deoxynucleotide Triphosphate
dTTP	Thymidine Triphosphate
dsDNA	Double Stranded Deoxyribonucleic Acid
DNA	Deoxyribonucleic Acid
EDC	1-Ethyl-3-(3-dimethylaminopropyl)carbodiimine
EDTA	Ethylenediaminetetraacetic Acid
FAM	5-(and 6-)-carboxyfluourescein
FRET	Förster Resonance Energy Transfer
G	Guanine
GM19	3,5-dimethoxy-4-(6'-azobenzotriazoyl)-phenylamine
HEG	Hexaethylene Glycol
HEX	6-Carboxy-2',4',4',5',7,7'-hexachlorofluorescein
HIV	Human Immunodeficiency Virus
IR	Infrared
ITC	Isothiocyanate
LNA	Locked Nucleic Acid
LOD	Limit of Detection
LSPR	Localised Surface Plasmon Resonance
LWD	Long Working Distance
MPY	4- Mercaptopyridine
MRSA	Methicillin-resistant *Staphylococcus aureus*

NHS	*N*-hydroxysuccinimide
PBS	Phosphate Buffered Saline
PCR	Polymerase Chain Reaction
R6G	Carboxyrhodamine 6G
ROX	X- Rhodamine
RNA	Ribonucleic Acid
RRS	Resonance Raman Scattering
SA	*Staphylococcus aureus*
SAM	Self-Assembled Monolayer
SE	*Staphylococcus epidermis*
SPR	Surface Plasmon Resonance
SSC	Saline Sodium Citrate
SERS	Surface Enhanced Raman Scattering
SERRS	Surface Enhanced Resonance Raman Scattering
SNP	Single Nucleotide Polymorphism
ssDNA	Single Stranded Deoxyribonucleic Acid
T	Thymine
TAMRA	5-(and-6)-carboxytetramethylrhodamine
TBE	Tris Borate EDTA
T_M	Melting Temperature
TRITC	TAMRA Isothiocyanate
UV	Ultra Violet

Contents

1. Introduction

DNA is the fundamental genetic material which is the basis of life in all organisms. It is due to the biological importance of DNA that it has become a vastly studied area of molecular biology. Since Griffith's "transforming principle" in 1928[1] and the subsequent Avery-MacLeod-McCarty experiment in 1943,[2] DNA has been established as the material which carries genetic information. This has led to an expanding area of research into the structure and function of DNA which has hugely impacted the understanding of life, genetics and the cause of disease. DNA detection of specific sequences has become increasingly important in the diagnosis and treatment of genetic diseases and infections. Therefore, DNA testing is continually evolving to create methods which are quicker, more sensitive, inexpensive and safer.

1.1 Structure of Deoxyribonucleic Acid (DNA)

1.1.1 Primary Structure

Friedrich Miescher first isolated and identified nucleic acid in 1869, through extraction of an acidic substance rich in phosphorus from the nuclei of red blood cells.[3] This was called nuclein and was later discovered to be nucleic acid. In 1905, Phoebus Levene gave further clarification to Miescher's work showing that the large nucleic acid molecules could be split into much smaller components which he named nucleotides.[4] Deoxyribonucleic acid (DNA) is a nucleic acid composed of a large number of monomeric nucleotide repeating units, each consisting of a sugar, a base and a phosphate group (Figure 1.1).

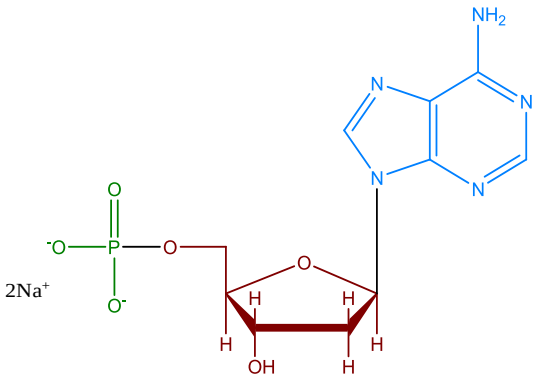

Figure 1.1: Adenosine monophosphate; red: deoxyribose sugar, blue: adenine base group and green: phosphate.

The four nitrogenous base groups which carry genetic information within the DNA structure are adenine (A), thymine (T), cytosine (C) and guanine (G) (Figure 1.2). Between 1895 and 1901, Albrecht Kossel isolated and described the four organic DNA bases and uracil (U), the nucleobase which replaces thymine within ribonucleic acid (RNA).[5] Uracil and thymine are chemically very similar differing only by the absence of the methyl group at the C-5 position of the ring of uracil.[6] RNA is a biologically important molecule that plays an essential role in protein synthesis.

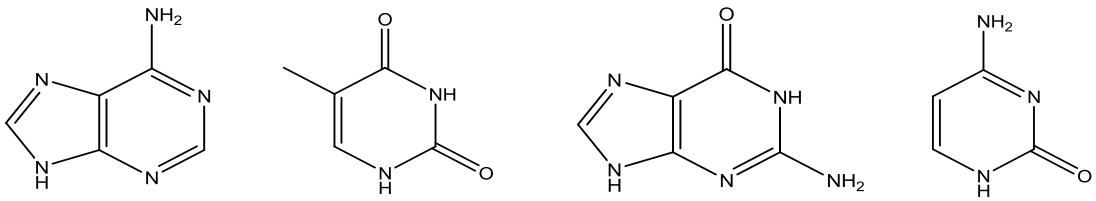

Adenine ***Thymine*** ***Guanine*** ***Cytosine***

Figure 1.2: DNA bases; adenine, thymine, guanine and cytosine.

The nucleotide bases are heterocyclic aromatic organic compounds and can be classified into two types, bicyclic purines and monocyclic pyrimidines. Adenine and guanine fall into the purine category, composed of a pyrimidine ring fused to an imidazole ring. Thymine and cytosine are pyrimidines which are composed of a 6 membered ring containing nitrogen atoms. A single base group is bound *via* an N-glycosidic bond to the C-1' of the 2-deoxy-β-D-ribose sugar group to N-9 of the purines and N-1 of the pyrimidines. This bond fixes the sugar ring into a β configuration (Figure 1.3).

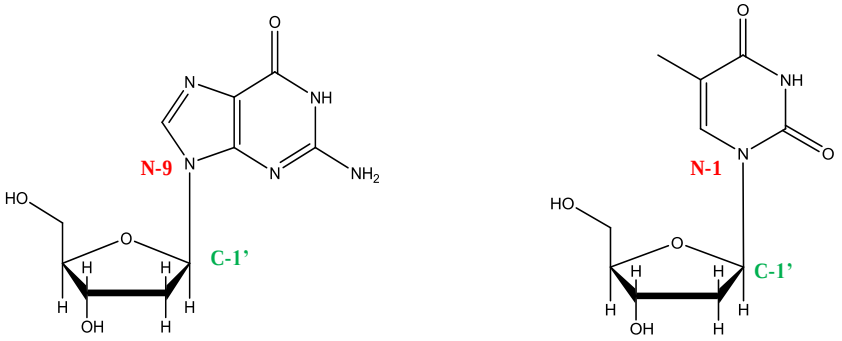

Deoxyguanine ***Deoxythymine***

Figure 1.3: N-glycosidic bonds in deoxyguanine (purine) and deoxythymine (pyridine) units.

The bases are complementary in nature, this was first noted by Chargaff in 1950.[7] Chargaff recognised that the number of adenine groups was equal to the number of thymine and the number of cytosine groups was equal to the number of guanine. This strongly suggested specificity within the base pairings, adenine will only bind to thymine and cytosine will only bind to guanine.[8] This work lead to the sudden realisation by Watson and Crick, that the results were compatible with a DNA spiral structure, in which every adenine was paired with thymine and every cytosine with guanine.[9,10] The consequential model could only be fully confirmed through invaluable x-ray diffraction patterns of DNA generated by Franklin.[11] This resulted in the elucidation of the double helix DNA structure in 1953, suggesting that the secondary structure of DNA was composed of two helical chains wound around the same axis.[12]

1.1.2 Secondary Structure

Each DNA strand is composed of nucleoside units joined through phosphodiester bonds between the 3'-hydroxyl of the sugar and the 5'-hydroxyl of the next sugar (Figure 1.4). The sugar and phosphate groups perform a structural role forming a backbone of alternating phosphate and deoxyribose sugar groups which create polynucleotide chains of DNA. Each single nucleotide strand (ssDNA) has directionality, containing a terminal 5' phosphate group and a 3' hydroxyl group.

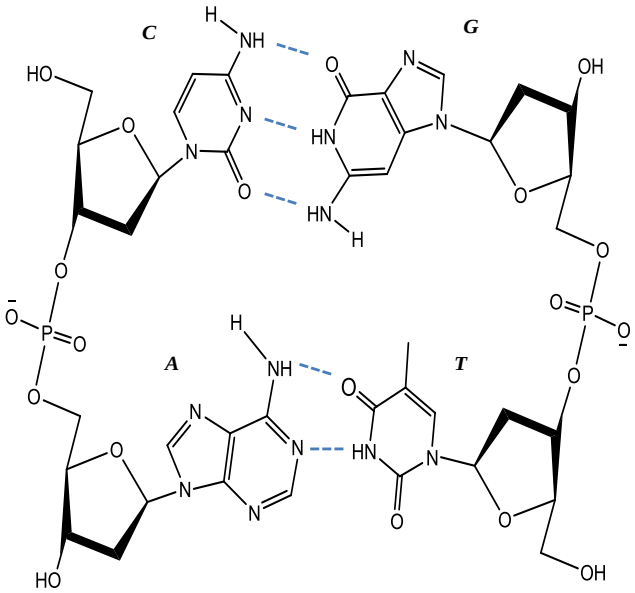

Figure 1.4: DNA strands with bonding between thymine and adenine *via* 2 hydrogen bond, bonding between cytosine and guanine *via* 3 hydrogen bonds.

Two antiparallel strands bind together through hydrogen bonding between complementary base pairs, with two H-bonds for each A-T pair and three for a G-C pair (Figure 1.4). A hydrogen bond is a relatively weak bond, in comparison to covalent bonding, with an average strength of 6 – 10 kJ mol^{-1}, but the relative strength is increased due to the large number of hydrogen bonds between the complementary pairs which stabilises the DNA helix structure.[8] This generates the formation of the DNA double helix (Figure 1.5).

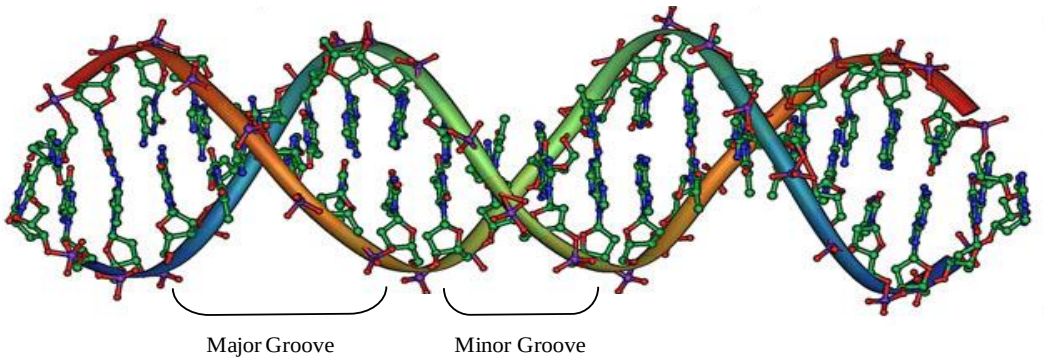

Figure 1.5: DNA double helix.[13]

The double helix structure develops differently sized grooves within the backbone as a result of each strand being closer together on one side of the arrangement than the other. Major grooves are formed where the backbone is further apart whereas minor grooves are smaller and occur when the backbone is closer together (Figure 1.5).[14] Grooves within DNA structure provide binding sites for biological material, such as proteins, one minor groove binding protein is distamycin A which acts as an anti tumour agent.[15] These groove sites can also be utilised to allow base modifications without disrupting the duplex.

The stability of the DNA duplex can be determined by UV-visible spectroscopy (Figure 1.6). Double stranded DNA will become denatured by increasing the temperature, resulting in the transition of double stranded DNA to single stranded DNA. This can be monitored by inspection of the UV-visible absorbance at 260 nm, as only the nucleotide bases significantly contribute to absorption above 230 nm. This phenomenon is a result of the π interactions in the benzene rings, when double stranded the rings stack face-to-face causing a decrease in absorption at 260 nm due to the shielding of the bases. When these strands become denatured at higher temperatures, the bases in the single strands become exposed generating an increased absorption at 260 nm. This is known as hyperchromicity and is reversible by denaturing the hybridised duplex.

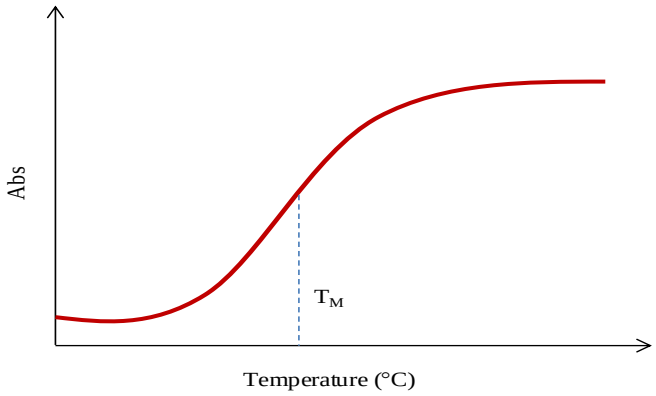

Figure 1.6: UV DNA melting curve, T_M indicates the melting temperature of complementary DNA strands.

A sigmoidal shaped melting curve is produced and the point of inflection is referred to as the melting temperature (T_M). T_M is the temperature at which half the sample exists as a double helix and half exists as single stranded DNA (ssDNA). Consequently, the T_M is used to indicate the thermal stability of the duplex. Many factors can affect stability including salt, pH and sequence modifications such as locked nucleic acids (LNA). The length and guanine (G) and cytosine (C) content of a sequence are also highly influential. A higher number of GC pairs within a DNA strand will increase the strength of the duplex, as there are a higher number of hydrogen bonds compared to AT base pairings. Consequently, long chain sequences with higher GC base pairings will have a greater stability and an increased melting temperature. However, research has found that oligonucleotides with an elevated number of guanine bases are prone to form self associating duplexes.[16] Through Hoogsteen base pairings, secondary structures including G-tetrads or guanine-quartets and -hairpins are formed by the stabilising guanine–guanine bonds,[17] which may adversely affect DNA analysis.

The study of the structure of DNA is a vast area of research. In 1990, the largest international DNA research investigation was undertaken which aimed to identify and map the sequences of all genes within human DNA.[18,19] The human genome project took over 13 years to complete and it was found that humans contain approximately 23,000 genes, roughly 3 x 10^9 DNA bases. This vast quantity of DNA makes it extremely difficult to detect a single genetic mutation within the human genome.[20] However, the development of the polymerase chain reaction (PCR) enables DNA regions containing the target sequence to be selectively amplified as well as reducing the complexity of the reaction.

1.2 Polymerase Chain Reaction (PCR)

The quantity of DNA available for analysis is often very small, therefore amplification of the nucleic acid sequence of interest is necessary. This is almost always achieved through PCR, which is an innovative *in vitro* technique used to amplify and detect double or single stranded DNA sequences. It is an exponential amplification technique which generates multiple copies of specific desired DNA sequences from trace amounts of sample. PCR was first developed in 1983 by Kary Mullis, with the first publication of the technique in 1985.[21] In 1993, Mullis won the Noble prize for his pioneering work on PCR.

The reaction relies on thermal cycling, consisting of repeated cycles of heating and cooling enabling DNA denaturation and enzymatic elongation. The essential components required for PCR are:

DNA template, the target sequence of bases to be amplified and analysed.

Primers, a pair of synthetic sequences are needed which are polynucleotides of between 10 and 30 bases. The primers are composed of sequences which are complementary to specific regions on the template that are within amplifiable distance of the area of interest. The primer sequences should have sufficient complexity to ensure they do not bind to other sites within the template. However, a balance between complexity and similarity to one another is required to prevent the formation of primer-dimers caused by self complementary. Primer design is a crucial component of PCR which, when successful, will produce a high yield of product and reduce the amplification of unwanted sequences.

Deoxynucleoside triphosphates (dNTP's), these are the "building blocks" within DNA and are required for strand amplification. Conventional PCR generally uses equal amounts of dATP, dTTP, dCTP and dGTP.

A thermostable polymerase enzyme is required which will catalyse the addition of deoxynucleoside triphosphates onto the annealed primers resulting in the formation of a new strand of amplified DNA. In order for elongation to take place, primers must have annealed to the template DNA strand as enzymatic extension can only occur on an existing polynucleotide strand. The enzymes that are used are relatively thermostable but will eventually denature after continual exposure to elevated temperatures. Often heat stable enzymes are used to reduce enzyme degradation at the high temperatures needed during

PCR. Commonly used thermostable enzymes inhibit polymerase activity at ambient temperature through the binding of an antibody or covalently bonded inhibitor that dissociates only after a high temperature activation step. The enzyme is activated through an incubation step (generally 5 – 15 minute at around 95 °C), minimising non-specific amplification products and primer–dimers at lower temperatures. This also limits degradation of the enzyme by preserving activity until the inception of the reaction.

Buffer solution, is essential to provide a suitable chemical environment for amplification and ensuring the pH is maintained throughout the reaction. The buffer contains a mixture of monovalent and divalent cations which have a large effect on success and efficiency of amplification. Repulsion between the negatively charged strands can inhibit PCR and so it is necessary to introduce cations which will neutralise the phosphate backbone and allow successful hybridisation to take place. Monovalent cations, generally in the form of KCl and divalent cations, $MgCl_2$, improve amplification through binding to the phosphate backbone, stabilising the annealing of the primers to the template. Magnesium divalent cations, Mg^{2+}, are often used as one ion can neutralise two phosphate groups within the DNA strand. However, the concentrations of the cations must be carefully controlled as an excess of Mg^{2+} ions in the sample can produce high levels of non-specific amplification and a deficient Mg^{2+} supply will inhibit PCR. Also the use of thermostable DNA polymerase enzymes require free divalent ions to produce effective activity within the reaction.[22]

PCR consists of repetitive thermal cycles, with each cycle containing a denaturation, annealing and elongation step (Figure 1.7). Within the first cycle of PCR, the temperature is increased to 90-95 ºC for between 30 and 60 seconds, disrupting the hydrogen bonds between the base pairings in the double stranded DNA template separating the strands. This is known as denaturation (Figure 1.7, step (a)). The annealing step then follows (Figure 1.7, step (b)), and involves lowering of the temperature to 40 – 60 ºC to allow the primers to hybridise to the complementary DNA template. The annealing temperature is critical since if it is too high, then primer hybridisation will be poor resulting in a low yield of product. However, if the temperature is too low, non-specific binding of primers could occur resulting in unwanted sequences being amplified. The elongation step (Figure 1.7, step (c)) involves the extension of the annealed primers in the 3’ → 5’ direction, through the use of a polymerase enzyme which catalyses the addition of dNTPs. This takes place at the optimum temperature for the enzyme activity which is usually 72-78 ºC.

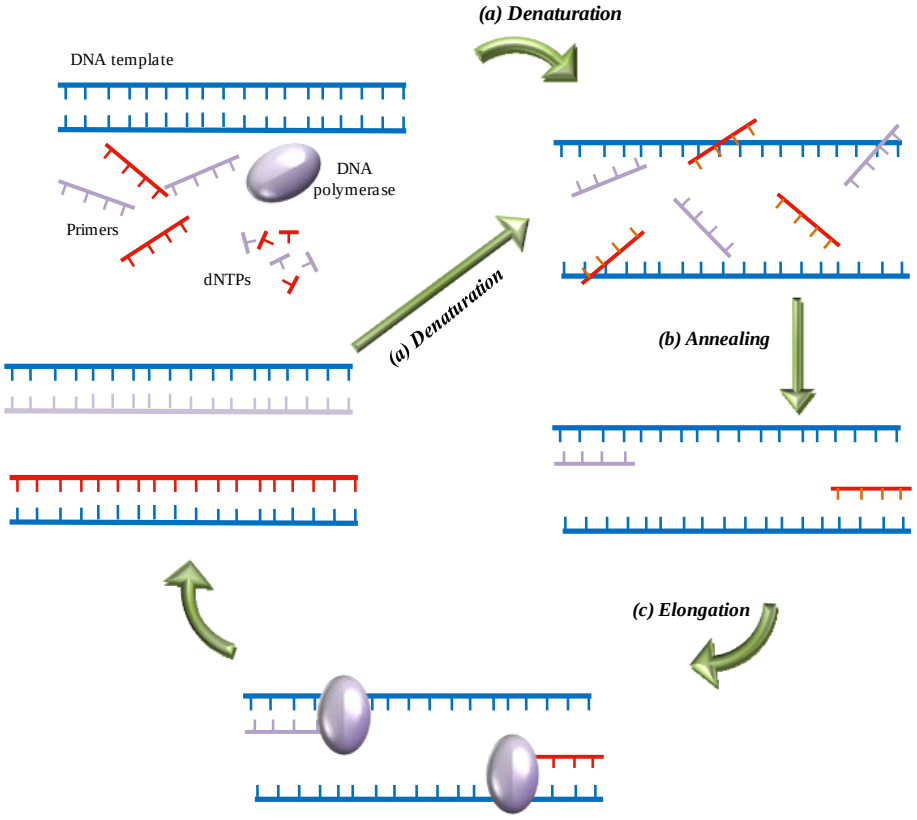

Figure 1.7: PCR cycle with 3 steps; **(a)** denaturation, **(b)** annealing and **(c)** elongation.

Initially, primer extension occurs along the template sequence beyond the secondary primer binding site. However, after the first few cycles DNA sequences produced are equal in length to the region between annealed primers, generating identical complementary strands with reduced complexity to the original template whilst maintaining sequence specificity.[22] These steps are then continuously repeated, doubling the amount of DNA template sequence in every cycle. Consequently, 1billion DNA copies would be produced after 32 cycles.

PCR is a highly complex reaction in which careful consideration of components and conditions must be taken to ensure that the optimum amount of product is efficiently generated during the reaction.

1.2.1 PCR Considerations

1.2.1.1 Plateau Effect

An increasing number of cycles should theoretically increase the yield of amplified DNA. In reality, however, there is another limiting factor to the number of cycles. While the reaction

proceeds, the amplicon will begin to accumulate and the reactants will decrease and degrade. In particular, the primer to template ratio will decrease and all available enzyme will become occupied. This will result in slow product formation and the rate of reaction will begin to level off, this is known as the plateau effect (Figure 1.8). For most reactions performing more than 30 cycles results in no greater quantity of product, thus shows no significant advantage.[23]

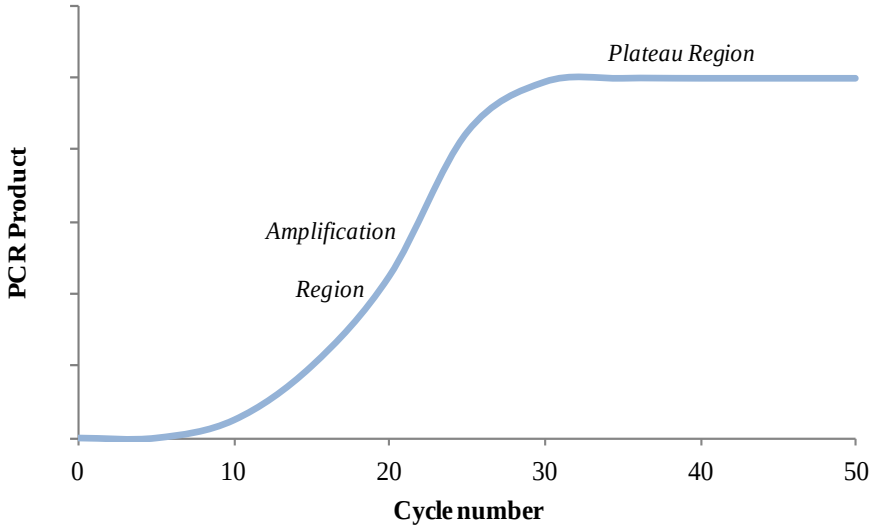

Figure 1.8: Plateau effect for a PCR reaction.

1.2.1.2 Contamination

PCR has been shown to be a robust and highly efficient technique which if carried out correctly generates high amounts of target DNA sequences. However, as a result of the sensitive nature of the reaction, contamination from undesirable DNA sequences is possible. To help overcome this, real-time PCR can be used to monitor the accumulation of amplicon throughout PCR, allowing detection to be carried out in a "closed tube" format. Consequently, reducing the risk of cross contamination as no manipulation of the sample is required during or after PCR.

1.2.1.3 Monitoring Real-Time PCR

The amplification of DNA PCR can be monitored through the inclusion of a fluorescent dye binding agent, such as SYBR Green I,[24] ethidium bromide[25] and YO-PRO-1.[26] These small molecules have a low binding affinity for single stranded DNA and bind in high yields to double stranded DNA, permitting the detection of sequence amplification. In real-time PCR,

fluorescence from the dye is measured in each cycle to obtain an amplification curve, the intensity of which is proportional to the amount of PCR product formed (Figure 1.9(a)). This is a simplistic method to monitor the indiscriminate amplification of double stranded DNA, which can be applied to a widespread sample basis with no requirement for specialised design. In addition, post-PCR melt curves can be obtained through heating the sample to melt the probe-PCR product duplex and chart the fluorescence from the intercalating dye (Figure 1.9(b)). Fluorescent dyes, such as SYBR Green I and LC Green, strongly bind to double stranded DNA and fluoresce at low temperatures, however as the temperature is increased the strands denature to single sequences and the dye fluorescence decreases. The fluorescence is continually monitored and a melting curve is obtained.

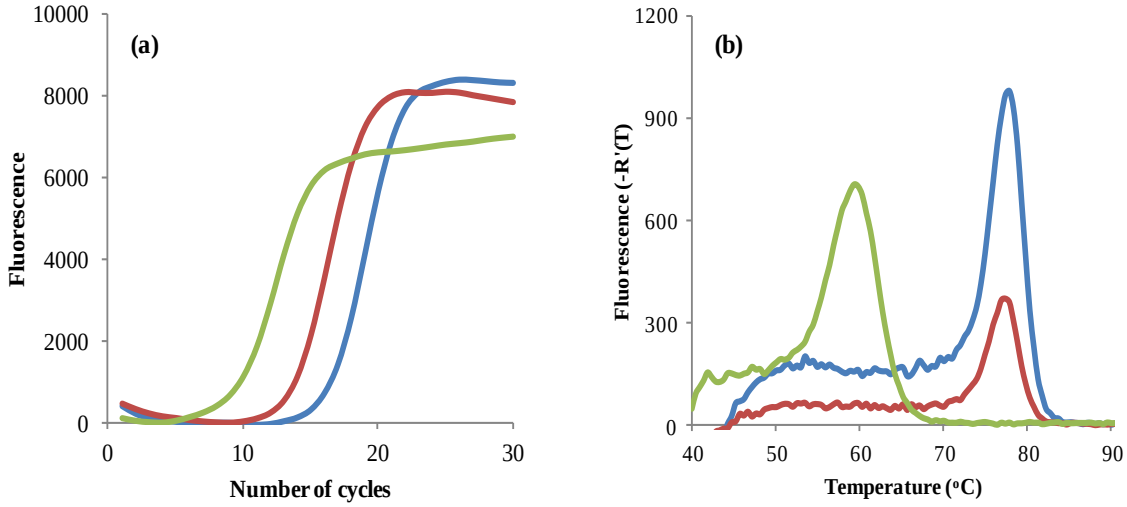

Figure 1.9: **(a)** Real-time PCR amplification, **(b)** first derivative of post-PCR melting curve.

Real-time PCR amplification can generate highly sensitive DNA quantification in a low cost and simplistic approach, however, the intercalating dyes will bind indiscriminately to double stranded sequences. Consequently, false positive results may be generated from the amplification of undesired sequences, preventing sequence-specific information being obtained. One method to avoid non-specific accumulation of fluorescent signal is by PCR assays. These methods incorporate labelled oligonucleotides which have been designed to probe specific regions of the target sequence and generate signal only through selective hybridisation events.

1.3 Specific DNA Detection Assays

The continual development into the understanding and interpretation of specific DNA sequences is fundamental in the progression of rapid and routine analysis, with the need for this information vital within a vast number of fields, including proteomics, genetics and human diagnostics.[27] Therefore, research into the specific detection of nucleic acids is continually being progressed. Sequencing methods have been used to determine specific DNA sequences, including the Maxam-Gilbert method,[28] Sanger dideoxy[29,30] and Pyro sequencing.[31] The advent of these techniques has significantly accelerated biological research and the use of modern sequencing technology has been instrumental in the elucidation of the human genome. However, the sequencing process can often generate much more detailed information than is often necessary, for example, the detection of a single nucleotide polymorphism (SNP) through sequence analysis will yield vast amounts of surplus information. Consequently, other methods for efficient and specific DNA detection have been developed. Discussing all these methods is beyond the scope of this thesis, however, a commonly taken approach employs fluorophore probes, short oligonucleotide strands labelled with fluorescent dyes.

1.3.1 Fluorophore Probes

Fluorophores are coloured molecules that fluoresce by absorbing a specific wavelength of light and emitting it at another wavelength, this process can then be detected and measured. Fluorescent molecules can be covalently attached to specific DNA oligonucleotides, enabling sequence determination *via* selective hybridisation and detection of the coloured molecule by spectroscopic analysis. The use of short oligonucleotide probes to determine the presence of specific complementary sequences has become a reliable and well-established technique.[27] These approaches often incorporate PCR, to amplify and reduce the complexity of the nucleic acid sequence of interest, allowing a higher probe binding capacity. Four DNA detection assays will be highlighted here, primer-probes, TaqMan, molecular beacon and scorpion probe assays.

1.3.1.1 Primer-Probe PCR

The simplest form of specific nucleic acid detection assays use labelled primers to detect the accumulation of PCR product. Fluorescently labelled primer-probes have been utilised within conventional PCR to generate an increasing fluorescent signal as PCR product

accumulates. The primers are designed to generate enhanced fluorescence through PCR extension, one such example is AmpliFluor primers (Figure 1.10).[32]

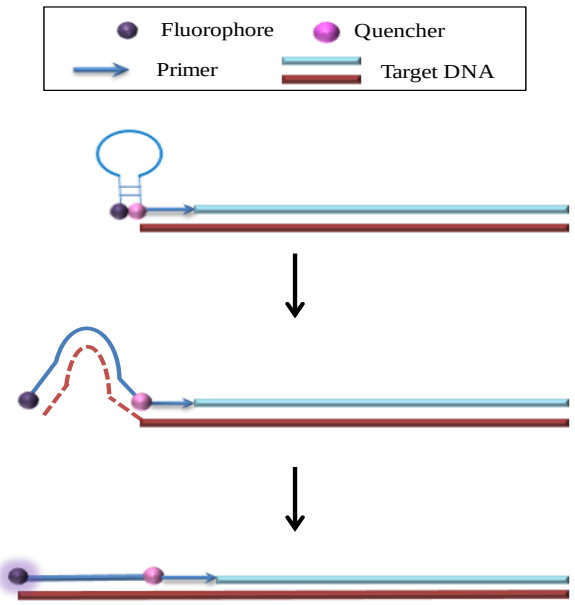

Figure 1.10: AmpliFluor primers demonstrate the accumulation of amplicon through the build up of fluorescence signal as the number of PCR cycles increases.

These primers are designed to conform to a stable hairpin loop structure, which inhibits the emission of fluorescence. Typically, probes are designed to be non-fluorescent until bound to the complementary target and often achieve this through Förster resonance energy transfer (FRET) quenching. FRET is a mechanism which describes the energy transfer between two chromophores. The efficiency of this energy transfer is inversely proportional to the 6^{th} power of the distance between the chromophores, thus FRET will diminish over distance. This quenching mechanism can therefore be utilised within DNA detection assays to maintain fluorescence quenching when the DNA is in the unbound state. However, upon hybridisation to the target sequence, the interfluorophore distance is increased leading to an increase in fluorescence emission. Extension of the AmpliFluor primers results in incorporation into the PCR product, consequently, the copying process opens the hairpin structure and increases the fluorescent signal. The use of labelled primer allows significantly increased specificity to be obtained since in the presence of non-specific target DNA no amplification should occur.

1.3.1.2 TaqMan Assay

TaqMan assays have been widely used as a DNA detection method[33-35] which involves signal generation through enzymatic probe cleavage. The assay utilises PCR and the 5'-exonuclease activity of a DNA polymerase enzyme to selectively build-up fluorescence signal. The fluorophore is incorporated into a specifically designed probe and any emitted fluorescence is absorbed by connecting the dye to a quencher through a short single stranded sequence. During PCR, the probe hybridises to a specific region within the target gene through the single stranded DNA probe sequence (Figure 1.11).

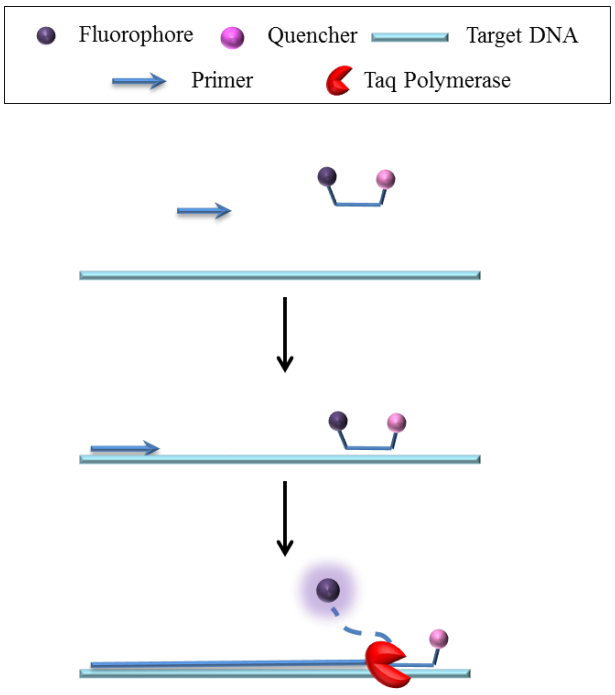

Figure 1.11: TaqMan assay illustrating enzymatic digestion of the FRET quenched probe enabling build up of fluorescence signal, demonstrating the presence of target DNA.

Conventional PCR can then be performed through elongation of the DNA primers by the *Thermus aquaticus* (Taq) polymerase enzyme. However, the enzyme also simultaneously digests the bound probe. The assay design ensures that the primer binding sites are adjacent to the probe, allowing the 5' to 3' exonuclease activity of the thermostable enzyme to be fully exploited. The probe digestion separates the fluorophore and quencher, enabling fluorescence emission. The accumulation of free fluorophore and hence, amplification of target sequence, can be monitored during the reaction through the build up of fluorescent signal.

The TaqMan assay is a closed tube method which allows signal to be generated within real-time PCR, reducing the need for post-PCR manipulation. High target selectivity is also obtained through the specific hybridisation of the probe and primers and amplification ensures low concentrations of target can be detected. However, the assay does suffer from some inherent drawbacks. TaqMan probes can show poor allelic binding and inefficient fluorophore quenching, which result in high background signals. Therefore, probe designs are continually being developed to improve upon assay shortcomings and reduce fluorescent background signals. These have included chemical modifications,[36] intramolecular TaqMan probes[37] and attachment of minor groove binders.[38]

1.3.1.3 Molecular Beacon Assays

Molecular beacons are competitive oligonucleotide hybridisation probes, which generate an increased fluorescent signal in the presence of specific target DNA. A molecular beacon contains an internally quenched fluorophore held within a stable hairpin-loop structure. The DNA sequences within the molecular beacon structure are carefully selected to form a stem and loop region. The DNA loop usually contains around 18 – 30 bases and is complementary to a specific region within the target gene. At both terminus ends of the loop, self complementary sequences are incorporated (~5-8 bases), which form a double stranded stem and holds the beacon within a stable hairpin structure. A fluorophore and quencher are covalently attached to the 5'- and 3'- ends of the stem and in the closed loop conformation fluorescence emitted by the dye is absorbed by the adjacent quencher. However, in the presence of target DNA, hybridisation between the loop region and target occurs, as this open formation is thermodynamically favoured due to a greater number of bases being integrated within the duplex. The open conformation separates the fluorophore from the quencher, increasing fluorescence emission and indicating the presence of target DNA (Figure 1.12). Molecular beacons have been widely used in homogeneous nucleic acid detection assays including DNA genotyping in human alleles[39] and drug resistance in *Mycobacterium Tuberculosis*.[40]

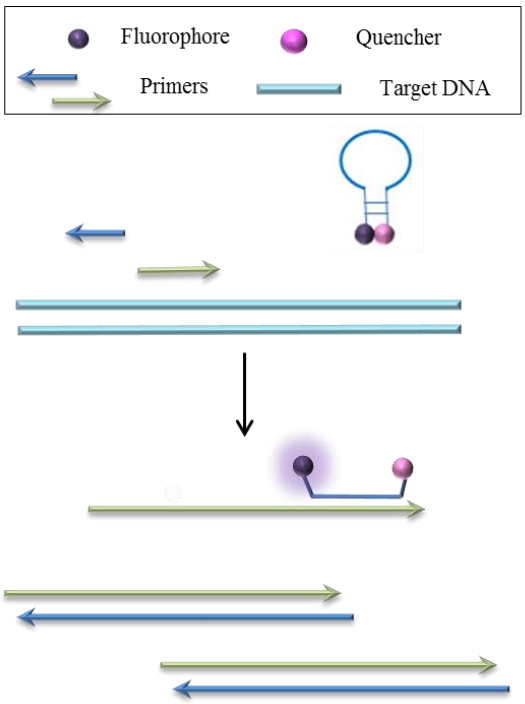

Figure 1.12: Molecular beacon assay which detects the presence of target DNA through selective hybridisation, changing the conformation of the beacon which permits fluorescence emission.

The probe-target duplex formation within the assay is a bimolecular binding event, thus, the intermolecular reformation of the stem-loop beacon is kinetically and entropically favoured. Consequently, under certain conditions the fluorescent signal obtained from the assay may decay rapidly as the beacon detaches from the target and returns to the beacon format. This can be eliminated through the design of unimolecular binding probes, the most well studied example is scorpion probes.

1.3.1.4 Scorpion Probe Assay

A scorpion detection assay utilises self-probing amplicons through incorporation of specially designed primer probes. These probes make use of a hairpin structure to quench any fluorescence from the fluorophore, however, unlike a molecular beacon the hairpin is attached to the 5' end of the primer through a PCR blocker. Initially, the scorpion primer hybridises and PCR extension results in the formation of an oligonucleotide which contains a region specific to the loop sequence (Figure 1.13). The loop region of the probe is designed to be longer than the stem, thus, binding to the amplicon is favoured over stem reformation. This conformational change within the scorpion probe results in separation of the fluorophore and quencher, allowing fluorescence emission.

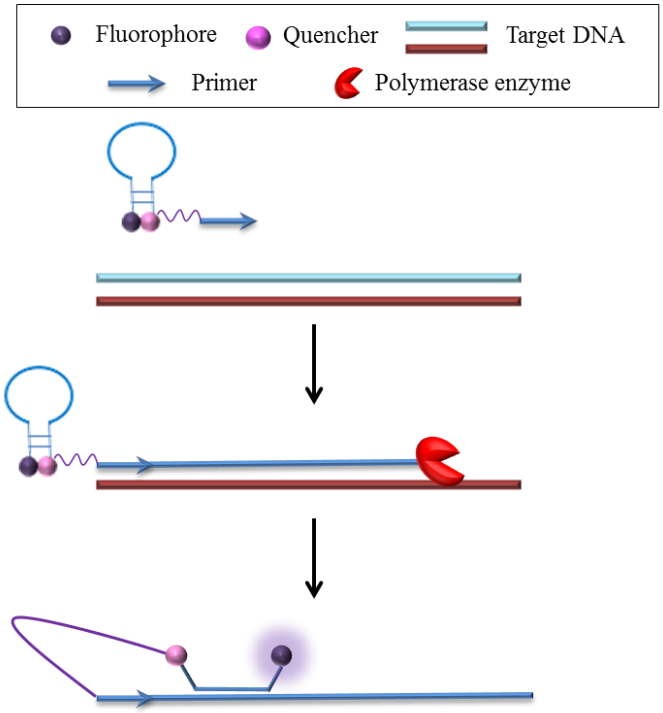

Figure 1.13: Scorpion probe assay detects target DNA through selective hybridisation of a unimolecular probe which changes conformation permitting fluorescence emission.

The design of the scorpion assay provides extra specificity due to the selective hybridisation of both the primer and probe sequences, however, sensitivity may be limited by the nature of this competitive hybridisation. This unimolecular probing event facilitates rapid probe binding and a high signal-to-noise ratio as a result of the probe target duplex being kinetically and thermodynamically more favourable than other structure formations. However, the complexity of the design and synthesis of the scorpion probes can introduce complications into their action producing inaccurate results through poor secondary structure formation. Therefore, care and experience must be used when initialising assay set up. Successfully designed scorpion assays have been effectively used to detect and quantify HIV-1 DNA[41] and muscular dystrophy.[42]

These solution based nucleic acid detection assays are some of the most successful and widely used methods to achieve qualitatively and quantitatively analysis of specific oligonucleotides. However, an alternative method of DNA detection utilises array platforms to accurately and sensitively detect DNA sequences which has rapidly emerged and developed significantly in recent years.

1.4 Surface DNA Detection Methods

The development of surface detection platforms, such as biosensors and microarrays for the detection of DNA has risen sharply over recent years.[43] These methods utilise surfaces to immobilise target DNA strands and detect their presence through the exploitation of preferential DNA strand binding. DNA surface detection techniques have become routinely used for the identification of specific nucleic acid sequences and can rapidly generate large quantities of DNA analysis information within one array which is unparalleled within solution based methods. These highly efficient methods of strand detection were initially developed from the original surface DNA detection method, the Southern blot.

1.4.1 Southern Blot

One of the first surface DNA detection methods was proposed by E. M. Southern who, in 1975, invented Southern blot analysis.[44] This molecular biology technique combines the transfer of electrophoresis separated DNA fragments to a membrane surface and subsequent DNA detection through probe hybridisation. Initially, DNA sequences are separated in an agarose gel using electrophoretic mobility.

1.4.1.1 Gel Electrophoresis

Gel electrophoresis is a commonly used method for the analysis and separation of DNA, allowing compounds to be separated according to their differing physical properties including size and charge (Figure 1.14).

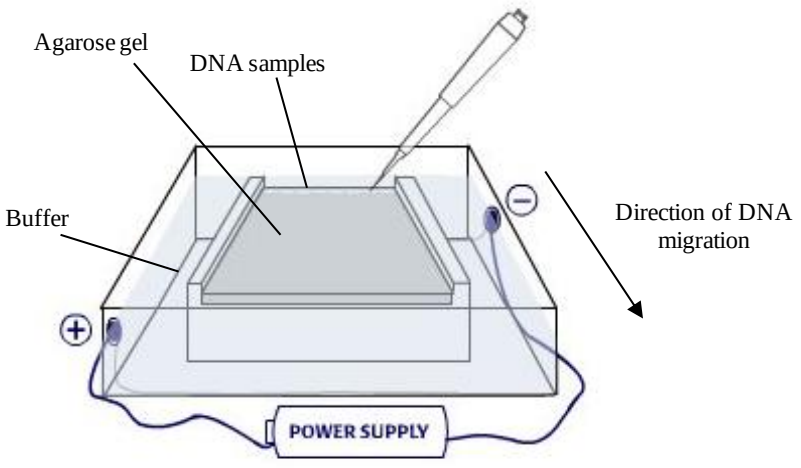

Figure 1.14: Gel electrophoresis equipment enabling the separation of DNA sequences on an agarose gel through differences in electrophilic mobility of DNA.

Electrophoresis is performed in an insulated chamber containing a buffer reservoir with a voltage applied across the system. The overall negative charge on the DNA phosphate backbone causes it to migrate through the gel towards the cathode. An agarose gel is generally used for nucleic acid separation. It is composed of a 3D network of crosslinked polymer strands which create large pores throughout the matrix. The porous gel acts as a molecular sieve and the DNA migrate at different rates across the gel depending on the charge-to-size ratio, known as the electrophilic mobility (μep) of the DNA. Smaller fragments of DNA migrate a further distance compared to larger fragments due to the frictional force. These can then be compared to a DNA ladder, fragments of DNA of known sizes utilised to the discrimination differently sized sequences. Capillary action is then used to transfer the DNA from the gel to the membrane through a stacking blot.

1.4.1.2 Capillary Blot

Within the stack, the gel is placed between several layers of blotting paper, with either a nylon or nitrocellulose membrane placed on top of the gel. A buffer solution is then drawn through the blotting paper layers by capillary action, causing the DNA fragments to migrate from the gel to the membrane. The membrane, which now has the target DNA bound, is removed from the blotting stack and placed within a hybridisation buffer. The buffer contains a blocking agent and a complementary DNA probe. The blocking agent blocks sites on the membrane that do not contain target DNA to prevent any non-specific binding of the probe. The probe hybridises to immobilised target on the membrane surface through aid of the cation rich buffer.[8] The DNA probe is labelled with radioisotopes, such as ^{32}P or ^{125}I, which after extensive washing steps can be visualised on x-ray film by autoradiography. While this is one of the most sensitive methods of DNA detection, radioactive labelling presents a serious hazard. Consequently, modern array methods have been developed which utilise optical detection techniques based on the use of fluorescent dye labels. The DNA microarray is one such innovative DNA detection technique which has greatly surpassed the traditional Southern blot method and has significantly enhanced DNA research over recent years.

1.4.2 DNA Microarrays

A DNA microarray is an orderly and systematic arrangement of a large number of oligonucleotides on a solid substrate, which are selectively detected through the principle of DNA hybridisation. Single stranded target DNA sequences are immobilised on a solid surface, generally glass, plastic or silicon support. The array is then treated with a solution

containing dye labelled DNA sequences, if the labelled DNA is complementary to the target strands, hybridisation occurs fixing the newly formed duplex to the surface. However, DNA strands which are non-complementary to the target will be washed from the surface, leaving only complementary labelled DNA to be detected. The hybridised sequences will generate colour from the dye label on the array and are commonly detected through fluorescence or colorimetric techniques. One single microarray can consist of tens of thousands of DNA target strands, therefore, many reactions can be performed simultaneously using different DNA sequences with a variety of dye labels (Figure 1.15). Subsequently, the use of DNA microarrays for strand detection has dramatically accelerated many types of investigation, including the diagnosis and drug treatment of many disease states.[45, 46]

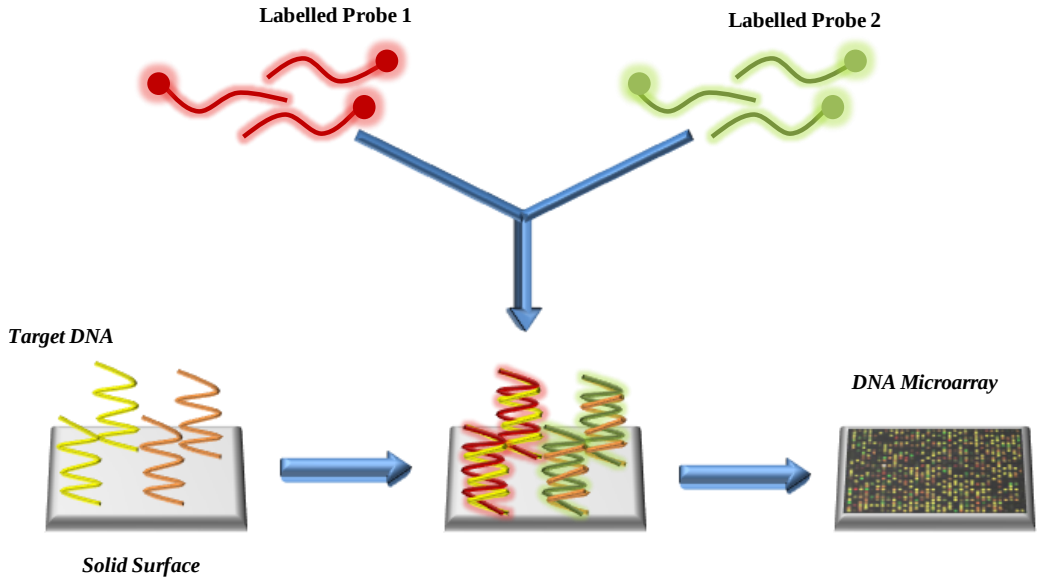

Figure 1.15: Schematic of DNA microarray in which target DNA is detected from a solid substrate through hybridisation of specifically labelled DNA.

The immobilisation of target DNA onto the sensory surface is essential in the development of DNA microarrays.[47] To achieve high sensitivity and specificity from the array, non-specific adsorption must been minimised. Therefore, the arrangement of target DNA on the surface must be controlled to ensure stability, orientation and accessibility. DNA immobilisation is mainly achieved *via* adsorption, covalent immobilisation and avidin-biotin interactions.

1.4.2.1 Adsorption

Adsorption is the simplest form of DNA immobilisation onto a surface as the target DNA requires no modifications. Adsorption of unmodified DNA sequences onto a surface substrate occurs through electrostatic charges between the DNA sequence and the charged surface layer. The orientation of DNA adsorption largely depends on the charge of the accepting substrate and can be driven through either the negatively charged groups on the DNA backbone[48,49] or through electrostatic charges on the constituent bases.[16,50] This will allow different DNA groups to be exposed depending on the requirements of the surface array. Often, DNA can be further fixed onto the surface through heating or UV crosslinking.

1.4.2.2 Covalent Immobilisation

DNA immobilisation by covalent attachment is generally carried out through chemisorptions and the covalent coupling of a modified probe onto a functionalised surface. Chemisorption describes the chemical attachment of DNA to the surface, with thiol – metal interactions frequently employed to bind biomolecules to gold surfaces. Thiol groups have a strong affinity to the metal surface, enabling the formation of a covalent bond between the sulphur and gold atoms. This phenomenon has been widely utilised within surface arrays for the specific detection of DNA.[43,51,52] Covalent attachment can also be generated through the coupling of modified probes onto functionalised surfaces. *N*-hydroxysuccinimide (NHS) and 1-Ethyl-3-(3-dimethylaminopropyl)carbodiimine (EDC) are frequently used activation coupling reagents which can form self-assembled monolayers through an esterification reaction.[53] These methods of attachment encourage the sequences to adopt an orientation perpendicular to the surface and pack more densely.

1.4.2.3 Avidin – Biotin Interactions

Avidin and streptavidin are tetrameric proteins that have four identical binding sites (Figure 1.16). These sites have a very high binding affinity ($K_a = 10^{15}$ M^{-1}) for the small molecule, biotin. This specific binding event has been widely exploited within detection assays to immobilise DNA as a result of the stable and fixed orientation of nucleic acids.[54,55] DNA microarrays and biosensors have also utilised this strong interaction to form self-assembled monolayers (SAMs) of target oligonucleotides on the substrate surface.[56] This interaction also allows reuse of the array surface without significant loss of hybridisation activity, through the reversible binding on the probe.

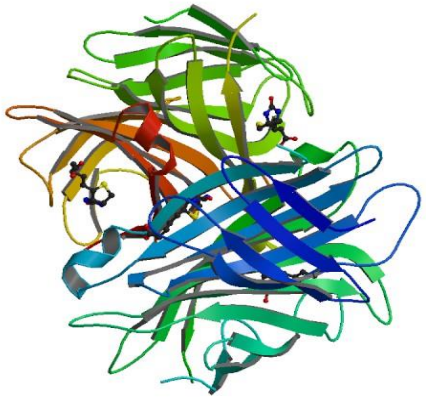

Figure 1.16: Streptavidin tetramer with four bound biotin molecules, PDB ID: 1MEP.

The successful immobilisation of DNA onto the surface substrate is a crucial step, ensuring the maximum amount of complementary probe is able to hybridise and generate accurate signals. The optical detection of successfully hybridised samples from the array surface is generally carried out using fluorescence, with laser fluorescence confocal microscopes routinely used to provide very sensitive scanning of high density microarrays.[57,58] Alternative detection methods include colorimetric detection in which the sample will change colour when complementary strands hybridise[43] and surface plasmon resonance (SPR) in which changes in the refractive index occur through biomolecular binding events.[59] More recently, surface enhanced resonance Raman scattering (SERRS) has emerged as an effective detection method for biomolecules on surfaces.[51,60]

1.5 Surface Enhanced Resonance Raman Scattering (SERRS)

SERRS is an optical spectroscopy method which has been shown to be capable of extremely sensitive and specific biomolecule detection with the potential for multiple analyte analysis.[61,62] Thus, to enable the potential of SERRS to be fully exploited, an understanding of the basic principles and theory of Raman spectroscopy must be first be introduced.

1.5.1 Spectroscopy

Spectroscopy is the measurement of discrete amounts of energy which are passed between molecules and electromagnetic radiation when they interact. These exchanges can either be in the form of absorption, emission or scattering. The main spectroscopic techniques utilised to detect vibrational changes in molecules are based on infrared (IR) absorption and Raman scattering. Both these techniques allow information on the structural properties of the molecule to be gained through identification of characteristic spectral patterns.

IR absorption requires direct excitation of the molecule by a photon corresponding to the energy gap between the ground vibrational energy level and the first excited vibrational level (Figure 1.17). This is achieved by directing IR energy covering a range of frequencies onto the sample and detecting the loss of energy from the radiation beam after it has passed through the sample. Each peak within an IR spectrum represents the energy of radiation absorbed, this allows information on the chemical structure to be obtained. The most intense IR absorptions are generated due to the oscillating dipole moment of the molecule, thus, IR active molecules require a permanent dipole. In contrast, light can be scattered by the molecule and detected by Raman spectroscopy.

1.5.1.1 Raman Scattering

In Raman scattering, the photon interacts with the electrons of the molecule causing a distortion. When the distorted electron cloud relaxes scattering occurs. Scattering results in two forms of radiation, Rayleigh and Raman scattering. Most scattering occurs at the same frequency as the incident photon, this is known as Rayleigh scattering. This dominant process produces elastic scattering in which the molecule is 'excited' to a virtual level and immediately returns back to the ground state. Therefore, the scattered radiation has the same frequency as the incident light (Figure 1.17).[63,64]

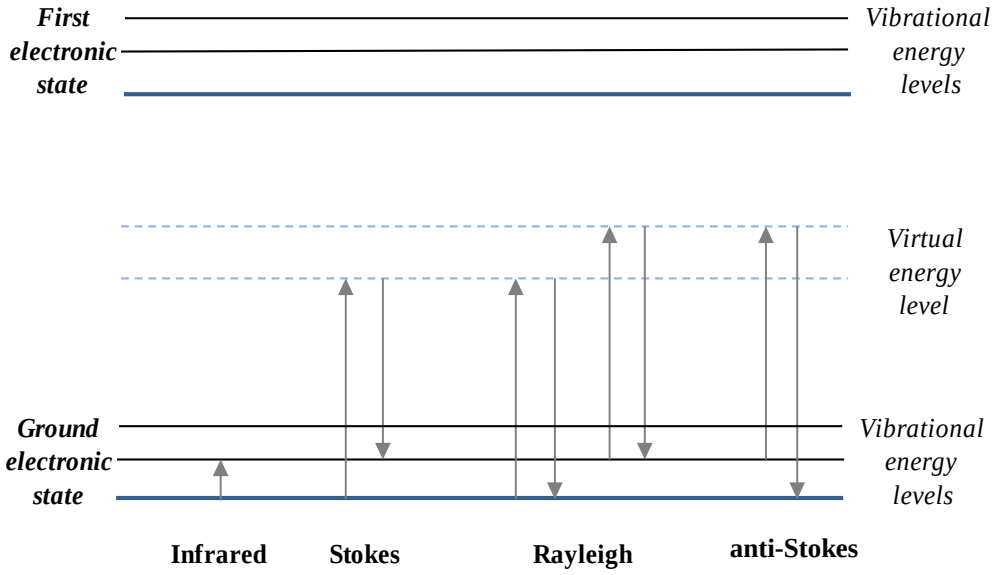

Figure 1.17: Vibrational transitions involved in Infrared (IR) absorption and Raman scattering.

However, a small fraction of the scattered radiation results in inelastic scattering where there is an induction of nuclear motion during the scattering process. Energy is transferred to or from the nucleii of the molecule, this is known as Raman scattering. The Raman effect was first experimentally demonstrated by Chandrasekhara Venkata Raman in 1928, who discovered that light passing through a transparent material will change some of the deflected lights wavelength.[65] In Raman scattering, photons interact with the molecule polarising the cloud of electrons around the nuclei, this generates the formation of a virtual energy state. This state is very unstable and the photon is immediately re-radiated from the molecule in the form of scattered radiation. The scattering is shifted in energy by one vibration unit and can be detected by irradiating the molecule with a single frequency of radiation. This process is described using the energy level diagram in Figure 1.17.

Raman scattering can be further split into two types, Stokes and anti-Stokes scattering. Stokes Raman scattering is generated from a molecule that relaxes to a higher vibrational level however, some molecules may already be present in an excited state as a result of thermal energy and will relax to a lower vibrational energy, this is anti-Stokes Raman scattering (Figure 1.17).[63]

Most molecules exist in the ground state at room temperature, therefore, the intensity of the Stokes scattering is generally greater than anti-Stokes. The population of the energy levels, and the relative intensities of both processes, can be predicted using the Boltzmann equation (Equation 1.1).[63] This equation takes into consideration the degeneracy (g) of all possible vibrational states in the ground level and can distinguish between individual components.

$$\frac{N_n}{N_m} = \frac{g_n}{g_m} \exp\left[\frac{-(E_n - E_m)}{kT}\right]$$

Equation 1.1: Boltzmann Equation.

N_n *is the number of molecules in the excited vibrational energy level (n)*

N_m *is the number of molecules in the ground vibrational energy level (m)*

g *is the degeneracy of the levels n and m*

$E_n - E_m$ *is the difference in energy between the vibrational energy levels*

k *is the Boltzmann's constant (1.3807 x 10^{-23} JK^{-1})*

T *is temperature in kelvin (K)*

Molecules which are Raman active must comply with selection rules. Intense Raman scattering occurs from vibrations which cause a change in polarisability of the electron cloud around the molecule, with symmetrical vibrations generating the greatest scattering. The selection rules also state that only vibrational changes by one unit are permitted.

Raman scattering has many advantages as an optical detection technique including the generation of molecularly specific vibrational spectra, the ability to use aqueous solutions without background interference and it is a non-destructive process.[66] Qualitative analysis can also be obtained as the energy exchange between the incident photon and the molecule results in scattering which returns the molecule to rotational and vibrational energy levels generating energies which correspond to particular vibrations of a molecule.[64] However, Raman scattering is a weak process i.e. only about 1 in every million photons within the incident beam are scattered, thus, weak lines are produced. Subsequent advances in modern instrumentation such as lasers, optics and detectors have improved the sensitivity of the technique. In addition, the use of molecules in resonance with the excitation radiation have increased the application of this technique.

1.5.2 Resonance Raman Scattering (RRS)

Resonance Raman spectroscopy has shown to be a sensitive technique able to enhance the strength of Raman signals. For RRS to occur, the absorption maximum of the molecule with a chromophore must coincide with, or be close to the excitation frequency of the laser beam. The excitation radiation is tuned to the energy of an electronic transition within a molecule, and instead of a molecule being excited to a virtual level as in Raman scattering, it is excited into a higher vibrational energy level within the excited electronic state (Figure 1.18). This generates strongly enhanced Raman bands and increases the scattering efficiency by a factor of $10^3 - 10^5$, with enhancements of 10^6 observed.[63]

The spectra produced by RRS are much simpler than Raman spectra as only the vibrations which are in resonance with the excitation frequency are enhanced. Since Raman scattering arises from a change in polarisation of the molecule, strong resonance enhanced Raman bands are generally produced by symmetrical vibrations that vibronically couple with the electronic state. This generates large polarisation changes and results in a simplified spectrum dominated by a few peaks.

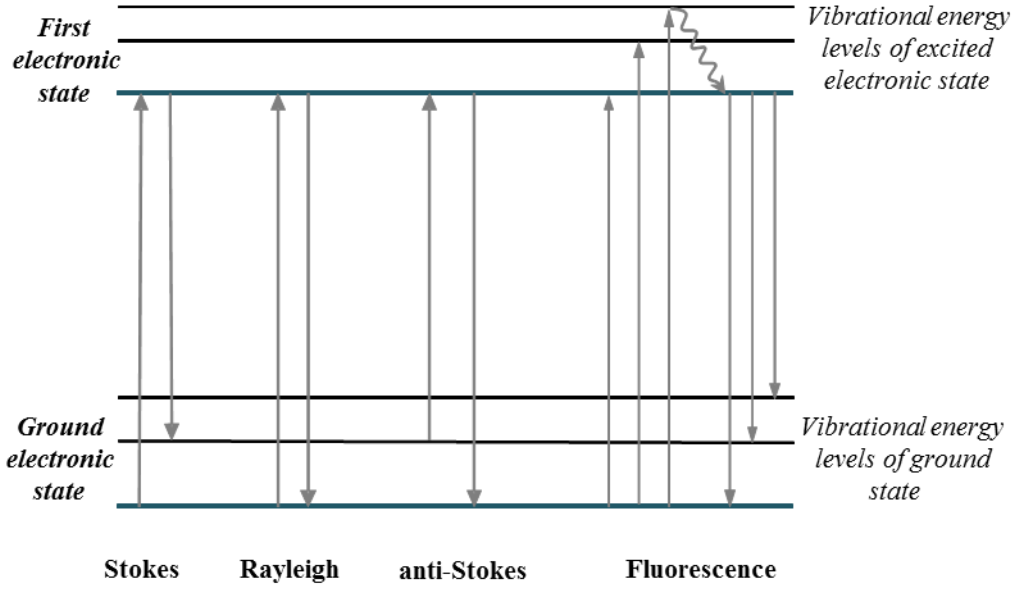

Figure 1.18: Electronic transitions involved in resonance Raman scattering.

The powerful visible lasers used for RRS generate the same energy required for absorption processes, thus, photodegradation and fluorescence can become a large problem. Photodegradation and heating will cause decomposition of the sample, however, sampling techniques such as spinning the sample or flowing it past the beam during analysis can overcome this. A more difficult problem in RRS is the obstruction of spectral bands by fluorescence as both processes share a similar mechanism (Figure 1.18). In fluorescence, an electron is excited into a higher electronic vibrational state where it relaxes to the vibrational ground state of the excited state *via* internal conversion and vibrational relaxation. It then returns to the electronic ground state with emission of a fluorescent photon. The difference between RRS and an electronic absorption is the length of time the molecule stays in the excited state. The scattering process is fast, occurring before the nuclei reach equilibrium positions in the excited state, producing very low quantum yields. Whereas, absorption is a slower process as the nuclei relax into the equilibrium geometry and has high quantum yields. Therefore, as a result of the low number of Raman scattered photons and narrow spectral bands produced, the spectra can be easily obscured by broad fluorescent bands. The dilution of samples, use of pulsed lasers and anti-Stokes scattering[67] have all been utilised to reduce fluorescence interference. However, the use of roughened metal surfaces has shown to increase the signal intensity as well as acting as a fluorescence quenching substrate. This technique is known as surface enhanced Raman scattering.

1.5.3 Surfaced Enhanced Raman Scattering (SERS)

In 1974, Fleishman and co-workers initially observed an increased intensity in Raman signal when pyridine was absorbed onto a roughened silver surface, they attributed this to a large increase in surface area.[68] In 1977, Albrecht and Creighton[69] and Jeanmarie and Van Duyne[70] independently reported proposed mechanisms for this enhanced Raman signal, now known as surface enhanced Raman scattering (SERS). SERS is a very simple and effective method of analysis that can increase the Raman enhancement by 6 orders of magnitude.[63] The technique requires a nanoscale roughened metal surface which has been provided through numerous substrates including structured metal arrays,[71,72] shaped nanoparticles[73,74] and spheres,[75,76] and specially designed solid surfaces.[77,78] However, this thesis will focus on the use of metallic nanoparticle suspensions.

1.5.3.1 Metallic Nanoparticle Suspensions

Different metals have been analysed for their potential use as enhancing nanoparticles[79,80,81,66] However, colloidal suspensions of silver and gold are predominately utilised as SERS substrates as they can be easily prepared and are relatively stable surfaces allowing target molecules to be effectively adsorbed.[66] Different techniques have been used to roughen the metal surface, original methods utilised electrochemically roughened metal electrodes, however colloidal suspensions[82] and metal films[83] have found to be more accessible and are frequently used. Metallic suspensions have been used to improve the Raman signal with an enhancement factor of up to $10^5 – 10^6$ observed.[84]

In 1982, Lee and Meisel published their work on SERS of dyes using silver and gold colloidal solutions. This outlined the first reported procedure for the preparation of silver and gold colloidal suspensions for SERS analysis.[85] Citrate-reduced silver colloid can be prepared by a modified Lee and Meisel procedure through reduction of a silver salt[86] and gold colloid is produced by the Turkevich method by reduction of $HAuCl_4$ by sodium citrate.[87] Other methods for preparing colloid suspensions can also be used these include hydroxylamine,[88] borohydride[89] and EDTA reduction methods.[90] These silver and gold nanoparticles have an overall negative charge on the surface generated by the formation of either a citrate or an EDTA surface layer.

The optical properties of nanoparticles are observed when an electromagnetic field interacts with metal particles causing surface electrons to move under the influence of the incoming

light, this is known as surface plasmon oscillations. Restorative forces arise from repulsion of the electrons producing collective oscillation of the electrons (Figure 1.20).

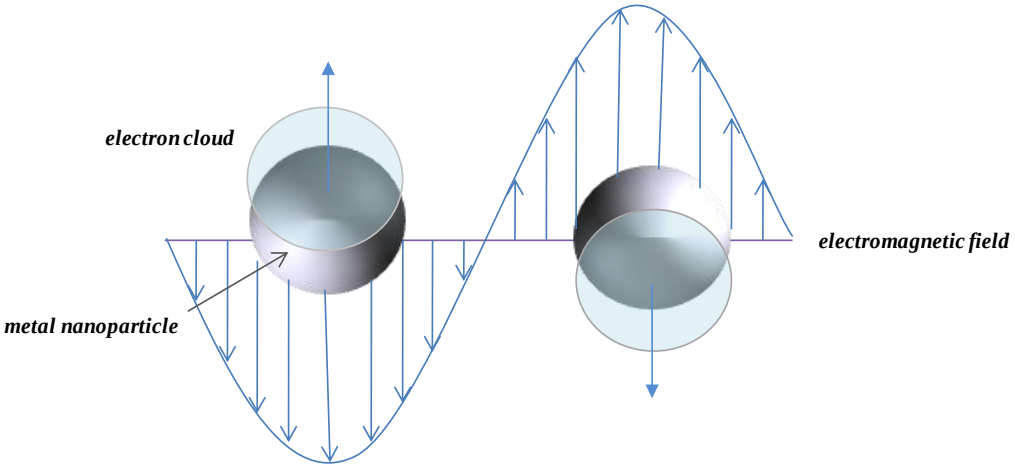

Figure 1.20: Displacement of electrons on metal nanoparticle surface induced by an electromagnetic field.

This process can be characterised by the plasmon resonance band in the extinction spectrum, with the resultant spectrum being strongly dependant on the dielectric environment of the metal and surrounding solution, in addition to the size and shape of the nanoparticles.[91] Theses factors can affect the position of the characteristic plasmon resonance band and influence the Raman signal obtained from the sample. When discrete nanoparticles are forced into close proximity individual nanoparticle plasmons will couple, resulting in the broadening and red-shifting of the longitudinal plasmon. This optical property of nanoparticles has been widely exploited during analysis with many methods utilising the aggregation of gold nanoparticles to detect biomolecular events through the resultant change in colour of the nanoparticle suspension from red to appearing blue to the eye.[92,93,94]

1.5.3.2 Proposed SERS Mechanisms

The SERS effect is believed to be a combination of 2 mechanisms, electromagnetic enhancement and chemical enhancement. The electromagnetic mechanism is thought to be the main enhancement effect and describes the interaction of the surface plasmon with the analyte molecule. When incident light interacts with the surface it causes the localised surface plasmon to oscillate, this will increase the local field experienced by the absorbed molecule causing greater polarisation around the molecule.[95,79] The greatest enhancement occurs when the plasmon frequency is in resonance with the laser excitation radiation and

the plasmon oscillations are perpendicular to the surface. Plasmon on each individual particle will only be in resonance over a small range of wavelengths, therefore in regions where particles or clusters of particles are touching, electrons can couple to adjacent particles allowing a larger range of frequencies in which resonance can occur. These active regions are known as 'hot spots' and form greater electromagnetic fields between the metal particles, giving an increased signal enhancement. The chemical mechanism is believed to contribute a smaller amount to the enhancement factor. It occurs due to bond formation between the molecule and the metal surface. This attachment induces a charge transfer, creating a new state which is in resonance with the laser excitation wavelength. This increases the polarisability of the molecule and in turn increases the scattering effect.[63,96]

Colloidal nanoparticles are synthesised in the form of a monodispersed suspension, which generates a large variation in the size and shape of the nanoparticles. Batch variation can produce inaccurate results, therefore, methods have been developed to reduce this effect. Reproducible signal responses can be obtained by aggregating the nanoparticles into discrete clusters. This is achieved through the partially controlled aggregation of the particles using reagents, such as NaCl, HNO_3 and NaOH.[97] The use of organic aggregating agents such as spermine tetrachloride and poly-l-lysine have been shown to generate strong signal enhancements.[20]

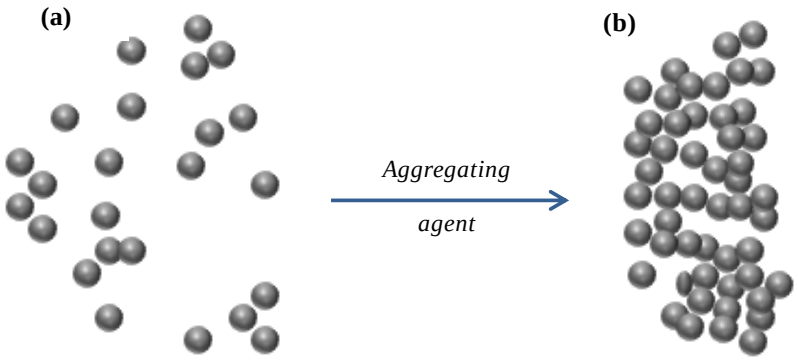

Figure 1.21: Aggregation of silver nanoparticles by addition of an aggregating agent **(a)** dispersed silver nanoparticles, **(b)** aggregated silver nanoparticles.

Aggregated nanoparticles create intense electromagnetic fields at the junctions between the particles. This increases the enhancement of the analyte molecule by shifting the range over which the plasmon resonates causing it to coincide with the laser and potentially the analyte

absorbance frequency.[63] The increased signal enhancement range also allows reproducible results to be obtained from different nanoparticle batches.

SERS has been shown to be an effective detection technique since fluorescence interference can be minimised through the direct adsorption of the analyte molecule onto the metal surface. Fluorescence generated during Raman scattering can be efficiently quenched by the metal allowing low background SERS responses to be obtained. However, the orientation of the molecule may be altered when adsorbed onto the metal surface, resulting in a change in symmetry and selection rules. Consequently, the SERS spectra produced are not always similar to spectra generated by Raman and RRS using the same sample. [7]

1.5.4 Surface Enhanced Resonance Raman Scattering (SERRS)

Further signal enhancement can be obtained through a combination of RRS and SERS, producing a separate synergic technique known as surface enhanced resonance Raman scattering (SERRS). SERRS was first reported in 1983 by Stacy and Van Duyne.[98] The technique incorporates the advantages of surface enhancement with a resonant molecule to achieve significantly improved signal enhancements.[63] SERRS requires a chromophore adsorbed onto a suitable roughened metal surface. The laser excitation frequency is chosen to be close to the absorption maximum of the chromophore. This allows only vibrations which are associated with the chromophore to be enhanced, giving highly increased sensitivity and selectivity.[99] Similarly to SERS, the use of a metal surface will also quench any fluorescence emitted. However, due to the increased sensitivity seen in SERRS, more intense peaks are produced which will also dominate over any residual fluorescence effect.[10]

Both SERS and SERRS, produce sharp spectral bands which allow individual molecular species to be easily discriminated within a mixture. Enabling multiple analytes to be detected, removing the need for separation of the sample into its components.[63] Fluorescence detection can be used for the multiplex analysis of DNA,[100] however, the technique suffers from broad overlapping spectra and photobleaching. Therefore, multiple analyte detection and the potential for low sensitivity have shown to be the main advantages that SERRS has over fluorescence detection.[101,102]

The use of SE(R)RS for the detection of biomolecules has shown to be an effective and sensitive analysis tool,[103] which is ideally suited for the selective and sensitive detection of DNA sequences and has become a widely researched area.[104,105]

1.6 Detection of DNA using SERRS Analysis

SE(R)RS has shown to offer many advantages as a detection technique, namely the ability for low sensitivity and the capability for multiple analyte analysis.[101] Consequently, much research has been carried out into developing SE(R)RS as an effective analytical technique for the quantitative detection of DNA.

1.6.1 Label-Free DNA Detection

The four DNA nucleobases contain aromatic chromophore rings which generate distinctive SERS peaks, therefore DNA detection methods have been exploited for the detection of individual DNA nucleotides.[106,107,16] Single base mismatches within DNA oligonucleotides can be identified through distinctive SERS responses.[108] This was achieved by adsorbing sequences non-specifically through the nucleotide side chains onto the enhancing surface, enabling the DNA to adopt a flat conformation on the metal surface. This ensures all the bases interact sufficiently with the surface providing good Raman signals. Single base mismatches can then be indentified through digitally subtracting the spectra of the target sequence and the mutated sequence. This generates spectra with positive and negative features corresponding to the exchange of a single nucleotide. Successful detection of individual nucleotide changes has been demonstrated in this approach. However, elucidation of the results can be time consuming and non-sequence specific signals are obtained. Therefore, detection assays which utilise specific hybridisation events and changes in surface orientation have been developed.[16] The understanding of DNA adsorption surface chemistry has been aided through use of metal nanoparticles and SERS. Papadopoulou *et al*. have used DNA sequences attached to gold nanoparticles *via* thiol linkers to determine the presence of specific nucleic acid sequences through the orientation of the surface oligonucleotides.[16] Thiolated poly A DNA sequences bound to gold nanoparticles give preferential enhancement of the adenine breathing SERS bands depending on the orientation to the enhancing substrate. Sequences which lie perpendicular to the surface have an increased signal intensity at 736 cm^{-1}, whereas sequences which adopt a flat conformation generate weaker bands. This principle was utilised within a molecular beacon assay to detect the presence of target DNA. The closed beacon was attached to a gold nanoparticle *via* a thiol linker generating weak adenine responses. However, in the presence of target, the hairpin structure opens allowing the adenine ring breathing mode to be enhanced. This method has illustrated the specific detection of unlabelled DNA through selective sequence hybridisation. However, the SERS signals obtained from DNA bases can be relatively weak and may be

obscured when detecting clinical samples within high background media. Therefore, a commonly utilised method which generates sequence specific detection with high intensity signals, rely on the attachment of a SERRS active label.[20]

1.6.2 Fluorophore Labelled DNA Detection by SERRS

SERRS active labels are incorporated into nucleic acids sequences through covalent attachment to the DNA strand, creating a SERRS labelled probe. Quantitative SERRS responses have been obtained through attachment of different commercially available fluorophores to DNA sequences generating low limits of sequence detection.[104] Illustrated in Figure 1.22 are two commonly utilised fluorescent dyes labels; FAM and TAMRA, with both dyes generating distinctively strong SERRS spectra.[20,109]

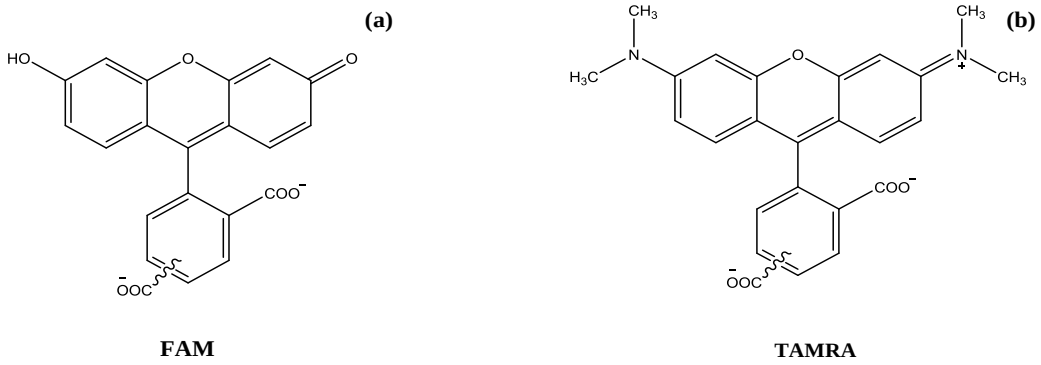

FAM **TAMRA**

Figure 1.22: **(a)** FAM dye label (5-(and 6-)-carboxyfluourescein) and **(b)** TAMRA dye label (5-(and-6)-carboxytetramethylrhodamine)

However, to obtain maximum SERRS responses the fluorophore probes must be adsorbed onto silver or gold nanoparticles. These citrate coated nanoparticles have an overall negative charge through a layer of carboxylate groups which repel the negatively charged DNA phosphate backbone. To overcome this, an aggregating agent is added to promote adsorption of labelled oligonucleotides onto the nanoparticle surface through elimination of repulsive charges. The optimum aggregating agent for SERRS analysis of DNA has been found to be spermine.[110] Spermine is a polyamine which acts as a bridge between the two negatively charged species by interacting with the phosphate groups of the DNA backbone, eliminating repulsion and enhancing SERRS signals.[101]

Commercially available dyes have the potential to generate high intensity SERRS signals, nevertheless, as a consequence of their fluorescent properties simultaneous high background signals may also be generated. The presence of the metal surface aids in the reduction of

these unwanted background signals through quenching fluorescence emitted by the label.[101,110] However, non-fluorescent dyes have also been synthesised to decrease fluorescence interference.

1.6.3 Non-Fluorescent Dyes

Molecular fluorophores have been used which are non-fluorescent due to the reduced constraint in the planar ring system, these include phenolphthalein and malachite green.[111,112] Highly SERRS active dyes have also been specifically synthesised to generate strong SERRS responses with no fluorescent background. These dyes have incorporated benzotriazole moieties which complex directly to the metal surface, forming bonds between the metal nanoparticle and dye.[113] The dyes have shown to be very effective in adsorbing onto metal nanoparticle surfaces by displacing the citrate layer and generating distinct SERRS spectrum through the azo group.[102,114] A commonly used non-fluorescent dye is GM19 (3,5-dimethoxy-4-(6'-azobenzotriazolyl)-phenylamine), the dye contains a benzotriazole (BT) group with three incorporated nitrogen atoms which strongly attach through covalent bonding to the silver nanoparticle surface. This ensures the molecule is fixed in one orientation on the nanoparticle surface during analysis, resulting in increased reproducibility. GM19 also contains an azo dye that acts as a chromophore, generating a highly intense SERS peak at 1370 cm^{-1}. The non-fluorescent dye can be incorporated into the DNA sequence of interest, enabling low background SERRS detection (Figure 1.23).

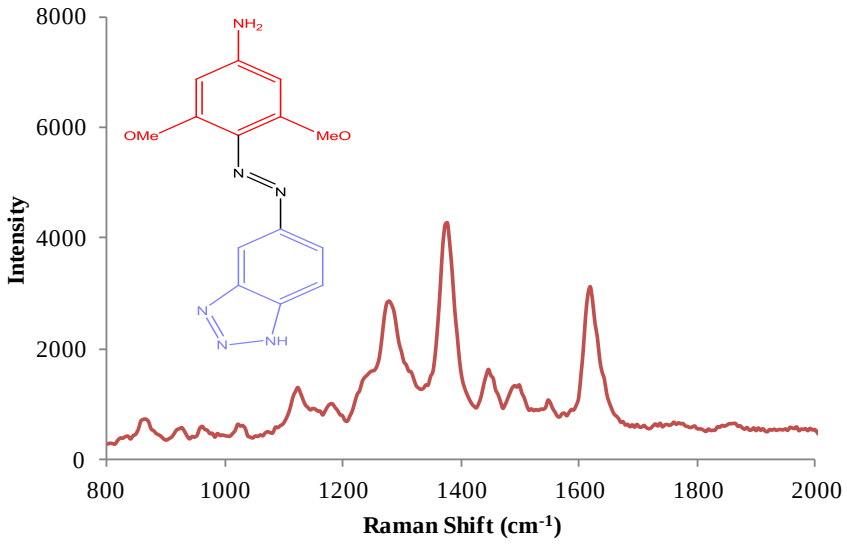

Figure 1.23: SERRS spectrum of GM19 dye using 532 nm laser excitation. Insert contains structure of GM19 3,5-dimethoxy-4-(6'-azobenzotriazolyl)-phenylamine; blue – benzotriazole (BT) group, red – dimethoxyphenylamine chromophore group.

Studies have shown that the use of fluorescent and non-fluorescent labels attached to oligonucleotides can enhance the sensitivity of the detection of biomolecules as well as generating sequence specific information. Consequently, many studies have been carried out using DNA labelled probes for detection by SERRS.[115,104]

1.7 Detection of Labelled DNA using SERRS

Conventional DNA analysis methods have employed fluorescence emission spectroscopy as the detection technique. This market leading technique is a well-established and robust detection analysis method with low limits of detection routinely obtained[116] and single molecule detection achievable.[117,118] However, recent advances in the use of SERRS within the bioanalysis field have demonstrated the potential of this technique in becoming a disruptive technology to fluorescence detection. The distinct advantages SERRS can offer, in terms of successfully detection of multiple labelled oligonucleotides and the potential of surpassing fluorescence detection by three orders of magnitude,[119] demonstrate the promise of developing this analysis method into the principle nanotechnology technique for diagnostic applications.

1.7.1 Quantitative Labelled DNA Detection

SERRS has been shown as a highly sensitive analysis method which has shown successful detection of many different fluorophore probes. Stokes *et al.* have demonstrated the versatility of the technique through detection of numerous dye labelled DNA oligonucleotides using 3 excitation wavelengths and both silver and gold nanoparticle suspensions.[104] This work was further developed through the simultaneous detection of multiple probes within a single sample mixture. SERRS analysis generates strong narrow spectral bands which are ideally suited for the detection of numerous dyes within one sample. Faulds *et al.* used two excitation wavelengths to simultaneously detect five labelled DNA probes within one sample. The distinctive spectra obtained from each dye enabled probes to be distinguished without the need for chemometric analysis.[101] Subsequent progression was achieved by the detection of six different DNA sequences using one excitation wavelength and the aid of multivariate analysis.[109] These initial studies have shown the potential application of SE(R)RS as a diagnostic tool and initiated the use of SE(R)RS as a replacement technique within many standard fluorescence based DNA assays.

1.7.2 SE(R)RS based DNA Assays

Standard PCR assays are frequently used within modern genetic analysis and predominately utilise fluorescence analysis. Graham *et al*. demonstrated the use of SERRS detection for specific genetic sequences through use of labelled primers and PCR.[120] The detection of the cystic fibrosis transmembrane conductance regulator (CFTR) gene was shown using SERRS active primers in an amplification refractory mutation system (ARMS) assay. This assay reported the first SERRS multiplex for DNA genotyping. Three possible variants of the gene can be present, wild type, heterozygote and mutant homozygote. Specially designed primers containing either HEX or rhodamine dyes were used to differentially detect these gene sequences. The primers were incorporated into PCR product and any remaining dye labelled primer was removed through a biotin–streptavidin wash step. SERRS was used to successfully detect each variant *in situ* without sample separation.

Many SE(R)RS DNA assays have also been developed which utilise molecular beacons. This approach uses competitive hybridisation to generate an increase in fluorescent signal in the presence of specific target DNA sequences.[121] In 2007, Vo-Dinh *et al.* reported a plasmonics-based nanoprobe approach using molecular sentinels.[122] The sentinels adopt a hairpin loop conformation, with one end of the stem functionalised with a thiol group, allowing attachment to a silver nanoparticle and the other end functionalised with R6G (carboxyrhodamine 6G) dye. In the closed loop conformation, an intense SERS signal is obtained due to the close proximity of the dye and the silver nanoparticle. However, in the presence of complementary PCR target a reduced SERS signal was observed due to the dye being held distal to the metal surface upon target hybridisation. Subsequent to this study, multiplex detection of molecular sentinels was demonstrated.[123] Two genes associated with *erbB-2* and *ki-67* breast cancer biomarkers were used to design two sentinels labelled with either TAMRA or Cy3 dyes, allowing each sentinel nanoprobe to be distinctly detected. Jung et al. have also utilised molecular beacon probes to detect the azoospermia target gene, DYS 209 within a microfluidic device.[124] Silver nanoparticles were premixed with the beacon probe, generating strong SERS signals through adsorption of the Raman reporter within the beacon to the metal surface. Subsequent addition of complementary target DNA, fixed the beacon loop into the open conformation through specific hybridisation. This event diminished the SERS response, as the dye was moved further from the surface.

SE(R)RS and the specific hybridisation of complementary DNA sequences have also been exploited to determine the presence of target DNA through differing affinities of DNA to

silver and gold nanoparticle surfaces. MacAskill *et al.* developed a homogeneous assay that discriminately detected multiple target sequences through correlation to specific DNA hybridisation events.[125] The assay exploited the principle that single stranded DNA has a stronger affinity to a metal nanoparticle surface than double stranded DNA, consequently generating SERRS spectra with significantly different intensities. Within the assay, the absence of complementary target results in no sequence binding to the single stranded dye labelled probe, producing strong SERRS responses from the probe electrostatically binding to the nanoparticle surface. Whereas, in the presence of target sequence, hybridisation occurs forming double stranded DNA. The dye labelled helix has a lower affinity for the metal surface and the SERRS signal is significantly lowered. Three clinically relevant sequences of methicillin resistant *Staphylococcus aureus* (MRSA) were discriminately detected within a closed tube assay without sequence separation. This study illustrates the potential SERRS has to quantitatively discriminate between single and double stranded DNA with vastly reduced analysis times compared to standard culturing methods, however, this assay has a distinct disadvantage in the fact that it is a negative assay and a decrease in signal intensity is generated in the presence of target DNA. Recent work has investigated a positive homogeneous assay which produces enhanced SERS signals in the presence of target DNA.[126] The assay utilises the different propensities of DNA for silver nanoparticles surfaces using specifically designed SERS primers. Genomic DNA from *Staphylococcus epidermis* (SE) was detected through higher intensity SERS signals obtained when compared to the presence of no target DNA. Increasingly, the surface of metal nanoparticles has been exploited to recognise and detect specific DNA detection with surface arrays being progressively exploited.

1.7.3 Surface Array based SERRS Detection Assays

A wide variety of surfaces have been studied as SE(R)RS detection substrates, including nanoparticles,[127] metal surfaces[128] and membrane surfaces.[129] Conventional DNA assays have been modified to incorporate metal nanoparticles, opening up novel applications within molecular biological development. This work has been significantly progressed since the ability to detect DNA using localised surface plasmon resonance (LSPR) through thiol modified DNA on nanoparticles was demonstrated.[130,131] The surface plasmon of silver and gold nanoparticles lie within the visible wavelength region and have shown to be ideal substrates for SERS analysis. Much research has now focused on the utilisation of DNA functionalised nanoparticles that use specific hybridisation events to promote aggregation and enhance signal output. Cao *et al.* have shown detection of labelled oligonucleotides

using a DNA array format and gold nanoparticles.[51] Gold nanoparticles probes were prepared by labelling with thiolated DNA and Raman-active dyes. These functionalised nanoparticle conjugates were immobilised onto an array surface using a split probe hybridisation system. Captured dye labelled particles could then be detected through facilitation of a silver coating promoting SERS signals from the dye. Six different DNA targets with different Raman reporter molecules were distinguished with a 20 femtomolar limit of detection obtained.

Nanoparticles are often employed as metal surfaces for SERRS analysis and have enabled single molecule detection.[132] This remarkable sensitivity is attributed to signal enhancement produced by the areas of high electric field between aggregated nanoparticles, known as "hotspots". However, the use of colloidal nanoparticles as an enhancing substrate requires dynamic control of this aggregation event to obtain these detection levels. Nanostructured gold surfaces have been developed with plasmon bands tuned to commonly used Raman spectrometer wavelengths.[133] One such substrate which has shown to be an effective solid surface for the detection of DNA is Klarite™. Klarite™ is a gold surface specially engineered to consist of a lattice of inverted square pyramidrial wells, coated with a roughened layer of gold. It is anticipated that the surface will provide a means of sensitive and reproducible detection without the need for aggregation. Stokes *et al.* demonstrated Klarite™ could be used to obtained signal enhancement for the detection of SERRS active DNA from the gold surface.[128]

Membrane surfaces have also shown to be a practical substrate in which DNA can be captured and detected using SERRS. Vo-Dinh *et al.* studied surface-enhanced Raman gene (SERG) probes that had been hybridised to complementary target sequences on a nitrocellulose membrane.[129] After hybridisation probes and DNA fragments were blotted onto a SERS-active substrate for successful generation of SERS peaks. Control samples consisting of non-complementary labelled DNA probes exhibited no SERS responses.

Significant advances have been achieved in the use of SERS detection of DNA over the last 35 years. However, the technique has not been fully exploited and work so far has only scratched the surface this method. Subsequent work will aim to fully unearth this potential and establish SE(R)RS as one of the primary bottom-up nanotechnology techniques for diagnostic and clinical applications.

2. Aims

This thesis exploits surface enhanced Raman scattering (SERS) to detect the presence of specific unmodified oligonucleotides with the ultimate aim of developing more sensitive and selective diagnostic platforms. The main areas of research aimed to:

- Gain a clearer understanding of the adsorption of dye labelled oligonucleotides onto silver nanoparticle surfaces through differences in affinity when altering sequence and dye composition.
- Detect clinically relevant sequences of methicillin resistant *Staphylococcus aureus* (MRSA) within novel SERS detection assays utilising solution and surface based strategies. These were achieved through:

    - Developing a solution based assay by coupling a conventional fluorescence based TaqMan assay with SERS detection.
    - Preparing functionalised silver nanoparticles to develop a surface assay for the detection of unmodified DNA sequences from solid substrate surfaces.

Optimisation of both strategies aimed to development rapid, simple and effective detection methods. The applicability of the SERS techniques was established through obtaining the detection sensitivity and selectivity. Also the detection of multiple dye labelled probes without the need for sample separation was determined, indicating the presence of different target DNA sequences. Further illustration of diagnostic applications was determined through realistic sequence sampling.

3. Experimental

3.1 Preparation of Colloid

3.1.1 Preparation of Silver Citrate-Reduced Colloid

Silver citrate-reduced colloid was prepared *via* a modified Lee and Meisel method.[85] All glassware was soaked in Aqua Regia ($HCl:HNO_3$ 4:1 v/v) for 2-3 hours and rinsed with distilled water. 500 mL of distilled water was heated to 45 ºC with continuous stirring in a round bottom flask and 90 mg silver nitrate was added. Heating continued until 98 ºC then 10 mL of 1 % aqueous solution of sodium citrate was added. The temperature of the solution was maintained at 98 ºC for 90 minutes with continuous stirring throughout. Finally, the solution was left to cool whilst being stirred.

3.1.2 Preparation of Silver EDTA-Reduced Colloid

All glassware was soaked in Aqua Regia ($HCl:HNO_3$ 4:1 v/v) for 2-3 hours and rinsed with distilled water. 2000 mL of distilled water and 94.7 mg of EDTA (ethylenediaminetetraacetic acid) were added to a 3 L beaker and heated. Before boiling, 0.32 g of sodium hydroxide in 20 mL of distilled water was added then brought to the boil. At boiling, 0.088 g of silver nitrate in 20 mL of distilled water was added and the solution was left to boil for 15 minutes. The solution was left to cool to room temperature with continuous stirring.

The quality of the colloid was assessed by UV-visible spectroscopy using a Cary 300 Bio UV-visible spectrophotometer (Varian, USA). The silver citrate reduced colloid had an absorbance maximum of 407 nm and the full width half-height (FWHH) was measured to be 86 nm. The nanoparticles were determined to have a diameter of 39 nm and a concentration of 4.92×10^{-11} mol dm^{-3}. The silver EDTA reduced colloid produced was found to have an absorption maximum of 412 nm and the FWHH was measured to be 77 nm. The nanoparticles were characterised to have a diameter of 46 nm and a concentration of 1.14×10^{-10} mol dm^{-3}.

3.2 Preparation of Buffers

3.2.1 Phosphate Buffered Saline (PBS)

0.3 M phosphate buffered saline (PBS) was composed of 83 mL of phosphate (10 mM, pH 7) and 75 mL of sodium chloride (0.3 M) and made up to 500 mL with distilled water.

3.2.2 Tris-Tween Buffer

Tris-HCl (10 mM), sodium chloride (100 mM) and 0.05% Tween 20 were made up to a volume of 100 mL with distilled water. The pH of the solution was adjusted to pH 7.4 using 1 M NaOH.

3.2.3 Saline Sodium Citrate (SSC) Buffer

Saline sodium citrate (SSC) buffer was prepared in a stock and diluted as required. 20 x SSC was composed of sodium chloride (3 M) and trisodium citrate (300 mM) made up to required volume with distilled water. Buffer was adjusted to pH 7 with sodium hydroxide.

3.2.4 Trisborate EDTA (TBE) Buffer

Trisborate EDTA (TBE) buffer was prepared in a stock solution and diluted as required. 10 x TBE was composed of Tris-HCl (130 mM), boric acid (45 mM) and EDTA (2.5 mM) made up to the required volume with distilled water.

3.3 Instrumental

3.3.1 Surface Enhanced Raman Scattering (SERS)

All SERS analyses in this study were carried out using 1 cm^3 plastic cuvettes, the sample mixture and volumes used are stated within each individual study.

3.3.1.1 514.5 nm Laser Excitation

Two different instruments with laser excitation frequency of 514.5 nm as the source of radiation were used within this study, a Renishaw model 100 probe system with an argon ion laser and a Renishaw InVia Raman Microscope with an argon ion laser. Both lasers (6 mW) were focused onto the sample using a 20x long working distance (LWD) objective lens. Detection was achieved using a charge coupled device (CCD) detector and spectra were

recorded in the range 200 – 2500 cm^{-1}. After analysis all spectra were baseline corrected using GRAMS/AI software.

3.3.1.2 532, 633 and 785 nm Laser Excitations

The surface samples were analysed using a Witec Alpha 300 R confocal microscope (Ulm, Germany) using either 532, 633 or 785 nm laser excitation (~ 500 μW), the grating was centred at 1400 cm^{-1} and either a 5, 10 or 50x objective. Accumulation times of 0.1 and 0.5 seconds were used. The exact instrumental parameters were determined for each experiment and are stated within the results section. Spectra were processed using Witec Project v2.0 software.

3.3.1.3 785 nm Laser Excitation

Large surface sample areas were analysed using a Renishaw InVia Raman Microscope/Leica DMI 5000 M spectrometer (785 nm spot focus) using an acquisition time of 2.54 seconds and a 10x LWD objective lens. The grating was centred at 1100 cm^{-1} with 100 % laser power (13 mW). After analysis all spectra were baseline corrected using GRAMS/AI software.

3.3.1.4 SERS Data Analysis

Experimental data was obtained from the average intensity of the principle peak, as specified with individual SERS experiments. To obtain accurate peak heights, individual spectra were background corrected using GRAMS/AI or Witec Project v2.0 software and the average peak height was calculated from multiple replicates of each sample.

Data was normalised within concentration studies by dividing the average intensity of each concentration by the intensity obtained from the standard. The standard used within the SERS instrumentation was cyclohexane and was determined for individual experiments performed. Error bars for each point were calculated as ± one standard deviation.

3.3.3 Fluorescence Measurements

Fluorescence measurements and thermal cycling were carried out using a Stratagene MX3005P QPCR system (Agilent, UK) using 200 μL plastic PCR tubes (Agilent, UK). Results were analysed using MXPro software.

3.4 DNA Melting Experiments

3.4.1 UV-visible Melt

DNA sequences were diluted to 1 µM in 0.3 M PBS in a volume of 500 µL. The samples were analysed by UV-visible spectroscopy using a Cary 300 Bio UV-visible spectrophotometer (Varian, USA). The absorbance was monitored at 260 nm between 30°C to 90°C at a rate of 1°C/min. The sample was heated and cooled over a period of 6 cycles.

3.4.2 Fluorescent Melt

DNA sequences were diluted to 1 µM in 0.3 M PBS up to a volume of 24 µL and 1 µL of 1/1000th dilution of SYBR Green (Invitrogen) was added. The samples were analysed using a Mx3005P^{TM} Multiplex Quantitative PCR system (Stratagene, UK). The fluorescence of the SYBR Green was monitored using SYBR Green filter set (492 nm ex/516 nm em) between 30°C to 90°C at a rate of 1°C/min. The sample was heated and cooled over a period of 6 cycles.

3.5 DNA Affinity

3.5.1 DNA Hybridisation

All DNA hybridisations were carried out using a Minicycler PTC-150 system (MJ Research, Canada). An aliquot of the oligonucleotide probe and complementary sequence (combined volume of 500 µL, 1 µM) were added to a PCR tube and incubated in 0.3 M PBS. The temperature was raised to 95 °C for 2 minutes and slowly cooled by 1 °C/minute to 25 °C. This was also carried out using single stranded dye labelled probe and single TAMRA dye with no complement sequence present, excess 0.3 M PBS buffer was added to keep concentrations consistent. Dilution series were carried out for each sample by diluting in 0.3 M PBS.

3.5.2 Dye Preparation

The SERS-active TAMRA dye was prepared *via* deprotection of a commercially available 3'-TAMRA CPG column. The column was treated with a deblocking solution (3 % trichloroacetic acid and dichloromethane) to remove the dimethoxytrityl (DMTr) group, leaving an alcohol group. Concentrated ammonium hydroxide solution was then added to the column to cleave the O-succinyl bond.

3.5.3 SERS Analysis

Within the study two experimental methods were compared, the original and optimised experimental conditions. The methods differed in the composition of the analysis mixture, however both used the same SERS conditions.

Original Experimental Conditions: In a disposable cuvette either the single stranded, double stranded DNA or TAMRA dye samples (5 µL, X* µM) were added. To this, an aqueous solution of spermine hydrochloride (20 µL, 0.1 M), PBS buffer solution (220 µL, 0.3 M) and Tris-tween buffer (30 µL, pH 7.4) was added. Finally, the mixture was diluted by addition of silver EDTA reduced colloid (275 µL, pH 11).

Optimised Experimental Conditions: In a disposable cuvette either the single stranded, double stranded DNA or TAMRA dye samples (5 µL, X* µM) were added. To this, an aqueous solution of spermine hydrochloride (20 µL, 0.1 M), PBS buffer solution (100 µL, 1.65 M) and Tris-tween buffer (30 µL, pH 7.4) was added. Finally, the mixture was diluted by addition of silver EDTA reduced colloid (395 µL, pH 12).

** Where X ranges from 0.4 to 0.02 µM*

All samples were thoroughly mixed and the SERS spectra recorded within 1 minute of colloid addition on a Renishaw model 100 probe system with 514.5 nm laser excitation as detailed in Section 3.3.1.1 (1s, 6 mW, 20x obj). The spectra were baseline corrected using Grams/AI software. 5 replicate analyses of 5 replicate samples at each concentration were analysed. The differences between the ssDNA and dsDNA were calculated through subtraction of SERS intensity values at 1650 cm^{-1}. However, the calculation of standard deviation could not be obtained in a similar way.

$$SD_{tot} = \sqrt{(SD_1{}^2 + SD_2{}^2)}$$

Equation 3.1: Error calculation for results obtained from differences. SD = standard deviation

Equation 3.1 was used to accurately calculate the standard deviation error for differences between ssDNA and dsDNA values.

3.5.4 Colloidal pH Optimisation

Experimental optimisation was carried out to determine the optimum pH of EDTA silver colloid to be utilised within the assay. ssDNA and dsDNA were prepared according to section 3.5.1. In a disposable cuvette either the ssDNA or dsDNA (5 µL, 50 nM) were added. To this, an aqueous solution of spermine hydrochloride (20 µL, 0.1 M), PBS buffer solution (220 µL, 0.3 M) and Tris-tween buffer (30 µL, pH 7.4) was added. Finally, the mixture was diluted by addition of silver EDTA reduced colloid (275 µL). Three colloid samples were utilised which had been pH adjusted to 7, 11 and 12 using dilute hydrochloric acid or sodium hydroxide. Samples were thoroughly mixed and the SERS spectra recorded within 1 minute of colloid addition on a Renishaw model 100 probe system with 514.5 nm laser excitation as detailed in Section 3.3.1.1 and 3.5.3 (1s, 6 mW, 20x obj).

3.5.5 Colloidal Volume Optimisation

Experimental optimisation was carried out to determine the optimum volume of EDTA silver colloid to be utilised within the assay. ssDNA and dsDNA were prepared according to section 3.5.1. In a disposable cuvette either the ssDNA or dsDNA (5 µL, 0.4 µM) were added. To this, an aqueous solution of spermine hydrochloride (20 µL, 0.1 M), PBS buffer solution (220 µL, 0.3 M) and Tris-tween buffer (30 µL, pH 7.4) was added. Finally, the mixture was diluted by addition of silver EDTA reduced colloid (pH 12) using 155, 275, 345 and 395 µL. Samples were thoroughly mixed and the SERS spectra recorded within 1 minute of colloid addition on a Renishaw model 100 probe system with 514.5 nm laser excitation as detailed in Section 3.3.1.1and 3.5.3 (1s, 6 mW, 20x obj).

3.5.6 PBS Buffer Optimisation

Experimental optimisation was carried out to determine the optimum volume and concentration of PBS buffer to be utilised within the assay. ssDNA and dsDNA were prepared according to section 3.5.1. In a cuvette either the ssDNA or dsDNA (5 µL, 0.4 – 0.05 µM) were added. To this, an aqueous solution of spermine hydrochloride (20 µL, 0.1 M), PBS buffer (220 µL of 0.3 M or 100 µL of either 0.66 or 1.65 M) and Tris-tween buffer (30 µL, pH 7.4) was added. The mixture was diluted by addition of silver EDTA reduced colloid (pH 12, 345 or 395 µL). Samples were thoroughly mixed and the SERS spectra recorded within 1 minute of colloid addition on a Renishaw model 100 probe system with 514.5 nm laser excitation as detailed in Section 3.3.1.1 and 3.5.3 (1s, 6 mW, 20x obj).

3.6 TaqSERS Assay

3.6.1 TaqSERS PCR

To reduce the risk of contamination, samples were prepared by adding reagents in separate laboratories dedicated to individual reagents. Before preparation, the work surfaces were cleaned using MicroSol 3+ spray (Anachem, UK) to remove any contamination DNA. The template sequence was added within a UV hood (Sigma-Aldrich, UK) which had been decontaminated using UV radiation and MicroSol 3+ spray. Each sterile working cabinet contained its own dedicated pipettes, filter tips and waste tip box and a fresh pair of disposable gloves were used during preparation in each laboratory. The following PCR mixtures were used throughout this study:

Table 3.1: PCR mixture

Reagents	***SYBR Green sample (µL)***	***Non-SYBR Green sample (µL)***	***Notes***
PCR Buffer	2.5	2.5	10x buffer, Novagen or Qiagen
$MgCl_2$	1	1	25 mM solution
dNTP mix	0.4	0.4	1 mM dATP, 1 mM dCTP, 1 mM dGTP, 1 mM dTTP.
Taq Polymerase	0.5	0.5	5 units/µL* in storage buffer, Novagen or Qiagen
SYBR Green	1.5	-	1000x dilution
Primer 1	1	1	10 µM, IDT
Primer 2	1	1	10 µM, IDT
Probe	-	0.7	18 µM, ADT bio
Template	1	1	6 ng/µL
DEPC water	Up to 25	Up to 25	Bioline

* Unit definition: "One unit is defined as the amount of enzyme that will catalyze the incorporation of 10nmol of dNTP into acid-soluble form in 30 minutes at 74 °C in a reaction containing 25 mM TAPS (tris-[hydroxymethyl]-methyl-amino-propane-sulfonic acid, sodium salt), pH 9.3 at 25 °C. 50 mM KCl, 2 mM $MgCl_2$, 1mM β-metacaptoethanol, 0.2 mM dATP, dGTP and dTTP, 0.1 µM [α-^{32}P]dCTP and activated salmon sperm DNA."

Table 3.1 illustrates the PCR mixtures used, with and without SYBR green within the sample mixture. PCR mixture contained either Novataq DNA polymerase with Novagen PCR buffer (Merck, Germany) or Hot®Star polymerase with corresponding Qiagen PCR buffer (Qiagen, Germany), the enzyme and buffer used is stated within each study. Both enzymes and buffers were supplied at equal concentrations and equal volumes were added.

Sequence of primers and probe used:

Methicillin-resistant *Staphylococcus aureus* (MRSA)

***Forward primer*:** 5'- CAT TGA TCG CAA CGT TCA ATT T – 3'
***Reverse primer*:** 5' – TGG TCT TTC TGC ATT CCT GGA - 3'
Probe Sequence: 5' –Biotin-TGG AAG TTA GAT TGG GAT CAT AGC GTC AT –HEG-10A–TAMRA- 3'

Staphylococcus aureus (SA)

***Forward primer*:** 5'- TGC CTT TAC AGA TAG CAT GCC A – 3'
***Reverse primer*:** 5' – AGT AAG TAA GCA AGC TGC AAT GAC C - 3'
Probe Sequence: 5' –Biotin-TCA TTT CAC GCA AAC TGT TGG CCA CTA TG –HEG-10A-FAM 3'

A bacterial strain of *Staphylococcus aureus* (NCTC 8325) used in the study were obtained from the national health protection agency culture collections (HPACC Salisbury, UK) and cultured in sterile Tryptone Soy Broth (Oxoid). The cells were centrifuged at 16.110 *g* for 10 min at 4 °C; the supernatant was then removed, and 1 mL of Lysostaphin was added. The suspension was incubated for 30 min at 37 °C to lyse the cells. DNA was extracted from the lysate using a QIAamp DNA minikit (Qiagen, Crawley, UK).

PCR was carried out using a Mx3005P^{TM} Multiplex Quantitative PCR system (Stratagene, USA) over 25 amplification cycles using the following parameters:

Cycling conditions:

1 cycle	95 °C for 10 minutes
25 cycles	94 °C for 30 seconds, 60 °C for 1 minute, 72 °C for 1 minute
1 cycle	72 °C for 5 minutes

3.6.2 Bead Separation and Preparation

After TaqSERS PCR was carried out, any biotinylated probe present within the sample was removed with streptavidin coated paramagnetic beads (New England Biolabs, UK). In order to ensure the maximum amount of biotinylated probe would be removed, a 3 times excess of beads to DNA was used. The binding capacity of beads is 500 pmol mg^{-1} for biotinylated

oligonucleotide, therefore 1 mL of beads will bind to 2 nmol of biotinylated DNA. It was calculated that 25 µL of PCR product contained 12.5 pmol of TaqSERS probe, thus would require 6.25 µL of beads for a 1:1 binding and 19 µL for a 3 times excess. The binding capacity was also greater than this due to each bead containing 4 probe binding sites.

The required volume of beads (19 µL multiplied by the number of PCR reactions to be assayed) were aliquoted into a sterile 1.5 mL tube and placed into a magnetic separation rack for ~2 minutes until all the beads had migrated towards the magnet leaving a clear supernatant. The supernatant was removed and discarded leaving only the beads in the tube. The tube was removed from the rack and the beads were resuspended with 2 volumes of 2 x binding buffer (20 mM Tris, 300 mM NaCl and 5 mM $MgCl_2$). The tube was returned to the separation rack for ~2 minutes and the supernatant was removed again. This washing process was repeated a further 2 times before resuspending the beads in binding buffer to the starting volume.

3.6.3 Sample Separation

19 µL of the bead solution, prepared in section 3.6.2, was then transferred into an empty sample tube and placed in the magnetic separation rack for 2 minutes before removing the supernatant. 25 µL of PCR product was added to each aliquot of beads and left for 30 minutes at room temperature with gentle mixing to allow binding of the biotinylated probe to the streptavidin beads. After 30 minutes, the tubes were placed in a magnetic rack and left for ~2 minutes, 25 µL of supernatant was then removed and placed in new sterile tubes to be used for subsequent SERS analysis.

3.6.4 SERS Analysis

The samples analysed by SERS were a DNA assay positive (target template) and negative control (non-complementary template sequence). To each cuvette 5 µL of PCR product, 5 µL of spermine (0.1 M), 125 µL of distilled water and 250 µL of silver citrate-reduced nanoparticles were added. All samples were thoroughly mixed and the SERS spectra recorded within 1 minute of colloid addition on a Renishaw InVia Raman Microscope with 514.5 nm laser excitation as detailed in Section 3.3.1.1 (1s, 6 mW, 20x obj). 5 replicate analyses of 4 replicate samples were analysed and data processing was carried out as detailed in Section 3.3.1.4.

3.6.5 Enzymatic Digestion of the TaqSERS Probe

To determine the ability of the Taq polymerase enzyme (Qiagen) to digest the TaqSERS probe, a digestion experiment was performed. This study contained no template sequences and no PCR was performed. Samples were prepared incorporating the TAMRA labelled *mecA* probe (0.7 μL, 18 μM), Taq polymerase enzyme (0.5 μL) and Qiagen PCR buffer (23.8 μL). A negative control was also prepared which contained no enzyme and 24.3 μL of buffer. Samples were activated through heating for 10 minutes at 95 °C and then heating at 60 °C for 2 hours, which was the optimal temperature for the enzyme activity and the approximate time taken to carry out the full TaqSERS PCR reaction. After heating, both samples were washed with three times excess of streptavidin coated magnetic beads, before removing the supernatant for SERS analysis (Section 3.3.1.1).

3.6.6 Multiplex TaqSERS PCR

TaqSERS PCR was performed incorporating both the TAMRA labelled *mecA* probe (18 μM, 0.35 μL) and FAM labelled *femA-SA* probe (18 μM, 0.35 μL) within the same mixture. Three separate samples which had different template sequences; MRSA, SA and a nonsense control sequence were performed. To enable sample distinction principle component analysis (PCA) was performed on the SERS analysis data. The data was initially baseline corrected using asymmetric least squares algorithm, the data was then scaled and finally smoothed. Two principle components were calculated from the data sets and plotted to generate the largest possible variance between each sample.

3.6.7 Capillary Gel Electrophoresis

Capillary electrophoresis of the PCR products was carried out using an Agilent 2100 Bioanalyzer (Agilent, Germany) and the DNA 1000 reagent kit. Specially designed DNA chips were used for the separation of nucleic acid fragments based on their size. The chips contained an interconnected set of microchannels which were filled with a mixture containing agarose gel and an intercalating DNA dye. 1 μL of PCR product was added to each well containing the gel/dye mixture. 1 μL of a DNA ladder was also added to a designated well to enable accurate sizing of the DNA fragments. The gel was placed in the Agilent 2100 Bioanalyzer and run within 5 minutes of preparation. DNA within the size

range of 25 – 1000 bases can be analysed, this study investigated DNA sequences containing 104 bases.

3.7 DNA Detection Surface Array

DNA sequence of target and probe used:

Probe	TAMRA ITC - GGTTCATATAGTTATAATAA
Conjugate sequence	Thioctic Acid- $(HEG)_3$ – GGTTCATATAGTTATAATAA
Target	TTATTATAACTATATGAACC
Nonsense	CAATGTGAAAGGCTGGTTA
MRSA Conjugate Sequence	Thioctic Acid- $(HEG)_3$- TTGAAGTTAGATTGGGATCATAGCGTCAT
MRSA Target	ATGACGCTATGATCCCAATCTAACCTTCCA

3.7.1 Preparation of Conjugates

5’ thiolated oligonucleotides were conjugated to silver nanoparticles. The thiol-modified oligonucleotides were prepared in a solution of water to a concentration of 20 nM. The DNA was added to 500 µL of colloidal silver nanoparticles and the samples were incubated overnight at room temperature. The addition of 60 mM of pH 7 phosphate buffer gave a final concentration of 10 mM phosphate. Following 24 hours at room temperature, the salt concentration was brought up to 0.1 M by successive addition of NaCl over 48 hours. The nanoparticle conjugates were centrifuged at 5000 rpm for 20 minutes and resuspended in 0.3 M PBS. The DNA conjugates were then added to 500 µL of 1 µM solution of the chosen SERS active label molecule. This study utilised 5-(and-6)-carboxytetramethylrhodamine isothiocynate (TAMRA ITC), 3,5-dimethoxy-4-(6’-azobenzotriazoyl)-phenylamine (GM19) and mercaptopyridine (MPY). The oligonucleotide nanoparticle conjugates were incubated for 5 hours in the dark, and then centrifuged and resuspended in 0.3 M PBS.

The concentration of the nanoparticle conjugates was calculating using the Beer-Lambert Law.

$$A = \varepsilon l c$$

Equation 3.2: Beer-Lambert equation

The molar absorptivity (ε) of the nanoparticles was determined to be 2.87 x 10^{10} mol dm^{-3}, the pathlength (l) was 1 cm^3 and the absorbance (A) was deduced by UV-visible analysis. UV-visible spectroscopy was carried out using a Cary 300 Bio UV-visible spectrophotometer (Varian, USA). The conjugate sample (50 µL) was diluted in 0.3 M PBS (450 µL) and the absorbance was monitored from 200 – 800 nm. The absorbance maximum between 404 – 412 nm was used within the calculation.

3.7.2 Surface Hybridisation Procedure

3.7.2.1 Target DNA spotting

A 20 µM solution containing target DNA in Nexterion LE buffer (Schott, Germany) was prepared and 0.2 µL of the DNA solution was spotted onto the analysing solid surface. In this study three surfaces were compared, epoxysilane coated glass (Schott), nylon (Whatman) and nitrocellulose (Grace Bio-Labs). The sample slide was placed in a humidity chamber for 30 minutes and then baked at 80 °C for 60 minutes.

3.7.2.2 Surface Washing

The surface was washed to remove any unbound DNA. 100 µL of 0.1 % Tween 20 solution was added to each sample area for 5 minutes and then removed. 1 mM HCl solution was added for 2 minutes (twice) followed by 100 mM of KCl solution for 10 minutes. Finally, the surface was rinsed 3 times with distilled water. The slide was dried with nitrogen.

3.7.2.3 Surface Blocking

The surface was blocked using either Nexterion® Block E (Nexterion, UK) or sheared salmon testes DNA (Sigma-Aldrich, UK) to block any sites which had not already been blocked by the target DNA. Nexterion® Block E was activated *via* addition of dilute hydrochloric acid. 100 µL of either blocking buffer was then added to each sample, covered and placed in an oven at 50 °C for 1 or 2 hour with gently shaking. Exact experimental blocking times are stated within each study. The surface was then rinsed with water.

3.7.2.4 Hybridisation

25 µL of dye labelled DNA conjugates or DNA probe were added to 25 µL of 0.3 M PBS buffer or warm PerfectHyb solution (Sigma-Aldrich, UK) and applied to each sample area. The slide was incubated in a hybridisation oven with gently shaking. Various hybridisation

times and temperatures were investigated and the utilised times are given within each experiment.

3.7.2.5 Post Hybridisation Washing

The hybridisation solution was removed and the surface was rinsed with wash buffers; 100 µL of 0.1 % Tween 20 and 2x SSC buffer for 5 minutes (twice), 0.2x SSC for 5 minutes (twice) and then distilled water for 10 minutes, with gentle shaking. The wash solutions were removed and the slide dried with nitrogen.

3.7.2.6 SERS Analysis

Sample areas were mapped using a Witec Alpha 300 R confocal microscope (Ulm, Germany) using either 532, 633 or 785 nm laser excitation dependent upon the SERS active dye being analysed (Section 3.3.1.2). Accumulation times and instrumental parameters were determined for each dye labelled nanoparticle and are stated for each experiment within Section 6. The total area for each sample square was approximately 6 x 6 mm, therefore to obtain an accurate overview of the entire region a minimum of four SERS maps were obtained. These maps were approximately 100 x 100 µm and contained on average 500 spectra. The spectra obtained from each sample area were plotted by calculating the average of spectrum for each individual mapped region and plotting the average of the total number of maps. False colour SERS map images of the chosen dye peak on the substrate were collected using a 2 µm resolution. Data was processed using Witec Project v2.0 software.

3.7.3 Gel Electrophoresis

Functionalised nanoparticles were run on a 1% w/v agarose gel (1g of agarose in 100 mL of TBE buffer.) The gel was poured into a mould, protected from light and allowed to set. Once set, the gel was placed within an insulated chamber and filled with 1 x TBE buffer until the gel was just covered. To each, 10 µL of functionalised nanoparticles, 1/10th volume of tricolour loading buffer (Bioline) was added and mixed thoroughly. The gel was run at 160 V for an hour.

3.7.4 Detection Limits of Functionalised Nanoparticle Conjugates

The detection limits of DNA functionalised silver nanoparticles were determined from a nitrocellulose membrane. TAMRA ITC, GM19 and MPY conjugates were prepared (section 3.7.1) and a dilution series was prepared *via* addition of increasing volumes of 0.3 M PBS.

0.2 μL of a range of concentrations of each batch of conjugate were spotted onto a nitrocellulose membrane. The concentration samples were analysed using a Witec Alpha 300 R confocal microscope (section 3.3.1.2) using TAMRA ITC 1650 cm^{-1}peak (532 nm, 0.1s,10x), GM19 1370 cm^{-1}peak (633 nm, 0.1s,10x) and MPY 1095 cm^{-1}peak (785 nm, 0.5s,10x). Spectra were processed using Witec Project v2.0 software.

3.7.5 Three Dimensional Mapping of Nitrocellulose Membrane

A 3D image volume image of a sample area within a nitrocellulose membrane was generated through gathering multiple SERS maps at different depths through the target region. Individual SERS maps were stacked to generate a volume image of the cross section of the membrane. The approximate depth of the nitrocellulose membrane is 10 – 14 μm, therefore depth analysis was carried out by scanning 10 membrane layers at 1 μm intervals. Individual maps were produced using 785 nm laser excitation, 0.5 sec accumulation time, 10x objective and 2 μm resolution. The scans were then complied into a volume image through use of Image J software.

3.7.6 Large Mapping Analysis

To analyse the full area of each sample square, a Renishaw InVia Raman Microscope/Leica DMI 5000 M spectrometer with 785 nm laser excitation and 0.5 second accumulation times were used as detailed in Section 3.3.1.3. These maps enabled a representation of the sample square to be generated through accumulative white light images of the membrane. This instrument utilised a streamline mapping system to rapidly map analysis the full 6 x 6 mm sample area through cumulative image capture. The full sample area could then be mapped using SERS. This study utilised the MPY labelled DNA nanoparticle by applying them to the membrane surface *via* cotton wool swabbing in a cross shape.

4. DNA Detection via Differences in Surface Affinity for Silver Nanoparticles

The increasing need for sensitive and rapid DNA detection methods is continually driving molecular diagnostics research. Current DNA detection protocols utilise the specific hybridisation of labelled single stranded probes to selectively bind to a complementary target sequence corresponding to a chosen genetic infection or disease. One such approach utilises the differences in affinity between single stranded DNA (ssDNA) and double stranded DNA (dsDNA) towards silver or gold nanoparticle surfaces.[125,134] This method can be exploited to confirm the presence of target oligonucleotides within a sample.

Li and Rothberg have shown by colorimetric detection that ssDNA and dsDNA can be discriminated by their differences in propensities to adsorb onto gold nanoparticles.[134] This work has been further developed through designing molecular diagnostic assays which combine SERS detection with the differences in the electrostatic properties of DNA.[135,136] These diagnostic platforms are promising tools for the specific and rapid detection of DNA related to diseases. MacAskill *et al.* developed a homogeneous assay that discriminately detects multiple target sequences *via* correlation to specific DNA hybridisation events.[125] The assay exploited the principle that ssDNA has a stronger affinity to a metal nanoparticle surface than dsDNA, consequently generating SERRS spectra with significantly different intensities. The single stranded probe produced stronger SERRS responses due to electrostatic binding to the nanoparticle surface, whereas, double stranded DNA generated SERRS signals that were significantly lower. This study illustrates the potential SERRS has to quantitatively discriminate between single and double stranded DNA, however, one major drawback of this assay is the generation of decreased signal intensities in the presence of target DNA. Recent work has overcome this by developing a homogeneous assay which produces enhanced SERS signals in the presence of target DNA, through the incorporation of specially designed SERS active primers.[135] These primers contain a dye labelled segment which was rendered single stranded upon hybridisation to the target sequence. This single stranded region has a higher affinity for the metal surface, resulting in increased SERS responses in the presence of target DNA.

The DNA affinity methodology offers many advantages including high reproducibility, specific detection, simple application and has demonstrated the potential of SE(R)RS to

quantitatively discriminate between single and double stranded DNA. However, with current methods, the discrimination between ssDNA and dsDNA is often not large, therefore reliable conclusions may not be drawn. This also influences the concentration range over which the method is applicable and it is often limited as a result of reduced discrimination between ssDNA and dsDNA at lower concentrations. Therefore, a study was carried out to gain a clearer understanding of DNA surface adsorption and obtain results with greater confidence.

4.1 DNA Analysis of Single and Double Stranded DNA Sequences using SERS

Through the application of SERS, the differences in affinity of dye labelled ssDNA, dsDNA and an unattached dye label adsorbed onto silver nanoparticles were investigated, to determine the effect that this has on the resulting SERS signal. Sequences used in this section are shown in Table 4.1.

Table 4.1: DNA sequences and modifications

Name	*Sequence (5'- 3')*	*5' Modification*
T20 probe	GGT TCA TAT AGT TAT AAT AA	TAMRA
T20 complement	TTA TTA TAA CTA TAT GAA CC	-

The nucleobases within DNA contain aromatic chromophore rings which generate distinctive SERS peaks. This observation has been exploited within DNA detection methods for the identification of individual DNA nucleotides and the determination of single base mismatches.[106,108] However, the SERS signals obtained from DNA bases can be relatively weak and may be obscured when detecting samples within high background signals. Therefore, a commonly utilised method which generates sequence specific detection with high intensity signals, relies on the attachment a SERRS active label.[20] In this study, both the single and double stranded probe contained a 5' covalently attached 5-(and-6)-carboxytetramethylrhodamine (TAMRA) dye (Figure 4.1), to obtain clear and distinctive SERS signals.

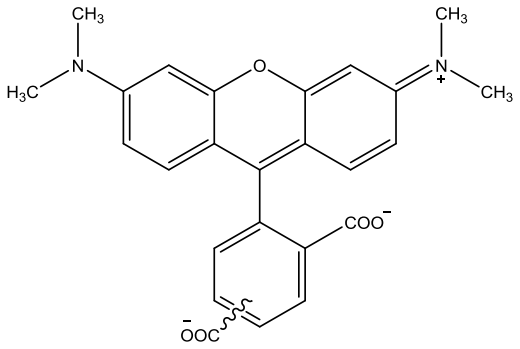

Figure 4.1: Structure of TAMRA dye.

TAMRA is a fluorescent dye molecule containing a chromophore with an excitation maximum at 565 nm and emission maximum at 580 nm. SERS analysis was performed by incorporating the TAMRA dye into the DNA sequences at the 5' position. The dye alone, with no sequence attached was also investigated to determine its role in surface adsorption. The T20 probe containing a 20 % content of guanine and cytosine bases was used to evaluate the differences between the electrostatic interaction of DNA sequences and the dye. The DNA samples were prepared by mixing either the exact complementary sequence or excess buffer with the T20 probe and hybridising in 0.3 M phosphate buffered saline (PBS), resulting in distinct samples; TAMRA labelled ssDNA (T20 probe) and TAMRA labelled dsDNA (T20 probe and T20 comp) samples. The single SERS-active TAMRA dye was prepared *via* deprotection of a commercially available 3'-TAMRA CPG column (section 3.5.1 and 3.5.2).

Double stranded DNA denatures by increasing the temperature, resulting in the transition of double to single stranded DNA sequences. This can be monitored by inspection of UV-visible absorbance at 260 nm, as a result of π interactions in the benzene rings. When double stranded, the rings stack face-to-face causing a decrease in absorption at 260 nm due to the shielding of the bases. However, when these strands denature at higher temperatures, the bases in the single strands become exposed generating an increased absorption at 260 nm. The melting curves for both ssDNA and dsDNA samples are shown in Figure 4.2. The melts were carried out to determine whether successful hybridisation of the ssDNA probe to its complementary target sequence had occurred within the dsDNA sample, while the ssDNA probe remained unhybridised as expected.

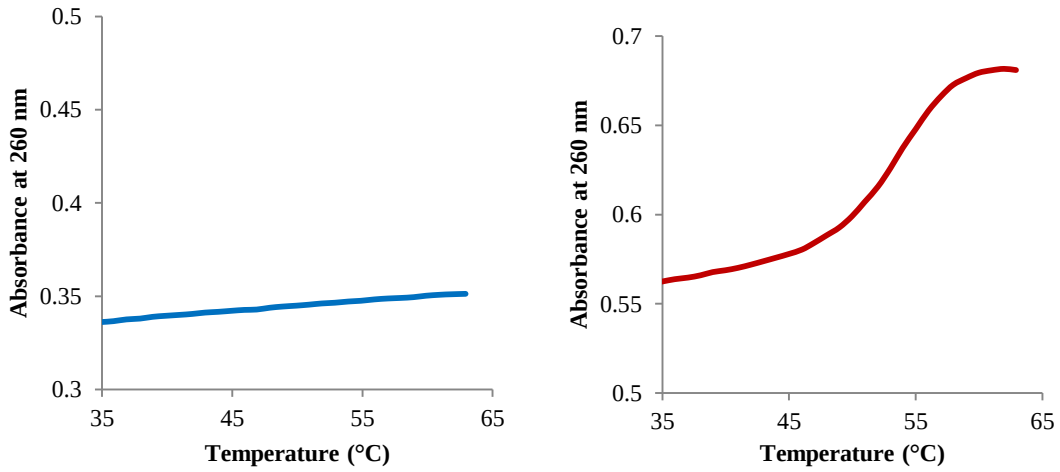

Figure 4.2: UV melting curves obtained by monitoring the absorbance at 260 nm in 0.3 M PBS; blue: ssDNA and red: dsDNA (DNA concentration 1 µM).

The dsDNA melt shows a point of inflection in the sigmoidal profile, this defines the melting temperature (T_M) and is representative of the thermal stability of the duplex. This indicates that at temperatures below 53 °C, the double stranded probe has successfully formed. As expected no sigmoidal curve and therefore, no hybridisation was obtained from the ssDNA sample.

SERS analysis was performed through addition of dye labelled DNA or single dye (0.4 µM) to a cuvette and then mixed with 0.1 M spermine, 0.3 M PBS buffer, tris-tween buffer and 1.14 x 10^{-10} M silver EDTA reduced nanoparticles (46 nm). EDTA-reduced silver nanoparticles were used as previous studies have reported that whilst citrate-reduced silver colloid gives greater SERS signal intensities, larger discrimination between samples is obtained using a silver EDTA colloidal suspension.[125] The silver nanoparticles were prepared through reduction of the corresponding metal salt forming a negatively charged EDTA layer on the nanoparticle surface. The negatively charged DNA backbone will be electrostatically repelled from the metal surface layer, preventing adsorption and eliminating the possibility of obtaining significant SERS responses. The reduction of charge repulsion can be efficiently achieved through use of an excess volume of spermine added into the sample mixture (Figure 4.3). Studies have shown that spermine serves a dual purpose of inducing maximum surface adsorption of oligonucleotides whilst also aggregating the nanoparticles.[99] The amine group strongly interacts with polyanionic backbone, effectively neutralising the charge and bridging between the two negatively charged species. This successfully promotes DNA adsorption onto the metal surface.

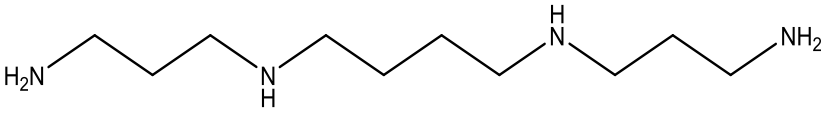

Figure 4.3: Structure of spermine.

The SERS samples for TAMRA labelled ssDNA, dsDNA and TAMRA dye were then analysed using 514.5 nm laser excitation, recording the SERS spectra within 1 minute of colloid addition. 5 replicate samples were analysed and Figure 4.4 shows the average spectra obtained from the SERS analysis.

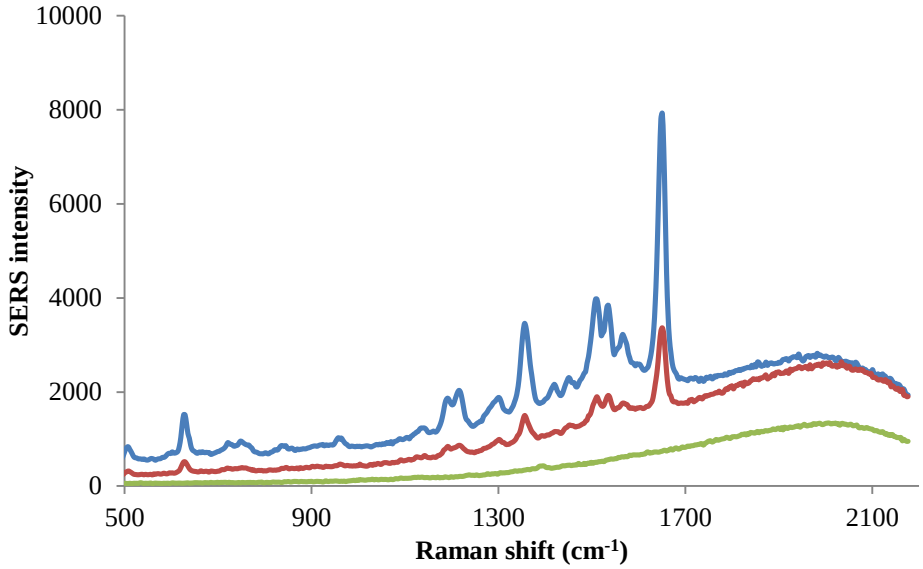

Figure 4.4: SERS spectra of TAMRA labelled DNA and single dye (final concentration 3.6 nM) obtained using 514.5 nm laser excitation (1s, 6 mW, 20x obj); blue: single stranded TAMRA labelled probe (T20), red: double stranded TAMRA labelled probe (T20+complement), green: TAMRA dye label.

Distinctive TAMRA SERS peaks were obtained from both the ssDNA and dsDNA with no differences in peak position observed. However, dsDNA samples gave a significantly lower signal intensity compared to ssDNA. This indicates that through differences in structure and electrostatic properties, ssDNA has a higher affinity for the silver surface than dsDNA. These differences can be attributed to the rigid helical structure which encapsulates the bases preventing electrostatic surface adsorption and complete coordination to the metal. Therefore, a lower SERS signal intensity is obtained. On the other hand, the flexibility of ssDNA permits uncoiling of strands enabling an increased number of the constituent bases to

be exposed. This enhances the attraction of the DNA strands onto the nanoparticle surface and generates a higher SERS signal intensity.

The TAMRA dye produced a broad fluorescent curve with no SERS peaks, this suggests that any charge on the TAMRA dye is not sufficient to facilitate surface absorbance. SERS enhancement drops off rapidly with distance to the metal surface with more than 90 % of scattering resulting from the first layer of adsorbed analyte.[95,137] Beyond the SERS enhancement distance, the quenching effect from the metal nanoparticle surface is diminished, enabling fluorescence emission to occur. Therefore, the single TAMRA dye was not held close enough to the metal nanoparticle to be identified by SERS. Within the final reaction mixture, the pH of the solution was determined to be pH 8.3. Under these experimental conditions the overall charge on the TAMRA dye molecule will be neutral. Therefore, these results show that the surface attraction is driven by attachment of nucleotides and not the TAMRA dye.

The results obtained in this section have shown that under these conditions, the electrostatic adsorption of DNA onto EDTA reduced silver nanoparticles is driven through constituent base groups and that more sensitive SERS detection will be obtained through detection of TAMRA labelled DNA rather than released free dye. Previous studies have used this DNA discrimination principle to evaluate the presence of target DNA through discrimination of ssDNA and dsDNA.[125,135] However, in these assays substantial differences between ssDNA and dsDNA at lower concentrations cannot be obtained to clearly establish the presence of target DNA. Consequently, as a result of smaller discriminations, the concentration range over which sequence differences can be observed is limited. Therefore, a subsequent study was carried out to investigate optimisation of the DNA affinity method to increase the discrimination between ssDNA and dsDNA and thus, the sensitivity range of the assay.

4.2 Method Optimisation

Various parameters of the experimental method were investigated to determine the optimal SERS detection conditions that gave the maximum increase in the discrimination between ssDNA and dsDNA sequence SERS intensities. Prior SERS experimental conditions were employed from a previously established DNA discrimination assay to provide a basis for optimisation.[125] The SERS conditions used previously and the order of addition are shown in Table 4.2.

Table 4.2: Initial SERS experimental conditions used

Order of Addition	*Sample Added*	*Volume (µL)*	*Concentration (M)*
1	ssDNA/dsDNA sample	5	0.4 to 0.02 x 10^{-6}
2	Spermine	20	0.1
3	PBS buffer	220	0.3
4	Tris-tween buffer	30	10 x 10^{-3}
5	EDTA-reduced silver colloid	275	1.4 x 10^{-10}

The colloidal nanoparticles play a primary role within the DNA discrimination assay that fundamentally impacts on the SERS intensities obtained for the DNA sequences. Therefore, this parameter was initially investigated.

4.2.1 Colloid Optimisation

Silver EDTA-reduced nanoparticles were used within this study as larger signal differences between ssDNA and dsDNA had previously been obtained compared to other colloid suspensions.[125] It was very important to ensure that the experimental conditions were favourable, ensuring the greatest signal discriminations could be obtained. Consequently, the pH and volume of colloid used were studied.

4.2.1.1 Colloidal pH

The pH of the colloidal suspensions of silver nanoparticles can have a large impact on DNA adsorption. Varying the pH of the reaction mixture can alter the electrostatic interactions of the DNA strand onto the roughened metal surface. Consequently, to determine the favourable pH of the solution, three samples of silver EDTA-reduced colloid were pH adjusted to either 7, 11 or 12, generating overall pH values in the final sample mixture of 6.8, 7.4 and 8.3 respectively. To determine whether the pH of the colloidal suspensions would affect the SERS responses, ssDNA and dsDNA with a final concentration of 0.45 nM, were added to colloidal suspensions with three different pH values and analysed by SERS. The average intensity of the principle peak at 1650 cm^{-1} was calculated from 5 replicates samples and used to determine the difference in intensity between single stranded and double stranded oligonucleotides for each pH adjusted colloidal sample. The difference between the SERS intensity of ssDNA and dsDNA for each pH are plotted in Figure 4.5. The differences between the ssDNA and dsDNA were calculated through subtraction of SERS intensity values at 1650 cm^{-1}. However, the calculation of standard deviation could not be obtained in

a similar way. Instead, to obtain the error within the results the standard deviation values for each sample were squared, added together and the square root of the sum was calculated (Section 3.5.3, equation 3.1). This calculation ensured accurate standard deviation values were obtained and was used throughout this study to calculate error bar values when differences between ssDNA and dsDNA values were calculated.

The increase in pH was shown to have a significant effect on the SERS responses with the largest discrimination between ssDNA and dsDNA being obtained when the sample reaction mixture had a pH of 8.3. Increasing the pH of the EDTA colloid generates a subsequent increase in the difference in signal intensity between DNA sequences. This is thought to be as a result of an increased charge density on the EDTA nanoparticle surface arising from the ionisable surface capping layer providing increased surface attraction at higher pH.

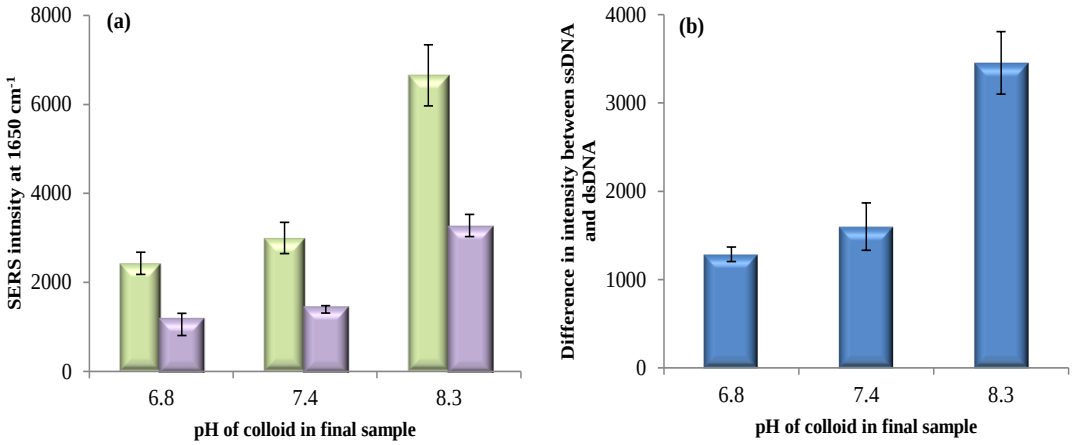

Figure 4.5: (a) SERS intensity of ssDNA (green) and dsDNA (purple) at 1650 cm^{-1} and **(b)** difference in SERS intensity between ssDNA and dsDNA of the 1650 cm^{-1} peak (DNA concentration 0.45 nM) using silver EDTA colloid generating final sample pH of 6.8, 7.4 and 8.3 obtained using 514.5 nm laser excitation (1s, 6 mW, 20x obj). Error bars represent one standard deviation for 5 x 5 replicate samples.

4.2.1.2 Volume of Colloid

The maximum adsorption of DNA strands onto the nanoparticle surface during analysis is essential to ensure optimum SERS responses. Thus, the volume of silver EDTA nanoparticles used within each SERS analysis sample was examined to determine whether altering the available nanoparticle surface area would have an effect on DNA strand discrimination. Theoretically, a large excess of nanoparticles within the reaction mixture would consequently generate a greater metal surface area accessible to the DNA strands.

Therefore, the majority of ssDNA sequences could adsorb onto the surface, giving maximum SERS signal intensities. Whereas, even with an excess of surface area the same concentration of dsDNA would give a markedly lower signal intensity due to the charge screening effect from enclosing of the bases. This theory was tested through analysis of four volumes of silver EDTA-reduced colloid; 155 µL, 275 µL, 345 µL and 395 µL. The previously published assay used a colloid volume of 275 µL (Table 4.2). Therefore, volumes below and above this value were chosen to gain an understanding of the effect of nanoparticle volume on DNA adsorption. To keep the total sample volume at 550 µL (see Table 4.2 for sample volumes and concentrations of other components) and ensure the concentration of DNA remained constant, the volume of PBS buffer was increased and decreased appropriately as the nanoparticle volume varied.

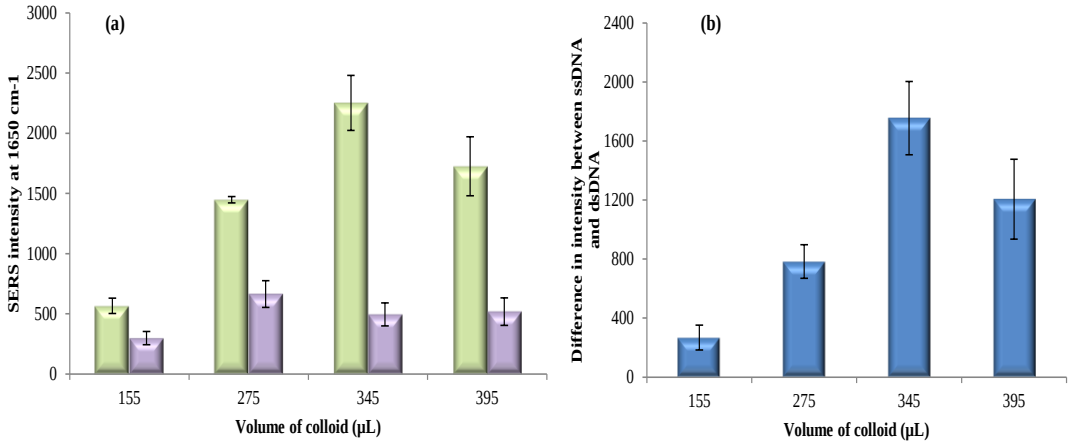

Figure 4.6: (a) SERS intensity of ssDNA (green) and dsDNA (purple) at 1650 cm^{-1} and **(b)** difference in SERS intensity between ssDNA and dsDNA of the 1650 cm^{-1} peak (final DNA concentration 3.64 nM) using different volumes of EDTA silver colloid obtained using 514.5 nm laser excitation (1s, 6 mW, 20x obj). Error bars represent one standard deviation for 5 x 5 replicate samples.

Results previously obtained in Figure 4.5, demonstrate that using colloid with a pH of 12 (pH 8.3 within final assay) gave the largest intensity differences, thus, this colloid was employed to evaluate the effect of colloid volume. Figure 4.6 illustrates that increasing the nanoparticle volume up to 345 µL generates an increase in the difference in intensity between single and double stranded samples. The use of 345 µL of colloid gave the largest discrimination. However, the highest volume of colloid investigated, 395 µL, gave unexpectedly lower discriminatory results. This trend has been shown within a previous study, where diminished SERS signals were generated through increasing the volume of colloid.[138] This resulted from the Raman scattered light becoming self-adsorbed as the

number of nanoparticles significantly increased, which reduced the amount of Raman scatter reaching the detector.

The diminished SERS response within this system was further investigated through a DNA concentration studying using both ssDNA and dsDNA probes. Using 395 µL of colloid, five concentrations of DNA within the nanomolar range were investigated since the SERS method must be applicable over a range of concentrations. The intensities of single and double stranded oligonucleotides versus DNA concentration are displayed in Figure 4.7.

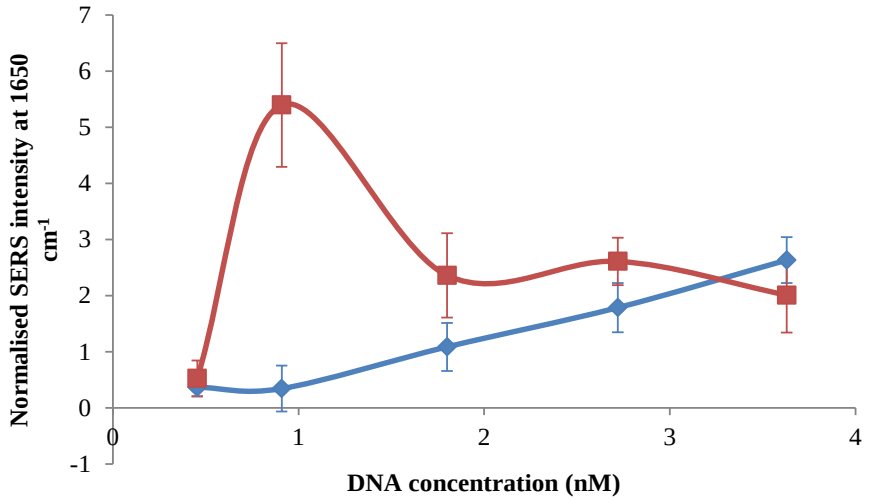

Figure 4.7: Intensity of ssDNA and dsDNA using 395 µL of pH 12 EDTA silver colloid over a concentration range of DNA; blue: dsDNA and red: ssDNA obtained using 514.5 nm laser excitation (1s, 6 mW, 20x obj). Each point represents the mean of 5 x 5 replicates and error bars represent ± one standard deviation.

The results obtained using 395 µL of colloid showed erratic ssDNA intensities over the concentration range analysed, indicating a reduction in the stability of the DNA samples. Although lower than expected error bars were obtained from the data, repeated experiments could not reproduce these results and inconsistent and variable signal intensities were obtained. Through the increase in colloid volume, the volume of PBS buffer was reduced to maintain sample concentrations. However, the PBS buffer contains an essential supply of monovalent ions necessary in sustaining DNA stability and as the buffer volume, and consequently salt concentration, was reduced the results became uncertain. Consequently, to stabilise the samples and obtain more accurate results, the concentration of NaCl within the PBS buffer was increased whilst maintaining the overall volume of buffer.

The initial experimental conditions used a 0.3 M PBS buffer that resulted in a final concentration of 0.12 M NaCl within the SERS analysis mixture. The use of 0.3 M PBS buffer enables stabilisation of DNA sequences and has been widely utilised within DNA analysis hybridisation studies. Therefore, the concentration of NaCl was increased, resulting in a 1.65 M PBS buffer that would maintain a salt concentration of 0.3 M within the final reaction mixture when reduced volumes of buffer were incorporated. The study carried out in Figure 4.6 was repeated changing only the initial concentration of PBS used, from 0.3 M to 1.65 M. Similarly, the difference in intensity between ssDNA and dsDNA samples were calculated from the SERS peak at 1650 cm^{-1} and plotted in Figure 4.8.

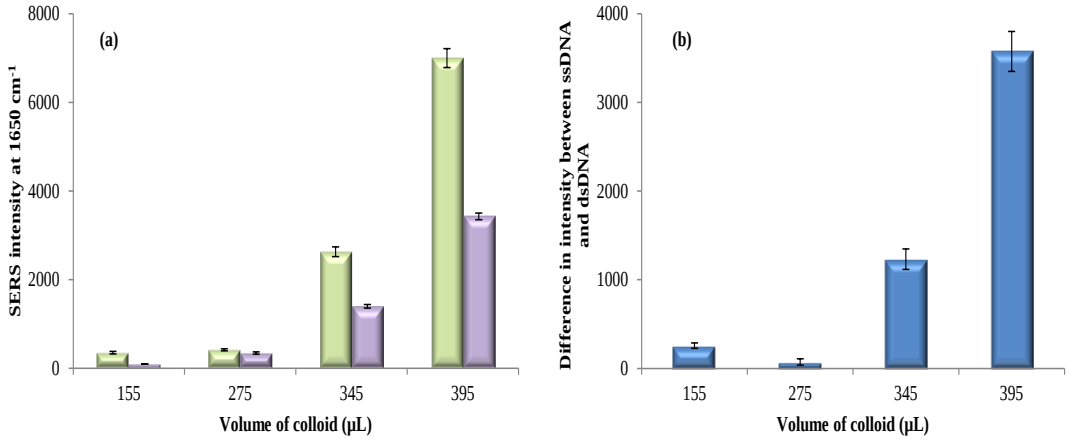

Figure 4.8: (a) SERS intensity of ssDNA (green) and dsDNA (purple) at 1650 cm^{-1} **(b)** difference in SERS intensity between ssDNA and dsDNA of the 1650 cm^{-1} peak (DNA concentration 3.64 nM) using 1.65 M PBS and different volumes of EDTA silver colloid obtained using 514.5 nm laser excitation (1s, 6 mW, 20x obj). Each point represents the mean of 5 x 5 replicates and error bars represent ± one standard deviation.

The higher salt concentration within the PBS buffer produced the largest discriminatory difference in intensity between ssDNA and dsDNA samples when using the highest colloid volume. Compared to Figure 4.6, the new PBS buffer concentration produced lower differences when lower colloid volumes were used this could result from higher salt concentrations causing colloid instability and aggregation. However, the highest SERS responses were obtained from the use of 395 µL of colloid, therefore, PBS buffer concentrations were further investigated to ensure full optimisation.

4.2.2 PBS Buffer Optimisation

The largest discrimination between ssDNA and dsDNA sequences was obtained through increasing colloid volume whilst maintaining the salt concentration within the SERS solution. The inclusion of higher salt concentrations has shown to be essential in obtaining accurate and reproducible results. Consequently, a study was carried out to determine the optimum concentration of salt used in the PBS buffer ensuring that the greatest SERS intensity differences were obtained. The original experimental conditions employed 0.3 M PBS buffer, generating a final concentration of 0.12 M within the final reaction mixture. Therefore, two concentrations of PBS buffer, 0.66 M and 1.65 M, were investigated generating final concentrations of 0.12 M and 0.3 M respectively when adding a lower volume of 100 µL within the final reaction mixture. SERS responses for both single and double stranded samples were obtained using 395 µL of silver colloid and 100 µL of either concentration of PBS. The difference between the samples was then calculated over a range of DNA concentrations (Figure 4.9).

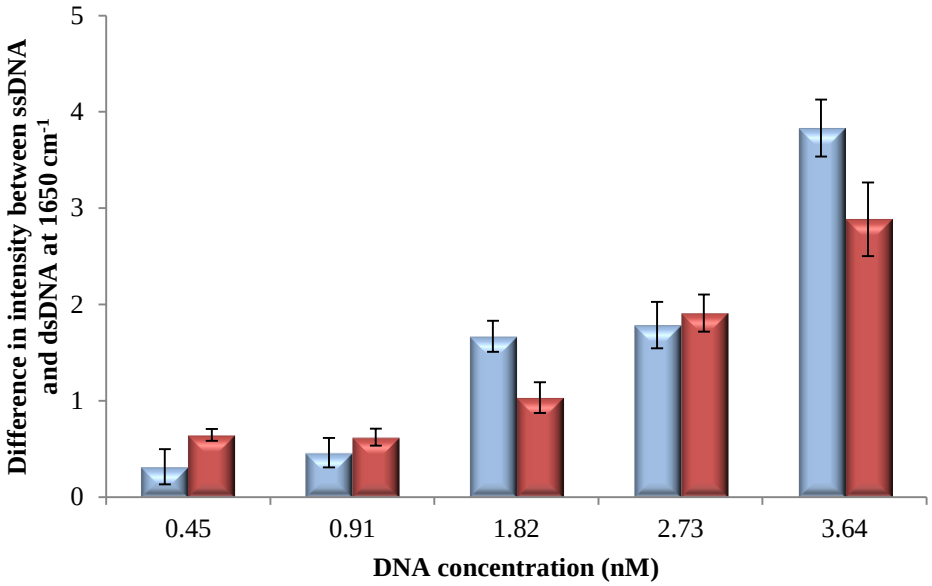

Figure 4.9: Difference in SERS intensity between ssDNA and dsDNA of the 1650 cm^{-1} peak comparing blue: 100 µL of 0.66 M PBS and red: 100 µL of 1.65 M PBS over a concentration range of DNA obtained using 514.5 nm laser excitation (1s, 6 mW, 20x obj). Each point represents the mean of 5 x 5 replicates and error bars represent ± one standard deviation.

It was shown that both PBS concentrations give comparable differences in SERS intensities. However, using the higher concentration of 1.65 M gives increased differences at lower

DNA concentrations with reduced error. This is advantageous in developing a DNA detection method as smaller volumes of DNA can be detected with greater confidence and was therefore chosen to be used within the optimised experimental conditions.

Optimisation of experimental conditions has demonstrated that the largest SERS intensity differences between ssDNA and dsDNA were obtained from the use of 395 µL of pH 12 EDTA reduced silver colloid and 100 µL of 1.65 M PBS buffer within the final SERS analysis mixture. A comparative dilution study was then carried out evaluating the original conditions against the optimised conditions (Figure 4.10).

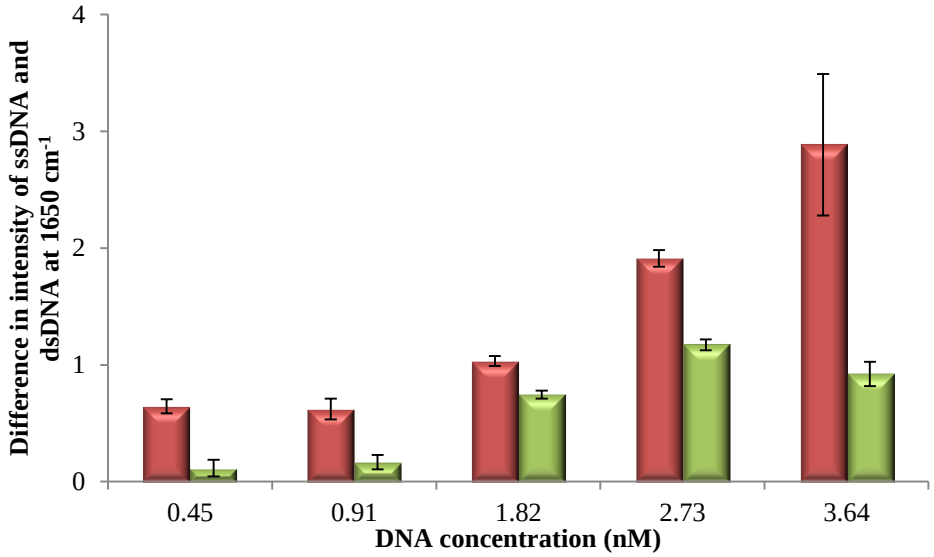

Figure 4.10: Difference in SERS intensity between ssDNA and dsDNA of the 1650 cm^{-1} peak comparing experimental conditions; red – optimised and green – initial experimental conditions obtained using 514.5 nm laser excitation (1s, 6 mW, 20x obj). Each point represents the mean of 5 x 5 replicates and error bars represent ± one standard deviation.

Significantly higher differences in SERS intensity between ssDNA and dsDNA sequences were obtained through utilisation of the optimised experimental conditions over the concentrations analysed. These results suggest that through slightly altering the experimental conditions considerably higher SERS intensity differences over an extended concentration range were achieved compared to employment of the original conditions. Subsequently, this improved DNA discrimination method was employed to further investigate the quantitative discrimination of ssDNA, dsDNA and a TAMRA dye.

4.3 Quantitative SERS Analysis of DNA Discrimination Principle

The determination of the quantitative discrimination of ssDNA, dsDNA and a free TAMRA dye label was achieved by analysing the SERS responses over a range of nanomolar concentrations. The average intensity of the principle peak at 1650 cm^{-1} was calculated and plotted against concentration to produce the linear concentration response shown in Figure 4.11.

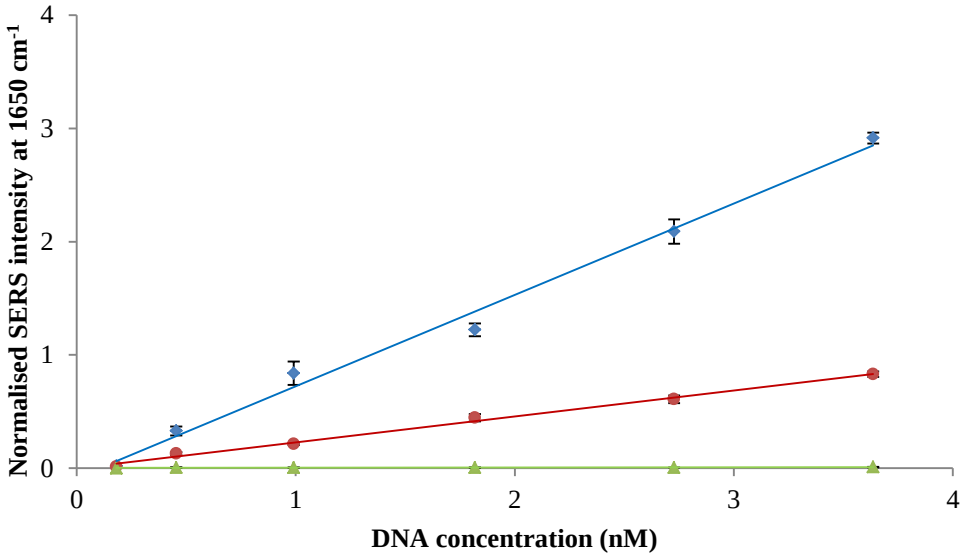

Figure 4.11: Dilution series of TAMRA labelled DNA and single dye at 1650 cm^{-1}; blue: single stranded TAMRA labelled probe (T20); red: double stranded TAMRA labelled probe (T20+complement); green: TAMRA label obtained using 514.5 nm laser excitation (1s, 6 mW, 20x obj). Each point represents the mean of 5 x 5 replicates and error bars represent ± one standard deviation.

Through utilisation of the optimised SERS method, significant discrimination between each sample at concentrations above 0.45 nM was observed. Linear responses were obtained for ssDNA and dsDNA sequences, illustrating the quantitative nature of the SERS method. Detection limits for the ssDNA and dsDNA were calculated by assigning the limiting signal intensity to be three times the standard deviation of the background signal. The limit of detection of the single stranded probe was calculated to be over a magnitude lower than the double stranded probe (Table 4.3), verifying the spectral observations. No SERS signal was obtained from the dye molecule at any of the chosen concentrations, therefore, the calculated signal intensity was fundamentally negligible and no limit of detection could be obtained.

Table 4.3: Limits of detection (L.O.D) for single and double stranded DNA

TAMRA labelled DNA probe	*L.O.D (mol dm^{-3})*
Single stranded	2.88 x 10^{-12}
Double stranded	1.15 x 10^{-11}

An understanding of the principle of DNA discrimination using differences in electrostatic attractions to silver nanoparticles has been shown. The potential of this principle as a DNA detection method has been demonstrated through significant discrimination intensities between ssDNA and dsDNA at concentrations above 0.45 nM. Results have also importantly demonstrated that the TAMRA dye does not contain sufficient charge to be adsorbed onto the metal surface and surface attraction is instead driven by attachment of nucleotide bases. To further extend this theory, a study was carried out using an analogous probe incorporating a negatively charged FAM dye to compare to the neutral TAMRA dye.

4.4 DNA Analysis of FAM sequences using SERS

The SERS responses of ssDNA and dsDNA probes containing a covalently attached 5-(and 6-)-carboxyfluourescein (FAM) dye were analysed using the optimised experimental conditions. FAM is a SERS active fluorescent dye with an excitation maximum at 492 nm and an emission maximum at 521 nm. The dye contains a carboxylic acid and hydroxyl group, which under experimental conditions will convey an overall negative charge on the molecule.

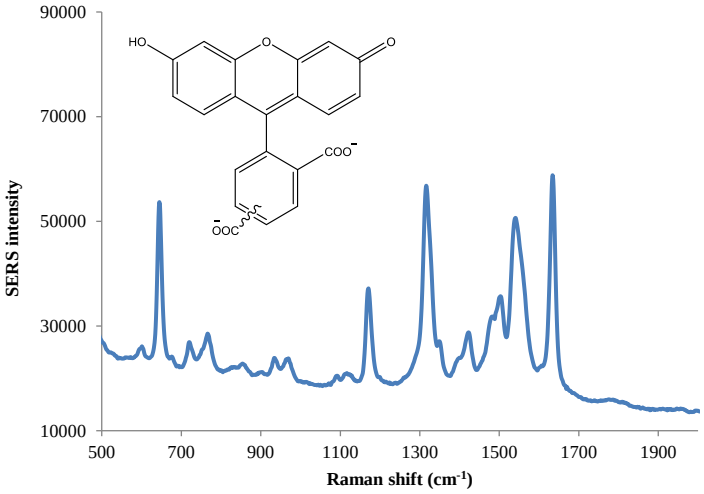

Figure 4.12: Structure and spectra of FAM labelled DNA obtained using 514.5 nm laser excitation (20x obj., 1 sec acc.).

The distinctive FAM spectrum generated by SERS demonstrates a principle peak at 1636 cm^{-1} which was chosen for analysis. The DNA sequences used remained unchanged from previous analysis of TAMRA sequences differing only in the dye attached to the 5' end of the DNA sequence, ensuring equivalent results could be determined (Table 4.4).

Table 4.4: FAM labelled DNA sequences and modifications

Name	***Sequence (5'- 3')***	***5' Modification***
F20 probe	GGT TCA TAT AGT TAT AAT AA	FAM
F20 complement	TTA TTA TAA CTA TAT GAA CC	-

The determination of the quantitative discrimination between ssDNA and dsDNA FAM probes was achieved by analysing the SERS responses over a range of concentrations. The average intensity of the principle peak at 1636 cm^{-1} was calculated and plotted against concentration to produce the linear concentration responses shown in Figure 4.13.

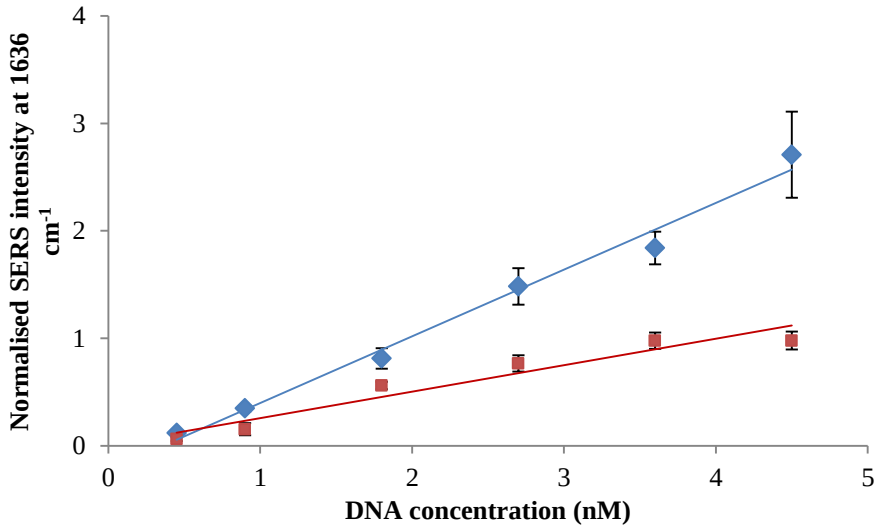

Figure 4.13: Dilution series of FAM labelled DNA at 1636 cm^{-1} comparing blue: single stranded FAM labelled probe (F20) and red: double stranded FAM labelled probe (F20+complement) obtained using 514.5 nm laser excitation (1s, 6 mW, 20x obj). Each point represents the mean of 5 x 5 replicates and error bars are ± one standard deviation.

Linear responses were again obtained for ssDNA and dsDNA sequences with discrimination between samples at concentrations above 1.8 nM. The detection limits for the ssDNA and dsDNA were also calculated by assigning the limiting signal intensity to be three times the standard deviation of the background signal (Table 4.5). Comparable limits of detection for the single stranded and double stranded DNA probes were calculated with a slightly lower

detection limit obtained from the ssDNA sequence. These similar detection limits may have been obtained as a result of both probes generating similar plot slopes. However, Figure 4.13 demonstrates that significantly distinct SERS intensities were obtained between ssDNA and dsDNA samples. This illustrates that discrimination between samples has not been compromised and clear signal discrimination was still obtained.

Table 4.5: Limits of detection (L.O.D) for double stranded and single stranded FAM labelled DNA

FAM labelled DNA probe	***L.O.D (M)***
Single stranded	1.73×10^{-11}
Double stranded	3.46×10^{-11}

The results obtained from the quantitative SERS analysis of FAM and TAMRA probes indicate that DNA sequences labelled with FAM generate reduced SERS responses. As identical oligonucleotide sequences were utilised and previous results have demonstrated that nanoparticle adsorption is driven through the nucleobases, the difference in detection limits appears to be due to the difference in dye. The Raman cross section of TAMRA and FAM dyes were analysed by comparing the SERS signal intensities utilising the same dye concentration, analysed under the same conditions (Figure 4.14).

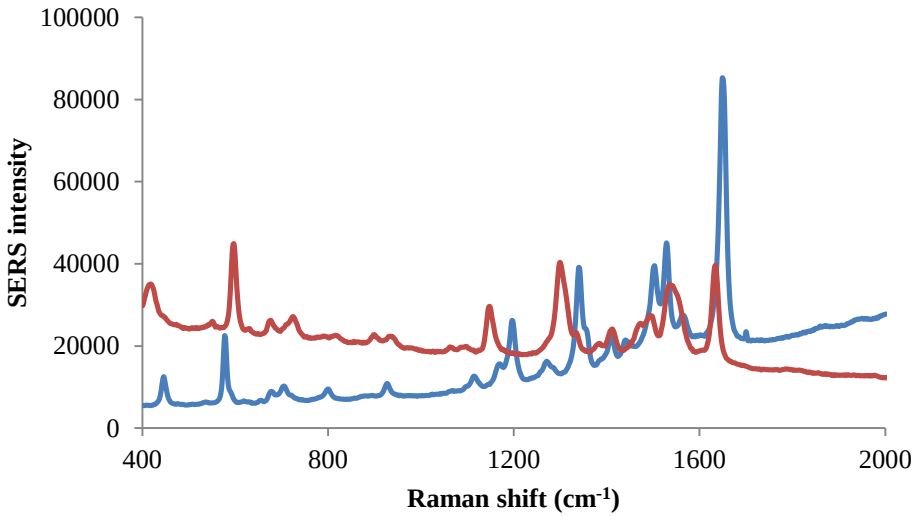

Figure 4.14: SERS spectra of TAMRA (blue) and FAM (red) labelled DNA (concentration 3.6 nM) analysed using 514.5 nm laser excitation. Spectra taken under same conditions and concentration.

The SERS signals generated from the TAMRA dye were higher in intensity than the FAM label, suggesting significant differences in the dye cross section. A larger Raman cross section on the TAMRA dye will result in stronger SERS responses over the FAM dye and therefore, higher detection limits would be achievable.[95]

Analysis of ssDNA and dsDNA sequences incorporating either a TAMRA or FAM dye have shown that surface attraction is heavily driven through the electrostatic attraction of the DNA bases. Thus, the sequence composition of the attached nucleotide chain was investigated using TAMRA labelled ssDNA and dsDNA sequences.

4.5 Dependency of Sequence Composition

The understanding of surface adsorption and sequence affinity for silver metal nanoparticle surfaces is vitally important in developing a DNA discrimination method based on silver nanoparticles. Therefore, since results have demonstrated a high dependence on the oligonucleotide sequence directing surface adsorption, the base composition of the DNA sequence was varied and analysed. The T20 probe used previously is composed of a nucleic acid sequence containing 20 % guanine (G) and cytosine (C) bases. As demonstrated, this sequence composition has shown distinctive differences between ssDNA, dsDNA and a TAMRA dye. To gain an understanding of the dependence that the number of G and C bases incorporated into the analysed sequence has, the GC content of the sequence was increased and analysed using the optimised SERS conditions. Three synthetic oligonucleotide probes containing a 5'-TAMRA label and consisting of either 20, 50 or 80 % GC content were investigated to determine the base composition effect on the SERS responses (Table 4.6).

Table 4.6: DNA sequences used and corresponding GC content

Name	*DNA Sequence (5'- 3')*	*5' Modification*	*GC content (%)*
T20 probe	GGT TCA TAT AGT TAT AAT AA	TAMRA	20
T20 comp	TTA TTA TAA CTA TAT GAA CC	-	20
T50 probe	TTG GAC GCG CTG GCT AAT AA	TAMRA	50
T50 comp	TTA TTA GCC AGC GCG TCC AA	-	50
T80 probe	TTG GAC GCG CTG GCG CCG CC	TAMRA	80
T80 comp	GGC GGC GCC AGC GCG TCC AA	-	80

Initially, a concentration study using only single stranded probes was carried out to determine the influence of varying the GC composition on the adsorption of single stranded DNA sequences. Evident differences were obtained between each of the single stranded TAMRA labelled probes, with the highest signal intensity obtained from the 20 % GC content samples, shown in Figure 4.15. Significantly reduced signal intensities were obtained from the T50 probe, with the lowest SERS response generated by the T80 probe.

This indicates that the increasing number of guanine and cytosine bases within the target DNA sequence is considerably reducing the SERS signal intensity obtained.

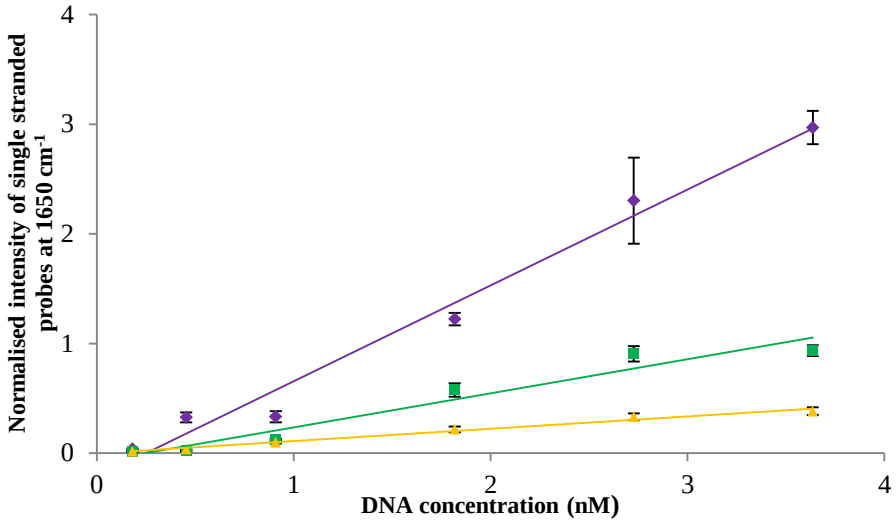

Figure 4.15: Single stranded TAMRA labelled probes over a concentration range of DNA comparing 1650 cm^{-1} peak; purple: 20 % TAMRA labelled probe (T20), green: 50 % TAMRA labelled probe (T50), yellow: 80 % TAMRA labelled probe (T80) obtained using 514.5 nm laser excitation (1s, 6 mW, 20x obj). Each point represents the mean of 5 x 5 replicates and error bars represent ± one standard deviation.

These results imply that the reduction in surface affinity is due to formation of secondary structures through self-hybridisation of sequences and a weaker binding affinity of guanine bases onto silver nanoparticle surface. Previous studies have shown that poly G DNA sequences form secondary structures through Hoogsteen base pairings.[17] Thus, guanine rich oligonucleotides are prone to self-association, forming G-tetrads or guanine-hairpins.[140,141] These structures are not sufficiently flexible to allow the nucleobases to adsorb directly onto the metal surface, reducing surface affinity and appreciably decreasing the SERS response. However, the fundamental aspect of this DNA discrimination method is obtaining the greatest signal intensity differences between ssDNA and dsDNA samples. Thus, an experimental study was carried out investigating the difference in SERS intensity between ssDNA and dsDNA probes containing 20 %, 50 % and 80 % GC content.

Initially, double stranded probes were prepared by hybridising single stranded probes with their exact DNA complements. To ensure hybridisation had occurred successfully, UV melting experiments were carried out.

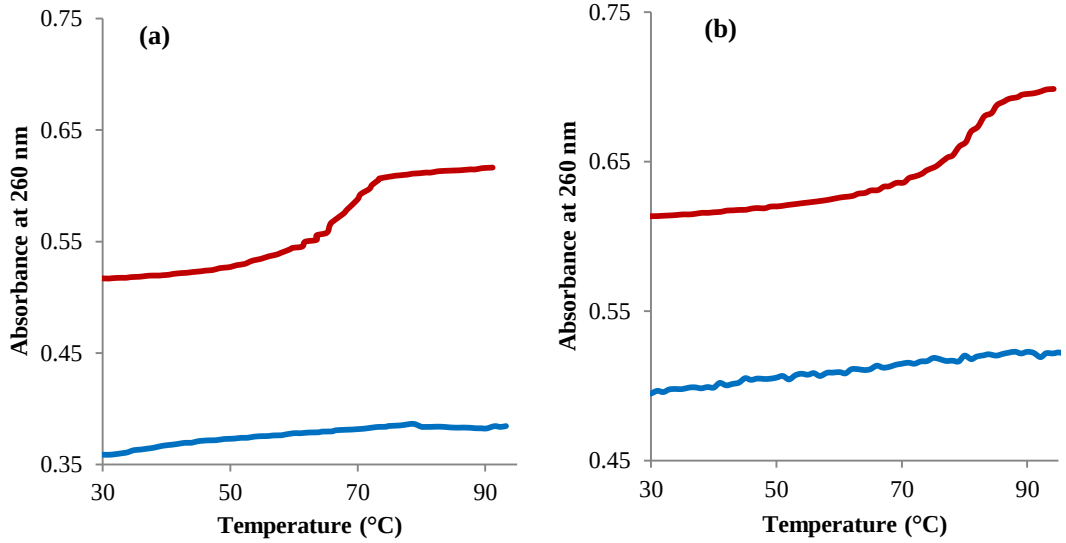

Figure 4.16: UV melting curves obtained at 260 nm. **(a)** DNA sequences containing 50 % GC content, **(b)** DNA sequences containing 80 % GC content; blue: ssDNA and red: dsDNA.

The melting curves for the ssDNA and dsDNA samples for both the 50% and 80 % GC content sequences are shown in Figure 4.16. The dsDNA melts show a point of inflection on the sigmoidal profile, this defines the melting temperature (T_M) of the double stranded T50 probe and T80 probe (Table 4.7). This shows that the formation of double stranded samples has been successfully achieved. As expected no sigmoidal curve and therefore no hybridisation was obtained from the ssDNA sample.

Table 4.7: UV melting temperatures for T50 and T80 dsDNA probes

Name	***Predicted T_M (°C)***	***Experimental T_M (°C)***
T20 probe	50.0	53.0
T50 probe	67.7	70.0
T80 probe	80.14	80.0

The predicted melting temperatures shown in Table 4.7 for the 20, 50 and 80 % GC content sequences were calculated using EndMemo software. These results show that increasingly high numbers of guanine and cytosine bases generate higher melting temperatures through increased hydrogen bonding between base pairs. This could also indicate that secondary structures are forming within higher GC content sequences, reducing the thermal stability of the complementary duplex.[142] After successful preparation of double stranded sequences, SERS analysis was carried out on the ssDNA and dsDNA samples (Figure 4.17).

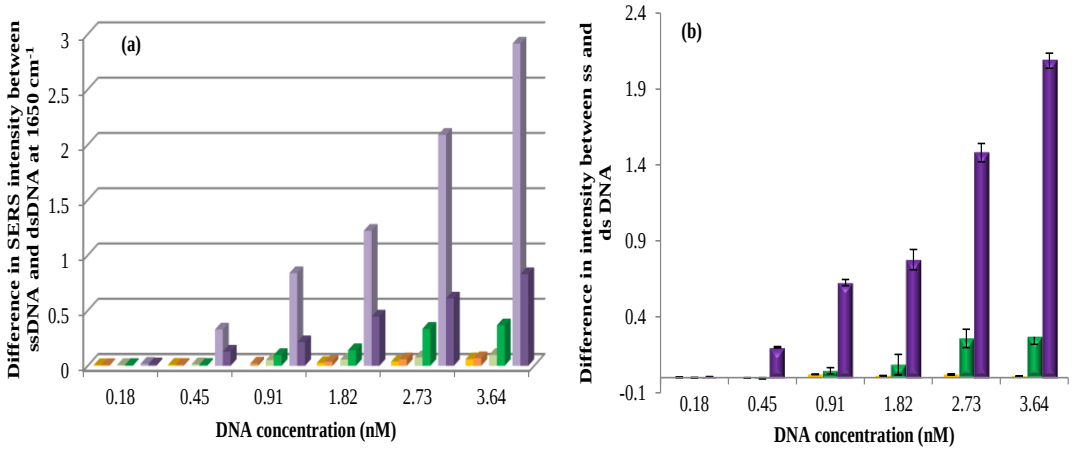

Figure 4.17: (a) SERS intensity of 20 % GC probe ssDNA (dark purple) and dsDNA (light purple), 50 % GC probe ssDNA (dark green) and dsDNA (light green) and 80 % GC probe ssDNA (dark yellow) and dsDNA (light yellow) at 1650 cm^{-1} **(b)** Difference in intensity of single and double stranded TAMRA labelled probes comparing 1650 cm^{-1} peak; purple: 20 % TAMRA probe (T20), green: 50 % TAMRA probe (T50), yellow: 80 % TAMRA probe (T80) obtained using 514.5 nm laser excitation (1s, 6 mW, 20x obj). Each point represents the mean of 5 x 5 replicates and error bars represent ± one standard deviation.

Significantly higher signal discrimination between ssDNA and dsDNA were obtained from sequences containing 20 % GC content. The 50 % GC content probes gave considerably lower signal intensities. However, distinctive discrimination was still obtained. No discrimination between ssDNA and dsDNA sequences was obtained from the 80 % GC probes. These results strongly indicate that as the number of guanine and cytosine base pairs increase within the oligonucleotide sequence, the surface affinity for silver nanoparticles is reduced as a result of the formation of secondary structures.

The coordination and attraction of DNA nucleosides (dA, dT, dG and dC) to silver and gold surfaces has been investigated.[143,144] SERS spectra have enabled constituent bases, nucleosides and nucleotides to be studied and the surface chemistries increasingly understood.[145] Adenine complexes have shown diverse spectra through altering pH and concentration.[107,146] This has generated multiple forms and varied structure orientations which can be detected through distinctive SERS responses. Studies have also shown that dT has a lower surface affinity than dA, dG and dC, this has been attributed to the lack of an exocyclic amino group with only the oxygen of the pyrimidine ring implicated in metal coordination (Figure 4.18).

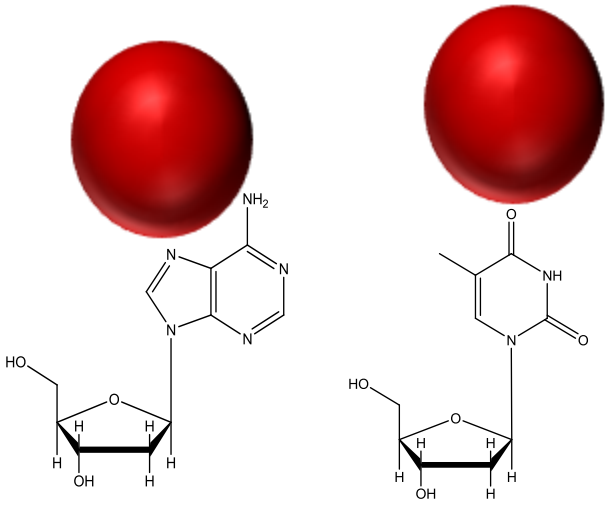

Figure 4.18: Deoxythymidine and deoxyadenosine coordination to gold nanoparticles.[143]

However, nucleobases are prevented from binding to the nanoparticle surface through the desired nucleoside orientations, due to the sugar phosphate backbone holding the structure in a fixed conformation.[147] Therefore, the hetero-oligonucleotide sequences used within this study mimic DNA sequences and surface adsorption which would be seen within diagnostic assays. Consequently, it has been demonstrated that sequence composition and experimental conditions have an extremely influential effect on the electrostatic attraction of DNA sequences to metal nanoparticles and careful consideration must be taken when designing DNA affinity assays.

4.6 Application of DNA Binding Affinity within Assay

A developed understanding of the DNA detection method based on differences in the affinity of ssDNA and dsDNA for silver nanoparticles has been illustrated within this study. However, to demonstrate the applicability and versatility of this method, the optimised SERS conditions were used within an established DNA detection SERS assay based on the principle of DNA discrimination.[125] Within this assay, the presence of target DNA was determined through the differentiation of non-complementary DNA (ssDNA) and complementary DNA (dsDNA) by the generation of distinctive SERS responses (Figure 4.19). Samples containing target DNA will hybridise to the added complementary dye labelled probe, forming a double stranded sequence. This rigid helical structure has a low affinity for a silver nanoparticle and generates a lower SERS intensity. Whereas, in the presence of non-complementary DNA, no hybridisation will occur and the probe will remain single stranded. The flexibility of the single stranded DNA allows it to be strongly adsorbed

onto the nanoparticle surface, generating higher SERS signals. As the concentration of target is increased the formation of dsDNA will also increase, resulting in further reduction in the SERS signals. Meanwhile, further addition of non-complementary DNA has no effect on the dye probe and a constant SERS intensity is maintained. These differences in SERS intensities allow the existence of target DNA to be determined.

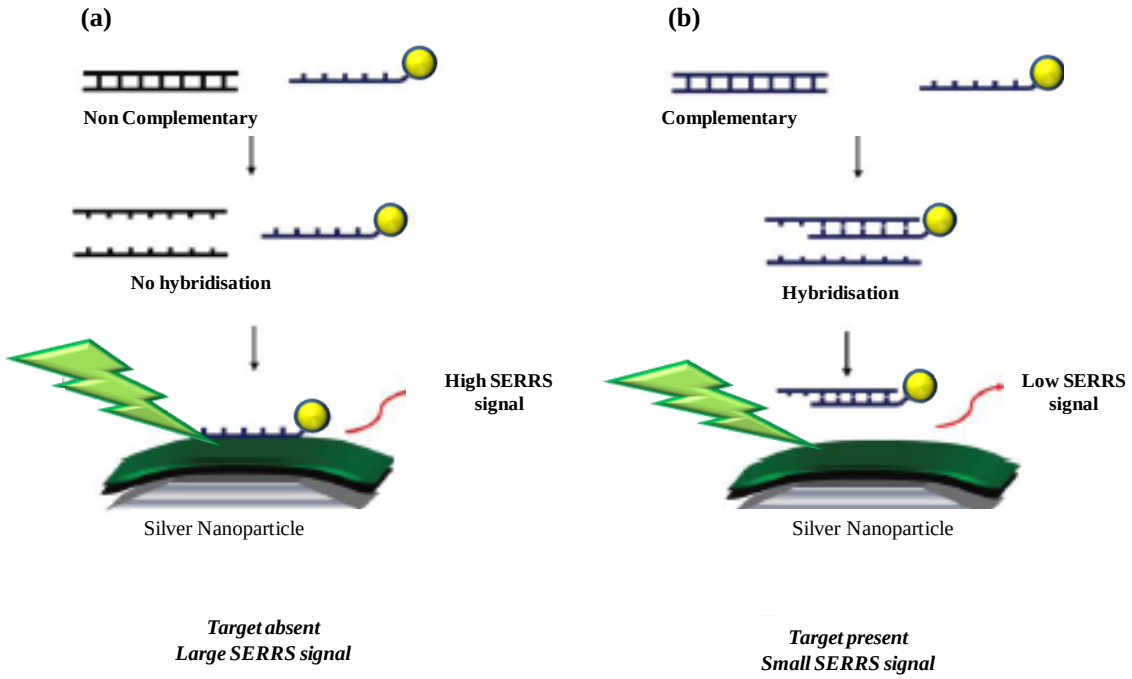

Figure 4.19: Schematic of DNA affinity assay. **(a)** Non-complementary DNA cannot hybridise to the dye labelled probe which remains single stranded and generates strong SERS responses. **(b)** Complementary DNA will hybridise to labelled probe forming dsDNA which has a lower affinity for nanoparticle surfaces and generates weaker SERS responses[125]

The detection assay was performed comparing the optimised SERS conditions with the original experimental conditions to determine the discrimination between ssDNA and dsDNA as a function of concentration (Figure 4.20). The T20 probe (20 % GC content) was initially used for this comparison study. The optimised conditions yielded significantly higher differences between complementary and non-complementary sequences at concentrations above 0.25 nM, with the highest signal discrimination of 7.4 times at 0.9 nM using optimised conditions compared to a 1.4 times using the original parameters.

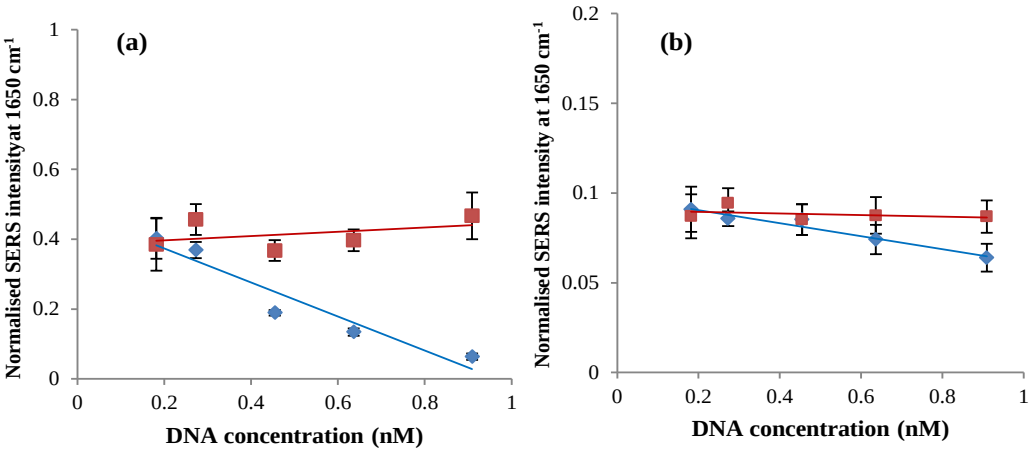

Figure 4.20: SERS intensity of T20 probe over concentration range blue: complementary and red: non-complementary DNA using 514.5 nm laser excitation (1s, 6 mW, 20x obj) **(a)** optimised SERS conditions, **(b)** original SERS conditions. Points represent the mean of 5 x 5 replicates and error ± one standard deviation.

The original DNA discrimination assay utilised a 45 % GC content probe containing locked nucleic acid (LNA) residues to determine the discrimination between ssDNA and dsDNA. LNA residues generate greater discrimination between exact match and mismatch sequences when used in the comparison of unmodified labelled DNA probes. Therefore, to enable a higher accuracy comparison to be obtained experiments using the higher GC content probes (T50 and T80) were performed using the original and optimised SERS conditions, within the DNA detection assay (Figure 4.21 and 4.22).

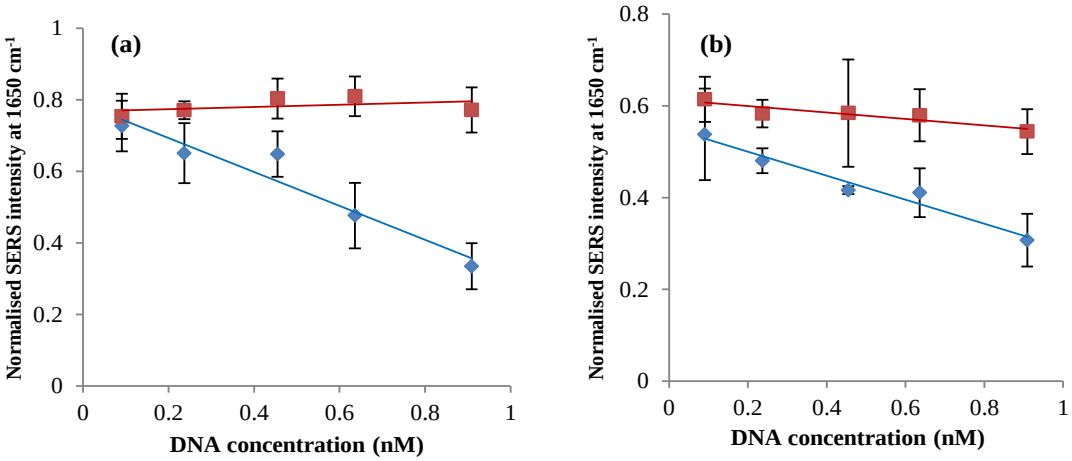

Figure 4.21: SERS intensity of T50 probe over concentration range blue: complementary and red: non-complementary DNA using 514.5 nm laser excitation (1s, 6 mW, 20x obj) **(a)** optimised SERS conditions, **(b)** original SERS conditions. Points represent the mean of 5 x 5 replicates and error ± one standard deviation.

Sequences containing 50% guanine and cytosine bases (T50 sequences) demonstrated discrimination between an exact match and control, with improved SERS differences obtained when employing optimised experimental conditions (Figure 4.21). Further illustrating that the optimisation of experimental conditions has considerably improved difference in SERS responses obtained using complementary and non-complementary oligonucleotides. These results have also shown that the use of the optimised experimental conditions have demonstrated significantly greater discrimination compared to the previous DNA affinity without the use or the expense of LNA residues.

Sequences containing higher proportions of GC bases (T80 sequences) illustrated no discrimination between complementary and non-complementary target using either experimental method. This indicates that sequences containing 80% or greater GC content are unable to be utilised within DNA detection assays based on the principle of differing surface affinity for silver nanoparticles.

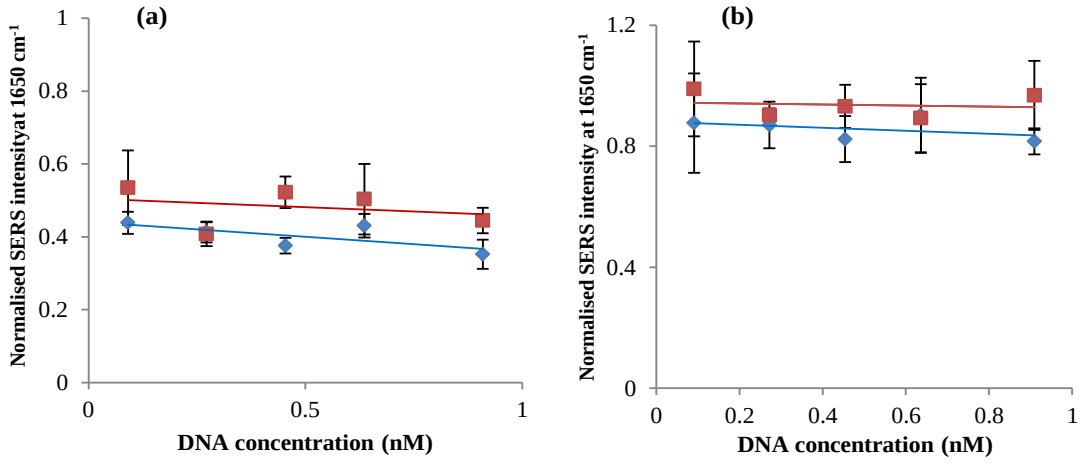

Figure 4.22: SERS intensity of T80 probe over concentration range blue: complementary and red: non-complementary DNA using 514.5 nm laser excitation (1s, 6 mW, 20x obj) **(a)** optimised SERS conditions, **(b)** original SERS conditions. Points represent the mean of 5 x 5 replicates and error ± one standard deviation.

The results obtained from the study of the effect of oligonucleotide chain length displayed varying SERS intensities over the sequence compositions analysed. The T20 probe generated the lowest SERS intensities, however, this experiment was performed on a separate day to the T50 and T80 experiments and is therefore not comparable due to daily variability in the SERS instrumentation and different reagents and colloid used. The T50 and T80 experiments were carried out simultaneously and therefore can be compared. The

optimised T50 results demonstrated higher signal intensities than the optimised T80 results, whereas, the original T80 probe was shown to generated greater SERS intensity signals than the T50 probe using the same conditions. This is likely to be due to inconsistent and fluctuating results produced by the T80 probe through self-hybridisation and weak surface binding.

4.7 Chapter Conclusions

This study has illustrated an understanding of the principle of specific DNA detection through differences in electrostatic interactions by SERS. SERS has been effectively utilised to quantitatively discriminate between TAMRA labelled single stranded, double stranded and a TAMRA dye molecule on silver nanoparticles, with higher SERS intensities observed for ssDNA compared to dsDNA. It was further demonstrated that surface attraction is driven through the constituent bases and the dye contributes minimally to surface adsorption. These results were obtained through the use of excess spermine, which effectively neutralised the negative charge on the DNA backbone. A comparative study also analysed the affinity of the DNA probes using a negatively charged FAM dye. Distinctive differences were also obtained between FAM labelled ssDNA and dsDNA sequences; however, the discrimination and limits of detection obtained were slightly lower than the calculated TAMRA results. This indicates that the charge on the SERS active FAM dye may be reducing surface affinity of the sequences compared to TAMRA labelled sequences through altering the surface orientation of the dye or through differences in the Raman cross sections of the dyes.

The optimisation of the experimental conditions enabled the development of a method that allows discrimination of DNA to be established with greater confidence and at lower DNA concentrations. Discrimination between single and double stranded sequences was obtained down to 0.45 nM for the TAMRA labelled sequences and 1.8 nM for FAM labelled sequences. The composition of the base sequence has proven to be highly influential on the discrimination of target samples, with an increasing percentage of GC content within oligonucleotides found to cause a decrease in surface affinity for silver nanoparticles. A DNA detection method has been shown here which through careful consideration of SERS conditions and target sequence, can provide a simple and selective biological assay method.

4.8 Further Work

To continue this work and gain a greater understanding of the principle of adsorption of labelled DNA onto nanoparticle surfaces, an extended study could be performed utilising a variety of labels and DNA sequences. This study has demonstrated that under these experimental conditions, identical DNA sequences containing either a TAMRA or FAM dye label generated differing SERS responses. Therefore, a more comprehensive understanding would prove beneficial when designing DNA detection assays, enabling customised systems to be easily devised. The detection of multiple probe sequences within one reaction mixture adds complexity to the system and surface interactions, therefore this study could be further extended to also investigate the differing affinities which dye labelled probes have for nanoparticle surfaces within SERS multiplex mixtures. This study has also demonstrated through slight experimental optimisations an increased discrimination at lower oligonucleotide concentrations was achieved. Further optimisation would enable the applicable concentration range to be extended detecting lower concentrations of DNA with a greater confidence.

5. Specific DNA Detection Coupling a TaqMan Assay with SERS

The treatment of clinical diseases and viruses is progressing towards prevention through early intervention. To achieve this goal DNA detection methods are continually improving to enhance sensitivity and multiplexing to enable generation of rapid and accurate results. Conventional methods for the detection of bacterial infections are based on cell culturing methods, which can be tedious and time-consuming. Generally, samples must undergo incubation for up to 48 hours on a mixed flora agar culture before identification and level of resistance can be measured.[148,149] This becomes problematic when detecting highly infectious disease causing pathogens, such as viruses and bacterium. Traditional detection methods can prolong diagnosis times and facilitate the spread of the infection. One such pathogen responsible for severe nosocomial infections is methicillin resistant *Staphylococcus aureus* (MRSA). This multiresistant strain has an increased resistance to many types of antibiotics, including methicillin and other β-lactam antibiotics, which considerably restricts treatment.[150,151] Consequently, rapid and accurate detection is essential for infection control. Modern techniques have been developed which utilise PCR combined with fluorescence detection to rapidly reduce analysis times. Francois *et al.* demonstrated the rapid detection of MRSA directly from clinical samples using a fluorescence detection TaqMan assay, which detected and identified MRSA within less than 6 hours.[152] This provided substantial benefits for infection control by enabling prompt and cost-effective implementation of contact precautions.

5.1 TaqMan Assay

The TaqMan assay (see Introduction, Section 1.3.1.2) has been the main focus of this study. Conventional TaqMan assays have been used for the detection of specific nucleic acid sequences.[33] The TaqMan assay utilises enzymatic probe cleavage to generate signal within a real-time PCR assay. The accumulation of dye as a result of target amplification is monitored through an increase in fluorescence signal. Morris *et al.* designed a fluorogenic probe-based PCR assay for the detection of hepatitis C virus RNA in serum and plasma.[34] The assay monitored the build up in fluorescence signal from the dye labelled DNA probe containing a FAM fluorophore and TAMRA quencher. This TaqMan assay demonstrated a

rapid detection method with increased throughput which reduced the opportunity for false-positive results due to the elimination of second-round amplification.

The TaqMan assay is highly effective and has many benefits including low post-PCR manipulation, selectivity through specific binding events and high sensitivity. However, TaqMan probes can show poor allelic binding and inefficient fluorophore quenching which will often result in high background signals, reducing assay sensitivity. Previous studies have overcome some of these issues through the incorporation of modified probes which reduce signal background.[38] Nurmi *et al.* utilised terbium chelates as a reporter molecule within a real-time TaqSERS PCR assay.[36] The fluorescence intensity of terbium chelate is lowered through attachment to a single stranded DNA sequence and increased when free in solution. This observation was exploited within a TaqMan 5'exonuclease assay. The chelate probe specifically binds to the complementary target amplicon and the 5' to 3' exonuclease activity of the DNA polymerase enzyme enables digestion of the probe. This action releases the chelate from the DNA sequence, generating an increased signal intensity which correlates to the presence of target DNA. This assay removes the need for efficient probe quenching, therefore, low backgrounds were obtained as well as a 1000-fold signal amplification.

Another drawback which significantly reduces assay productivity is the limited sequence analyses due to fluorescence detection. Fluorescence detection generally produces broad emission bands which make multiple dye combinations difficult to differentiate. Herein, we have investigated the benefits of coupling a TaqMan assay with SERS detection to obtain enhanced sensitivity limits and multiple analyte detection.

5.2 TaqSERS Assay

The TaqSERS assay has been developed to incorporate the advantages of SERS within an efficient DNA detection TaqMan assay. The polymerase chain reaction (PCR) is an essential component within the TaqSERS assay and a detailed perspective of the reaction and modified components must be introduced.

5.2.1 TaqSERS Polymerase Chain Reaction (PCR)

The TaqSERS assay relies on PCR to simultaneously amplify the target sequence whilst enzymatically digesting the hybridised probe. The standard fluorescent TaqMan probe had

to be redesigned within the TaqSERS assay, to enable specific and intense SERS response to be obtained. The probe was altered by replacing the 5'-terminus dye with a biotin residue, this was followed by a 29 base sequence complementary to a specific region within the target gene. Adjacent to the coding region, a hexaethylene glycol (HEG) spacer was incorporated, intended to prevent the further digestion of the probe by the enzyme. Finally, followed by 10 adenine bases terminated by a 3'-TAMRA dye (Figure 5.1).

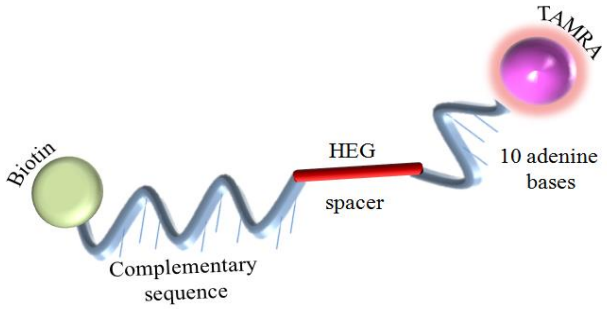

Figure 5.1: Schematic of TaqSERS probe.

Throughout each PCR cycle, the DNA primer and probe hybridise to specific regions of the target sequence within amplifiable distance. The binding of the primer enables the thermostable enzyme *Thermus aquaticus* (taq) polymerase to begin strand elongation (Figure 5.2). The enzyme also contains a 5' to 3' exonuclease activity which will cleave the obstructing TaqSERS probe, separating the attached TAMRA and biotin groups.

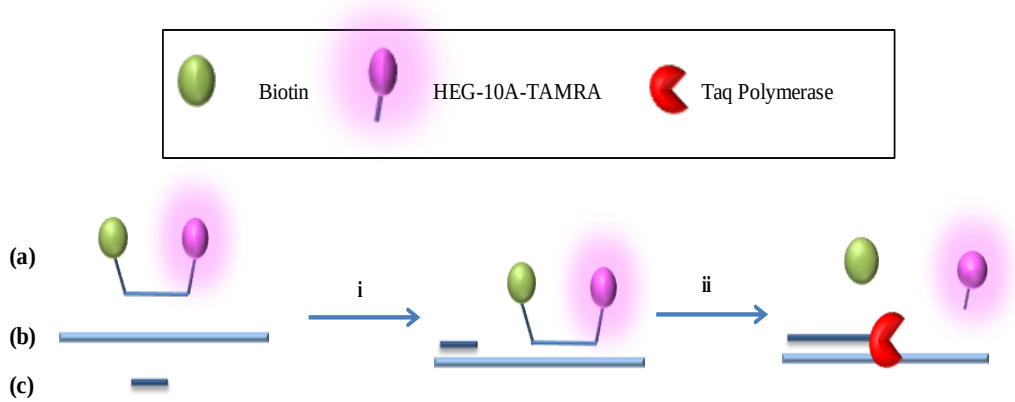

Figure 5.2: Schematic of TaqSERS PCR. TaqSERS probe containing biotin and TAMRA **(a)**, template **(b)** and primers **(c)**, (i) hybridisation of probe and primers to template, (ii) Taq polymerase enzyme simultaneously elongates primers and digests probe separating the biotin and TAMRA dye.

The biotin residue was incorporated into the TaqSERS probe to enable any undigested probe to be removed from the reaction mixture through addition of streptavidin coated magnetic beads (Figure 5.3). After PCR had been carried out, the resultant supernatant contained fully intact and digested TaqSERS probes. Streptavidin coated magnetic beads were utilised to remove any remaining intact probe to prevent the generation of false positive results. Streptavidin is a tetrameric protein with four binding sites, which have a very high binding affinity for biotin ($K_a = 10^{15}$ M^{-1}). Therefore, all biotin residues, whether single groups from the digested probe or biotin remaining with the TaqSERS probe, will bind strongly to the beads and magnetically removed from the sample mixture. This wash step leaves only the TAMRA dye with attached DNA remaining in the supernatant solution for SERS analysis.

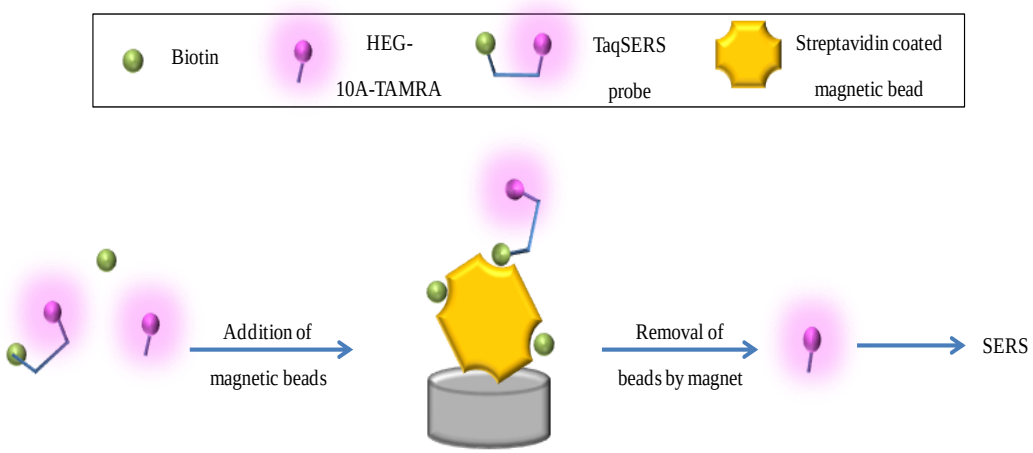

Figure 5.3: Schematic of removal of biotin group using streptavidin coated magnetic beads. Streptavidin coated magnetic beads are introduced to remove any undigested biotinylated probe and free biotin. A magnet then removes beads from the system leaving TAMRA labelled 10 adenine bases in the supernatant for SERS analysis.

The design of the probe ensures that a 10 adenine base "tail" remains attached to the TAMRA dye after enzymatic digestion. It was experimentally demonstrated that a DNA sequence attached to the fluorophore will generate significantly higher SERS signals.[153] This was shown in previous chapter, where a greater signal was obtained from dye-labelled DNA than dye alone (Chapter 4). SERS analysis was carried out comparing the SERS signal from a TAMRA dye and a HEG-10A-TAMRA sequence (Figure 5.4). Both samples were analysed through addition of 0.1 M spermine, distilled water and silver citrate-reduced nanoparticles. The mixtures were analysed using 514.5 nm laser excitation, recording the SERS spectra within 1 minute of colloid addition. Five replicates of each concentration were analysed 5 times and the average SERS intensity of the 1650 cm^{-1} peak was plotted against concentration.

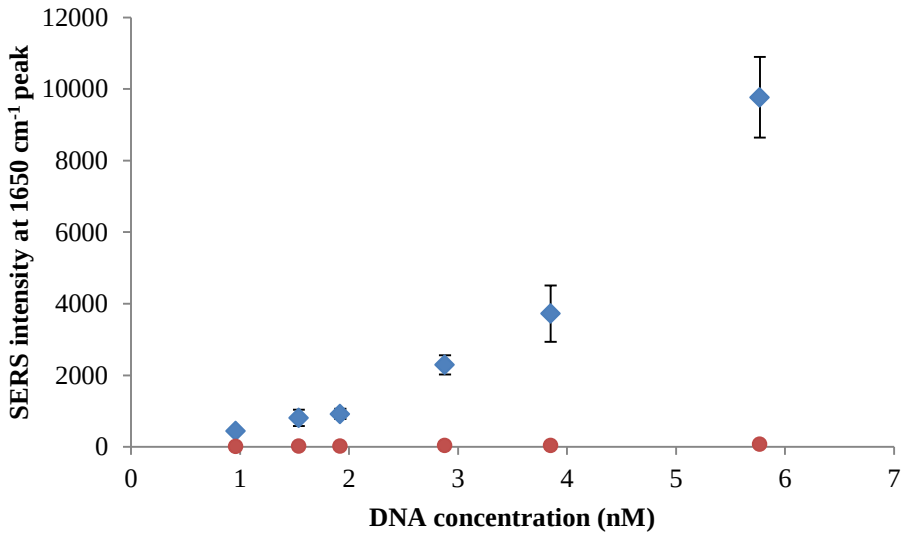

Figure 5.4: SERS intensity of 1650 cm^{-1} peak recorded using 514.5 nm laser excitation (1s, 6 mW, 20x obj); blue: HEG-10A-TAMRA, red: free TAMRA dye. Error bars represent ± one standard deviation.

Results clearly show that, under these conditions, no SERS signals were obtained from the TAMRA dye, whereas, high intensity SERS responses were obtained when analysing the dye labelled DNA sequence. Conventional TaqMan assays do not contain an enzyme blocking group and thus the full probe sequence is digested, allowing complete separation of fluorophore and quencher molecules. However, this study has demonstrated that through redesigning the probe to incorporate a HEG group, further progression of the enzyme is prevented. This enables a short oligonucleotide sequence to remain attached to the TAMRA dye and generate distinctive SERS responses. These findings support results obtained in Chapter 4, indicating that metal surface attraction of the DNA is driven by the nucleotide bases and not the TAMRA dye. This illustrates that more sensitive SERS detection can be achieved through detection of TAMRA labelled DNA rather than released free dye.

The probe design also removes the need for efficient fluorescence quenching within the intact form. The conventional TaqMan assay uses a quencher to avoid fluorescence being emitted before enzymatic digestion occurs. However, quenching can be poor, generating high background signals. The TaqSERS probe removes this issue as the assay does not rely on fluorescence signal quenching but instead biotin was incorporated into the sequence, allowing removal of excess probe using streptavidin coated magnetic beads.

5.3 SERS Analysis of TaqSERS Assay

The TaqSERS assay was employed for the detection of methicillin-resistant *Staphylococcus aureus* (MRSA). *Staphylococcus aureus* (SA) is a major pathogen responsible for severe nosocomial infections. Multiresistant strains of SA have emerged with an increased resistance to many types of antibiotics, including methicillin and other β-lactam antibiotics. The methicillin resistance gene within the strain is conferred through the *mecA* gene, which encodes the penicillin-binding protein 2a (PBP2a). This protein contains an active site which prevents the binding of β-lactam moieties. Thus, acquisition of the *mecA* gene within the SA chromosome, generates the methicillin resistance strain (MRSA).[150,151] This has considerably restricted the treatment of MRSA to the exclusive use of glycopeptides and oxazolidiones. Consequently, rapid and accurate detection is essential for infection control and to prevent use of last-line antibiotics.

Table 5.1: Oligonucleotide sequences and modifications

Name	***Sequence (5'- 3')***	***5' Modification***	***3'Modification***
mecA Probe	TGGAAGTTAGATTGGGATCATAGCGTCAT	Biotin	HEG-10A-TAMRA
MRSA Template	TGGTCTTTCTGCATTCCTGGAATAATGACGCTA TGATCCCAATCTAACTTCCACATACCATCTTCTT TAACAAAATTAAATTGAACGTTGCGATCAATG	-	-
Forward Primer	CATTGATCGCAACGTTCAATTT	-	-
Reverse Primer	TGGTCTTTCTGCATTCCTGGA	-	-

The assay was carried out using a synthetic MRSA oligonucleotide target sequence containing 99 bases and a probe nucleic acid sequence containing 29 bases which correspond to the *mecA* gene region within the MRSA strain (Tale 5.1).[152] To perform the assay, reagents were combined within a 200 μL PCR tube as described in detail in section 3.6.1. Each sample contained PCR buffer (2.5 μL), $MgCl_2$ (1 μL), dNTP mixture (0.4 μL), Taq polymerase enzyme (0.5 μL), forward and reverse primer (1 μL each, 10 μM), TaqSERS probe (0.7 μL, 18 μM) and target sequence (1 μL, 6 pg/μL) made up to a total volume of 25 μL with DEPC water. For each TaqSERS sample, a corresponding sample containing SYBR green was also prepared to enable the success of PCR to be determined through monitoring sequence amplification. SYBR green is an intercalating dye that has a low binding affinity for single stranded DNA and binds in high yields to double stranded DNA. In real-time PCR, fluorescence from the dye is measured in each cycle to obtain an amplification curve, the intensity of which is proportional to the amount of PCR product formed and

consequently, the increase in probe digestion. SYBR green samples contained all reagents and volumes as the TaqSERS assay with exception to the removal of the TaqSERS probe and addition of 1.5 μL of SYBR green (1/1000th dilution). Control assays, with and without SYBR green, were simultaneously performed using a nonsense oligonucleotide as a template sequence which was non-complementary to the TaqSERS probe, thus should generate minimal to no SERS responses. Samples were heated according to cycling conditions:

1 cycle	95 °C for 10 minutes
25 cycles	94 °C for 30 seconds, 60 °C for 1 minute, 72 °C for 1 minute
1 cycle	72 °C for 5 minutes

Both positive and negative samples containing SYBR green were monitored throughout PCR to determine the success of target sequence amplification. Figure 5.5 shows typical amplification profiles obtained from monitoring the SYBR green TaqSERS assay sample and negative control. Both the TaqSERS assay and negative control samples without SYBR green underwent PCR heating, however, the samples were not monitored during PCR as no information would have been gained.

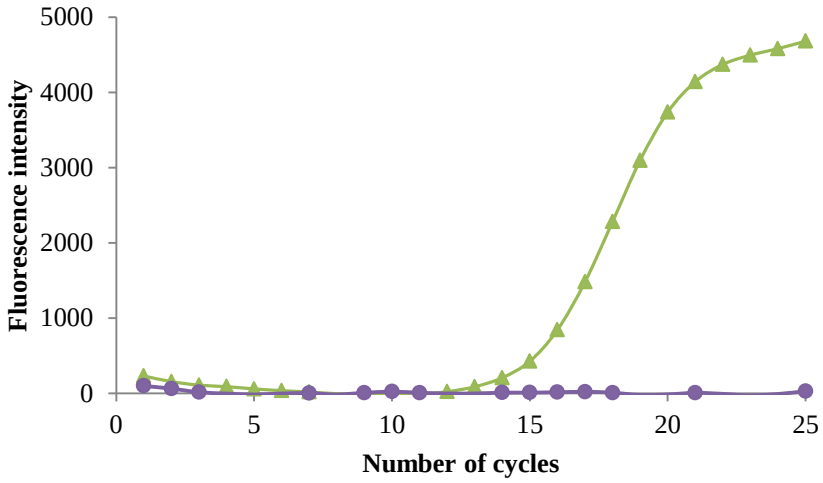

Figure 5.15: Real-time PCR cycles of amplification of template DNA through monitoring SYBR green fluorescence; green: MRSA template sequence and purple: nonsense template sequence.

The generation of a sigmoidal curve in the TaqSERS assay sample indicates the target DNA has been amplified and therefore, suggests optimum probe digestion has occurred. As expected no amplification of the nonsense control was generated. After PCR was determined to have been successfully performed, any undigested probe was removed through a streptavidin bead wash. This step was performed only on samples which did not contain

SYBR green dye as the intercalating dye may generate interfering signals during SERS analysis. Each 25 µL of PCR product was combined with 19 µL of streptavidin coated magnetic beads and left shaking for 30 minutes. The beads with attached biotinylated probe were then magnetically separated from the analysis mixture. The removal of the intact probe enables SERS signals to be generated from the remaining TAMRA dye formed *via* digestion of the TaqSERS probe, correlating to the presence of target amplicon. SERS analysis was carried out utilising 514.5 nm laser excitation with 1 second accumulations (Figure 5.6). Citrate-reduced silver nanoparticles were mixed with the TAMRA labelled adenine sequence and aggregated using spermine immediately prior to SERS analysis. Silver citrate-nanoparticles were used in this study as it has been reported that lower limits of detection and higher intensity signals can be achieved.[104, 125]

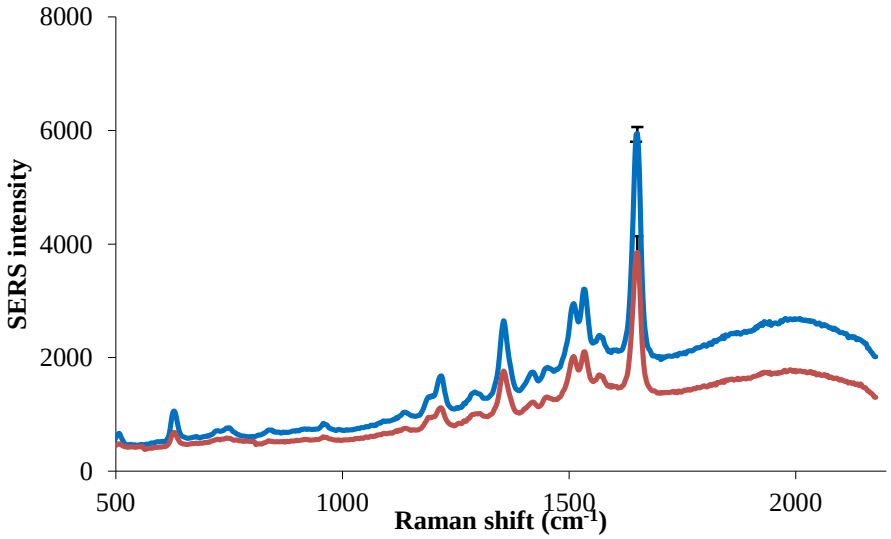

Figure 5.6: SERS spectra recorded using 514.5 nm laser excitation (1s, 6 mW, 20x obj) containing blue: synthetic MRSA target and red: synthetic nonsense control (final probe concentration 6.5 nM). Error bars represent ± one standard deviation.

The results in Figure 5.6 obtained from the assay show only a small difference between the detection of the MRSA sequence and a non-complementary sequence at the prominent 1650 cm^{-1} peak. This difference is not sufficient to definitively show the presence of the target sequence within the sample and significantly larger discrimination would be expected to obtain definitive conclusions. This minimal discrimination is due to high signals from the control, this could be a result of inefficient capture of excess probe within the bead washing step or through poor digestion of the probe by the enzyme which would lower the assay signal. Consequently, both theories were investigated.

5.3.1 Streptavidin Bead Wash Optimisation

To ensure the maximum amount of biotinylated probe was removed from the supernatant mixture prior to SERS analysis, a 3 times excess of streptavidin coated magnetic beads was initially utilised. A 1:1 binding capacity of beads was calculated to be 6.25 µL to 25 µL of PCR product containing biotinylated TaqSERS probe, with 19 µL of beads providing a 3 times excess. In reality, each streptavidin protein has four binding sites which further increases the binding capacity of each bead. However, results from Figure 5.6 demonstrate that high negative control signals were generated using this bead volume. Therefore, the TaqSERS assay was repeated incorporating increasing volumes of beads. Three different amounts of excess beads were investigated; 3 times (19 µL), 10 times (63 µL) and 15 times (94 µL) were each added to 25 µL of PCR product after TaqSERS PCR. The samples were analysed by SERS using 514.5 nm laser excitation after the biotinylated probe had been magnetically removed from the supernatant through the streptavidin bead wash. The difference in SERS intensity of the 1650 cm^{-1} peak between MRSA target sample and nonsense control could then be calculated and the efficiency of increased bead volumes assessed (Figure 5.7).

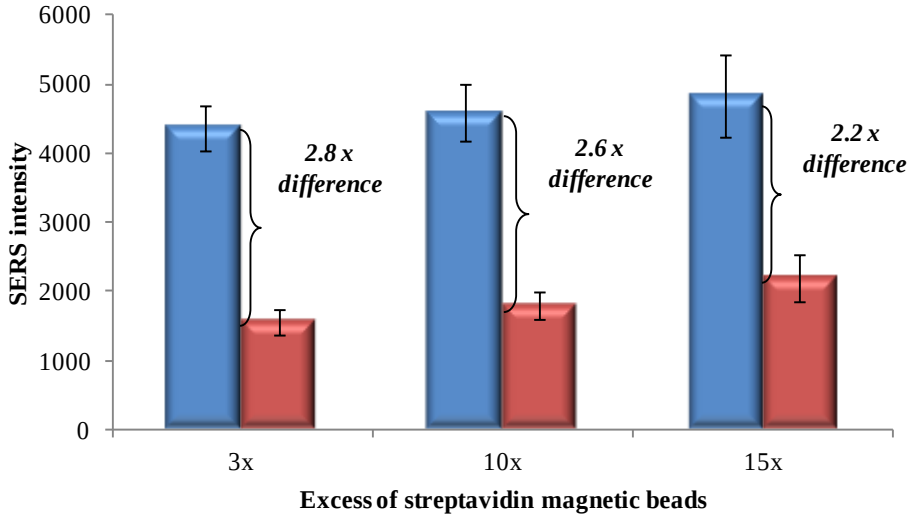

Figure 5.7: SERS intensities of 1650 cm^{-1} TAMRA peak recorded using 514.5 nm laser excitation (1s, 6 mW, 20x obj) comparing differences between blue: synthetic MRSA target and red: synthetic nonsense control using increasing volumes of streptavidin coated magnetic beads. Error bars represent ± one standard deviation.

The differences obtained between the MRSA target and control samples illustrate that no significant increase in the removal of the TaqSERS probe was achieved by increasing the

volume of beads employed. A 3 times excess of streptavidin beads provides a greater capturing efficiency than a 15 times excess. This demonstrates that a 3 times excess of beads is providing efficient probe removal. Larger intensity differences were obtained from results in Figure 5.7 than the assay performed in Figure 5.6. However, no experimental parameters were altered and a 3 times excess of beads was used, therefore these small differences are likely to be due to daily variances in the efficiency of PCR and SERS analysis. A noticeable SERS signal remains within the nonsense control, therefore the efficiency of the enzymatic digestion of the probe was investigated.

5.3.2 Enzyme Optimisation

The enzyme used within the TaqSERS assay was Nova*Taq* DNA polymerase (Merck), a chemically modified enzyme which is inactive at ambient temperature. The enzyme is activated by heating to 95 °C, providing specific amplification with minimum generation of non-specific products. To enable analysis of the enzyme a comparable hot start DNA polymerase enzyme was utilised. Hot®Star Taq DNA polymerase (Qiagen) is an alternative chemically modified enzyme with similar enzymatic properties. Both polymerase enzymes also contain 5' to 3' exonuclease activity which enables digestion of the probe when hybridised to the target sequence. Two simultaneous assays were performed incorporating each enzyme. The SERS intensities from the MRSA target and the non-complementary control were determined and the differences in intensity calculated (Figure 5.8).

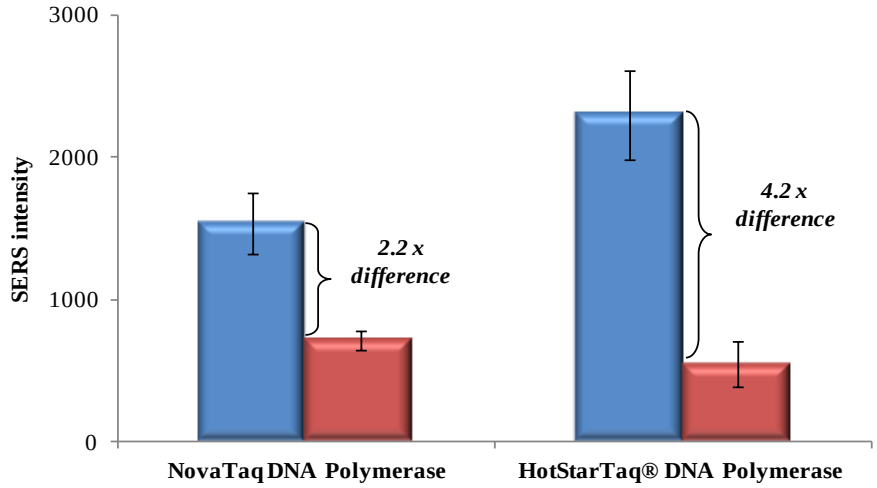

Figure 5.8: SERS intensities of 1650 cm^{-1} TAMRA peak recorded using 514.5 nm laser excitation (1s, 6 mW, 20x obj) comparing differences between blue: synthetic MRSA target and red: synthetic nonsense control using NovaTaq and Hot®Star Taq® DNA polymerase. Error bars represent ± one standard deviation.

The use of the Hot®Star Taq enzyme generated almost twice the discrimination between samples compared to utilisation of the Nova*Taq* enzyme. The discrimination generated by the Nova*Taq* enzyme was similar to results obtained from the same assay in Figure 5.6, with the small differences due to the daily variations in the efficiency of PCR. These results illustrate that the low discrimination previously obtained between samples can be enhanced through replacing the polymerase enzyme. The Hot®Star Taq enzyme generated lower SERS signals within the control sample as well as higher responses within the MRSA sample. This was thought to be as a result of increased probe digestion by the enzyme. Thus, to gain a further understanding of the activity of the Hot®Star Taq DNA polymerase enzyme, analysis of the enzymatic digestion of the probe was investigated.

5.3.3 Enzyme Digest

An enzyme digest experiment was carried out on the TaqSERS probe to establish the success of probe digestion within the assay. Two samples were prepared with enzyme added to one sample and only corresponding buffer added to the other. Both contained PCR buffer and the TaqSERS probe at the same volumes and concentrations used within the PCR assay. This experiment contained no template sequence and no PCR was performed. Both samples were activated through heating for 10 minutes at 95 °C and then heating at 60 °C for 2 hours, which was the optimal temperature for the enzyme activity and the approximate time taken to carry out the full TaqSERS PCR reaction. After heating, both samples were washed with three times excess of streptavidin coated magnetic beads, before removing the supernatant for SERS analysis.

Figure 5.9 shows the SERS intensity at 1650 cm^{-1} of samples with and without enzyme addition. Samples containing the enzyme gave higher intensity signals than samples without enzyme, indicating that the polymerase enzyme was able to successfully digest the probe and generate increased SERS responses through the build up of released dye. However, this result also indicates that the probe is being digested by the enzyme when free in solution and not hybridised to the target sequence. The Hot®Star Taq DNA polymerase enzyme contains a 5’ exonuclease activity which should digest single stranded DNA only when hybridised to the complementary target sequence. However, the strong exonuclease activity of the enzyme appears to indiscriminately digest a small volume of the free probe.

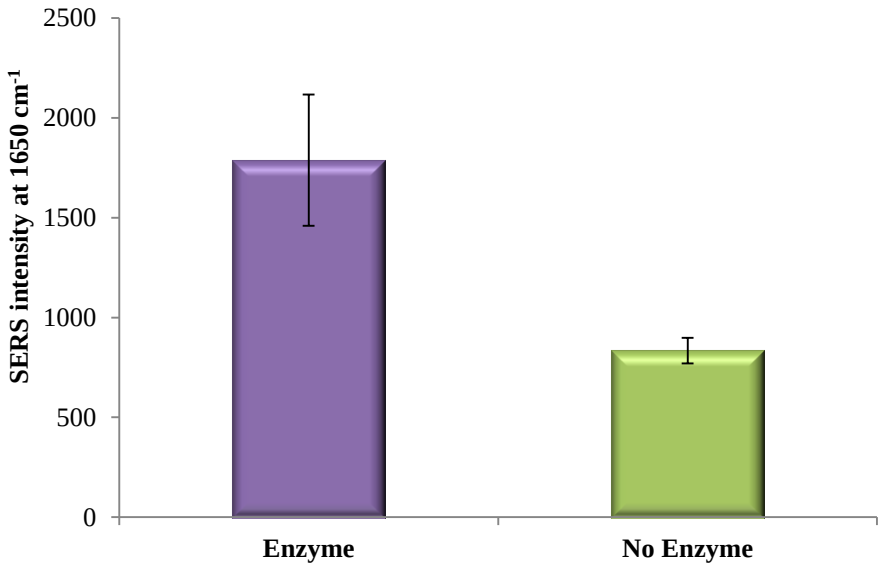

Figure 5.9: SERS intensities of 1650 cm^{-1} TAMRA peak recorded using 514.5 nm laser excitation (1s, 6 mW, 20x obj) analysing digestion of the probe purple: containing Hot®Star Taq DNA polymerase and green: omitting Hot®Star Taq DNA polymerase. Error bars represent ± one standard deviation.

This result also suggests that the bead removal step is not 100 % efficient due to the presence of the TAMRA signal within the "No Enzyme" sample. Weak but distinctive TAMRA spectra were generated despite the use of a 3 times excess of beads which was previously shown to produce sufficient probe removal. This indicates that not all biotin-streptavidin interactions are occurring to remove excess probe, regardless of the volume of beads added. The PCR mixture contains large quantities of by-products; template, primers and ions, which could compete with the biotinylated probe for the bead surface. This could result in free binding sites being obstructed by the probe as well as species remaining in the "dirty" PCR mixture.

This study has demonstrated that a combination of both non-specific enzymatic probe cleavage and reduced efficiency of the bead removal step appear to be the reason for the unwanted background signal in the negative control. However, the weak signals obtained in Figure 5.9 demonstrate that this is a minimal effect which in the presence of strong SERS responses from the target assay would become negligible. Thus, to definitively show the presence of target oligonucleotide, the signal intensity obtained from the full assay must be significantly enhanced compared to the control signal.

The TaqSERS assay was repeated incorporating the Hot®Star Taq DNA polymerase enzyme as results in Figure 5.8 have shown greater signal differences between the target assay and negative control. Synthetic MRSA template was utilised as the target sequence and a nonsense control of non-complementary DNA. After the streptavidin bead wash had removed the undigested probe, SERS analysis was performed on the resulting supernatant samples through addition of silver citrate nanoparticles and analysed using 514.5 nm laser wavelength. The average spectra generated are shown in Figure 5.10.

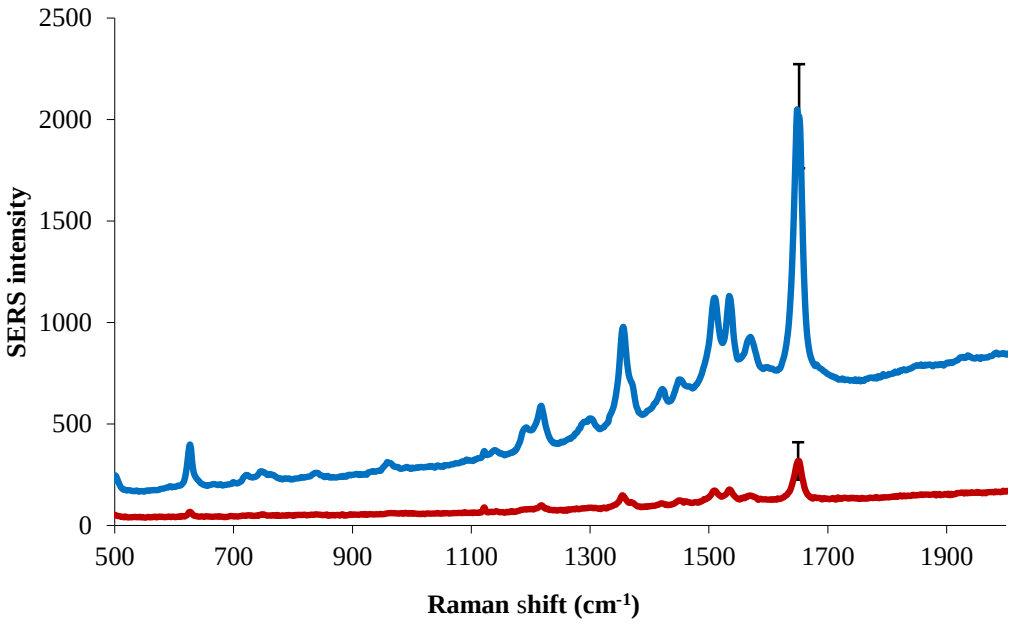

Figure 5.10: SERS spectra recorded using 514.5 nm laser excitation (1s, 6 mW, 20x obj) containing blue: synthetic MRSA target and red: synthetic nonsense control (final probe concentration 6.5 nM). Assay was performed using Hot® Star DNA polymerase. Error bars represent ± one standard deviation.

The spectra obtained demonstrated that only in the presence of MRSA target were intense characteristic TAMRA responses observed, with considerably weaker SERS signals generated by the nonsense control. A noticeable signal intensity difference of 6.3 was observed between samples from the principle spectral band at 1650 cm^{-1}. This was significantly improved from the initial assay results obtained from Figure 5.6. The SERS signals obtained were dependant on the final concentration of digested probe remaining within the sample after PCR had been performed. Therefore, a novel assay combining SERS detection with a conventional TaqMan DNA detection assay has been established which can determine the presence of specific target DNA.

5.4 Quantification of TaqSERS Assay

To demonstrate the potential of the TaqSERS assay as a diagnostic analysis method, the sensitivity of the assay had to be determined. Clinical samples often contain minimal amounts of target DNA. In light of this, it is essential for diagnostic assays to be able to detect low concentrations of oligonucleotide. Thus, the limit of detection of the TaqSERS assay was calculated to determine the lowest concentration of target MRSA which could be positively identified. The use of PCR within the assay has the advantage of enhancing sensitivity by amplification of low concentrations of target DNA. However, as PCR is an exponential reaction, obtaining detection limits for the assay can be difficult. Different initial concentrations of template will produce similar levels of DNA amplification through increasing the number of PCR cycles performed. This results in comparable levels of target amplification, probe digestion and undistinguishable SERS intensities.

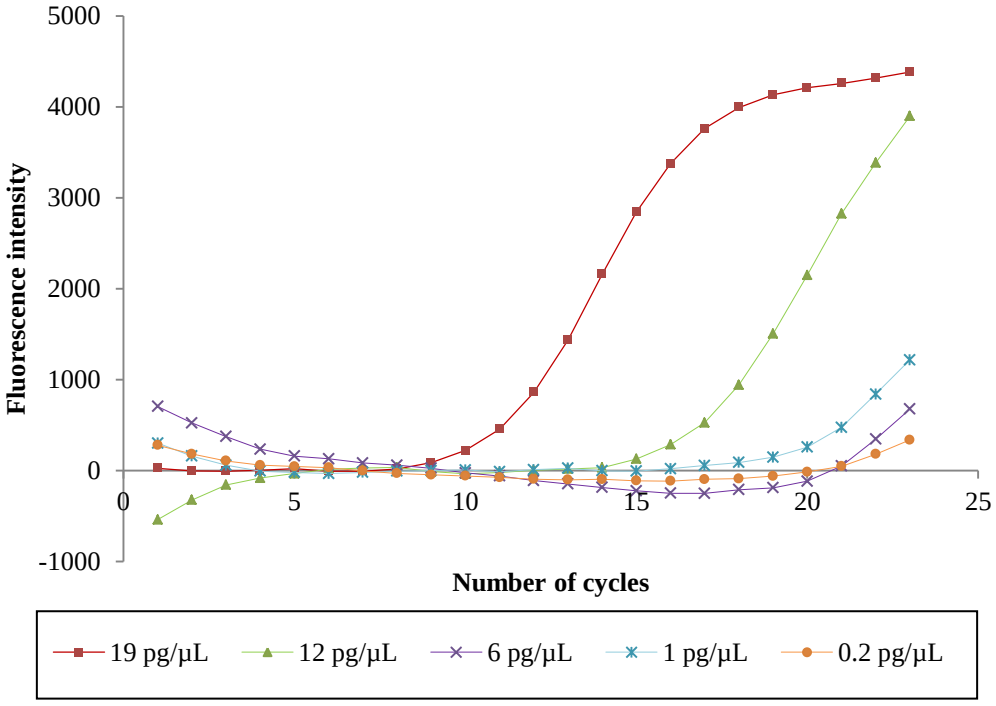

Figure 5.11: Real-time PCR cycles with varying initial DNA template concentrations. Amplification was monitored *via* fluorescence emission of SYBR green.

To overcome this issue and enable a limit of detection to be calculated, the number of PCR cycles performed was fixed. The TaqSERS assay was performed employing decreasing initial concentrations of synthetic MRSA target (19, 12, 6, 1 and 0.2 pg/µL) and it was determined that the highest template concentration had fully amplified by 23 cycles (Figure

5.11). Therefore, the assay was carried out with the number of cycles fixed at 23, enabling all concentrations of the template to begin amplification whilst maintaining discrimination between each concentration. The samples were then analysed by SERS to establish the limit of detection, four replicates of each concentration were analysed 5 times and the average SERS intensity of the 1650 cm^{-1} peak was plotted against concentration (Figure 5.12).

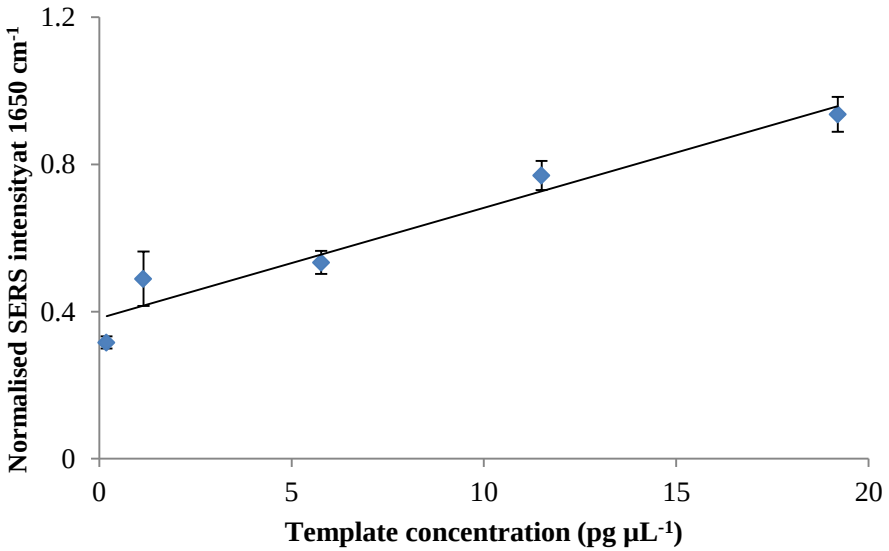

Figure 5.12: Limit of detection of TaqSERS assay using SERS, analysed using 514.5 nm laser excitation (1s, 6 mW, 20x obj) and average intensity of TAMRA peak at 1650 cm^{-1} plotted. Each point represents the mean of 4 replicates and error bars represent ± one standard deviation.

A quantitative linear response was obtained for the SERS results and the gradient of the line was used to calculate the limits of detection by assigning the limiting signal intensity to be three times the standard deviation of the background signal. The limit of detection of the TaqSERS assay using SERS analysis was calculated to be 7 fM (Table 5.2). This detection limit demonstrates the potential of the assay as a diagnostic method which can accurately detect low concentrations of DNA.

Table 5.2: Limit of detection (L.O.D.) of TaqSERS assay for MRSA template using SERS and fluorescence

Detection Method	***L.O.D (g µL^{-1})***	***L.O.D (mol dm^{-1})***
SERS	6.0×10^{-14}	7×10^{-15}
Fluorescence	6.6×10^{-13}	7.5×10^{-14}

The same samples were also analysed using fluorescence analysis to enable comparison of detection methods (Figure 5.13). Each sample concentration was analysed using a MX3005P fluorescence system utilising a TAMRA filter set (556 nm ex/580 nm em). A similar response was obtained from the fluorescence results and the limit of detection was calculated in the same way as the SERS concentration study. The limit of detection using fluorescence was calculated to be 75 fM (Table 5.2), over a magnitude higher than using SERS detection. Through the use of SERS, increased sensitivity has been achieved over its fluorescence counterpart, demonstrating one of the main benefits of SERS as a detection technique.

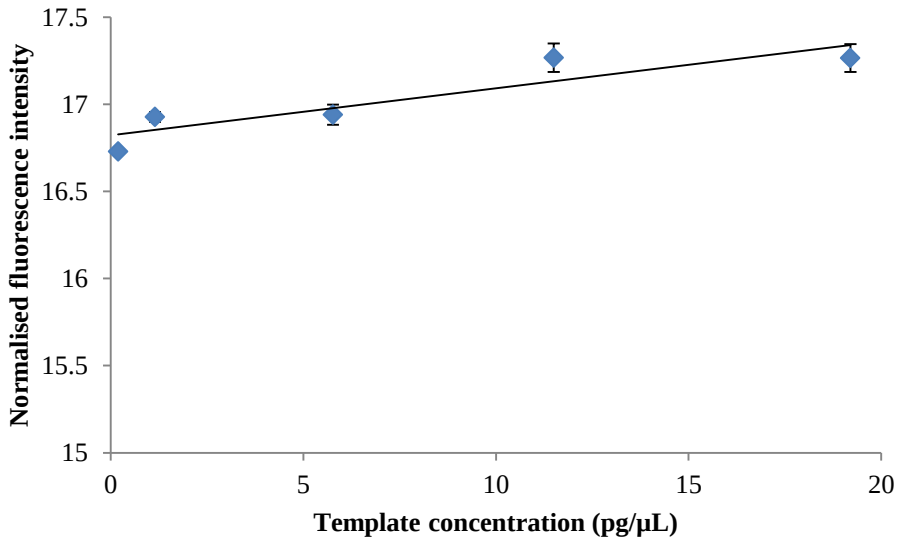

Figure 5.13: Limit of detection of TaqSERS assay using fluorescence detection, analysed using TAMRA filter set (556 nm ex/580 nm em) and average fluorescence intensity was plotted for each concentration. Each point represents the mean of 5 replicates and error bars represent ± one standard deviation.

5.5 Specificity of TaqSERS Assay

The TaqSERS assay has so far shown highly sensitive detection of clinically relevant samples of MRSA. However, to obtain meaningful results, clinical diagnostic assays must be able to specifically detect target sequences. Real clinical samples are complex mixtures of bodily fluids which contain unknown quantities of molecules, proteins, cell organelles as well as vast concentrations of genomic DNA. Therefore, analysis methods must be able to discriminately detected target sequences within these complex mixtures. Therefore, the TaqSERS assay was investigated to show its selectivity *via* the detection of clinically relevant samples of the *mecA* gene within a genomic MRSA strain. Genomic sequences of

MRSA containing the *mecA* gene were cultured from the bacterial *staphylococcus aureus* (SA) strain (NCTC 8325) obtained from the national health protection agency culture collection (HPACC Salisbury, UK). A SA strain was employed as a control. The SA strain does not contain the methicillin-resistant gene and no amplification should occur in this case. Therefore, the *mecA* probe should not be digested and will be removed from the reaction during the streptavidin bead wash step. Figure 5.14, shows the SERS intensity of the target MRSA and control SA sequences as well as the spectral responses.

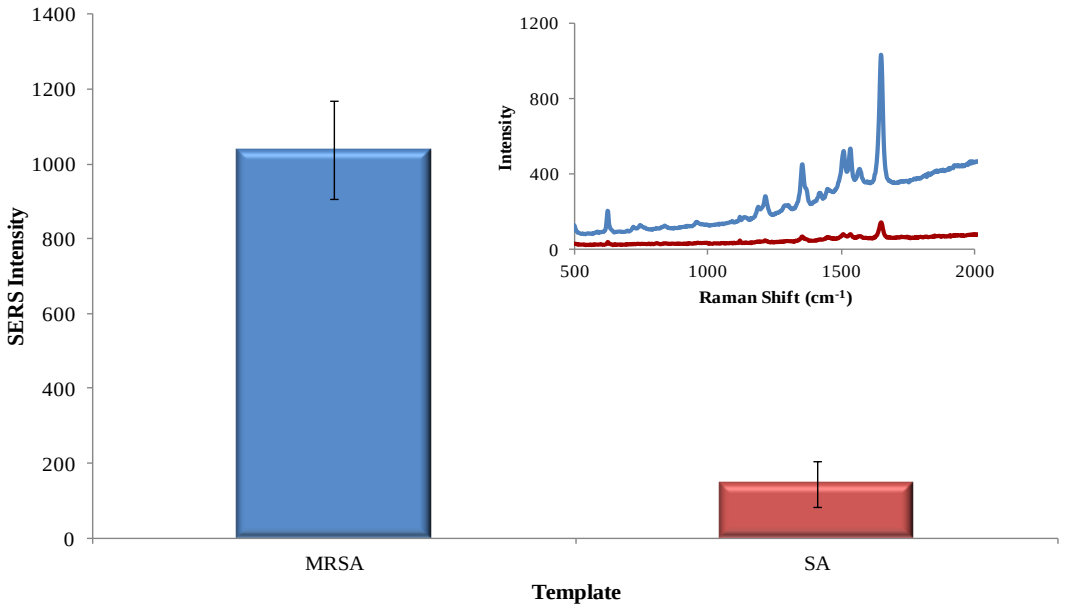

Figure 5.14: SERS spectra recorded using 514.5 nm laser excitation (1s, 6 mW, 20x obj) containing blue: genomic MRSA target and red: genomic SA control. Insert contains raw SERS spectra. Both used template concentration of 1.2 x 10^{-10} g mL^{-1} Each bar represents 4 x 5 replicates and error bars ± one standard deviation.

A clear distinction between the full assay using target MRSA and the SA control samples was obtained, with a 7.2 times difference obtained at 1650 cm^{-1}. These results demonstrate the selectivity of the TaqSERS assay since specific amplification and hybridisation of the *mecA* TaqSERS probe was observed between similar genomic strains. The higher SERS responses obtained from samples containing MRSA strain indicate preferential binding of the probe with consequently increased digestion and signal build-up. The weak control signal can be attributed to the non-specific digestion of the probe and inefficient probe removal, as discussed in section 5.3.

To further demonstrate the amplification and subsequent probe hybridisation within the TaqSERS assay, gel electrophoresis was undertaken using the PCR products from the MRSA and SA samples. A microfluidic-based gel platform (Agilent 2100 bioanalyzer) enabled sizing and quantification of PCR products through generation of an electropherogram. Marker samples were also incorporated into the gel to enable sizing of the DNA sequence samples. Results are shown in Figure 5.15, marker bands are depicted by green and purple peaks at 15 and 1500 bases respectively.

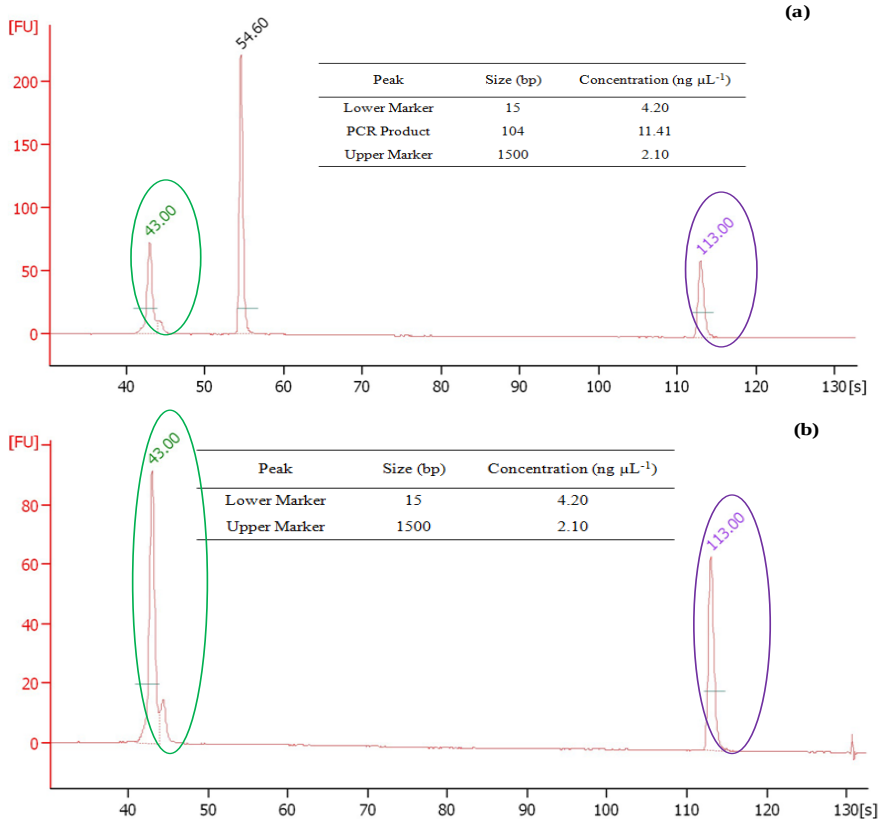

Figure 5.15: Electropherogram and quantitative data of **(a)** MRSA and **(b)** SA PCR product. Green and purple circles highlight lower and upper marker peaks.

An intense peak present within the MRSA electropherogram shows specific amplification of the *mecA* gene region within the MRSA strain has occurred. Quantitative analysis also indicated that the generated PCR product was approximately 104 bases, corresponding to the template amplification region. No product peaks were obtained from the SA control, supporting the SERS results and illustrating no amplification of the control has taken place. These results also demonstrate efficient PCR has been accomplished within the TaqSERS assay.

5.5.1 Specific Detection of SA using *femA-SA* Probe

The TaqSERS assay was also used as a method for the detection of the SA strain using another TaqSERS probe. To enable distinguishable sequence detection, a different fluorophore dye, 5-(and 6-)-carboxyfluourescein (FAM), was incorporated onto the 3' end of the probe. Figure 5.16, shows the structure of the FAM dye as well as the generated SERS spectra obtained using 514.5 nm excitation wavelength.

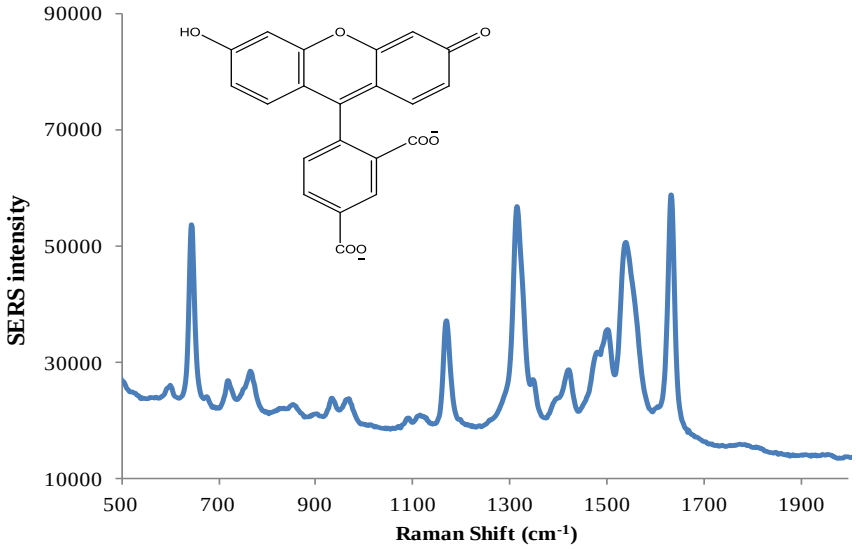

Figure 5.16: SERS spectra recorded using 514.5 nm laser excitation (1s, 6 mW, 20x obj) of *femA-SA* probe containing FAM (final DNA concentration 6.5 nM).

The probe also contained a DNA sequence complementary to the *femA-SA* region. The *femA-SA* gene was chosen as it is contained within both MRSA and SA strains, therefore the TaqSERS assay could differentially determine the presence of both, simultaneously in a multiplex. Probe and primer sequences utilised for detection of the *femA-SA* gene are shown in Table 5.3.

Table 5.3: *femA –SA* oligonucleotide sequences and modifications

Name	***Sequence (5'- 3')***	***5' Modification***	***3'Modification***
femA-SA Probe	TCATTTCACGCAAACTGTTGGCCACTATG	Biotin	HEG-10A-FAM
Forward Primer	TGCCTTTACAGATAGCATGCCA	-	-
Reverse Primer	AGTAAGTAAGCAAGCTGCAATGACC	-	-

The TaqSERS assay was performed utilising the FAM labelled *femA-SA* probe, primers and genomic SA sequence as template. A nonsense sequence, which was non-complementary to

any region within the SA template, was similarly employed as a control. SERS analysis was carried out using 514.5 nm laser excitation with a 1 second accumulation. The average intensity of the principle peak at 1636 cm^{-1} was plotted in Figure 5.17.

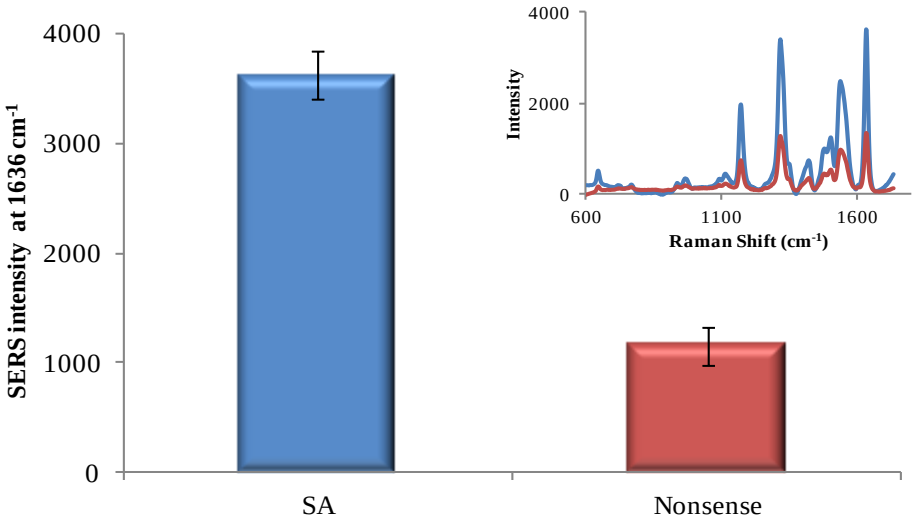

Figure 5.17: SERS spectra recorded using 514.5 nm laser excitation (1s, 6 mW, 20x obj) containing blue: genomic SA target, red: nonsense control. Insert contains raw SERS spectra. Both used template concentration of 1.2 x 10^{-10} g mL^{-1}. Each bar represents 4 x 5 replicates and error bars ± one standard deviation

Distinctive FAM spectra were obtained from SERS analysis of both the SA target and nonsense control. However, significantly stronger signal intensities were obtained from the SA target sample, with a 3.2 times difference. These results have shown that significant differences in intensity can be generated from the assay utilising the *femA-SA* probe as well as the *mecA* probe, demonstrating the versatility of the TaqSERS assay. Consequently, as the detection of both probes was shown to be successful, multiple sequence detection was investigated by SERS analysis.

5.6 Multiple Strain Detection

Conventional DNA detection methods are often performed using fluorescence spectroscopy and quantitative PCR. Fluorescence detection offers many advantages including a large number of available dye labels and low sensitivity with single molecule detection achievable.[117,118] Spatial multiplex analysis of DNA has been shown through use of array based fluorescence,[154] however, multiple analyte detection is limited due to the generation of

broad overlapping spectra, reducing the number of fluorophore-labelled oligonucleotides that can be analysed at one time. SERS is considered to be a powerful analytical technique with the potential to simultaneously discriminate between several targets. The spectra generated by SERS analysis produce sharp, narrow bands distinctly unique to specific molecules. Therefore, molecular identification and structural assignments can be made easily with minimal peak overlap.[101] Commercially available fluorescent labels have been widely utilised in SERS analysis due to the quenching of fluorescence emission by the metal surface.[20]

SERS analysis was performed using a TAMRA labelled *mecA* probe and a FAM labelled *femA-SA* probe, before performing the TaqSERS assay to determine the multiplexing potential of both probes. Citrate-reduced silver nanoparticles were mixed with the dye-labelled probes and aggregated using spermine immediately prior to SERS analysis. A laser excitation wavelength of 514.5 nm was utilised to generate strong responses from both dyes. The duplex spectra obtained from combination of the TAMRA and FAM probes as well as the individual spectra for each dye is shown in Figure 5.18.

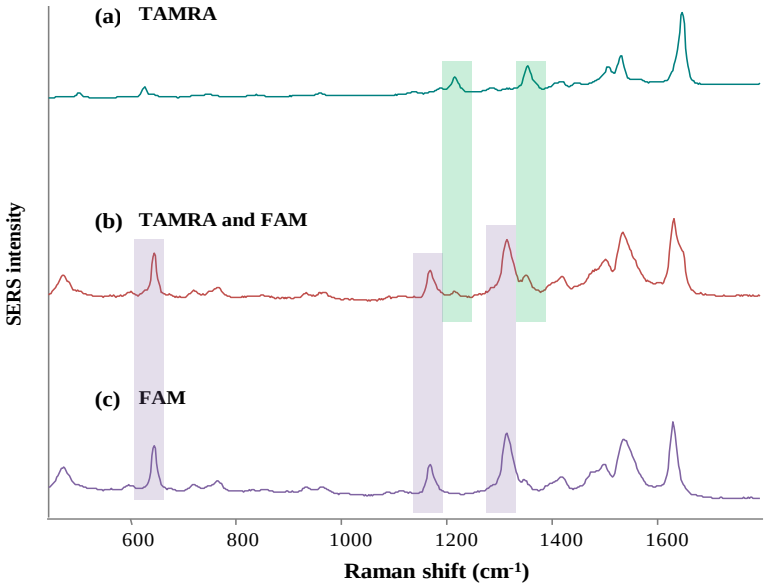

Figure 5.18: SERS spectra recorded using 514.5 nm laser excitation (1s, 6 mW, 20x obj) showing **(a)** TAMRA spectra, **(b)** TAMRA and FAM duplex spectra, **(c)** FAM spectra. Distinctive TAMRA peak at 1220 cm^{-1} and FAM peak at 1170 cm^{-1} shown within multiplex spectra

The discrimination of both TAMRA and FAM peaks can be clearly identified by eye, with numerous peaks unique to each dye within the duplex mixture. In this study, the TAMRA

peak at 1220 cm^{-1} and FAM peak at 1170 cm^{-1}, were chosen to give distinguishable peaks for multiplex analysis and data interpretation. The ease of SERS discrimination between the *mecA* and *femA-SA* probe enabled the TaqSERS assay to be performed with the aim of multiple strain discrimination. Equal concentrations of both probes and primers were added to the PCR mixtures, with the addition of different template sequences. The template DNA used 60 ng/µL of genomic MRSA or SA and a non-complementary nonsense sequence was used as a control. After PCR and a streptavidin bead washing step was carried out, the sample mixtures were analysed by SERS through addition of silver nanoparticles and spermine.

The intention of the multiplex TaqSERS assay was to obtain distinctive SERS spectra from each sample. The presence of both the *mecA* and *femA-SA* regions within the MRSA sequence should generate a duplex spectra as a result of hybridisation of the TAMRA and FAM probes. Genomic SA contains only the *femA-SA* gene, thus through *mecA* probe removal in the bead washing step, a predominately FAM spectra would be expected. The nonsense sequence was non-complementary to both probe sequences and should produce minimal SERS responses from either dye. Therefore, if MRSA was present a signal from both TAMRA and FAM would be observed, whereas, if SA was present, only FAM signal should be observed. However, the SERS spectra of the three sample mixtures in Figure 5.19, demonstrated unexpected results.

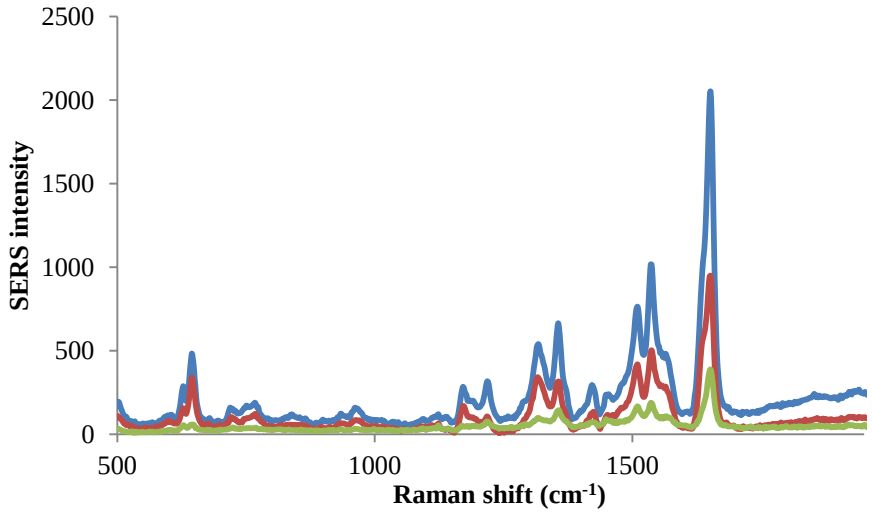

Figure 5.19: SERS spectra recorded using 514.5 nm laser excitation (1s, 6 mW, 20x obj) containing blue: genomic MRSA target; red: genomic SA control; green: nonsense sequence. All samples contain both *mecA* and *femA-SA* probes. Each spectra was generated from 4 x 5 replicate samples.

Analysis of the spectra by eye shows that dominant peaks corresponding to both the TAMRA and FAM dye labels were obtained in all three samples. Previous results have demonstrated that due to a combination of non-specific probe digestion by the polymerase enzyme and incomplete removal of uncleaved probe through the biotin-streptavidin interaction, a low intensity multiplex signal would be expected within the nonsense control. The SA sample lacks the methicillin resistant region, therefore, the TAMRA labelled *mecA* probe should produce minimal intensity signals within a FAM dominated spectra as a result of specific hybridisation of the FAM labelled *femA-SA* probe. However, results demonstrated the presence of intense FAM and TAMRA peaks within the SA sample.

Consequently, distinctive spectra from each template could not be visually obtained, however, the relative intensity of the peaks within the spectra varied between samples. This can be clearly seen in Figure 5.19, when comparing the TAMRA peak at 628 cm^{-1} and the FAM peak 645 cm^{-1}. The spectra obtained from analysis of genomic SA sample demonstrated an increase in peak height ratio between the peaks compared to the MRSA sample peaks. The reduction in the height of the TAMRA peak within the SA spectra appears to show less TAMRA labelled probe has remained within the supernatant and distinguishes the generated spectra from MRSA spectral responses. This trend was demonstrated throughout the spectra, including peak ratios of TAMRA and FAM peaks at 1220 cm^{-1} and 1170 cm^{-1} as well as 1650 cm^{-1} and 1636 cm^{-1}.

To determine whether these small differences could be resolved to discriminate each template sample chemometric analysis was performed on the data. Principle component analysis (PCA) was used to convert the SERS analysis data into a set of linearly uncorrelated variables, i.e. principle components. This method uses orthogonal linear transformation to convert data sets into a new coordinate system such that the greatest variance in the data comes to lie on the first coordinate, principle component 1 and the second greatest on the second coordinate, principle component 2 and so on. Two principle components were calculated from the data sets, with principle component 1 giving the largest possible variance.

Loading plots for the principle components were calculated and demonstrate the variances in spectral data through correspondence to positive and negative correlations (Figure 5.20). The peaks above 0 show a positive correlation for the allocated principle component and peaks below 0 demonstrate a negative correlation.

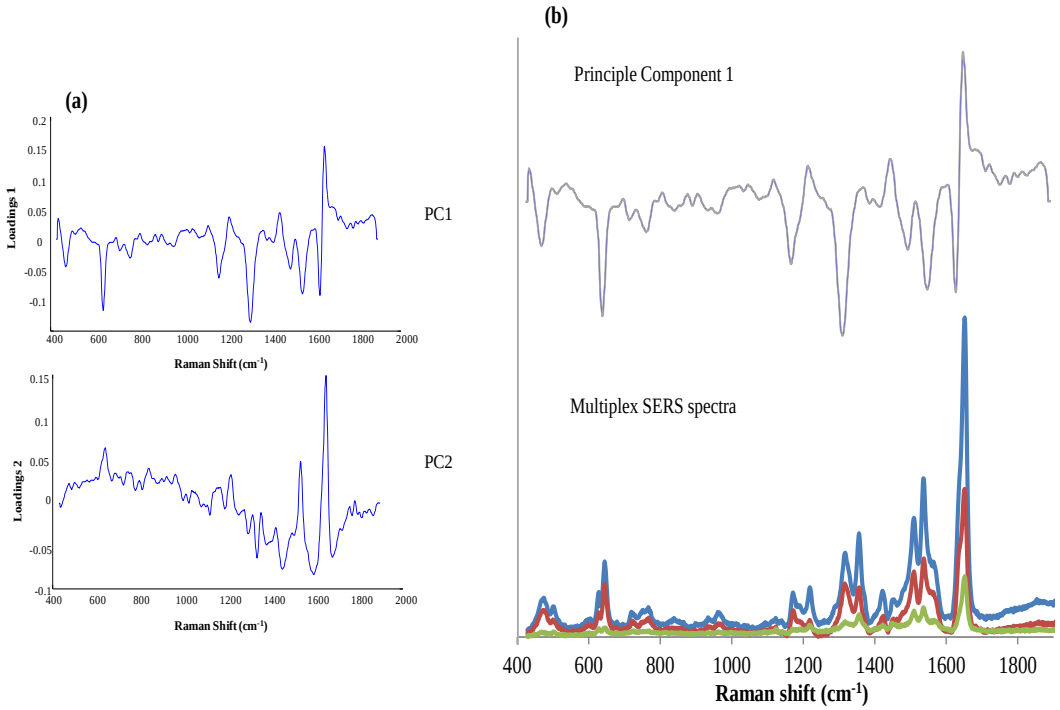

Figure 5.20: (a) Loading plots for principle components 1 (PC1) and 2 (PC2), illustrating the positive and negative correlations of each component and **(b)** Comparison of peaks in PC1 and raw SERS multiplex spectra

Amalgamating principle components 1 and 2, generated a data plot which combined points with similar loadings (Figure 5.21). This enabled any sample discrimination due to the varying of relative peak heights to be clearly determined.

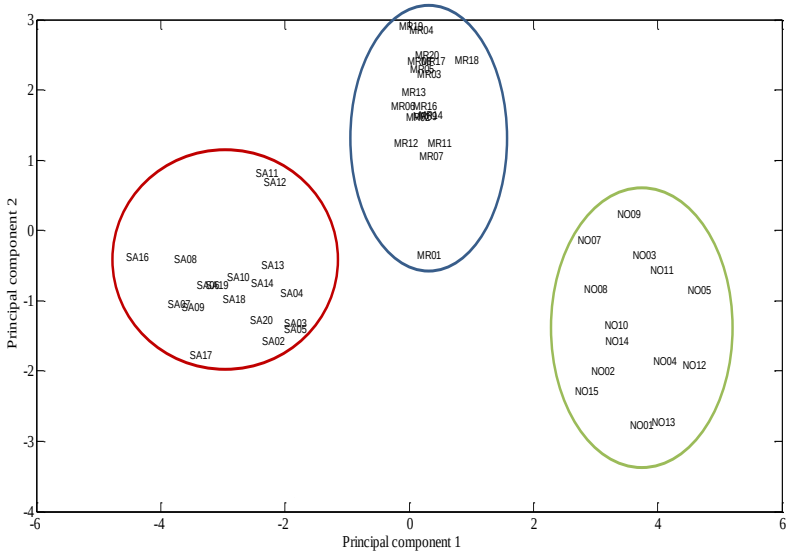

Figure 5.21: Principle component plot containing data points for blue: genomic MRSA target (MR), red: genomic SA control (SA), green: nonsense control (NO). Template conc. of 1.2 x 10^{-10} g mL^{-1}.

Both principle components were plotted in Figure 5.21, illustrating distinctive variances within each data set. Results illustrate that each template sample generated similar principle component values and the MRSA, SA and nonsense template samples can be evidently grouped together. This data analysis method has shown that multiple strain detection within the TaqSERS assay is achievable through use of chemometric analysis.

5.7 Quantitative Detection of Multiple Probes

Quantitative SERS analysis was performed on the *mecA* and *femA-SA* probes within the duplex spectra. The detection limit for each probe within the multiplex was determined through decreased concentrations by serial dilutions with DEPC water and determination of the intensity of specific dye peaks. Figure 5.21, illustrates a typical SERS spectra obtained using 514.5 nm laser excitation of the TAMRA and FAM duplex. Previous, analysis used the dominant 1650 cm^{-1} TAMRA peak (*mecA* probe) and 1636 cm^{-1} FAM peak (*femA-SA*) for quantification, however, within the duplex spectra these peaks are difficult to differentiate. Therefore, distinct peaks for TAMRA at 1220 cm^{-1} and FAM at 1170 cm^{-1} were used for multiple probe analysis.

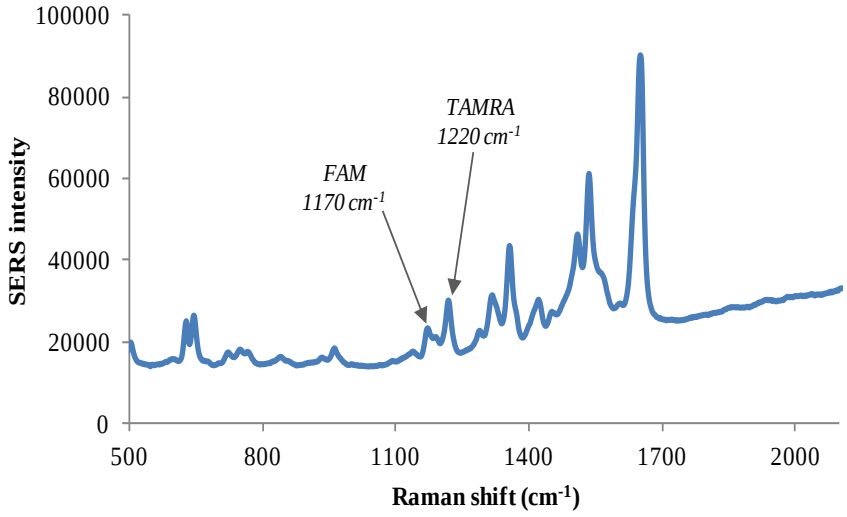

Figure 5.21: SERS spectra of TAMRA (1220 cm^{-1}) and FAM (1170 cm^{-1}) duplex obtained using 514.5 nm laser excitation (1s, 6 mW, 20x obj), with corresponding dye peaks (combined final probe concentration 6.4 nM).

A multiplex concentration study was performed by premixing equal concentrations of the *mecA* and *femA-SA* probes. To the probe mixture, 0.1 M spermine, water and silver citrate-reduced colloid were added to enable strong SERS detection. For each data point, the

concentrations of both probes were decreased with the ratio of probes to each other always being 1:1. Each sample was analysed 5 times to obtain the average intensity for the determined peak for each dye. The average SERS intensities were plotted against probe concentration as shown in Figure 5.22.

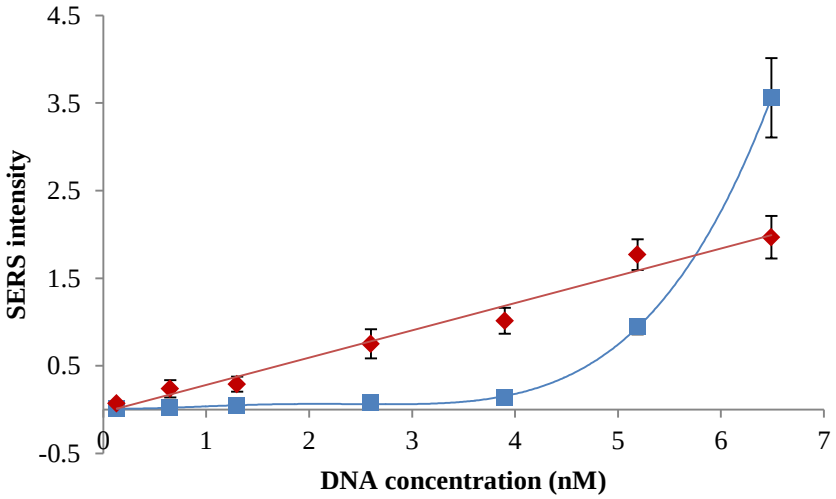

Figure 5.22: Dilution series of multiplex with the SERS peak intensity of blue: TAMRA dye (1220 cm^{-1}); red: FAM dye (1170 cm^{-1}) plotted against DNA probe concentration, obtained using 514.5 nm laser excitation (1s, 6 mW, 20x obj). Represent mean of 5 x 5 replicates and error bars ± one standard deviation.

Previous studies have demonstrated linear responses from the individual detection of TAMRA and FAM labelled oligonucleotides using silver citrate nanoparticles and SERS.[101,104] This study has also demonstrated the generation of linear responses using silver EDTA nanoparticles from the individual SERS analysis of TAMRA and FAM labelled DNA sequences (see Chapter 4).[50]

The FAM labelled *femA-SA* probe generated a linear plot over the analysed concentration range as expected. However, the TAMRA labelled *mecA* probe produced a curved plot (Figure 5.23, *blue plot*). This curved TAMRA plot was consistently obtained through SERS analysis of the combined *mecA* and *femA-SA* probes. Whereas, SERS analysis of the individual TAMRA labelled *mecA* probe over the same concentration range generated a linear response (Figure 5.23, *green plot*).

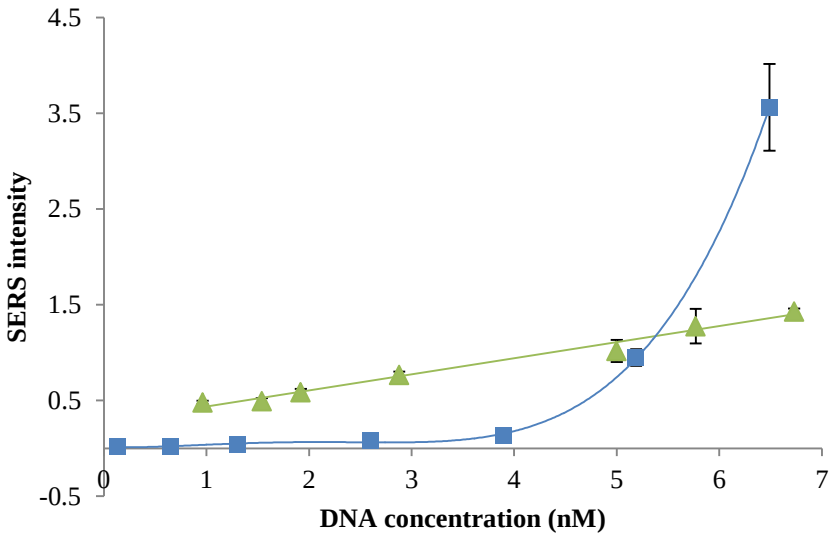

Figure 5.23: SERS plots of 1220 cm^{-1} TAMRA peak against DNA probe concentration, blue: TAMRA /FAM duplex, green: individual TAMRA probe obtained using 514.5 nm laser excitation (1s, 6 mW, 20x obj). Points represent mean of 5 x 5 replicates and error bars ± one standard deviation.

The results obtained in Figure 5.22 and 5.23, indicate that at concentrations below 5 nM the TAMRA signal from the *mecA* probe is reduced at lower concentrations as a result of the presence of the FAM labelled *femA-SA* probe. However, as the probe concentration is increased above 5 nM the signal intensity from the TAMRA labelled probe is significantly enhanced within the duplex in comparison to the responses from the individual TAMRA probe. This demonstrates that two distinct adsorption processes are occurring depending on the probe concentration. To gain an understanding of this interaction and the resultant SERS responses, further investigation was performed.

Initially, the SERS spectra generated from the probe dilution study were analysed to establish any spectral changes over the concentration range. Results indicated that a corresponding decrease in background fluorescence as well as TAMRA signal was obtained as the probe concentration decreased. This can be observed from the spectral background between 1650 and 2250 cm^{-1} in Figure 5.24, as the multiplex probe concentration is reduced the baseline and TAMRA signals diminish.

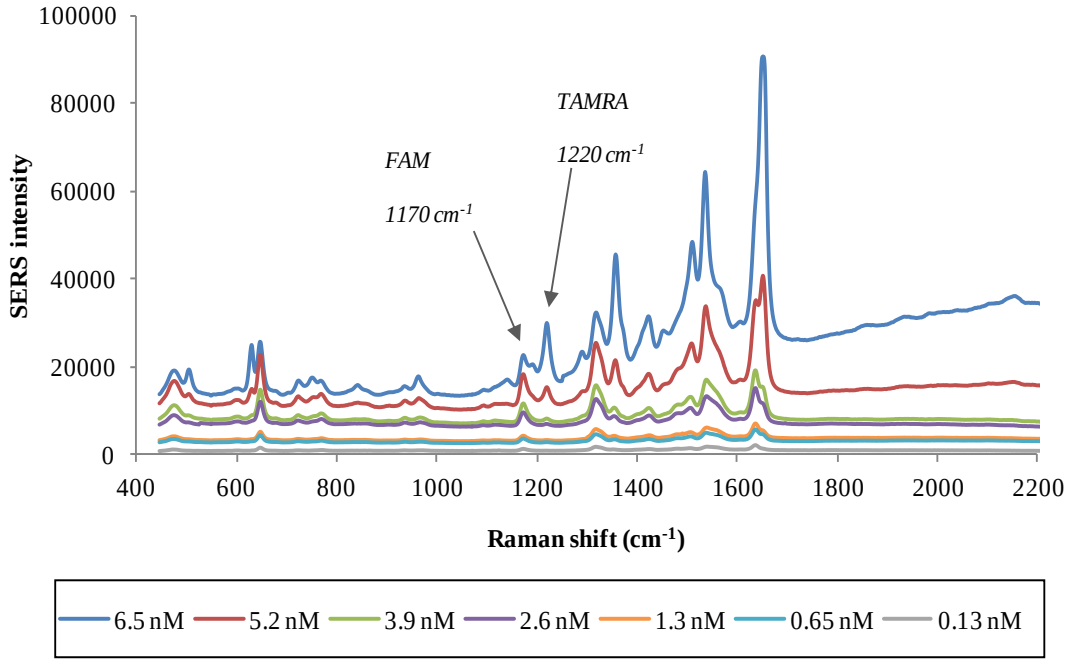

Figure 5.24: SERS spectra of *mecA* and *femA-SA* probe duplex over concentration range obtained using 514.5 nm laser excitation (1s, 6 mW, 20x obj). The raw spectra shown were not baseline corrected.

To clearly highlight this observation, two points, 1000 and 1700 cm^{-1}, on the spectral baseline were plotted and are shown in Figure 5.25. The plots generated demonstrate that at probe concentrations below 4 nM, the spectral baselines and probe concentration increases linearly at both 1000 and 1700 cm^{-1}. However, as the concentration of probes increase the generation of enhanced fluorescence at 1700 cm^{-1}, which can be attributed to the TAMRA dye becomes evident. Interaction of dye labelled oligonucleotides close to a metal surface will result in either fluorescence quenching or electromagnetic enhancement. The quenching process generally occurs within 5 -10 nm of the planar metal surface, whereas enhanced fluorescence can be generated at tens of nanometers from the surface.[155] Therefore, these results suggest that as the DNA concentration is increased above 4 nM, multi layers of probe are covering the nanoparticle surface. Strong SERS signals from the TAMRA dye are generated from the layer directly adsorbed onto the surface and enhanced fluorescence is produced from subsequent probe layers which lie further from the metal surface. This suggests that at higher probe concentrations monolayer coverage of the nanoparticle surface has been achieved, preferentially enhancing the SERS responses from the TAMRA labelled probe.

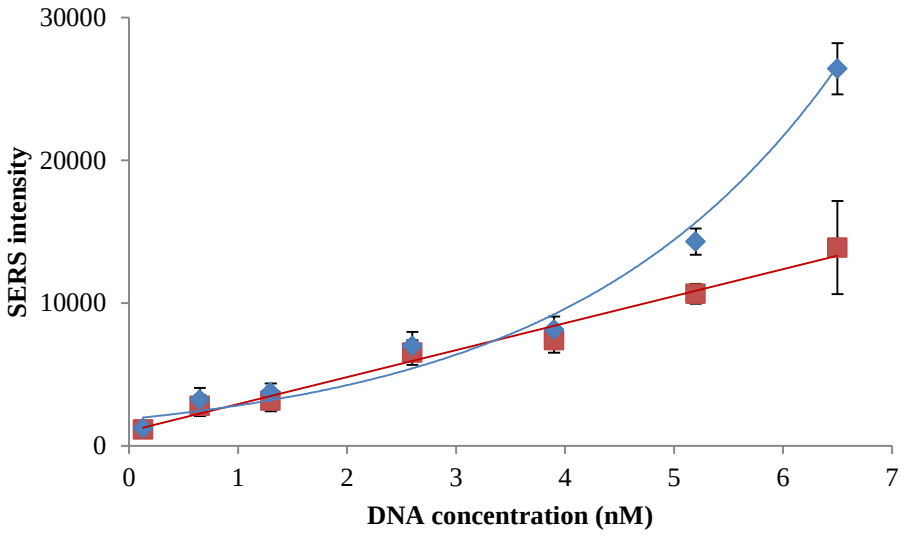

Figure 5.25: SERS intensities of the background signal of *mecA* and *femA-SA* probe duplex over concentration range at blue: 1700 cm^{-1} and red: 1000 cm^{-1} obtained using 514.5 nm laser excitation (1s, 6 mW, 20x obj).

One theory which may explain these results is that the probes are forming mixed clusters prior to adsorption onto the nanoparticle surface. The use of excess spermine in the analysis mixture reduces the charge on the DNA enabling probe interactions to occur. The results suggest the cluster formation preferentially positions the FAM probe onto the surface enabling strong SERS responses whilst inhibiting the adsorption of the TAMRA probe. This would account for the low TAMRA SERS and fluorescence responses obtained. However, an increase in the probe concentration forces reorganisation of the mixed cluster layers, allowing the TAMRA closer to the enhancing surface. This results in higher TAMRA SERS responses and production of enhanced fluorescence from the TAMRA dye to be observed.[156,155] Cluster formation would enable comparatively even surface coverage at low probe concentrations. This would account for distinctive FAM spectra being observed at DNA concentrations below monolayer coverage of the nanoparticle surface.

To gain a further understanding of the probe interactions, sequential analysis of the probes was investigated. The study of multiple probes has so far analysed sequences which had been premixed prior to SERS detection. However, the preferential surface adsorption of the probes was analysed by incorporating the individual probes separately into the SERS analysis mixture. The primary probe was initially analysed by addition of aggregated silver nanoparticles and collection of the SERS spectra at 0 minutes (t = 0). After initial spectral collection, the second probe was added. Spectra were then collected at 5 minute intervals for

25 minutes (t = 5 – 25). Two concentrations of each probe were analysed; 6.5 nM and 1.3 nM. These were chosen to enable analysis of interactions at both ends of the curved TAMRA plot in Figure 5.22. Figure 5.26 illustrates the SERS spectra generated from analysis of the *mecA* and *femA-SA* probes at concentrations of 1.3 nM. Whereas, Figure 5.27 demonstrates the spectral responses for the higher concentration of probe, 6.5 nM. For each concentration two data sets are shown, one was obtained through initially adding the TAMRA probe and the other by initially adding the FAM probe.

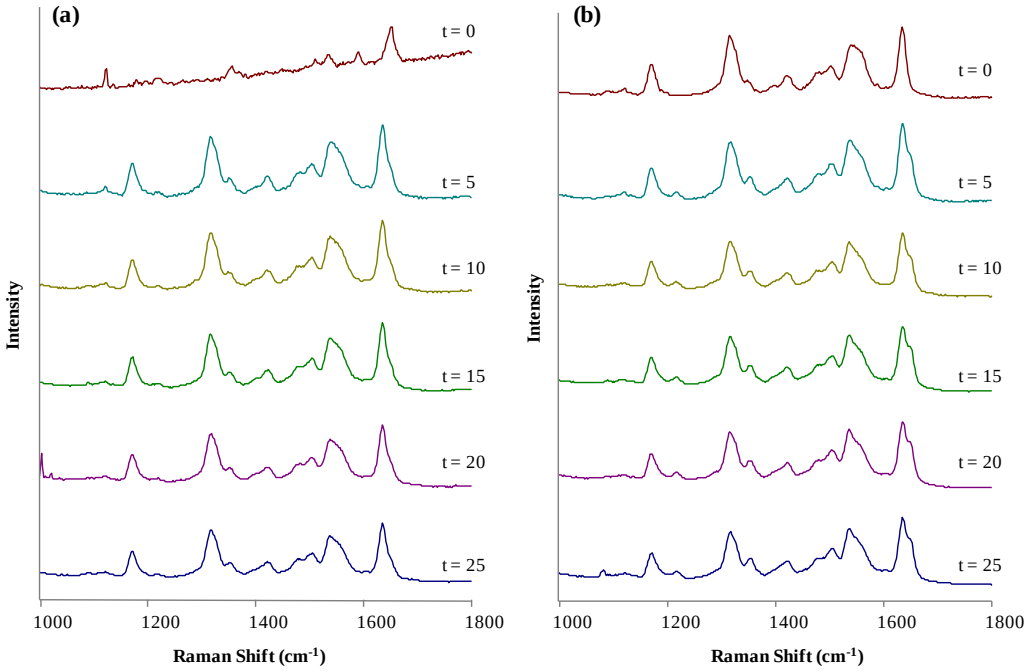

Figure 5.26: SERS plots over 25 minutes containing 1.3 nM of **(a)** TAMRA probe added initially **(b)** FAM probe added initially. t = 0 mins contained only primary probe, t = 5 mins onwards contained both probes obtained using 514.5 nm laser excitation (1s, 6 mW, 20x obj).

Analysis of the probes at the lower concentration of 1.3 nM, illustrated that the initial addition of the TAMRA labelled probe generated distinctive spectra at 0 minutes (Figure 5.26(a)). However, when the FAM labelled probe was added the TAMRA signal was completely replaced by FAM spectra, illustrated by distinctive FAM peaks at 1636, 1319 and 1170 cm^{-1}. The FAM spectra dominated in all subsequent spectra within the time study. This suggests the FAM probe is inhibiting TAMRA signal emission by displacing the TAMRA probe from the surface. Conversely, when the FAM probe was added to the SERS analysis mixture first, clear FAM spectra were obtained (Figure 5.26(b)). After addition of the *mecA* probe distinctive TAMRA peaks can be visualised within the duplex spectra from t

= 5 minutes. The appearance of the TAMRA peak at 1220 cm^{-1} and the shoulder peak at 1650 cm^{-1} from 5 minutes onwards clearly demonstrates the presence of the *mecA* probe. Although, these distinctive TAMRA peaks increase in intensity over time, duplex spectra from both probes were consistently observed over the study.

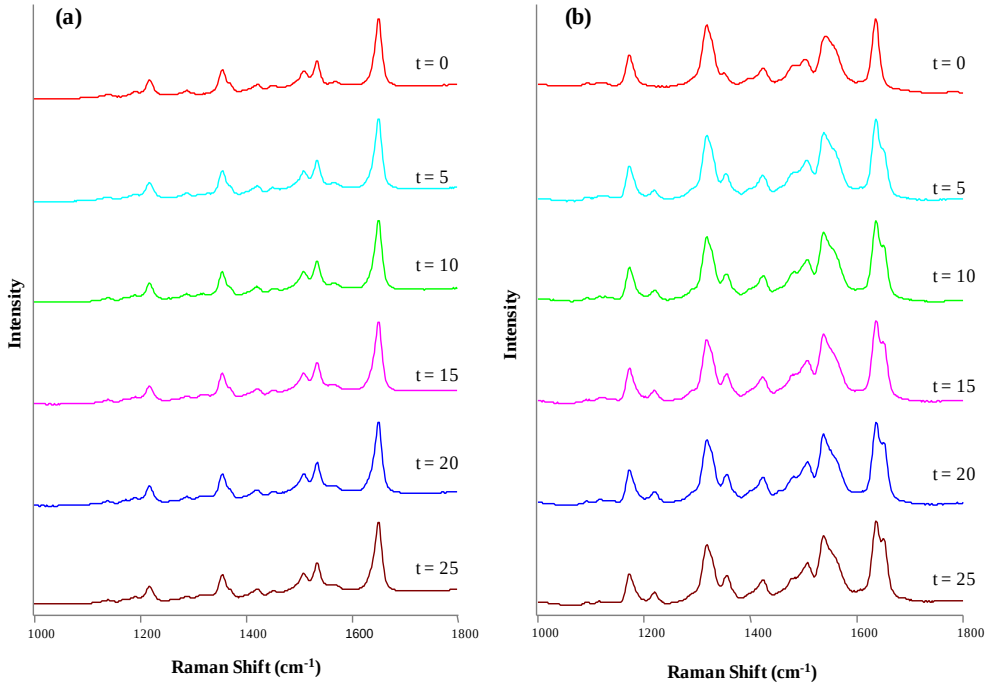

Figure 5.27: SERS plots over 25 minutes containing 6.5 nM of **(a)** TAMRA probe added initially **(b)** FAM probe added initially. t = 0 mins contained only primary probe, t = 5 mins onwards contained both probes obtained using 514.5 nm laser excitation (1s, 6 mW, 20x obj).

Analysis of the probe responses at the higher concentration of 6.5 nM, illustrated that TAMRA signals were significantly stronger compared to results for lower probe concentrations. When the TAMRA labelled probe was initially added to the silver nanoparticles, a characteristic TAMRA spectra was obtained (Figure 5.27(a)). After addition of the *femA-SA* probe no clear or distinctive FAM peaks within the spectra were observed after 25 minutes. Whereas, characteristic TAMRA peaks were increasingly observed when the FAM probe was added first (Figure 5.27(b)). Strong TAMRA peaks at 1220 and 1650 cm^{-1} can be clearly visualised after *mecA* probe addition from the 5 minute SERS spectra. Over time the intensity of these distinctive TAMRA peaks increased, suggesting that at higher concentrations preferential binding of the *mecA* TAMRA probe has occurred.

These results have defied standard SERS theory, in that the expected linear SERS responses from the adsorption of labelled oligonucleotides onto silver nanoparticle surfaces was not obtained. The collected data strongly implies that an interaction between the probes is occurring within this system to generate the spectra obtained. At higher probe concentrations a complex multi-layer appears to have formed, which changes the orientation of probes on the nanoparticle surface. The probes are driven to attach to the metal surface through attachment of the nucleobases, therefore, an increase in probe concentration will generate a shift in the packing of the surface adsorbed sequences. This appears to result in closer stacking of the probes, possibly fabricating a perpendicular probe alignment on the surface. This would arrange the TAMRA label in an orientation which generates enhanced SERS responses. When lower concentrations of the probe were present, it is assumed that the nanoparticle surface had below monolayer coverage and would enable equal surface binding of the probes. However, FAM responses overwhelmed the spectra obtained with only weak TAMRA signals observed. Previously, TAMRA labelled oligonucleotides have demonstrated linear responses at submonolayer concentrations (below 10^{-8} mol dm^{-3}), with a degree of curvature introduced into the concentration plot as the DNA concentration is increased.[61] These results suggests that probe interaction is occurring at lower concentrations which is preferentially enhancing the FAM signals whilst inhibiting the TAMRA probe, through diminished SERS responses.

The three possible interactions which could be occurring are DNA-DNA, DNA-dye or dye-dye interactions. The interaction of the bases within the two DNA sequences was shown to be highly unlikely by analysing the DNA sequences utilising computational analysis from integrated DNA technologies (IDT) (Figure 5.28).

The *mecA* probe generates one possible secondary structure through formation of a small loop within the sequence, however, sufficient single stranded regions remain free to promote surface adsorption. Likewise, the *femA-SA* probe produces two similar secondary structures which are likely to result in negligible hindrance to the surface adsorption. Minimal formation of secondary structure within each probe as well as interaction between individual sequences was determined (IDT analysis).

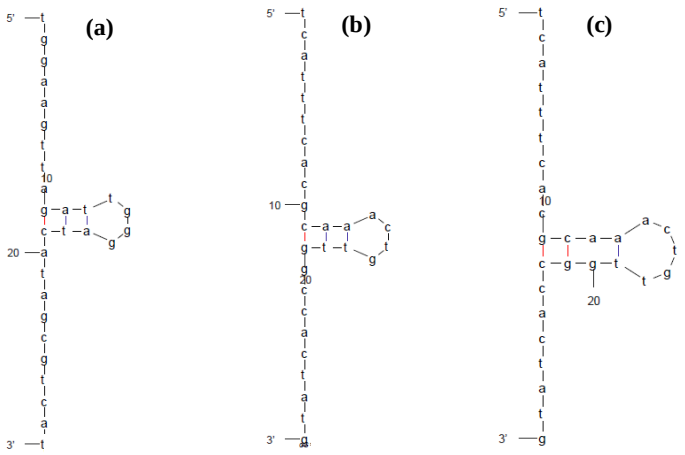

Figure 5.28: Secondary structures formed with **(a)** *mecA* probe, **(b)** and **(c)** *femA-SA* probe.

Therefore, probe interaction appears to be directed through the dye labels. Previous studies have demonstrated the interaction of TAMRA and FAM dye labelled sequences through FRET.[33] An energy transfer occurs from the emission of energy from the FAM dye which is quenched through absorption by the TAMRA dye. This mechanism is strongly dependant on the distance between the dyes, therefore the dyes must be held within close proximity to generate this strong interaction. However, within this system the results obtain do not suggest a FRET interaction between the dyes. The signal from the FAM dye is not inhibited which would be expected from a FRET interaction, therefore, to gain a fuller understanding of probe interactions in this system further investigation would be required to obtain a confident conclusion.

An alternative proposal for the unexpected TAMRA response within the multiplex sample is through intrinsic difference in Raman intensities characterised by Raman cross section of the dyes. Previously, the cross section of the Raman active dyes have been determined.[157] In the 1980s, Pettigner *et al.* and Hildebrandt *et al.* independently reported the Raman cross section of rhodamine 6G at sub-monolayer coverage on aggregated silver colloid to be on the order of 10^{-16} cm^2 per molecule.[158,159] However, determining the cross section of a molecule can be rigorous as a number of factors and calculation have to be considered to produce precise solutions.[160] Analysis of individual TAMRA and FAM dyes at the same concentration and using the same SERS reagents and instrumentation, demonstrated higher intensity responses for the TAMRA label (Figure 4.14). However, within this system FAM signal intensities dominated at lower concentrations and appeared to displace the TAMRA probe from the nanoparticle surface. Therefore, it seemed that the Raman intensities from either dye may

contribute to the obtained results but it is unlikely that this effect would fully elucidate the results.

These results have illustrated a fresh perspective on the detection of labelled oligonucleotides. The data obtained strongly suggest an interaction between the TAMRA labelled *mecA* probe and FAM labelled *femA-SA* probe is occurring through a dye interaction, which significantly affects the SERS responses generated. Interactions on this scale are extremely difficult to monitor and analyse, however, SERS has enabled an insight into this process to be proposed. To improve the obtained conclusions further investigation must be undertaken.

5.8 Chapter Conclusion

A novel DNA detection method was developed through adapting a TaqMan assay to give SERS detection which has enhanced the sensitivity whilst maintaining the selectivity of the assay. Quantitative SERS responses were obtained from the TaqSERS assay showing increased sensitivity over comparable fluorescence analysis by over an order of magnitude. Significantly distinct SERS signals were obtained from the detection of the *mecA* and *femA-SA* gene from two different genomic strains, methicillin resistant *Staphylococcus aureus* (MRSA) and *Staphylococcus aureus* (SA), when compared to a control sequence. Incorporation of SERS analysis generates the potential for multiple target strains to be detected due to the molecularly specific narrow spectral bands obtained. The assay has demonstrated the selective detection of both probes within a single reaction mixture. Principle component analysis (PCA) enabled individual genomic strains to be differentially detected *via* specific hybridisation of the TAMRA labelled *mecA* probe and FAM labelled *femA-SA* probe. These results show the applicability that the TaqSERS assay has to be utilised for detection of multiple clinical samples in situ.

The SERS analysis of the combined TAMRA labelled *mecA* and FAM labelled *femA-SA* probes demonstrated unexpected results. The data indicates that in the presence of the FAM probe the TAMRA probe is being inhibited and under some circumstances completely displaced from the surface. However, this effect reverses as the concentration of probe increases. It appears that the formation of a complex multilayer forces probe rearrangement to occur, significantly enhancing the SERS responses from the TAMRA label. This interaction effects the SERS intensity obtained from individual probes, which may account for the presence of *mecA* probe signals within SA and nonsense samples when performing

the multiplex TaqSERS assay. Results suggest that when both probes are incorporated at a concentration of 6.5 nM, the TAMRA peaks dominate the spectra. Therefore, repeating the multiplex assay using lower probe concentrations might enable distinctive strain discrimination to be established without the need for chemometric analysis.

5.9 Further Work

Surface enhanced Raman scattering (SERS) detection of DNA sequences using the novel TaqSERS assay can be developed further by advancing the detection of multiple sequences simultaneously. The ultimate aim of this study would be to demonstrate the diagnostic application of the TaqSERS assay through real clinical samples. Therefore, the multiplexing capabilities of SERS should be further exploited to extend the number of detectable disease strains. The TaqSERS assay has demonstrate the successful detection of MRSA and SA strains, therefore, this could be extended to triplex detection of Staphylococcus epidermis (SE) through addition of a *femA-SE* probe. However, careful consideration would need to be given to the design and dye incorporation of the probe.

This study has demonstrated the complex interactions which occur within SERS analysis mixtures. Interactions on this scale are extremely difficult to fully understand, however, SERS has enabled an insight into this process to be gained. To investigate this further, a study should be performed increasing the probe concentration range studied to enable a full overview of the process to be obtained. To achieve a greater insight into the interaction, modified probes would be implemented into the assay. Modified probes which did not contain dye labels would enable verification of probe interactions being directed through the dye labels. This work should be continued to compare the SERS responses obtained through altering probe design to narrow the possibly of a dye-dye or dye-DNA interaction. It is unlikely that an absolute understanding of this concept will be attained. However, further work will enable confident proposal of a working theory, enabling a highly valuable understanding of DNA detection by SERS to be achieved.

6. Detection of DNA on Solid Substrates using SERS

The detection of specific oligonucleotide target sequences utilising surface arrays has rapidly evolved in recent years.[43] DNA surface detection techniques are routinely used for the identification of specific nucleic acid sequences, generating large quantities of DNA analysis information, unparalleled within solution based methods. One such methods is the DNA microarray, which has enabled large quantities of unlabelled DNA to be detected through molecular specific hybridisation.[51,161,162] The orderly and systematic arrangement of large numbers of oligonucleotides on a solid substrate enables selective detection through the principle of DNA hybridisation (Section 1.4.2). Single stranded target DNA sequences are immobilised on a solid surface, generally glass, plastic or silicon support. In this study epoxysilane coated glass, nylon and nitrocellulose membranes were investigated as potential immobilisation substrates through bulk spotting of target sequences. However, reducing the size of the biosensor array into the low-micron and nanoscale can be valuable, providing lower detection limits for more efficient disease screening. Recently, nanoscale fabrication has been achieved through Dip-pen Nanolithography (DPN). The DPN technique was first reported by Mirkin *et al.* in 1999.[163] This technique utilised the self-assembly of alkanethiols on a gold surface through covalent chemisorptions to successfully pattern nanoscale features of 1-octadecanethiol (ODT) and 16-mercaptohexadecanoic acid (MHA). Throughout the last decade, DPN of alkanethiols has been used for the immobilisation of biomolecules, proving to be an effective combinational nanopatterning and analysis technique.

To enable detection of the surface immobilised DNA, the array is probed with dye labelled DNA sequences. Labelled sequences that are complementary to the target strand will hybridise and are fixed to the surface, whereas DNA strands which are non-complementary will be washed from the surface. This leaves only complementary labelled DNA to be detected. Traditionally, surface array detection methods are detected through colorimetric or fluorescence analysis. Colorimetric analysis is a rapid and simple detection method enabling the distinction of biomolecules through perceived differences in the colour of different samples. Taton *et al*. developed a DNA array which analysed two different DNA targets *via* a two-colour labelling system.[162] 50 and 100 nm diameter gold nanoparticles were functionalised with two different target sequences and immobilised within a three-component sandwich assay using a DNA probe and the DNA targets to be detected. Green

light was observed when 50 nm gold particles were attached to the surface and orange light was observed only from the attachment of 100 nm particles. This successfully allowed oligonucleotide distinctions to be observed. However, this method relies heavily upon individual perception and may become increasingly difficult as the number of dye labelled sequences within one sample grows.

The use of fluorescence for both qualitative and quantitative analysis extends to numerous biological research avenues including cell imagining,[164,165] biomolecule detection assays[166,167] and protein/sugar pathway monitoring.[168] Albelda *et al.* used fluorescent dyes to discriminate DNA sequences based on comparative intensities.[161] In this method, the DNA sequences were labelled with distinctive dyes which generated non-overlapping fluorescent spectra. The labelled oligonucleotides were mixed and hybridised to the DNA on the array surface. The quantity of binding of each probe was dependent on the expression level of the targeted disease enabling specific detection. This two-colour system has been used by Agilent technologies to selectively determine the presence of DNA. Spatial multiplex analysis of DNA has been shown through use of array based fluorescence,[154] however, multiple analyte detection is limited due to the intrinsic spectrum generated by fluorescent dyes being broad and easily obscuring competing signals. Consequently, the number of dyes that can be distinguished within one sample is restricted.

Surface enhanced Raman scattering offers many advantages over these more popular techniques, including low sensitivity, molecularly specific identification and multiple analyte detection. Cao *et. al.* used a three-component sandwich assay in a microarray format to detect multiple target DNA sequences from a solid substrate surface.[51] Gold nanoparticles were modified with Cy 3–labelled alkylthiol-capped oligonucleotides and were used as a probe to monitor the presence of specific target DNA. These functionalised nanoparticle conjugates were immobilised onto an array surface using a split probe hybridisation system. Captured dye labelled particles could then be detected through facilitation of a silver coating promoting SERS signals from the dye. Six different DNA targets with different Raman reporter molecules were distinguished with a 20 femtomolar limit of detection obtained. This approach gives a SERS readout representative of the target analyte present and is often used as a diagnostic analysis tool.

The aim of this study was to develop a membrane assay which utilised SERS for the detection of unmodified target DNA sequences using a simple and cost effective platform.

This body of work investigated the detection of clinically relevant sequences of methicillin resistance Staphylococcus aureus (MRSA) to demonstrate the applicability of the method as a diagnosis technique and demonstrate the advantages over that of fluorescence and colorimetric analysis.

6.1 DNA Probe Detection Assay

A DNA detection assay based on Southern blot analysis and a DNA microarrays was designed to enable the detection of target DNA through SERS analysis. The assay utilised the complementarity of DNA to detect unlabelled and unmodified sequences bound to a substrate surface through hybridisation of a dye labelled DNA probe. A schematic of the surface assay utilised within this study is given in Figure 6.1 and a detailed experimental procedure is outlined in Section 3.7.2.

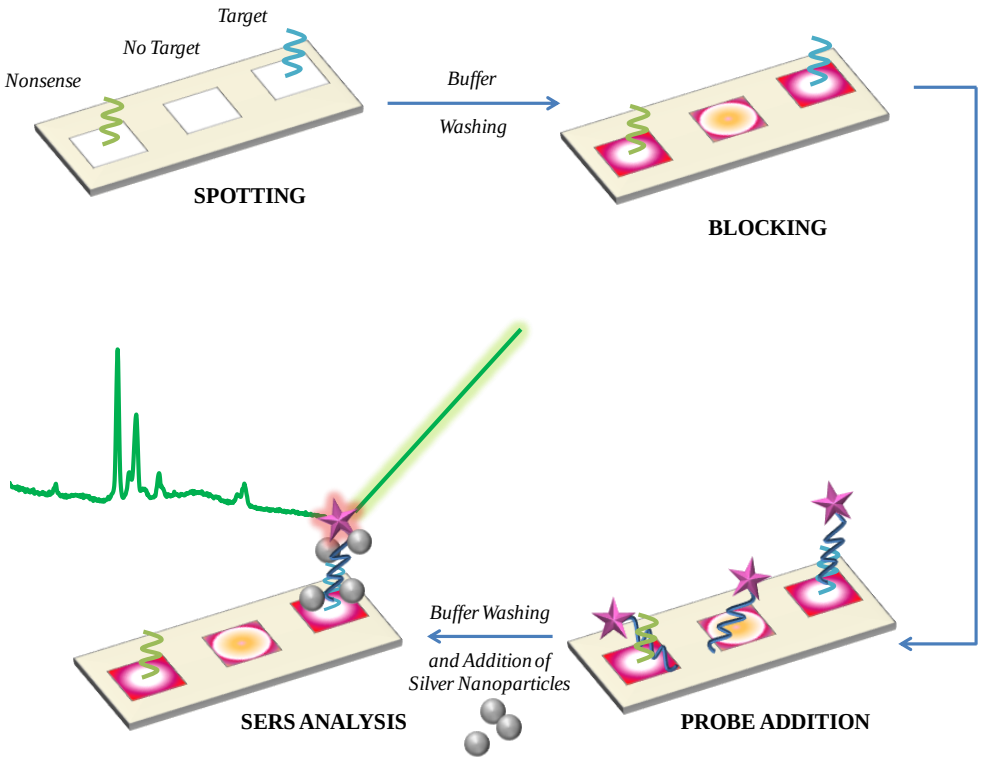

Figure 6.1: Schematic detailing the sequential steps involved in DNA detection surface assay on solid substrate. Spotting – target DNA applied to membrane, Blocking – blocking agent applied to prevent non-specific binding to the surface, Probe Addition - complementary probe added to the surface to bind to target DNA, SERS Analysis – silver citrate nanoparticles added to enable detection of the SERS dye labelled probe. A no target and nonsense control were simultaneously performed which altered only in the spotting step.

A bulk sample of 20 µM target DNA (0.2 µL) was spotted onto the solid substrate (surface functionality used within this study included epoxysilane glass and nitrocellulose membrane). The sequences were fixed through UV-crosslinking and baking at high temperatures (approximately 80 °C). Conventional microarray assays utilise split probe systems which require two specific hybridisation steps. However, this study aimed to reduce the complexity of the assay through investigating a one step hybridisation by directly attaching the capture target sequence to the surface. Comprehensive washing steps were carried out to remove any DNA which was not bound to the substrate. An incubation chamber was used during the surface assay, to enable spatially separate assays to be carried out simultaneously on the surface without the mixing of reagents. This is highly beneficial as multiple samples can be analysed from the same surface without target sequence contamination invalidating results. A blocking agent was then applied to the substrate surface at 50 °C for 60 minutes. This step was to prevent non-specific binding by blocking regions which did not contain bound target DNA. Most common hybridisation assays use long chain sequences, such as salmon or herring sperm DNA to block the surface or long chain ethanolamine molecules.[169,170] To enable detection of the unmodified target sequence, a complementary dye labelled probe was added. The probe was suspended in 0.3 M PBS buffer and was applied to each sample area while heating at 45 °C for 18 hours. Through selective hybridisation the probe binds to the immobilised surface DNA, whilst unbound probe was removed from the surface by a final washing step. In order to carry out SERS analysis of the fluorescent dye, silver citrate-reduced nanoparticles were applied enabling distinctive spectra to be generated and establishing the presence of the target DNA.

To ensure the generated signals were obtained through selective sequence hybridisation, negative control samples were performed in parallel. The two controls consisted of a "no target" area whereby a blank area of the surface had no DNA applied in the initial spotting step and a "nonsense" sequence control in which a separate spot was applied with DNA non-complementary to the detecting SERS probe. The further assay steps remained identical to the target assay. Throughout this study, sample areas will be referred to as target, no target and nonsense.

6.1.1 Surface Detection Assay from Epoxysilane Glass

Initially, the chosen surface substrate for the detection of unmodified DNA was epoxysilane coated glass. The glass slide was coated with a multi-purpose epoxysilane layer which covalently binds biomolecules applied to the surface. The surface epoxy groups enable

amino-modified nucleic acids as well as unmodified DNA sequences to bind with similar efficiency *via* the exocyclic amino groups of the bases or through the hydroxyl groups of the sugar-phosphate backbone. The sequences used through this study are shown in Table 6.1.

Table 6.1: Oligonucleotide sequences and modifications

Name	***Sequence (5'- 3')***	***5' Modification***
Probe	GGTTCATATAGTTATAATAA	TAMRA ITC
Conjugate sequence	GGTTCATATAGTTATAATAA	Thioctic Acid-$(HEG)_3$
Target	TTATTATAACTATATGAACC	-
Nonsense	CAATGTGAAAGGCTGGTTA	-

5-(and-6)-carboxytetramethylrhodamine isothiocynate (TAMRA ITC) labelled DNA sequences were applied to the surface to enable SERS detection. Previous studies have demonstrated strong SERS responses can be obtained through incorporation of TAMRA ITC using 532 nm laser excitation.[153] The surface assay was performed analysing target, no target and nonsense sample regions. Results were generated through multiple SERS maps of replicate areas within each sample. The total sample area was approximately 6 x 6 mm, therefore to obtain an accurate overview of the entire region a minimum of four SERS maps within each sample spot were obtained. Each map took an average of 500 spectra over 100 x 100 μm area and the spectral average was calculated and plotted (Figure 6.2). This data collection method was utilised throughout this study to generate SERS spectra representative of the analysed areas of interest.

TAMRA ITC generates distinctive SERS spectra with the principle peak positioned at 1650 cm^{-1}. However, analysis of the glass slide showed minimal TAMRA ITC signals within the target sample with no SERS peak obtained within the control spectra. The extremely weak SERS spectra and high fluorescence background signals appear to be generated due to increased distances between the dye labelled DNA probe and the nanoparticle surface. SERS enhancement drops off rapidly with distance to the metal surface with more than 90 % of scattering resulting from the first layer of adsorbed analyte.[95,137] Beyond the SERS enhancement distance, a reduced SERS signal is obtained from the dye and fluorescence quenching provided by the roughened metal particles is diminished.

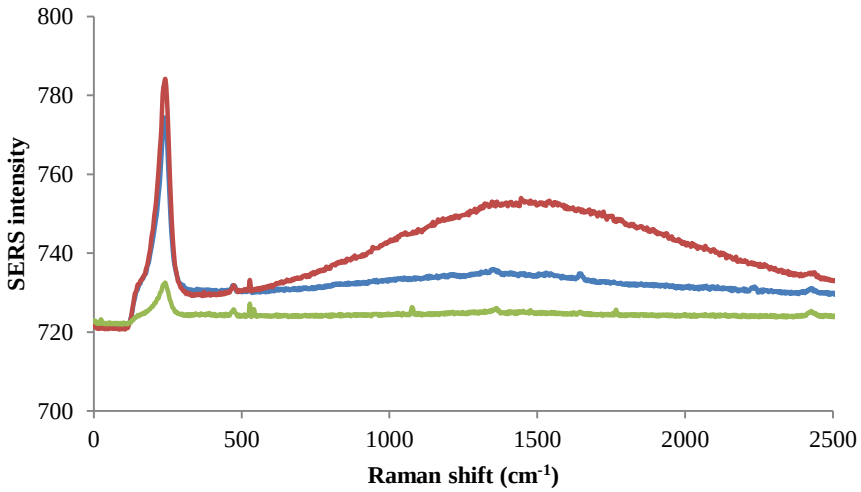

Figure 6.2: SERS spectra of epoxysilane coated glass slide containing TAMRA ITC labelled probe recorded using 532 nm laser excitation (10 x obj., 0.1 sec. acc.) blue: target DNA, red: no target DNA, green: nonsense DNA.

Therefore, these results suggest that the dye label is unable to adsorb onto the nanoparticle surface and be identified by SERS. To overcome this, a new approach was investigated through incorporating the dye labelled probe and metal nanoparticle within one species. This was achieved through synthesis of dye labelled DNA conjugates.

6.2 Functionalised Nanoparticles Preparation and Characterisation

The surface plasmon of silver and gold nanoparticles lie within the visible wavelength region and have been shown to be ideal substrates for SERS analysis. Much research has now focused on the detection and analysis of DNA *via* utilisation of functionalised nanoparticles.[92, 171, 172] These systems consist of metal nanoparticles coupled to modified target sequences and distinct Raman reporter molecules, enabling selective and distinct detection to be achieved. DNA functionalised nanoparticles are often prepared *via* attachment of thiol modified DNA sequences.[51] Modification of nanoparticles with DNA and Raman labels offers several distinct advantages for diagnostic applications. These include SERS signal enhancements and resistance to photobleaching and quenching, due to the close proximity of the SERS active dye to the nanoparticle surface. Also the narrow and specific spectra generated by SERS labels enable multiple dye functionalised nanoparticles to specifically detect a number of target sequences within one sample.

In this study, DNA conjugates were prepared by adsorbing the thiol modified DNA sequence onto bare silver citrate-reduced nanoparticles. The DNA sequence used within the probe

detection assay was redesigned, incorporating a three hexaethylene glycol (HEG) molecule and a 5' thioctic acid group (Table 6.1). Silver nanoparticles (40 nm) were prepared *via* citrate reduction of silver nitrate (method described in section 3.1.1). The silver particles adsorb excess citrate anions, rendering a negatively charged surface layer which stabilises the nanoparticles against irreversible aggregation. The thioctic acid sulphur atoms strongly bind through covalent bonding to the silver nanoparticle surface, enabling effective and direct attachment of the nucleic acid sequence. The protocol utilises a gradual salt ageing process in the presence of excess oligonucleotide, to encourage increased surface coverage of the DNA strands. The sodium chloride effectively screens the electrostatic charge repulsion between neighbouring sequences and reduces secondary interactions between the oligonucleotides. The three HEG groups were used as spacer molecules, assembling the subsequent DNA sequence into a perpendicular direction from the nanoparticle surface. This orientation allows further molecule attachment to the surface as well as providing accessible sequences for DNA hybridisation.[173]

Following DNA attachment, the SERS active molecule was adsorbed onto the nanoparticle surface. Throughout this study, 3 distinct molecules were employed to obtain SERS responses; 5-(and-6)-carboxytetramethylrhodamine isothiocynate (TAMRA ITC), 3,5-dimethoxy-4-(6'-azobenzotriazoyl)-phenylamine (GM19) and mercaptopyridine (MPY). Each molecule generates distinctive SERS spectra and contains a surface seeking group which chemisorbs onto the metal surface *via* thiol or amine bonding. The structure and SERS spectra of each dye are shown in Figure 6.3.

The TAMRA isothiocynate dye has been specifically modified through attachment of the strong surface seeking group containing a sulphur and nitrogen atom. Both molecules have a high binding affinity for the nanoparticle surface, generating strong dye attachment and SERS responses (Figure 6.3(a)). Characteristic TAMRA ITC spectra generate a prominent peak at 1650 cm^{-1}.

The specifically designed GM19 dye strongly adsorbs onto silver nanoparticles through the benzotriazole (BT) moiety. The molecule directly complexes to the metal nanoparticle through displacement of the citrate layer and is essentially irreversibly attached in a fixed conformation.[113] GM19 contains an azo dye that acts as a chromophore generating characteristic SERS spectra with the principle peak obtained at 1370 cm^{-1} (Figure 6.3(b)).

Mercaptopyridine (MPY) is a small molecule which is highly suited for SERS analysis as a result of generating strong SERS signals and enabling straightforward nanoparticle functionalisation *via* the thiol group. MPY consists of a pyridine ring system with a terminal thiol group. The thiol group enables strong surface adsorption, whilst the aromatic ring provides high SERS responses (Figure 6.3(c)). Strong intensity peaks were generated at 1005 and 1095 cm^{-1}.

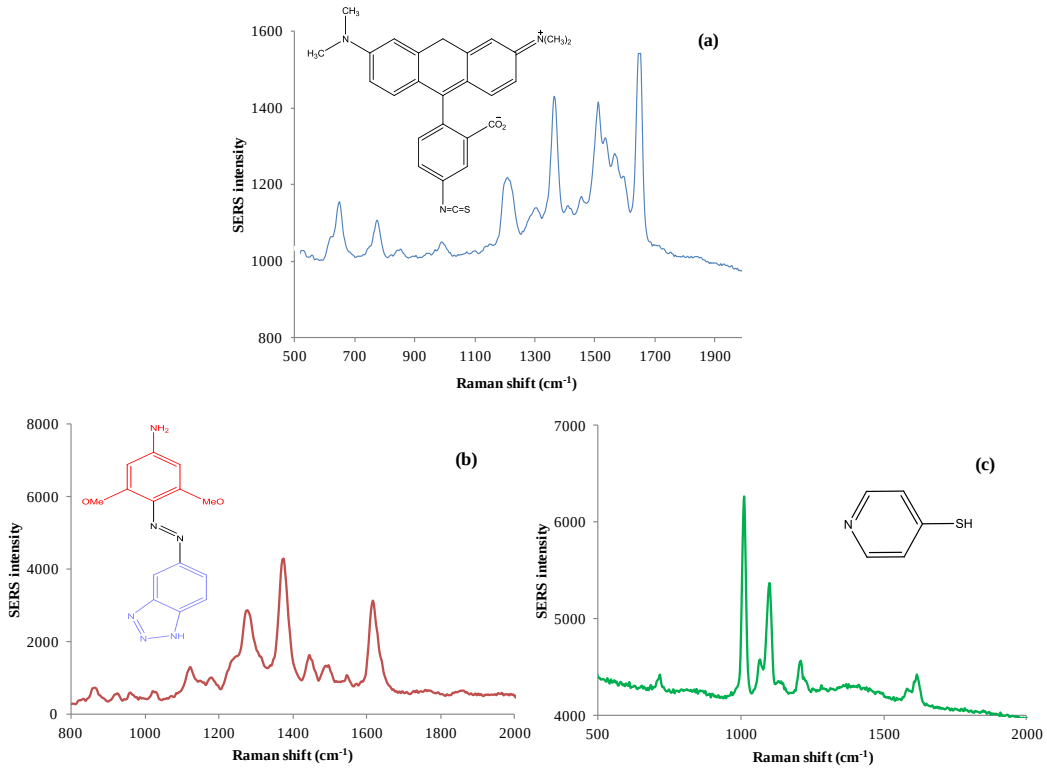

Figure 6.3: (a) TAMRA ITC structure and spectra obtained using 532 nm laser excitation (10 x obj., 0.1 sec. acc.), **(b)** GM19 structure and spectra obtained using 532 nm laser excitation (10 x obj., 0.1 sec. acc.), **(c)** MPY structure and spectra obtained using 785 nm laser (10 x obj., 0.1 sec. acc.) from substrate surface.

6.2.1 Wavelength and Dye Combinations

A study was performed analysing the SERS spectra generated from the combinations of each dye utilised within the study and the three available wavelengths; 532, 633 and 785 nm. This experiment was performed through applying samples of each dye labelled conjugate; TAMRA ITC, GM19 and MPY, onto a substrate surface and analysing the sample spots using each laser excitations. Figure 6.4 illustrates the SERS spectra for each dye and wavelength combination.

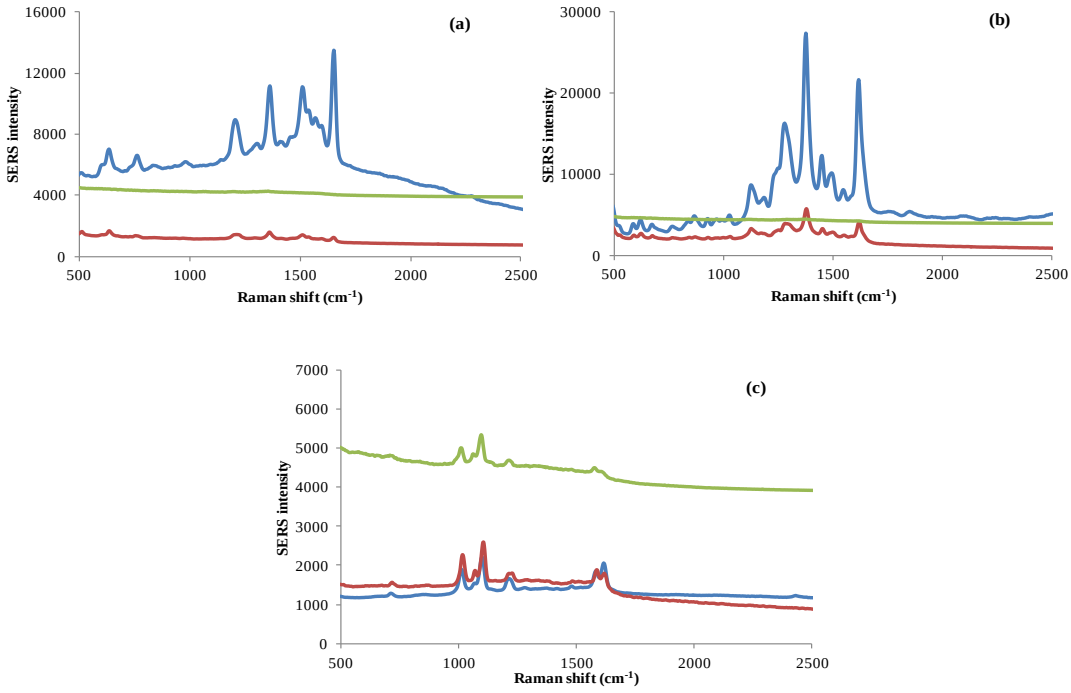

Figure 6.4: SERS spectra of dye labelled conjugates **(a)** TAMRA ITC, **(b)** GM19, **(c)** MPY recorded with blue: 532 nm (0.1 sec. acc. 10 x obj.), red: 633 nm (0.1 sec. acc., 10 x obj.) and green: 785 nm (0.5 sec. acc. 10 x obj.) laser excitation wavelength.

Analysis of the TAMRA ITC dye generated the strongest signals using 532 nm excitation wavelength, whereas, minimal SERS responses were obtained from the higher wavelengths of 633 and 785 nm. This was expected as TAMRA ITC possesses an excitation maximum at 565 nm and analysis with the closely resonant 532 nm excitation wavelength will enhance signal responses. GM19 has an excitation maximum at 435 nm and similarly generated the highest intensity peaks using 532 nm laser, however, strong and distinct peaks were also obtained through analysis of conjugates using 633 nm laser excitation. No significant SERS peaks from the GM19 dye were utilising 785 nm wavelength. The small molecule MPY generated similar intensity SERS responses when analysed by each laser wavelength. This demonstrates the versatility of MPY as a SERS reporter molecule.

The successful preparation of each batch of functionalised nanoparticle conjugates were then characterised by UV-visible analysis, gel electrophoresis and SERS spectroscopy.

6.2.2 UV-visible Analysis of Functionalised Nanoparticles

The optical properties of nanoparticles have been widely exploited to detect biomolecular events through changes in the plasmon resonance band in the extinction spectrum.[92,172] UV-visible analysis has also been utilised in determining the functionalisation of nanoparticles by the position of the characteristic plasmon resonance band. It has been demonstrated that nanoparticle functionalisation with DNA results in an increase in particle size as well as changes in the refractive index of the medium surrounding the nanoparticles. This gives rise to a shift in the plasmon resonance.[91] UV-visible analysis was performed on each batch of dye labelled nanoparticle conjugates, with bare silver citrate nanoparticles employed as a comparison. The conjugates were diluted in 0.3 M PBS and the bare nanoparticles were diluted in distilled water, as PBS buffer induced particle aggregation. The absorbance spectra were generated by monitoring the 200 – 800 nm region. The absorbance maximum for each sample is shown in Table 6.2 in addition to the calculated nanoparticle concentration. The nanoparticle concentration was calculated using the Beer-Lambert law (section 3.7.1, equation 3.2).

Table 6.2: Absorbance maximum and concentration of bare silver nanoparticles and dye labelled DNA conjugates

Name	Absorbance Maximum	Nanoparticle Concentration (pM)
Bare silver nanoparticles	407	49
TAMRA ITC labelled DNA conjugates	412	19
GM19 labelled DNA conjugates	404	22
MPY labelled DNA conjugates	406	6

In this study, functionalisation of the nanoparticle with 3 different DNA conjugates resulted in a red shift of 5 nm for the TAMRA ITC labelled conjugates and blue shifts of 3 and 1 nm for GM19 and MPY conjugates compared with the unmodified bare nanoparticles. A decrease in intensity of the extinction spectra for all three conjugate batches were obtained, however, no broadening of the peaks was observed indicating no particle aggregation had occurred. This provides a good indication that the thiolated DNA has successfully adsorbed onto the nanoparticle surface in each batch. The attachment of the thiol modified DNA to the nanoparticle was further verified by gel electrophoresis.

6.2.3 Gel Electrophoresis of Functionalised Nanoparticles

Gel electrophoresis is a commonly used method for the analysis and separation of DNA fragments. A voltage applied across the system enables DNA to migrate through the gel as a

result of the overall negative charge on the phosphate backbone. This model can also be applied to DNA functionalised nanoparticles.[174]

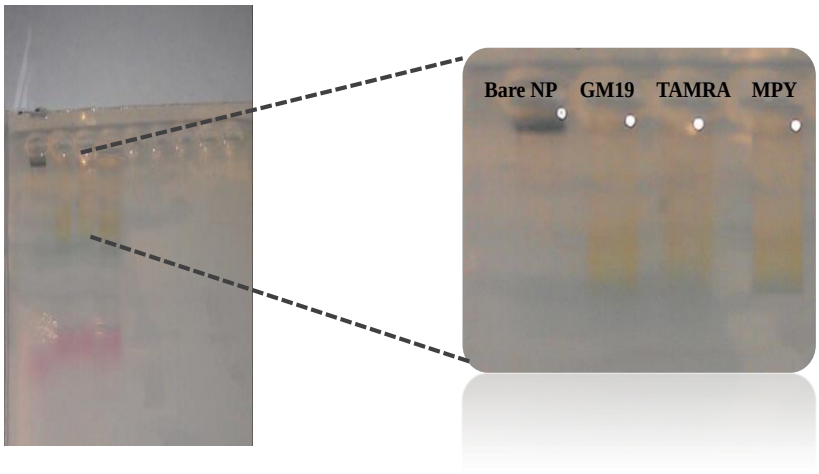

Figure 6.5: Image of agarose gel containing bare silver nanoparticles, TAMRA ITC, GM19 and MPY labelled DNA conjugates**.** The presence of blue and pink bands is due to loading buffer.

The attachment of DNA strands to the surface generates a strong electrostatic pull on the conjugates through the gel, providing an indication of the successful attachment of DNA to bare nanoparticles through particle mobility. Four nanoparticle samples were run in a 1 % agarose gel; bare silver nanoparticles, TAMRA ITC labelled DNA conjugates, GM19 labelled DNA conjugates and MPY labelled DNA conjugates. The gel image in Figure 6.5 shows that the bare silver nanoparticles have remained within the loading well and not moved through the gel. Whereas, the mobility of functionalised DNA nanoparticles can be seen by the distinctive brown colouration from all three batches of silver nanoparticle conjugates. The loading buffer (Bioline) contains bromophenol blue and cresol red dyes, which migrate at different rates depending on the concentration of agarose gel used and generate distinctive blue and pink bands on the gel. This allows DNA migration to be monitored as well as aiding the uptake of samples into the loading wells through increasing sample density. This result coupled with UV-visible analysis of the conjugates strongly suggests the attachment of the DNA to the nanoparticles has been successful. Consequently, the success of the dye attachment to the DNA labelled nanoparticles was investigated through SERS analysis.

6.2.4 SERS Analysis of Functionalised Nanoparticles

The attachment of the Raman active molecules to the metal nanoparticle surface was analysed *via* SERS responses. The molecules were attached to the silver nanoparticle surface between the bound DNA sequences by chemisorptions of either thiol or nitro groups. Any unattached SERS label was removed from the conjugate sample by centrifuging (preparation method in section 3.7.1). A bulk spot (0.2 µL) of the stock concentration of each dye labelled conjugate was applied to a solid surface substrate and analysed using 532 nm laser excitation for the TAMRA ITC and GM19 conjugates and 785 nm laser excitation for the MPY labelled DNA conjugates.

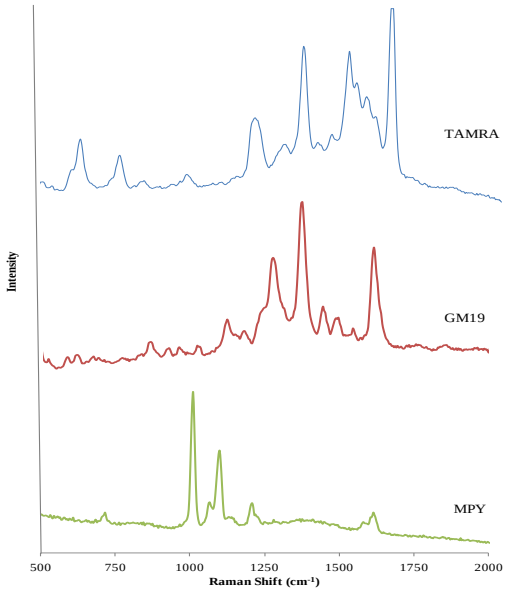

Figure 6.6: SERS spectra of DNA silver conjugates labelled with blue: TAMRA ITC (532 nm, 0.1 sec. acc.), red: GM19 (532 nm, 0.1 sec. acc.) and green: MPY (785 nm, 0.5 sec. acc.) all analysis used 10 x obj.

During analysis the laser radiation generates an electric field at the metal surface, which is inversely proportional to distance, therefore the magnitude of SERS enhancement drops off rapidly with increasing distance of the analyte from the surface. Therefore, only surface bound molecules will generate distinct and enhanced signals. The SERS spectra obtained in Figure 6.6 demonstrates successful dye attachment through the generation of high intensity SERS spectra from each functionalised nanoparticle using the selected excitation wavelength for each label.

Characterisation of the three batches of DNA nanoparticle conjugates using UV-visible absorption, gel electrophoresis and SERS analysis have demonstrated successful functionalisation. These conjugates have the potential for utilisation within a surface assay to detect unlabelled DNA by SERS. However, to ensure that maximum SERS responses were obtained from the nanoparticle conjugates, a study was carried out varying the volume of dye added to the DNA labelled nanoparticles.

6.2.5 Dye Optimisation

The optimum amount of dye on the surface is essential to obtain the maximum possible SERS responses within the assay. Insufficient dye produces weak signals and a large dye excess can over saturate the particles, causing destabilisation and aggregation. Thus, the optimum dye amount was determined by SERS analysis of five different dye concentrations adsorbed onto DNA functionalised nanoparticles.

According to standard protocols developed for attachment of monothiol labels to DNA conjugates, the addition of 500 µL of SERS active molecules at a concentration of 1 µM to the DNA functionalised nanoparticles (with a starting nanoparticle volume of 500 µL) is suggested.[92,175] TAMRA isothiocynate dye (1 µM) was added to 500 µL DNA conjugates at volumes of 125, 250, 375, 500 and 625 µL. The conjugates were centrifuged to remove any unattached dye and the fully functionalised nanoparticles were applied to a solid substrate surface and analysed using 532 nm laser excitation with 0.1 second accumulation times.

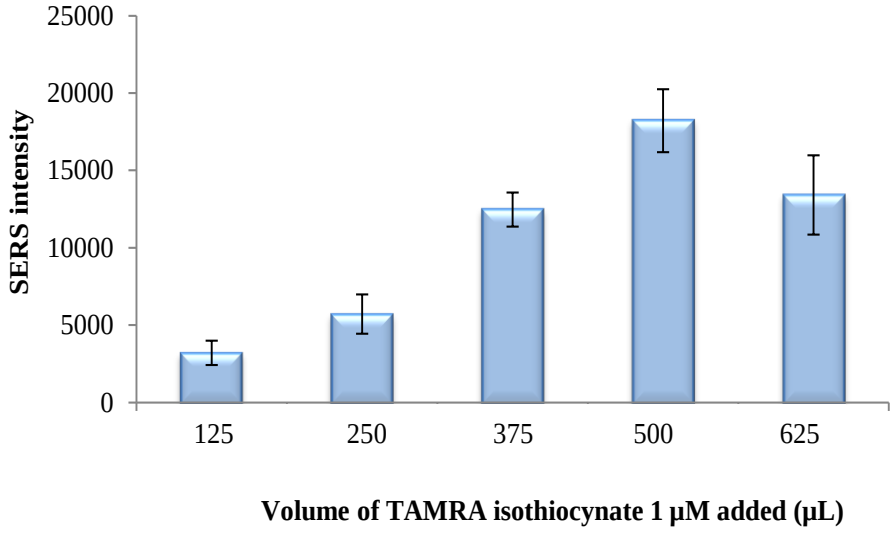

Figure 6.7: Volume of 1 µM TAMRA isothiocynate dye added to 500 µL of 26 pM DNA labelled nanoparticles obtained using 532 nm laser excitation. (10 x obj., 0.1 sec. acc.)

The average intensity of the principle peak at 1650 cm^{-1} was calculated and plotted for each dye concentration (Figure 6.7). The dye volume of 500 µL at 1 µM generated the greatest SERS signals, supporting previous findings. Utilisation of a higher dye volume shows slightly reduced signal intensities indicating that the nanoparticle surface may be saturated with dye. Therefore, from these results conjugates were prepared through addition of 500 µL of dye to DNA functionalised nanoparticles.

This study has so far demonstrated the successful preparation of three dye labelled DNA conjugates and ensured strong SERS responses would be generated from each batch through optimum dye adsorption. Therefore, the functionalised nanoparticles were incorporated into a surface detection assay.

6.3 Functionalised Nanoparticle Detection using Surface Assay

A surface detection assay was performed using DNA nanoparticle conjugates with an adsorbed TAMRA isothiocynate dye. The conjugate arrangement enables complementary hybridisation of the nanoparticle DNA to the surface adsorbed target DNA. This binding event can subsequently be detected by characteristic SERS responses (Figure 6.8).

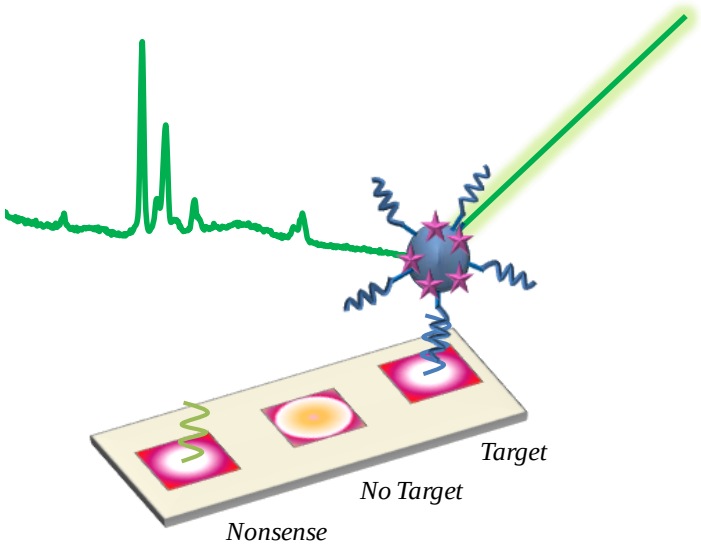

Figure 6.8: Schematic of DNA detection surface assay on solid substrate using nanoparticle conjugates.

In the first instance, the assay was performed on an epoxysilane coated glass slide with TAMRA ITC labelled DNA conjugates. The glass surface was coated with a multi-purpose

epoxysilane layer which covalently binds biomolecules and has successfully been employed as a detecting substrate.[176,177] The assay was performed as per the previous method (Section 6.1 and 3.7.2), whereby target, no target and nonsense DNA were applied to the surface. The surface was blocked using Nexterion® Block E, which contained ethanolamine molecules activated through addition of hydrochloric acid to block the activity of the surface epoxy groups. The TAMRA ITC labelled DNA conjugates were applied during the hybridisation step to enable sequence specific detection to be established. TAMRA ITC labelled DNA conjugates were suspended in PBS buffer and applied to the glass surface while heating at 45 °C for 18 hours. Multiple SERS spectra were gathered through mapping a minimum of four areas within each sample spot on the glass slide using an excitation wavelength of 532 nm. Each map took an average of 500 spectra over 100 x 100 µm area and the spectral average was calculated and plotted in Figure 6.9.

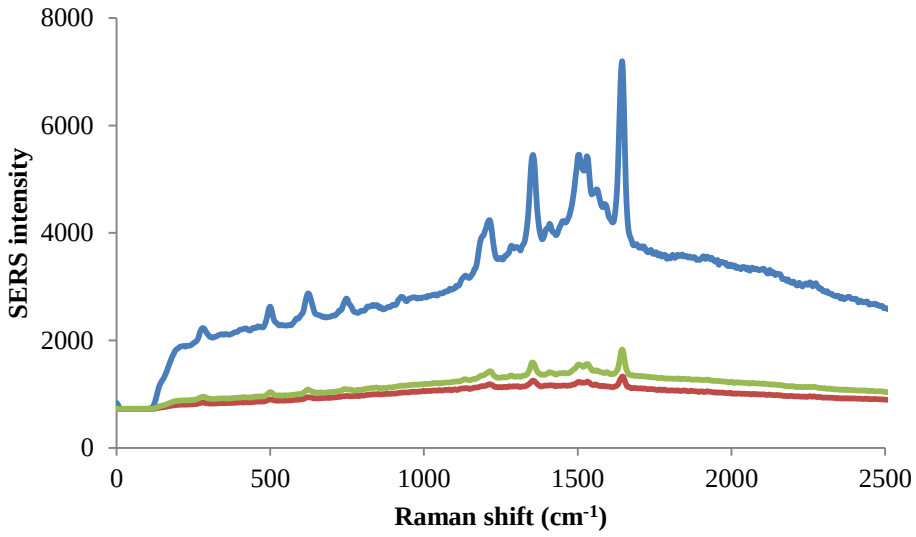

Figure 6.9: SERS spectra of epoxysilane coated glass slide containing TAMRA ITC labelled DNA conjugates recorded using 532 nm laser excitation (10 x obj., 0.1 sec. acc.); blue: target DNA, red: no target DNA, green: nonsense target DNA. Each spectrum was calculated from an average of 4 replicate SERS maps which were representative of sample area.

Significantly more intense and distinct TAMRA ITC peaks were achieved through the employment of nanoparticle conjugates for sequence detection over the use of a TAMRA ITC labelled detection probe and subsequent application of nanoparticles (Figure 6.2). Analysis of the target DNA region generated considerably higher intensity SERS responses than both control samples. The discrimination in signal indicates that an increased number of conjugates are binding to the target DNA sample. However, noticeable dye peaks were

obtained from control samples, suggesting non-specific binding of the conjugates to the surface is occurring at a significantly reduced level. These results enabled the distinctive detection of target DNA from an epoxysilane coated glass slide. The positive results obtained from the surface assay indicate the high potential for DNA analysis. Therefore, the assay was repeated multiple times to optimise the method and determine the reproducibility.

Further surface assays were performed on the epoxysilane glass slides using the method demonstrated in this section and variable results were generated. Several results demonstrated no differences between the target sample and controls. Figure 6.10 demonstrates typical spectra generated demonstrating minimal differences between the target assay and controls.

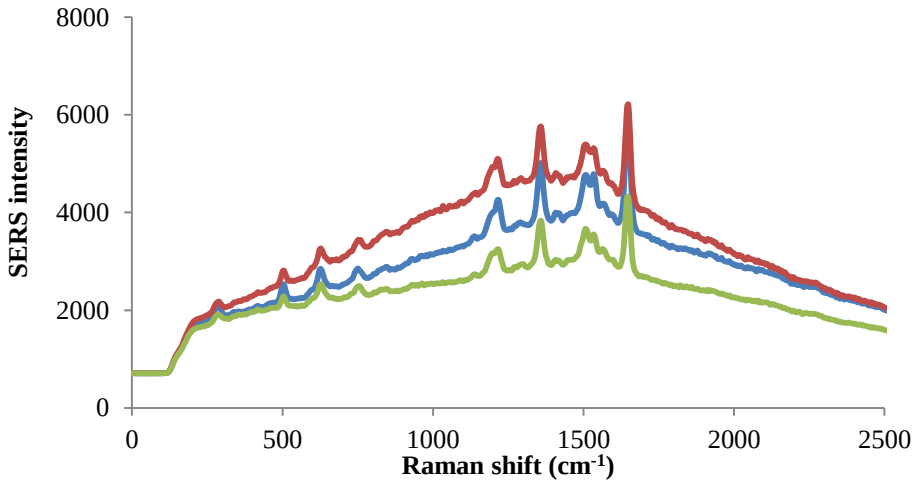

Figure 6.10: SERS spectra of epoxysilane coated glass containing TAMRA ITC labelled DNA conjugates recorded using 532 nm laser excitation (10 x obj., 0.1 sec. acc.); blue: target DNA, red: no target, green: nonsense. Each spectrum was calculated from an average of 4 replicate SERS maps which were representative of sample area.

These results indicate that the glass surface has not been adequately blocked by the ethanolamine molecules and reactivity of the free epoxy groups on the surface is facilitating the attachment of the functionalised conjugates. To overcome this issue other substrate detection surfaces with reduced surface reactivity were investigated.

6.3.1 Surface Comparison

DNA detection surface assays have utilised numerous solid substrates including glass, plastic and membranes.[178,179] Two of the most commonly used membrane substrates are nylon and

nitrocellulose surfaces which are composed three-dimensional matrices of synthetic polymers and cellulose strands respectively. Both surfaces form a three-dimensional microporous structure which will bind biomolecules at a lower affinity than epoxysilane surfaces. Both surfaces have previously been used successfully for DNA detection using blotting methods.[180,169] A comparison study was performed on both platforms to determine whether distinctive SERS signals from the nanoparticle conjugates could be obtained.

Analysis was performed by directly spotting TAMRA ITC labelled DNA conjugates onto each substrate surface. Multiple SERS spectra were gathered using 532 nm laser excitation and mapping four 100 x 100 µm surface regions within the target, no target and nonsense samples. The average spectrum from each sample was plotted in Figure 6.11. The spectrum illustrates that detection from the nylon and nitrocellulose membrane substrates generate characteristic TAMRA ITC peaks with similar intensities. However, the peak intensities obtained from the TAMRA ITC functionalised nanoparticles on these membrane surfaces demonstrated significantly lower signals than illustrated from detection of the epoxysilane coated surface (Figure 6.9 and 6.10). The reduced intensity of the SERS peaks from the membrane surfaces may indicate that due to the differences in surface structure, of the glass and membrane substrates, the conjugates are more widely spread and may be adsorbed into the porous membrane.

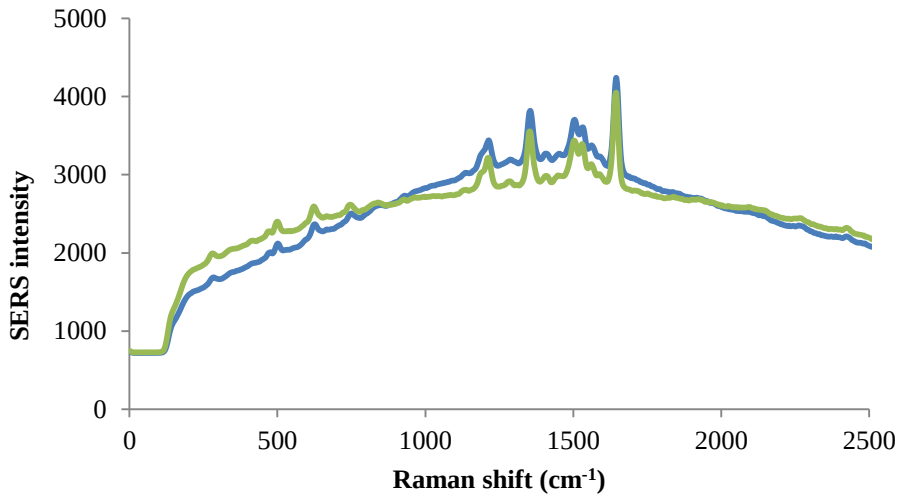

Figure 6.11: SERS spectra of TAMRA ITC labelled DNA conjugates recorded using 532 nm laser excitation (10 x obj., 0.1 sec. acc.) on blue: nylon, green: nitrocellulose. Each spectrum was calculated from an average of 4 replicate SERS maps which were representative of sample area.

Furthermore, the substrate employed for DNA analysis is required to be simple to use, handle and visualise the sample spots for analyse. This was investigated for each membrane by mapping the edge of the target spot and obtaining a definitive circular shape in which signal is only generated from areas inside the target spot. Therefore, the edge of each sample spot was analysed and false colour images generated using the intensity of the 1650 cm^{-1} peak (Figure 6.12). A distinctive spot edge was obtained from the functionalised nanoparticles applied to the nitrocellulose membrane and strong characteristic SERS spectra were generated. Whereas, the spot edge on the nylon surface proved difficult to locate, demonstrating a more challenging analysis would be obtained. The nitrocellulose surface is a three dimensional microporous membrane attached to a glass slide, whereas, nylon membrane used where not attached to a rigid surface. This may have influenced the degree of conjugate spreading through the substrate. As a result the nitrocellulose membrane was shown to be more practical and was further investigated by performing a full surface assay.

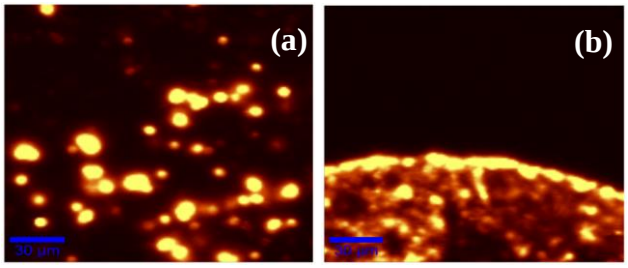

Figure 6.12: False colour maps of 1650 cm^{-1} peak on **(a)** nylon, **(b)** nitrocellulose membrane obtained using 532 nm laser excitation (10 x obj., 0.1 sec. acc.). Maps were 120 x 120 μm using 2 μm resolution.

6.4 Surface Assay on Nitrocellulose Membrane

The nitrocellulose membrane was utilised to perform a surface assay employing the same experimental conditions as used for the epoxysilane slide assay (Section 6.2.5). Similarly, complementary DNA, used as the target and non-complementary DNA used as a nonsense control were applied to the separate nitrocellulose regions. A blank area was also utilised for the no target control. SERS mapping analysis using 532 nm laser excitation and a 0.1 second accumulation time was carried out within each sample region and the average spectra of target, no target and nonsense areas are shown in Figure 6.13.

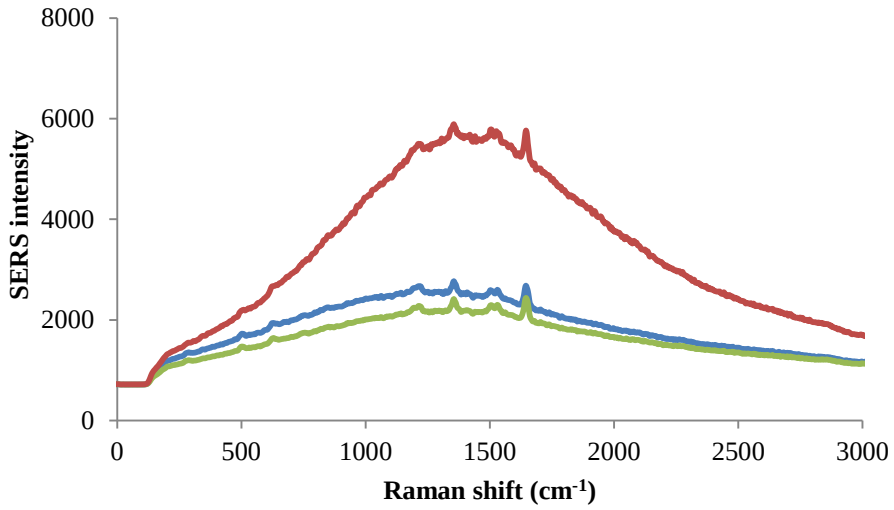

Figure 6.13: SERS spectra of nitrocellulose membrane containing TAMRA ITC labelled DNA conjugates recorded using 532 nm laser excitation (10 x obj., 0.1 sec. acc.); blue: target DNA, red: no target DNA, green: nonsense target DNA. Each spectrum was calculated from an average of 4 replicate SERS maps representative of sample area.

The average spectra obtained from each sample generated similar intensity peaks, indicating that no specific hybridisation of the conjugates to the target sequence adsorbed onto the membrane surface had occurred. In actuality, the conjugates appear to be non-specifically bound to the membrane, consequently generating SERS responses. This is likely to be due to a combination of inadequate blocking of the membrane and poor sequence hybridisation. Enhanced background signals were also obtained from each sample which may obscure the SERS signals. This could be due to a background signal obtained from the membrane or fluorescence emission from the TAMRA ITC dye. The experimental conditions used in this assay were favourable for analysis from an epoxysilane glass surface. Therefore, the method had to be modified and optimised for detection on a nitrocellulose membrane surface. Consequently, the blocking and hybridisation steps were investigated.

6.4.1 Optimisation of Surface Assay Blocking Step

The nanoparticle conjugates are designed to be self-contained SERS active species which can individually generate strong SERS signals without the need for activation. It is for this reason, that an efficient blocking step is essential to reduce the non-specific binding of the dye labelled DNA conjugates to the surface and ensure SERS signals are only produced through sequence specific hybridisation to immobilised target sequences. Previously, Nexterion® Block E had been employed to prevent unwanted binding on the surface (Section 6.1 and 3.7.2). This blocking solution utilises amine molecules which have been

activated through addition of water and HCl, to cap the epoxy groups on the glass slide and prevent unwanted DNA binding. However, using this blocking agent on the porous membrane surface may not provide sufficient or indeed any surface blocking. Consequently, a membrane blocking agent was investigated. Single stranded DNA fragments of between 587 to 831 base pairs are commonly utilised to block surfaces reducing the non-specific binding of probes to membrane surfaces.[170,43] Salmon testes DNA is a long chain oligonucleotide routinely used as a blocking reagent within membrane assays, including Southern blots, [169] and was therefore employed within an comparison assay.

Simultaneous surface assays were performed comparing both blocking agents, Nexterion® Block E and salmon testes DNA, on a nitrocellulose membrane. Both assays contained target, no target and nonsense control samples and the full experimental assay was performed as per section 3.7.2. An incubation chamber was applied during development of the surface assay, to enable separate membrane regions to be analysed without the mixing of reagents. Within the blocking step, both blocking agents were applied to the surface for 60 minutes while heating at 50 °C. All sample areas were then applied with TAMRA ITC labelled DNA nanoparticle conjugates at 45 °C for 18 hours.

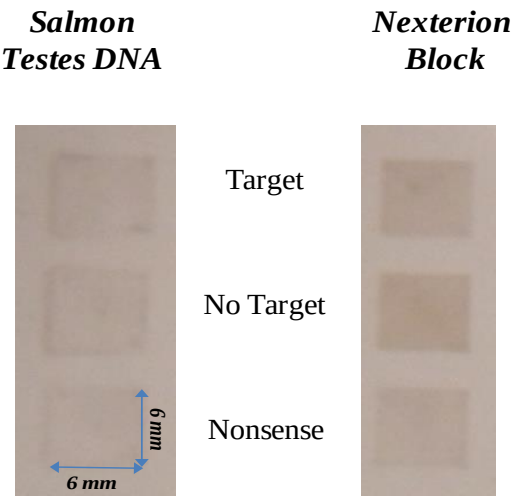

Figure 6.14: Nitrocellulose membrane applied with TAMRA ITC labelled DNA conjugates with either salmon testes DNA or Nexterion® Block E.

Figure 6.14 shows an image of the nitrocellulose membrane after the final assay washing step had been performed. The discolouration of the membrane squares were produced through the addition of functionalised nanoparticles during the hybridisation step. Clear differences between each blocking agent can be visually distinguished from the membrane,

with distinctly darker areas obtained from use of Nexterion® Block E within the assay. This demonstrates that inefficient surface blocking of the membrane has increased the amount of non-specific conjugate binding. Comparably, the same assay performed using salmon testes DNA block generated considerably lighter sample regions, suggesting a reduction in unwanted nanoparticle binding through increased surface blocking.

The sample regions were also analysed by SERS mapping using a laser excitation wavelength of 532 nm. The average spectra of the target, no target and nonsense sample areas were calculated and plotted in Figure 6.15. SERS spectra showed high background signals with low peaks from both blocking agents. The SERS spectra obtained for the assay using Nexterion® Block E generated more distinct peaks, however, no discrimination between samples was achieved. This indicates that a high level of non-specific binding of functionalised nanoparticles is occurring through inefficient surface blocking. The use of salmon DNA produced minimal SERS intensities, with only weak responses obtained from the target sample.

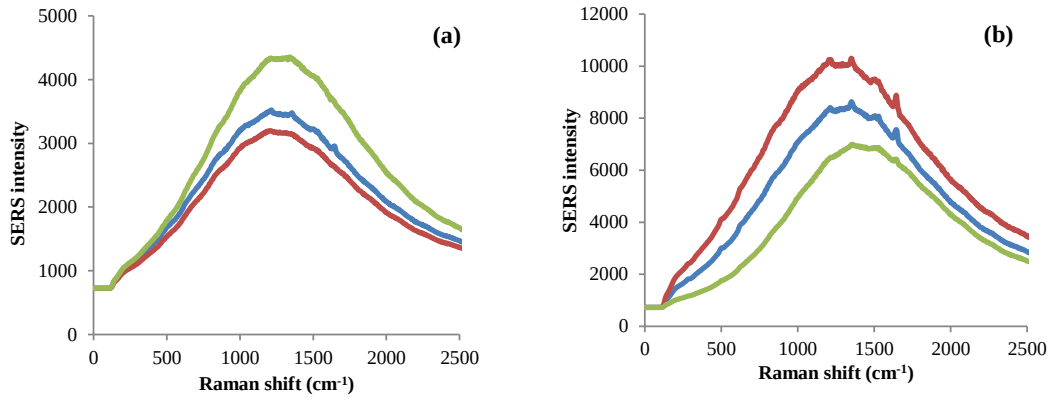

Figure 6.15: SERS spectra of nitrocellulose membrane containing TAMRA ITC labelled DNA conjugates recorded using 532 nm laser excitation (10 x obj., 0.1 sec. acc.) applied with **(a)** salmon testes DNA, **(b)** Nexterion® Block E; blue: target DNA, red: no target, green: nonsense. Each spectrum was calculated from an average of 4 replicate SERS maps which were representative of sample area.

Figure 6.14 and 6.15 show that preferential membrane blocking is obtained using salmon testes DNA as a block for the nitrocellulose membrane. Consequently, salmon testes DNA was used as the blocking reagent for nitrocellulose surface assay. However, to be able to distinctively determine the presence of target DNA, the SERS responses obtained must be significantly enhanced to dominate over the membrane background signals generated. This

can be achieved by increasing the number of conjugates hybridised to the DNA on the membrane surface.

6.4.2 Optimisation of Hybridisation Step

The hybridisation of the complementary target to the conjugate oligonucleotides was initially investigated in order to ensure sequence specific hybridisation occurred and determine the optimum temperature for this event. This was attained through performing a fluorescent DNA melt. The intercalating dye, SYBR green, has a low binding affinity for single stranded DNA, generating low fluorescence emission. However, the dye binds in high yields to double stranded DNA which significantly increases the fluorescence produced. This can be monitored by inspection of fluorescence emission using a filter set with 492 nm excitation and 516 nm emission. Consequently, the target sequence and conjugate DNA sequence were analysed prior to adsorption onto the silver nanoparticles. The probes were diluted to 1 μM in PBS buffer, routinely used for DNA hybridisations. This was also the chosen buffer for conjugate hybridisation within the surface assay. An intercalating dye, SYBR Green, was additionally included into the mixture. SYBR Green strongly binds to double stranded DNA and fluoresces at low temperatures, however as the temperature is increased the strands denature to single sequences and the dye fluorescence decreases. Monitoring of this process enables the temperature of sequence denaturation to be determined.

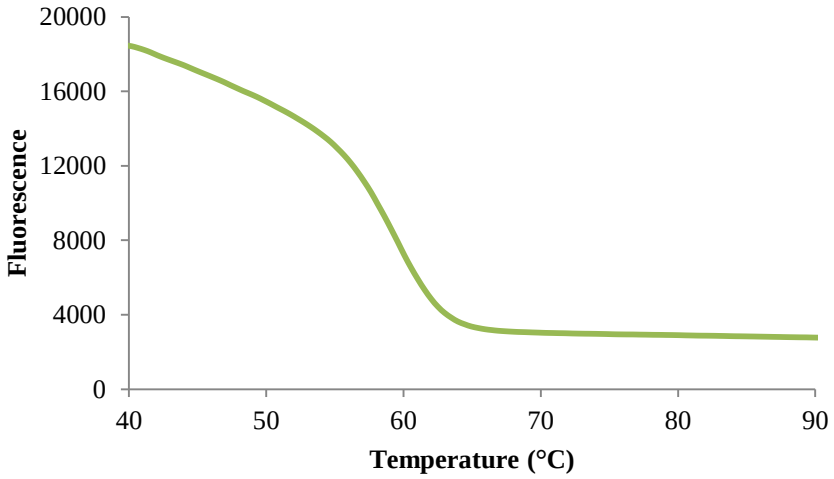

Figure 6.16: Fluorescent melt using SYBR green of unmodified target DNA and conjugate DNA sequence.

The fluorescence was continually monitored from 40 – 90 °C and a sigmoidal melting curve was obtained (Figure 6.16), demonstrating the successful hybridisation of the target and

conjugate sequence. The melting temperature was determined to be 60 °C, thus temperatures below this will be favourably driven towards sequence hybridisation.

The DNA melting experiment demonstrated hybridisation of complementary DNA sequences diluted in PBS buffer. PBS buffer contains a suitable volume of salt ions to ensure sequence stability and promote DNA hybridisation within solution assays. However, use of PBS buffer within the hybridisation step of the surface assay, demonstrated poor conjugate binding through the generation of weak SERS responses and high background signals (Figure 6.13 and 6.15). Additionally, to achieve these low signals, the hybridisation step had to be performed for over 18 hours at 45 °C. Consequently, to generate stronger SERS spectra in a vastly reduced time, an alternative to PBS as a hybridisation buffer was investigated.

6.4.2.1 Hybridisation Buffer Optimisation

PerfectHyb Plus buffer (Sigma-Aldrich,UK), is an alternative hybridisation solution recommended for use in surface DNA hybridisations. The buffer has been specifically optimised for sequence hybridisation on membrane surfaces and is able to generate high signal-to-noise ratios using significantly reduced hybridisation times. The PerfectHyb Plus buffer was employed as a replacement to PBS and the nanoparticle conjugates were premixed with Perfect Hyb Plus buffer before application to the membrane. The assay hybridisation time was also reduced from 18 to 2 hours and performed at 30 °C as recommend by the buffer application guidelines.

The performance of the assay utilising the new optimised buffer, showed significantly improved SERS responses (Figure 6.17). Distinct SERS peaks were obtained in the target sample with lower intensity signals. This could result from a lower number of conjugates binding non-specifically to the surface and the generated spectra representative of selective strand hybridisation. Nonsense samples generated only membrane background signals whereas, the no target control illustrated significant regions of non-specific binding of the functionalised nanoparticles, generating high intensity SERS signal. Therefore, further investigation into hybridisation times below 2 hours was carried out.

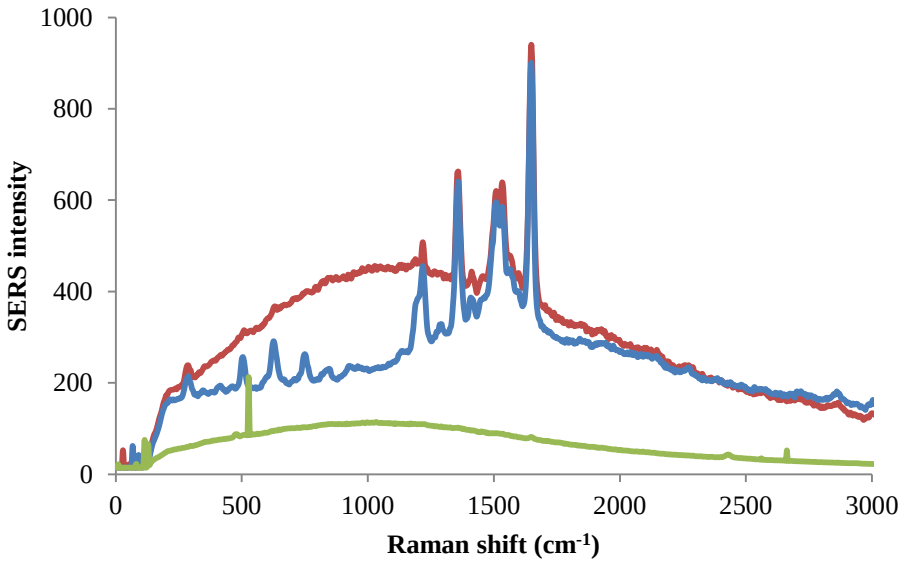

Figure 6.17: SERS spectra of nitrocellulose membrane containing TAMRA ITC labelled DNA conjugates with PerfectHyb Plus buffer with a 2 hour hybridisation time recorded using 532 nm laser excitation (10 x obj., 0.1 sec. acc.); blue: target DNA, red: no target, green: nonsense. Each spectrum was calculated from an average of 4 replicate SERS maps which were representative of sample area.

6.4.2.2 Hybridisation Time Optimisation

The change of hybridisation buffer has enabled prominent SERS responses with reduced background signals to be achieved whilst utilising a considerably lower hybridisation time. However, a 2 hour hybridisation generated no discrimination between the target and no target control. Consequently, reduced hybridisation times were investigated to determine the time at which complementary DNA hybridisation would occur prior to the surface attachment of non-specifically bound conjugates. A simultaneous surface detection assay was performed (use of an incubation chamber enabled individual assays to be performed on the same surface without the possibility of sample mixing), incorporating the decreasing hybridisation times of 60, 30, 20, 10 and 5 minutes. During the hybridisation step, TAMRA ITC labelled silver nanoparticle DNA conjugates were applied into each separate region of the nitrocellulose membrane and heated at 30 °C. The average intensity of the principle SERS peak at 1650 cm^{-1} was plotted for target, no target and nonsense samples over the range of hybridisation times is shown in Figure 6.18.

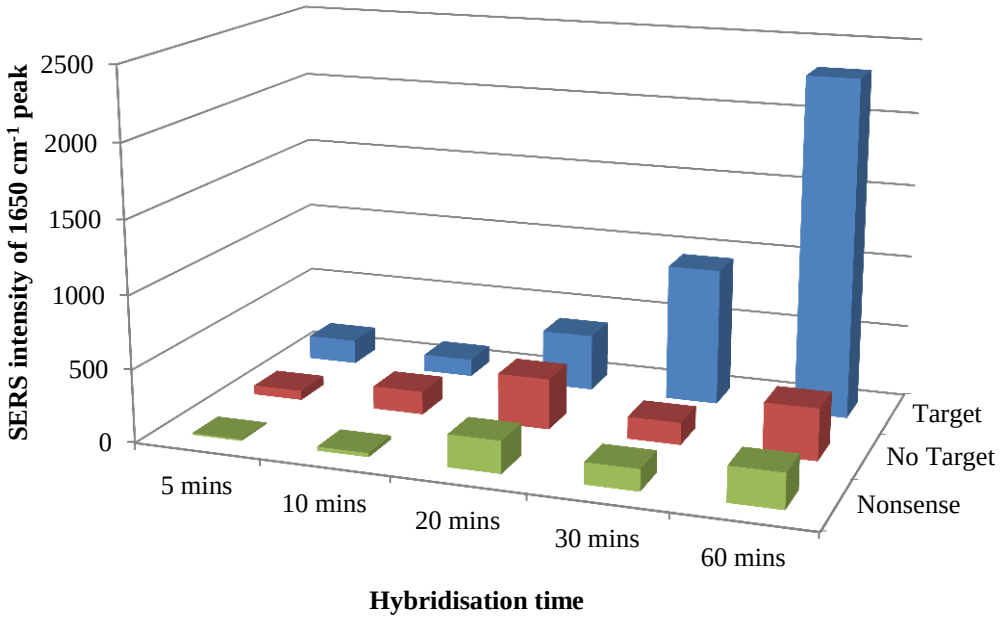

Figure 6.18: SERS intensity of 1650 cm^{-1} peak obtained using 532 nm laser excitation (10 x obj., 0.1 sec. acc.) of TAMRA ITC labelled DNA conjugates on nitrocellulose membrane assay using PerfectHyb Plus buffer over a range of hybridisation times; blue: target DNA, red: no target, green: nonsense

The largest discrimination between the target sample and the assay controls was obtained when a 60 minute hybridisation time was employed within the surface detection method. Hybridisation times of 20, 10 and 5 minutes, illustrated no significant discrimination between the target and controls. At these faster hybridisation times, the ratio of discrimination of signal between target sample and controls does not linearly or exponentially increase. Target sequences appear still to be available for hybridisation at these times, therefore the membrane surface is not fully saturated with conjugates. This indicates that signal is generated through non-specific binding of the conjugates to the surface. However, hybridisation times of 30 and 60 minutes demonstrated significantly increased target intensities compared to control signals. These results appear to indicate utilisation of 60 minute hybridisation times will promote specific conjugate hybridisation. The assay was repeated using the optimised blocking and hybridisation time incorporating the PerfectHyb buffer, with results similarly demonstrating large signal differences between target and controls (Figure 6.19). The principle peak in the target spectra at 1650 cm^{-1} was calculated to be 2.7 times greater than the no target peak and 53.4 times greater than the nonsense control.

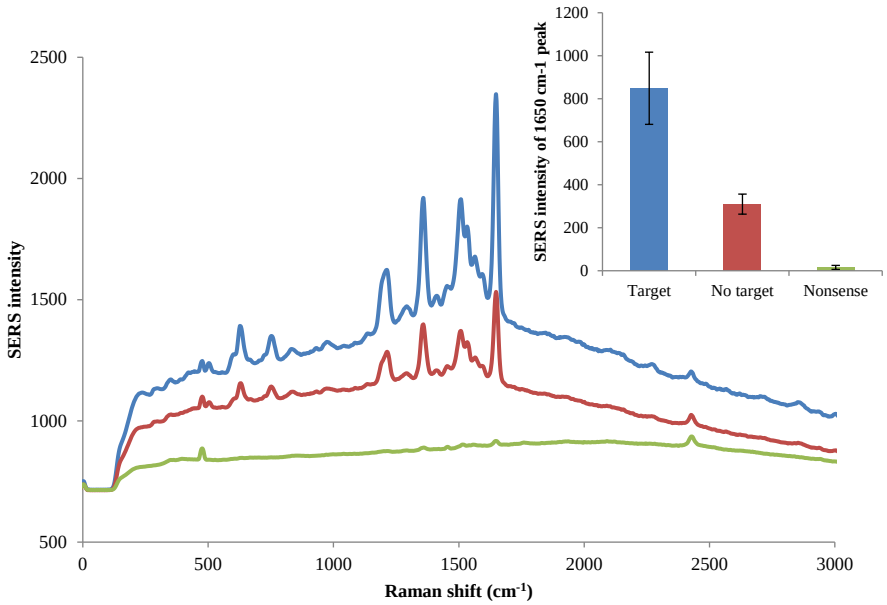

Figure 6.19: SERS intensity of 1650 cm^{-1} peak obtained using 532 nm laser excitation (10 x obj., 0.1 sec. acc.) of TAMRA ITC labelled DNA conjugates on nitrocellulose membrane; blue: target DNA, red: no target, green: nonsense. Insert contains average signal intensity of 1650 cm^{-1} peak, each bar represents 4 replicate SERS maps and error bars ± one standard deviation

These results have demonstrated that the optimised conditions for a SERS based DNA surface assay should be performed on a nitrocellulose membrane, using salmon testes DNA as a blocking agent along with a 60 minute hybridisation step at 30 °C using PerfectHyb buffer.

6.5 Dye and Wavelength Investigation

The experimental conditions utilised for the detection of unlabelled DNA from a membrane surface have been optimised, enabling significantly enhanced SERS responses to be generated. The surface assay has so far been performed utilising TAMRA ITC and DNA functionalised silver nanoparticle conjugates. However, the versatility of the assay was investigated through detection of other SERS active labels using the laser excitation wavelengths, 633 and 785 nm. Two distinct SERS active molecules, GM19 and the small molecule mercaptopyridine (MPY), have previously been shown to generate strong signals at 633 and 785 nm respectively (Figure 6.4). Therefore, these dyes were incorporated onto DNA functionalised silver nanoparticles and analysed within the surface membrane assay using these longer excitation wavelengths.

6.5.1 Nitrocellulose Surface Assay using GM19 Conjugates

GM19 dye strongly adsorbs onto silver nanoparticles through the benzotriazole (BT) moiety and contains an azo dye that acts as a chromophore generating characteristic SERS spectra with the principle peak obtained at 1370 cm^{-1}. The functionalised conjugates generated distinctive SERS signals when applied to a nitrocellulose membrane and analysed using 633 nm laser excitation (Figure 6.4). Therefore, a DNA surface detection assay was performed utilising GM19 conjugates and the optimised experimental conditions, determined from use of TAMRA ITC labelled conjugates. The average spectra of target, no target and nonsense sample areas were calculated and plotted in Figure 6.20. The principle peak in the target spectra at 1370 cm^{-1} was calculated to be 2.8 times greater than the no target peak and 6.2 times greater than the nonsense control. This indicates the detection of unmodified target DNA on a nitrocellulose is possible through SERS detection of hybridised DNA labelled nanoparticles utilising 633 nm laser excitation. The spectral background obtained is likely to be due to the use of 633 nm laser excitation generating background signal from the nitrocellulose membrane.

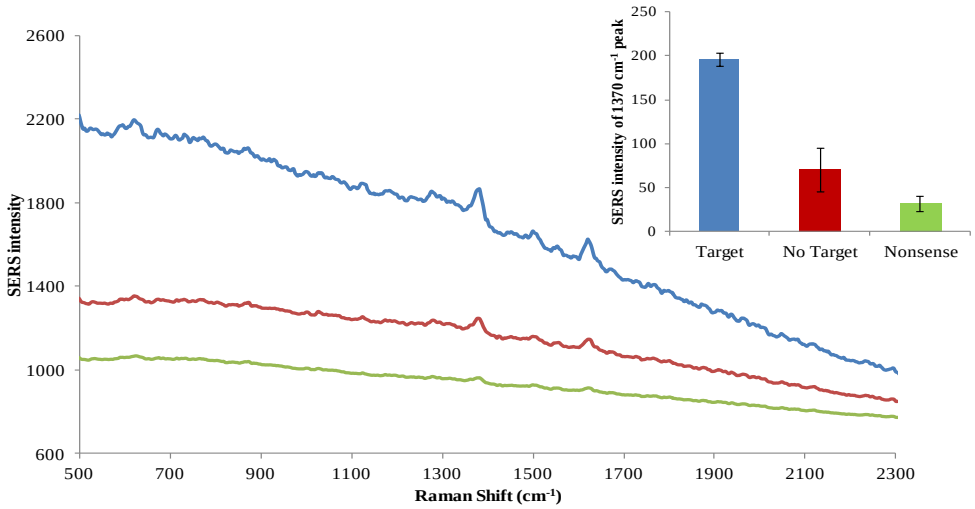

Figure 6.20: SERS spectra of nitrocellulose membrane containing GM19 labelled DNA silver conjugates recorded using 633 nm laser excitation (10 x obj., 0.1 sec. acc.); blue: target DNA, red: no target, green: nonsense. Insert contains average signal intensity of 1370 cm^{-1} peak, each bar represents 4 replicate maps and error bars ± one standard deviation.

6.5.2 Nitrocellulose Surface Assay using MPY Conjugates

Mercaptopyridine (MPY) is a small molecule which consists of a pyridine ring system with a terminal thiol group. The thiol group enables strong surface adsorption, whilst the aromatic ring generates strong SERS responses with prominent peaks at 1005 and 1095 cm^{-1}. The molecule was shown to generate intense spectra through adsorption onto the metal surface using an exciting laser line at 785 nm from a nitrocellulose membrane (Figure 6.4). The surface detection assay was performed under optimised experimental conditions utilising the MPY silver DNA conjugates within the hybridisation step to enable the detection of unmodified surface bound sequence. The average SERS spectra for each sample was collected from the membrane substrate and analysed using 785 laser excitation and a 0.5 second accumulation time (Figure 6.21).

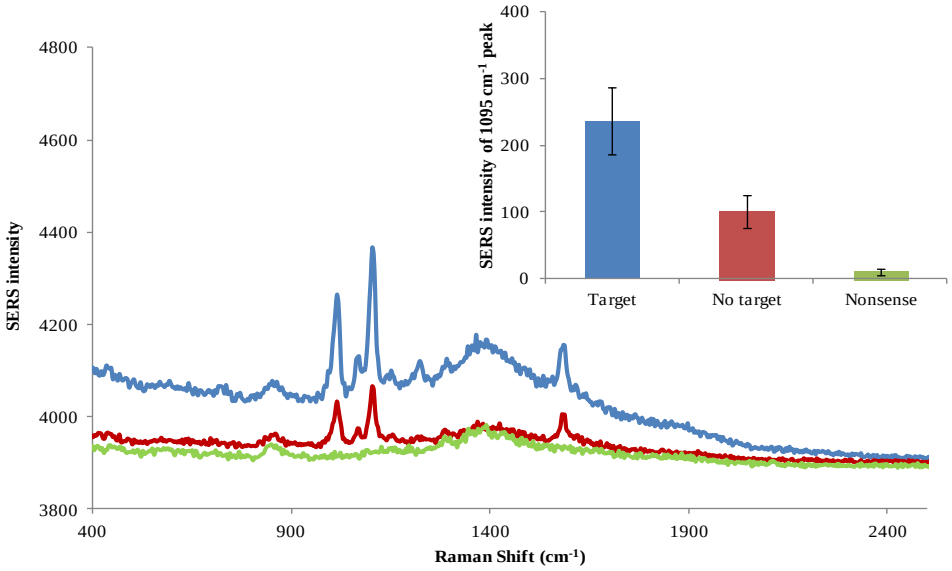

Figure 6.21: SERS spectra of nitrocellulose membrane containing silver MPY labelled DNA conjugates recorded using 785 nm laser excitation (10x obj., 0.5 sec. acc.); blue: target DNA, red: no target, green: nonsense. Insert contains average signal intensity of 1095 cm^{-1} peak, each bar represents 4 replicate maps and error bars ± one standard deviation.

The successful detection of the target sequence was achieved through binding of the MPY conjugates and analysis with 785 nm laser excitation. Characteristic MPY spectra obtained from the target sample area illustrated significantly increased intensity signals compared to the control samples. The highest intensity peak in the target spectra at 1095 cm^{-1} was calculated to be 2.4 times greater than the no target peak and 22.5 times greater than the nonsense control.

The nitrocellulose membrane was fixed onto a glass slide, enabling easier surface analysis. However, a broad background peak at approximately 1400 cm^{-1} was generated in all sample spectra, which can be attributed to signals from the glass surface. Analysis of the surface using 785 nm excitation wavelength has generated SERS signals from the membrane surface as well as the glass support slide. However, the glass peaks do not obscure the MPY identification peaks.

This study has illustrated the successful detection of unlabelled DNA from a nitrocellulose surface using three distinct functionalised nanoparticles and three different laser excitation wavelengths. Subsequently, the next step was to determine the detection limits from a nitrocellulose surface of the three conjugates using SERS analysis of a dilution series.

6.5.3 DNA Dilution Series for Functionalised Nanoparticles

To determine the detection limits for the conjugates the full surface assay was not carried out, instead the conjugates were diluted in PBS buffer and applied to the membrane surface. Five regions of each sample area were SERS mapped and the average spectra combined to determine the intensity of the principle peak for each label; TAMRA ITC at 1650 cm^{-1}, GM19 at 1370 cm^{-1} cm and MPY at 1095 cm^{-1}. The signal intensity was plotted against nanoparticle concentration to obtain a linear response for each batch of conjugates (Figure 6.22). Inherently, the synthesis of nanoparticle conjugates can make the controlled concentration of batches extremely difficult. The three batches utilised were comprised of differing stock concentrations and as a result different concentration ranges were analysed. However, each batch of nanoparticle conjugates demonstrated linear responses over a concentration range and the detection limits were calculated by assigning the limiting signal intensity to be three times the standard deviation of the background signal. The limits of detection are shown in Table 6.3.

Table 6.3: Limit of detection of nanoparticle conjugates from nitrocellulose membrane

Conjugate Label	***Limit of Detection of Nanoparticle Conjugates (M)***
TAMRA ITC	2.4×10^{-13}
GM19	8.3×10^{-13}
MPY	3.9×10^{-13}

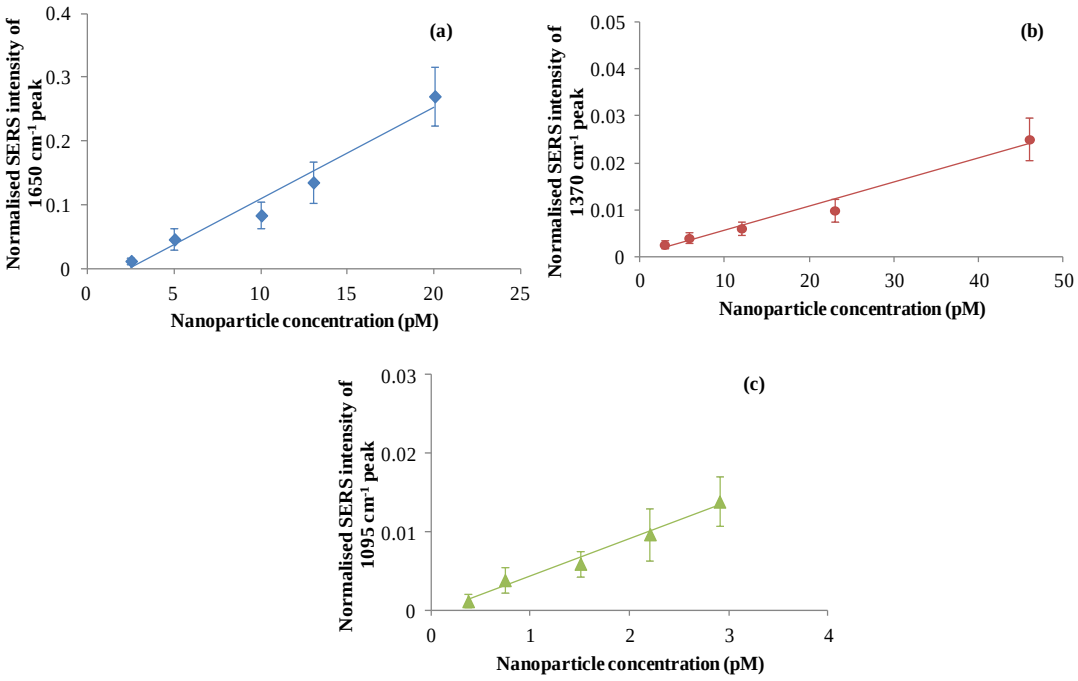

Figure 6.22 Dilution series of silver nanoparticle conjugates; **(a)** blue: TAMRA ITC 1650 cm^{-1}peak (532 nm, 0.1s, 10x obj), **(b)** red: GM19 1370 cm^{-1}peak (633 nm, 0.1s, 10x obj), **(c)** green: MPY 1095 cm^{-1}peak (785 nm, 0.5s, 10x obj).

Similar limits of detection were obtained for each batch of functionalised nanoparticles with limits below picomolar concentration evidently achieved. The GM19 conjugates generated a slightly higher detection limit, probably due to the use of the off resonant 633 nm excitation wavelength.

This study has demonstrated the successful detection of dye functionalised DNA nanoparticles through use of optimised experimental SERS conditions. Therefore, it was useful to demonstrate the application of the assay as a diagnostic detection method. An application of a nitrocellulose surface assay was analysed through the diagnostic detection of methicillin-resistant *Staphylococcus aureus* (MRSA) *via* selective hybridisation of DNA functionalised nanoparticle conjugates.

6.6 Nitrocellulose Surface Assay for the Detection of Methicillin-Resistant Staphylococcus Aureus (MRSA)

The aim of this study was to develop a membrane assay which utilised SERS for the detection of unmodified target DNA sequences from a simple and cost effective platform. The detection of sequences corresponding to MRSA were analysed to demonstrate the

applicability of the method as a diagnosis technique. MRSA sequences have been previously used within this thesis and are discussed in detail in Section 5.2.3. The sequences immobilised on the nitrocellulose surface (target) and adsorbed onto the nanoparticle surface (conjugate) are shown in Table 6.4.

Table 6.4: MRSA oligonucleotide sequences and modifications

Sequence Name	***Sequence (5'- 3')***	***5' Modification***
Conjugate	TGGAAGTTAGATTGGGATCATAGCGTCAT	Thioctic Acid-$(HEG)_3$
Target	ATGACGCTATGATCCCAATCTAACCTTCCA	-

A fluorescent DNA melt was initially performed, in order to identity the optimal temperature to achieve successful hybridisation between the MRSA conjugate and target sequences. Both the target and conjugate sequences were diluted in PBS to 1 μM and heated from 60 – 90 °C. The addition of the intercalating dye SYBR Green enabled monitoring of strand hybridisation.

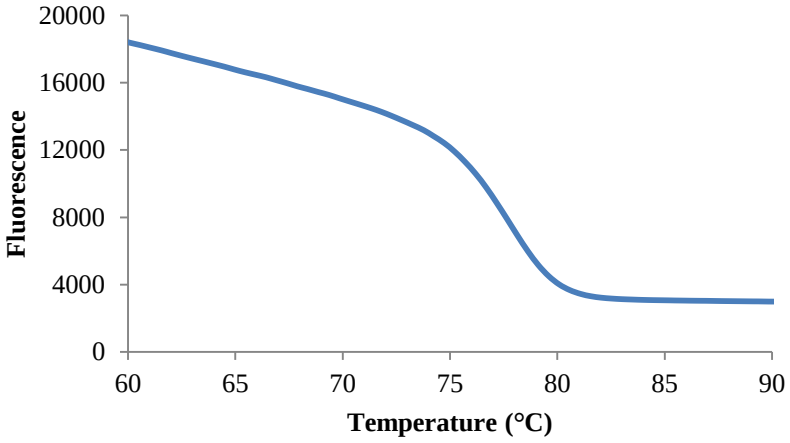

Figure 6.23: Fluorescent melt using SYBR Green of unmodified MRSA target DNA and conjugate MRSA sequence.

A sigmoidal melting curve demonstrates successful hybridisation of the complementary MRSA sequences was obtained (Figure 6.23). The temperature at which the DNA sequences hybridise was determined to be 78 °C. This temperature was higher than that of the hybridisation of the original sequences, due to the longer sequence being analysed. However, the hybridisation temperature utilised within the surface assay of 30 °C will nevertheless promote sequence hybridisation.

The detection of an unlabelled MRSA sequence from the nitrocellulose membrane was performed using the optimised assay conditions. Initially, TAMRA ITC labelled nanoparticles incorporating the complementary MRSA sequence were utilised to determine the presence of the target oligonucleotide. The average intensity of the 1650 cm^{-1} peak for target, no target and nonsense samples was generated through SERS analysis of the membrane surface (Figure 6.24).

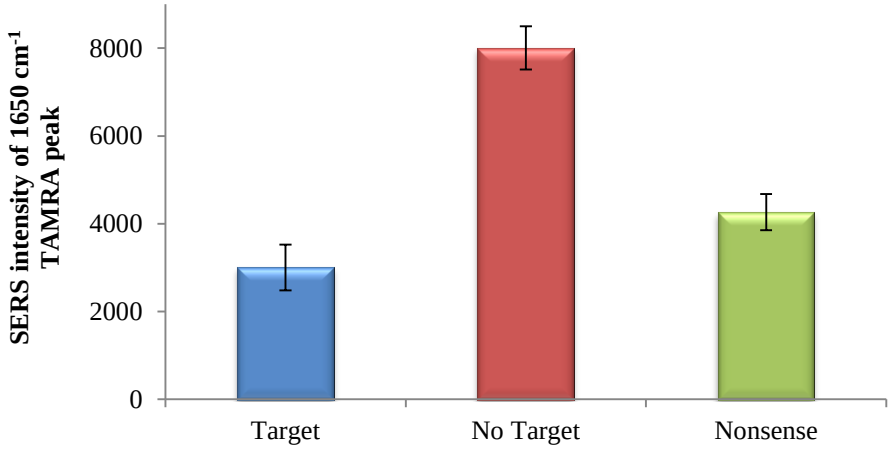

Figure 6.24: SERS intensity of 1650 cm^{-1} TAMRA ITC peak for target, no target and nonsense samples from MRSA detection surface assay obtained using 532 nm laser excitation (10 x obj., 0.1 sec. acc.). Each bar represents 4 replicate maps and error bars ± one standard deviation.

The no target sample gave unexpectedly high intensity signals, with the target and nonsense regions generating similarly lower responses. These results suggest that the blocking step has not sufficiently blocked the surface, increasing the amount of non-specific conjugate binding. The high no target signal appears to result from inefficient surface blocking. Whereas, the target and nonsense samples generated lower intensity signals due to intrinsic blocking of the surface from the presence of the target and nonsense sequences spotted on the membrane during the first assay step.

TAMRA ITC labelled nanoparticles have demonstrated varying degrees of successful reproducibility within the surface detection assay. Much work has been carried out into optimising and developing the assay procedure and although great improvements have been observed, the accurate reproducibility of the method remains the fundamental focus. Initial promising results from the use of MPY conjugates were achieved suggests an overall improved consistency (Section 6.2 and 6.5.2). Previous results have demonstrated that the use of the small molecule mercaptopyridine as a Raman reporter on silver nanoparticle

conjugates generated comparable limits of detection and low background signals. Consequently, a batch of functionalised silver nanoparticles were prepared incorporating the MRSA conjugate sequence and MPY molecule.

6.6.1 Detection of MRSA using MPY functionalised DNA nanoparticles

The initial detection of MRSA using the surface assay and TAMRA ITC labelled DNA conjugates demonstrated a reduction in the efficiency of the membrane blocking step (Figure 6.24). Consequently, the surface blocking step using the MPY conjugates was investigated. DNA detection surface assays, such as Southern blotting methods, often utilise blocking agents diluted in volumes of saline sodium citrate (SSC) buffer to obtain the greatest surface blockage. The SSC buffer contains essential salt ions which may enhance DNA stability and surface attachment. Thus, three blocking conditions were analysed; 100 % block (which had been used previously with the optimised experimental conditions), 50 % block plus 50 % 5x SSC buffer and 10 % block plus 90 % 5x SSC buffer. To further ensure adequate blocking of the membrane surface had been achieved, the time taken for the blocking step was also increased to 2 hours at 50 °C (previously a 1 hour blocking time was used). The blocking agent used throughout was salmon testes DNA. The SERS intensities for each blocking parameter were generated and the average intensity of the 1095 cm^{-1} peak was plotted against blocking conditions. This is shown as a 3D bar chart in Figure 6.25.

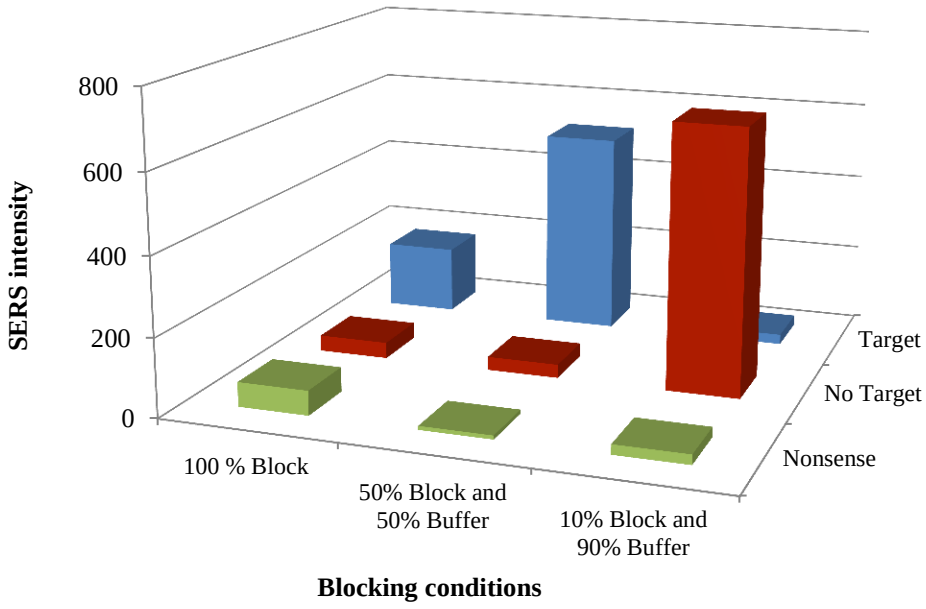

Figure 6.25: SERS intensity of the 1095 cm^{-1} peak of MPY labelled DNA conjugates on nitrocellulose membrane assay using different blocking conditions using 785 nm laser excitation (10 x obj., 0.5 sec. acc.); blue: target DNA, red: no target, green: nonsense.

Results generated from use of 100 % block as well as 50 % block and 50 % buffer demonstrated successful target sequence detection. However, stronger target DNA SERS responses and weaker control signals were obtained when applied with a 50 % mixture of block and SSC buffer, indicating that the highest blocking was obtained. The use of 10 % block in 90 % SSC buffer, clearly demonstrated minimal surface blocking has been achieved, as a high SERS signal intensity was found within the no target control assay. The raw spectra for the target, no target and nonsense samples generated using 50 % block and 50 % buffer mixture is shown in Figure 6.26.

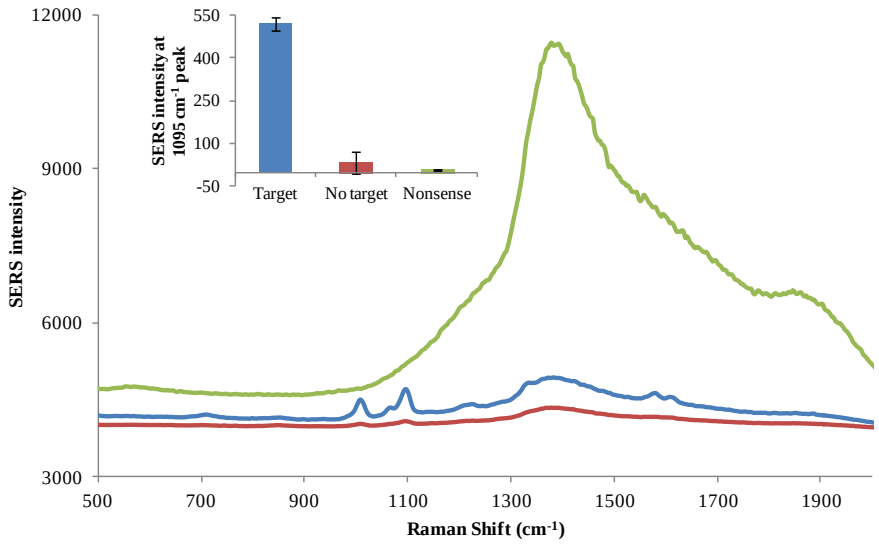

Figure 6.26: SERS spectra of nitrocellulose membrane containing MPY labelled DNA conjugates recorded using 785 nm laser excitation (10x obj.,0.5 sec. acc.); blue: target DNA, red: no target, green: nonsense. Insert contains average signal intensity of 1095 cm^{-1} peak, each bar represents 4 replicate maps and error bars ± one standard deviation.

The successful detection of unmodified labelled DNA from the membrane surface through SERS detection has been shown. These results have demonstrated that a combination of increased blocking times, altered blocking conditions and the use of MPY conjugates, which is analysed at the higher excitation wavelength of 785 nm, has improved the spectral responses obtained through increased hybridisation of the DNA conjugates to the surface adsorbed DNA sequence. This specific binding event was analysed further.

6.6.2 Specific Hybridisation of MRSA Conjugates

To confirm that the MRSA nanoparticle conjugates were selectively hybridising to the immobilised surface target DNA and were not bound to the membrane by embedding in the porous substrate, a depth profile SERS map was carried out on the assay surface. The ability to bind molecules to a membrane substrate, whilst retaining functionality and accessibility is highly beneficial in understanding surface interactions. Irvine *et al*. demonstrated the absorbing structure of a nitrocellulose matrix was key in retaining the activity of surface bound proteins.[181] In this study, a 3D volume image was obtained through the gathering of multiple SERS maps at different depths through the target region (Figure 6.27). The individual SERS maps were then stacked to generate a volume image of the cross section of the membrane. The approximate depth of the nitrocellulose membrane is 10 – 14 μm, thus depth analysis was carried out by scanning 10 membrane layers at 1 μm intervals. The scans were then complied into a volume image through use of Image J software.

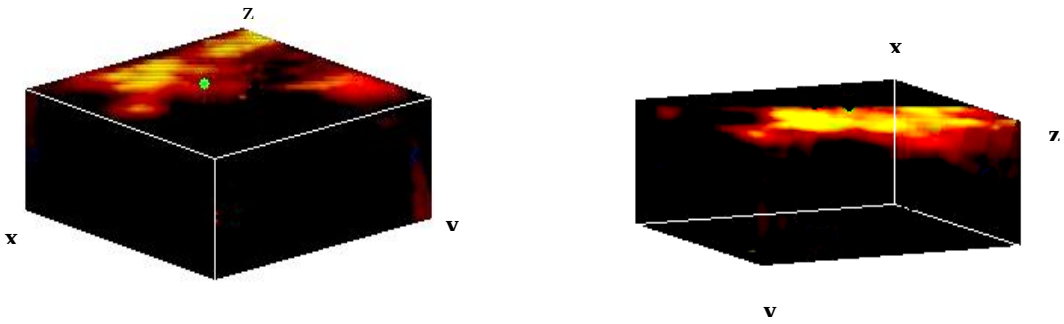

Figure 6.27: False colour volume image of cross section of nitrocellulose membrane at two different angles. The signal was generated from the 1095 cm^{-1} MPY peak using 785 nm laser excitation (10x obj., 0.5 sec. acc.) with a 2 μm resolution.

The generated volume image of the membrane illustrates that the strongest SERS signals were obtained from the surface layers of the nitrocellulose membrane. This suggests that the nanoparticle conjugates are not fully penetrated into the membrane but are being held near the surface layer. However, to demonstrate conjugate immobilisation is occurring through DNA hybridisation, the selectivity of the assay had to be determined.

This was achieved through preparation of two batches of functionalised nanoparticles with each set incorporating different SERS active molecules and DNA sequences, the original conjugate sequence and the MRSA conjugate sequence. Subsequent addition of both

conjugates to the nitrocellulose membrane containing immobilised target MRSA oligonucleotide, should bind only the nanoparticles containing complementary MRSA DNA. Whilst, conjugates containing the non-complementary sequences will be washed from the substrate, producing no SERS responses. This selective binding event will generate specific SERS spectra from the hybridised conjugates.

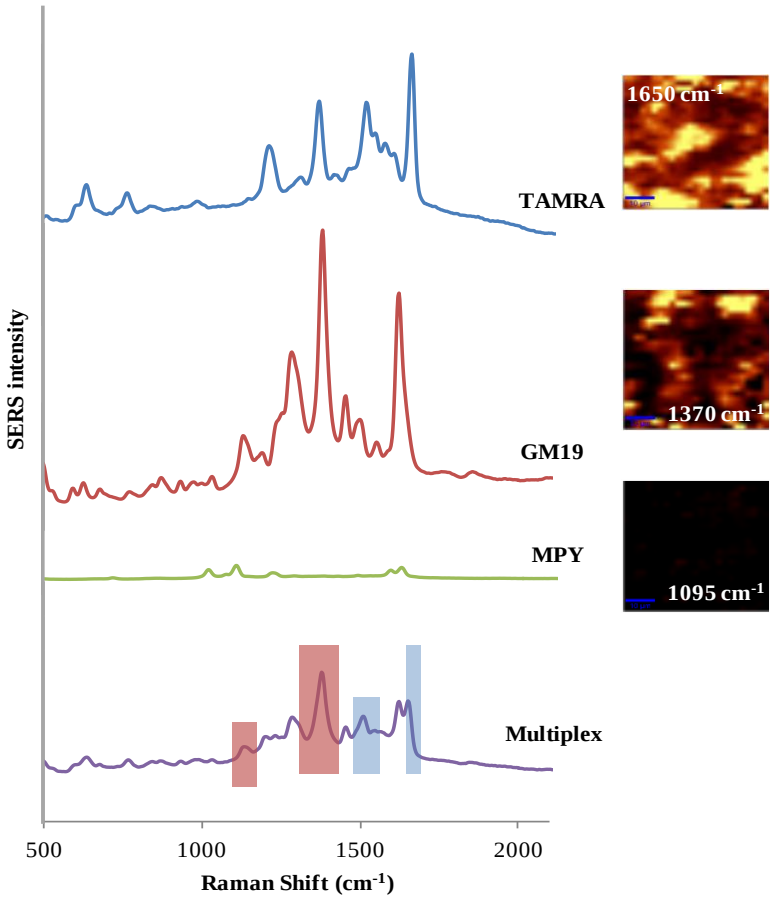

Figure 6.28: SERS spectra of nitrocellulose membrane containing individual silver TAMRA ITC, GM19, MPY labelled DNA conjugates and multiplex region containing all three conjugates recorded using 532 nm laser excitation (10x obj., 0.1 s acc time). Blue (TAMRA ITC) and red (GM19) squares within the multiple spectra illustrate distinctive peaks for each dye. False colour images with corresponding dye peak were generated from the multiplex nitrocellulose sample area containing all 3 conjugates (2 µm resolution).

Initially, distinct peaks for each label within a mixture had to be determined. Combinations of the three functionalised nanoparticles containing the SERS active dyes; TAMRA ITC, GM19 and MPY were analysed at 532, 633 and 785 nm excitation wavelengths, to determine which conjugates and excitation wavelength would generate the strongest peaks for each

labels. Optimal SERS signals resulted from batches of silver nanoparticles incorporating TAMRA ITC and GM19 dyes using 532 nm excitation wavelength (Figure 6.28). This combination generated the highest intensity and most distinct peaks for each of the two dyes. Clear peaks for the TAMRA ITC dye at 1650 cm^{-1} and GM19 at 1370 cm^{-1} enabled accurate detection of the presence of either nanoparticle conjugates from the membrane surface. No peaks from the MPY molecule were obtained using 532 nm laser excitation from the multiplex spectra.

Two batches of silver nanoparticle conjugates containing different DNA and dye were prepared. One batch incorporated the MRSA conjugate sequence and the TAMRA isothiocynate dye adsorbed onto the surface, whilst the other was functionalised with the original conjugate sequence and GM19 dye.

A surface assay was performed immobilising MRSA target DNA onto the substrate. During the hybridisation step equal concentrations of each dye labelled conjugate were premixed and then applied to the membrane surface. The original conjugate DNA is non-complementary to the target MRSA sequence and was utilised as a control, therefore, no signals should be obtained from the surface assay. SERS analysis was then carried out by mapping the sample region and generating false colour images corresponding to the distinct spectral peaks of each dye labelled conjugate. A typical map generated from the sample region is shown in Figure 6.29, illustrating the same analysed membrane region evaluating both the 1650 and 1370 cm^{-1} peaks.

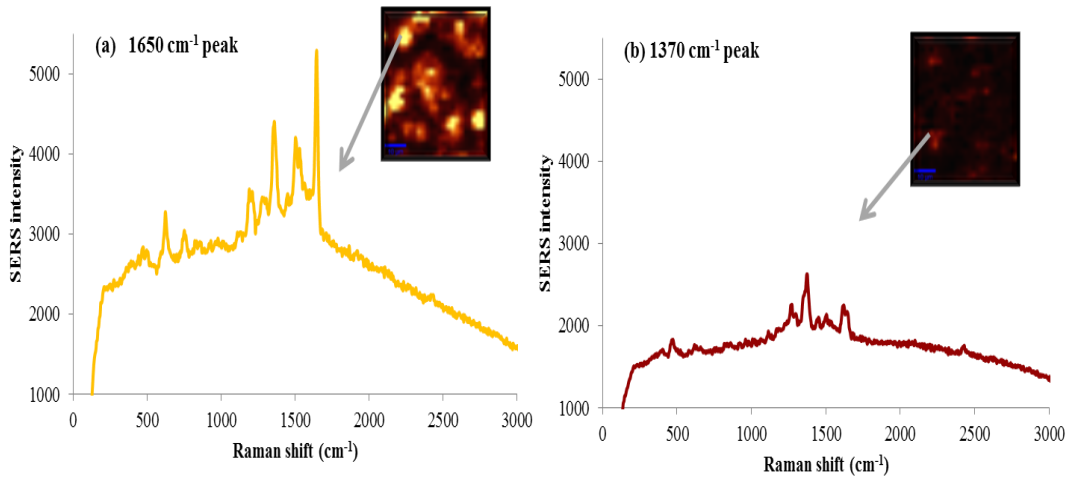

Figure 6.29: SERS spectra of nitrocellulose membrane containing target MRSA DNA recorded using 532 nm laser excitation (10x obj., 0.1 s acc time) with **(a)** addition of complementary TAMRA ITC functionalised nanoparticles and **(b)** non-complementary GM19 functionalised nanoparticles.

Brighter pixels within the false colour images indicate stronger signal intensities of the principle peak. The abundance and intensity of the TAMRA ITC signals obtained were significantly higher compared to the peaks corresponding to the GM19 labelled conjugates within an identical sample region (Figure 6.29(a)). The weak GM19 signals obtained can be attributed to a limited level of non-specific surface binding, however, the spectra also demonstrates a signal contribution from the TAMRA ITC dye (Figure 6.29(b)). Distinctive peaks at 1650 and 1505 cm^{-1}, show the presence of TAMRA ITC labelled conjugates which have bound to the target MRSA through complementary hybridisation.

The selective binding of the TAMRA ITC labelled MRSA DNA nanoparticle conjugates has been demonstrated through the specific DNA hybridisation events on the membrane surface. To investigate the further selectivity and potential of this surface assay as a clinical diagnostic method, an alternative of swabbing samples onto the membrane was analysed.

6.6.3 Application of Surface Assay through DNA Swabbing

The potential of a diagnostic SERS surface assay has been demonstrated through the selective detection of complementary nanoparticle conjugates from a nitrocellulose surface. In the work so far, bulk spots of the target DNA sequence (0.2 µL) were pipetted onto the membrane, producing large diffuse areas of DNA sample. Therefore, to further demonstrate the specific detection ability of the assay, the target DNA was applied to the surface in a distinctive shape.

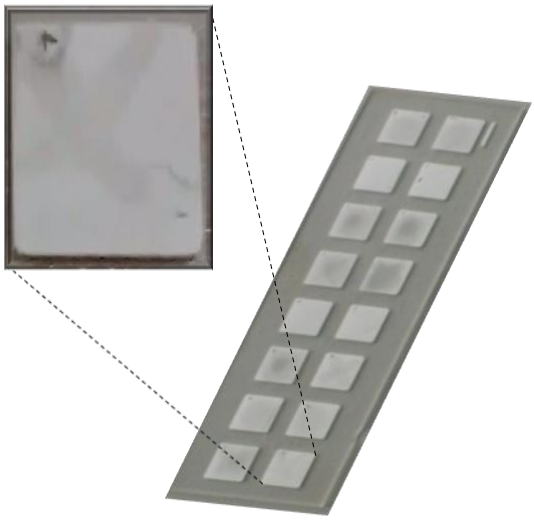

Figure 6.30: Swabbing of "X" onto nitrocellulose membrane slide with enlarged white light image of target DNA applied to surface after full assay

This would allow the functionalised nanoparticles to selectively hybridise to the membrane and be visualised through reproducing a SERS map of the shape. This is beneficial in demonstrating the successful and specific detection of target DNA with greater confidence. Within the assay, the MRSA target oligonucleotides were applied to the tip of a cotton wool swap and applied to the nitrocellulose membrane in a cross shape (Figure 6.30).

The use of the Nexterion® LE buffer for spotting the target DNA unexpectedly allowed the sample shapes to be visualised throughout the study, however, the initial coverage of the unmodified target DNA onto the membrane by SERS could not be determined. Therefore, a preliminary experiment was performed by swabbing a cross of SERS active nanoparticle conjugates onto a nitrocellulose surface and mapping the entire sample area. This would establish a proof of concept to ensure the DNA conjugates could be detected when shaped onto the membrane. The DNA was applied to the surface in a distinctive cross shape approximately 5 x 5 mm.

The Witec Alpha 300 R confocal microscope used throughout this study (Section 3.3.1.2) enabled highly sensitive analyses and contained three laser excitation wavelengths; 532, 633 and 785 nm, allowing comparable dye and wavelength combinations to be investigated. However, the instrumentation was limited to Raman mapping small micron sized areas, approximately 100 x 100 μm, which is only a small fixed region of the 6 x 6 mm membrane square. Therefore, to obtain full sample analysis the Raman instrumentation had to be altered. A Renishaw InVia Raman Microscope (Section 3.3.1.3) was utilised to enable a representation of the sample square to be generated through accumulative white light images of the membrane. This instrument utilised a streamline mapping system providing the capability to rapidly map large areas through cumulative image capture. The full sample area could then be mapped using SERS. This study utilised the MPY labelled DNA nanoparticles and a 785 nm excitation wavelength. The MPY label was utilised as results had previously demonstrated effective results using this label and wavelength combination (Section 6.6.1). The conjugates were applied to the membrane by cotton wool swabbing onto the surface in a cross shape and analysed by SERS (Figure 6.31).

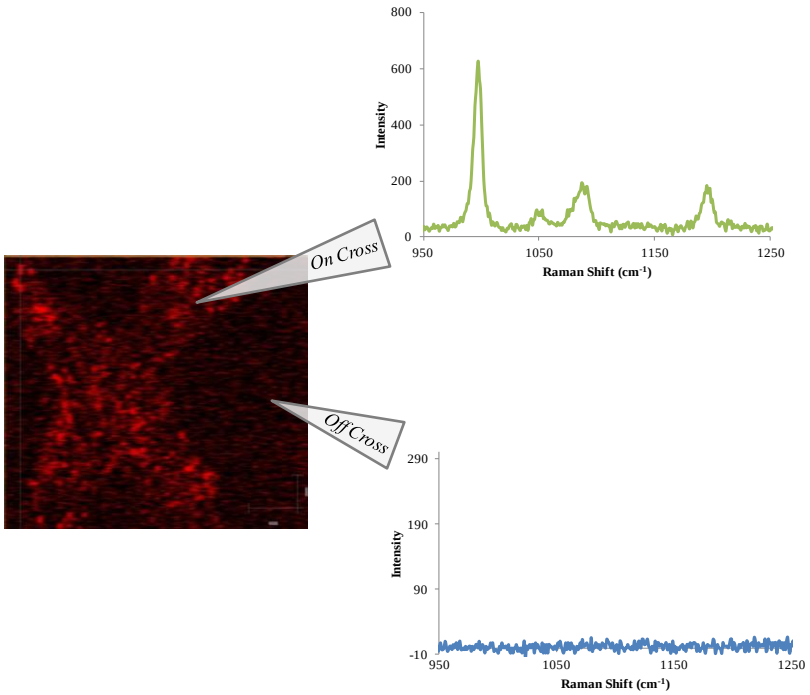

Figure 6.31: SERS false colour map of the 1005 cm^{-1}peak of MPY DNA silver nanoparticle conjugates swabbed onto nitrocellulose membrane in an "X" shape obtained using 785 nm laser excitation (10 x obj., 0.5 sec. acc.)

A false colour image of the MPY conjugates swapped directly onto the nitrocellulose surface area was obtained. Analysis of the conjugates using the Renishaw InVia Raman instrument generated distinctive MPY peaks with the most intense peak obtained at 1005 cm^{-1}. A clear cross shape can be visualised from the surface with strong MPY spectral peaks obtained from areas on the cross with no SERS responses from regions off the cross. This indicates that sufficient surface coverage can be obtained and also demonstrates that a distinct cross shape can be achieved from the porous nitrocellulose membrane.

A full detection assay was then performed using previously optimised experimental conditions with the unmodified target MRSA sequence applied through swabbing instead of bulk spotting. The samples were again applied in a cross shape to demonstrate accurate detection of the target DNA. Control samples of a no target and nonsense region were also analysed, the nonsense DNA was swabbed onto the surface in a cross shape. The complete membrane sample regions were SERS mapped and the average peak height at 1005 cm^{-1} was calculated. This generated false colour images of each sample and highlighted the strongest regions corresponding to the MPY peak (Figure 6.32).

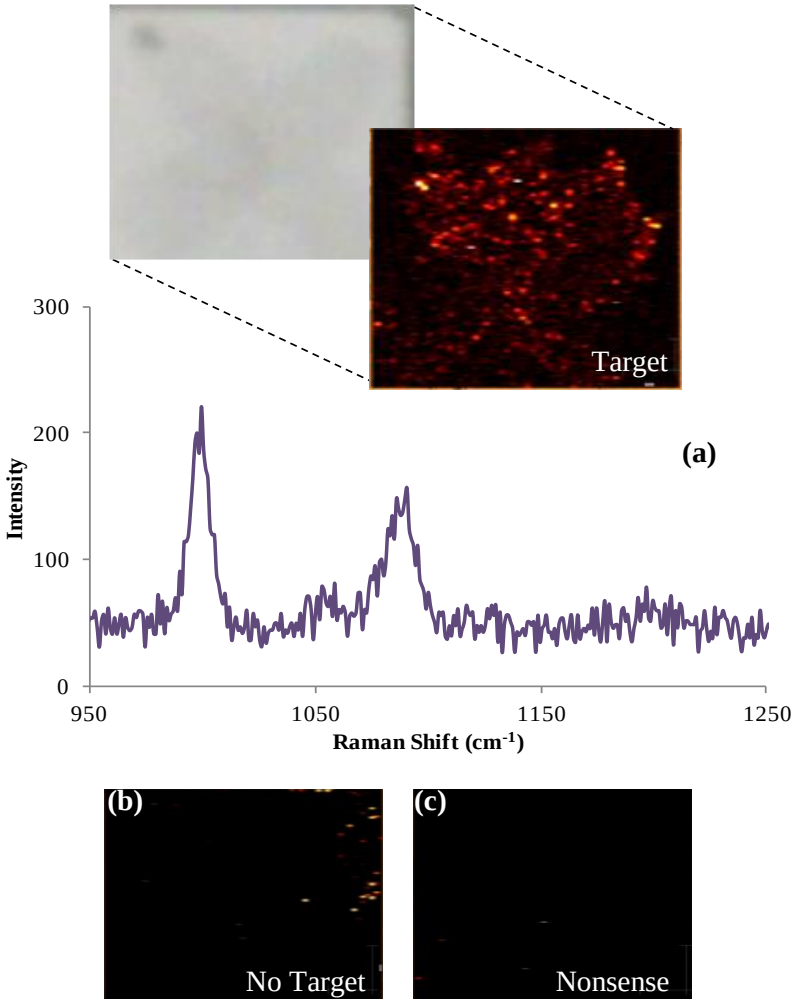

Figure 6.32: (a) SERS false colour and white light images of 1005 cm^{-1}peak of MPY DNA silver nanoparticle conjugates by swabbing "X" onto nitrocellulose membrane slide obtained using 785 nm laser excitation (10 x obj., 0.5 sec. acc.). SERS false colour image of MPY conjugate peak at 1005 cm^{-1} **(b)** no target, **(c)** nonsense

The false colour images generated from the control regions generated low SERS responses, with the weak signals generated attributed to a minimal amount of non-specific binding of the nanoparticle conjugates to the membrane. However, significantly stronger MPY responses were obtained from the target area. The generated target map illustrates areas in which the MPY conjugate have bound and an outline of a cross shape corresponding to the white light image. However, comparing this image to the distinct cross images obtained from the direct swabbing of nanoparticle conjugates onto the membrane (Figure 6.31), it can be seen that a more distorted cross shape was obtained. This could be as a result of incomplete coverage of the target sequence and reduced sequence hybridisation efficiency due to the random orientation of the target DNA which reduces strand accessibility.

This investigation has demonstrated a progression of the surface assay through the application of target DNA to the SERS substrate using a cotton wool swab. Swabbing techniques are often utilised to detect DNA samples from surfaces, therefore, this application method has been highly advantageous in showing an initial step to developing a practical DNA detection technique.

6.7 Chapter Conclusion

This study has demonstrated initial experiments showing the potential of a surface assay for the detection of unlabelled and unmodified DNA sequences by SERS. Intensive optimisation has progressed the technique from producing weak SERS responses, high background signals and poor discrimination between controls, to the illustration of significant and specific detection of clinically relevant sequences. However, to develop the method into a reliable clinical detection assay, further optimisation and development must be carried out to obtain accurate and reproducible results that are consistently obtained every time.

Functionalised nanoparticles were utilised to demonstrate the successful detection of unmodified DNA from both epoxysilane and nitrocellulose substrates. Silver citrate-reduced nanoparticles were successfully functionalised through chemisorption of specific DNA sequences and SERS active molecules. This enabled strong and distinct SERS responses to be obtained from three separate batches using TAMRA ITC, GM19 and MPY molecules. Hybridisation of these labelled DNA conjugates to complementary target DNA immobilised onto solid surfaces has successfully been shown by SERS.

MRSA related sequences have been successful detected from nitrocellulose membrane surfaces. This was demonstrated through specific conjugate hybridisation of complementary sequences on the membrane surface. Distinctive false colour maps relating to the MPY spectra have also shown distinctive cross shapes can be definitively reproduced by the selective hybridisation and SERS analysis. These promising results illustrate applications for DNA surface detection methodologies.

The early stages of a promising SERS detection assay have been illustrated within this study, however, significant work is still necessary to unearth the full potential of this method and ensure accurate results are consistently achieved.

6.8 Further Work

The reproducibility of the assay is a major problem. Early work has demonstrated variability in the detection of TAMRA ITC labelled DNA conjugates with the high energy 532 nm laser excitation wavelength. However, the latter stages of this investigation have shown improvement through use of mercaptopyridine (MPY) functionalised nanoparticles and detection using 785 nm laser excitation wavelength. Throughout this study, results have demonstrated that the assay shows high promise when performed successfully. Therefore, research must aim to investigate and improve the reproducibility through further investigation of the MPY detection system. This would enable accurate results to be consistently obtained and allow the full potential of the assay to be investigated.

Reducing the size of the surface array into the low-micron and nanoscale would prove to be highly valuable in providing lower detection limits for more efficient disease screening. Therefore, work could be carried out to produce nanoscale fabrication through Dip-pen Nanolithography (DPN). The assay has demonstrated the potential of selective detection and through SERS analysis distinctive fingerprint spectra have been obtained. This is a huge advantage for the detection of multiple sequences on one substrate. Therefore, this work could be expanded to investigate the detection of multiple genomic strains from clinically biological samples. In the future, the ultimate aim of this assay would be to enable large numbers of clinically relevant sequences to be detected for one sample. Potentially, numerous diagnostic tests could be performed on one clinical sample using one substrate slide and SERS analysis. This work could be progressed to develop a DNA detection method able to work successfully and efficiently on a cost effective substrate such as filter paper.

7. Conclusions

Silver nanoparticles are commonly utilised as an enhancing substrate for the detection of DNA by SERS. The beneficial qualities such as increased scattering efficiencies and favourable coincidence of the surface plasmons enable silver nanoparticles to generate strong signal responses within the visible wavelength region. This has allowed a large number of SERS active labels to be attached to target sequences and be specifically detected by SERS as shown throughout this study. This technique has also shown to be an essential analytical tool for providing an understanding of the principle of DNA adsorption onto nanoparticle surfaces. The adsorption of DNA onto silver nanoparticles has been shown to be driven through attachment of nucleobases and the attachment of the TAMRA dye contributed minimally to surface adsorption. This observation can be exploited to differential detect target DNA through differences in affinity of ssDNA and dsDNA onto the metal surface. However, the interactions at the nanoparticle surface interface have shown to be complex and elaborate involving numerous unidentified processes and interactions. This was highlighted through investigating the interaction between TAMRA and FAM labelled DNA probes within a multiplex sample. Unexpected but significant results, suggest that over a concentration gradient the signal responses from the TAMRA probe are inhibited at lower concentrations but are significantly enhanced as the DNA concentration is increased. Results appear to indicate that probe interactions are preferentially orientating sequences onto the enhancing surface with further work needed to thoroughly evaluate this process. However, SERS has enabled an insight into the complex surface chemistry of DNA and nanoparticles.

This study has demonstrated the use of silver nanoparticles to successfully develop two distinct methods for the specific detection of DNA. These methods have targeted specific clinical sequences of methicillin resistant *Staphylococcus aureus* (MRSA) within a diagnostic detection assay and have demonstrated the ability to discriminate against non-complementary sequences. The TaqSERS assay combined the benefits of a TaqMan assay with SERS detection to develop a highly sensitive, selective and adaptable detection method. The assay was shown to generate detection of genomic MRSA and SA sequences with high sequence specificity and low levels of sensitivity. Successful strain discrimination within a duplex assay has shown the potential for further advancing the detection of multiple targets.

Nanoparticle labelling is an attractive method for identifying DNA sequences and has shown to be a successful method for the indirect detection of unlabelled DNA from solid substrate surfaces. Specific hybridisation of silver nanoparticles functionalised with thioctic acid labelled sequences and Raman reporter molecules have demonstrated the presence of MRSA sequences on nitrocellulose and epoxysilane coated surfaces. The versatility of SERS was demonstrated through the generation of strong and distinct SERS responses using three SERS active molecules; TAMRA ITC, GM19 and MPY and three laser excitation wavelengths; 532, 633 and 785 nm. The specific detection of nanoparticle conjugates on membrane substrates has been demonstrated through preferential hybridisation of complementary DNA labelled nanoparticles and the reproduction of a distinctive cross shape by SERS mapping.

Overall the effectiveness and versatility of SERS as a DNA detection method has been demonstrated throughout this study. SERS has shown the potential as a viable DNA analysis method within two diverse detection strategies and an increased understanding into DNA surface interactions has also been demonstrated through the utilisation of SERS.

8. References

1. Griffith, F., *J. Hygiene* **1928,** *27* (2), 113.
2. Avery, O. T.; MacLeod, C. M.; McCarty, M., *J. Exp. Med.* **1944,** *79* (2), 137.
3. Dahm, R., *Hum. Genet.* **2008,** *122* (6), 565.
4. Hargittai, I., *Struct. Chem.* **2009,** *20* (5), 753.
5. Jones, M. E., *Y. J. Bio. Med.* **1953,** *26* (1), 80.
6. Campbell, N.; Reece, J., *Biology*. 6 ed.; Benjamin Cummings: San Francisco.
7. Chargaff, E., *Experientia* **1950,** *6* (6), 201.
8. Blackburn, G. M.; Gait, M. J.; Loakes, D.; Williams, D. M., *Nucleic Acids in Chemistry and Biology*. 3rd ed.; Royal Society of Chemistry: Cambridge, 2006.
9. Watson, J. D.; Crick, F. H. C., *Nature* **1953,** *171* (4356), 737.
10. Watson, J. D.; Crick, F. H. C., *Nature* **1953,** *171* (4361), 964.
11. Franklin, R. E.; Gosling, R. G., *Nature* **2003,** *421* (6921), 400.
12. Crick, F. H. C.; Watson, J. D., *Proc. R. Soc. A* **1954,** *223* (1152), 80.
13. Commons WikiMedia, http://commons.wikimedia.org/wiki/File:DNA_double_helix_horizontal.png (accessed March 2013).
14. Wing, R.; Drew, H.; Takano, T.; Broka, C.; Tanaka, S.; Itakura, K.; Dickerson, R. E., *Nature* **1980,** *287* (5784), 755-758.
15. Baraldi, P. G.; Tabrizi, M. A.; Preti, D.; Fruttarolo, F.; Avitabile, B.; Bovero, A.; Pavani, G.; Carretero, M. D. N.; Romagnoli, R., *Pure and Applied Chemistry* **2003,** *75* (2-3), 187-194.
16. Papadopoulou, E.; Bell, S. E. J., *Chem. Commun.* **2011,** *47* (39), 10966-10968.
17. Poon, K.; Macgregor, R. B., *Biopolymers* **1998,** *45* (6), 427.
18. Collins, F. S.; Morgan, M.; Patrinos, A., *Science* **2003,** *300* (5617), 286.
19. Consortium, I. H. G. S., *Nature* **2001,** *409* (6822), 934.
20. Faulds, K.; Smith, W. E.; Graham, D., *Analyst* **2005,** *130* (8), 1125.
21. Saiki, R. K.; Scharf, S.; Faloona, F.; Mullis, K. B.; Horn, G. T.; Erlich, H. A.; Arnheim, N., *Science* **1985,** *230* (4732), 1350-1354.
22. Sambrook, J.; Russel, D., *Molecular Cloning A Laboratory Manual*. 3rd ed.; CSHL Press: 2001; Vol. 2.
23. McPherson, M. J.; Hames, B. D.; Taylor, G. R., *PCR 2 A Practical Approach*. Oxford University Press Inc.: New York, 1995; p Chapter 1.
24. Skeidsvoll, J.; Ueland, P. M., *Anal. Biochem.* **1995,** *231* (2), 359.
25. Higuchi, R.; Fockler, C.; Dollinger, G.; Watson, R., *Bio-Technology* **1993,** *11* (9), 1026.
26. Tseng, S. Y.; Macool, D.; Elliott, V.; Tice, G.; Jackson, R.; Barbour, M.; Amorese, D., *Anal. Biochem.* **1997,** *245* (2), 207.

27. Ranasinghe, R. T.; Brown, T., *Chem. Commun.* **2005,** (44), 5487.
28. Maxam, A. M.; Gilbert, W., *Proc. Natl. Acad. Sci. U.S.A.* **1977,** *74* (2), 560.
29. Sanger, F.; Coulson, A. R., *J. Mol. Biol.* **1975,** *94* (3), 441.
30. Sanger, F.; Nicklen, S.; Coulson, A. R., *Proc. Natl. Acad. Sci. U.S.A.* **1977,** *74* (12), 5463.
31. Ronaghi, M.; Karamohamed, S.; Pettersson, B.; Uhlen, M.; Nyren, P., *Anal. Biochem.* **1996,** *242* (1), 84.
32. Nuovo, G. J.; Hohman, R. J.; Nardone, G. A.; Nazarenko, I. A., *J. Histochem. Cytochem.* **1999,** *47* (3), 273.
33. Morris, T.; Robertson, B.; Gallagher, M., *J. Clin. Microbiol.* **1996,** *34* (12), 2933.
34. Kimura, B.; Kawasaki, S.; Fujii, T.; Kusunoki, J.; Itoh, T.; Flood, S. J. A., *J. Food Prot.* **1999,** *62* (4), 329.
35. Laurendeau, I.; Bahuau, M.; Vodovar, N.; Larramendy, C.; Olivi, M.; Bieche, I.; Vidaud, M.; Vidaud, D., *Clin. Chem.* **1999,** *45* (7), 982.
36. Nurmi, J.; Ylikoski, A.; Soukka, T.; Karp, M.; Lovgren, T., *Nucleic Acids Res.* **2000,** *28* (8), 6.
37. Solinas, A.; Thelwell, N.; Brown, T., *Chem. Commun.* **2002,** (19), 2272.
38. de Kok, J. B.; Wiegerinck, E. T. G.; Giesendorf, B. A. J.; Swinkels, D. W., *Hum. Mutat.* **2002,** *19* (5), 554.
39. Kostrikis, L. G.; Tyagi, S.; Mhlanga, M. M.; Ho, D. D.; Kramer, F. R., *Science* **1998,** *279* (5354), 1228.
40. Piatek, A. S.; Tyagi, S.; Pol, A. C.; Telenti, A.; Miller, L. P.; Kramer, F. R.; Alland, D., *Nat. Biotechnol.* **1998,** *16* (4), 359.
41. Saha, B. K.; Tian, B. H.; Bucy, R. P., *J. Virol. Methods* **2001,** *93* (1-2).
42. Taveau, M.; Stockholm, D.; Spencer, M.; Richard, I., *Anal. Biochem.* **2002,** *305* (2).
43. Sassolas, A.; Leca-Bouvier, B. D.; Blum, L. J., *Chem. Rev.* **2008,** *108* (1), 109.
44. Southern, E. M., *J. Mol. Biol.* **1975,** *98*, 503-517.
45. Laitala, V.; Ylikoski, A.; Raussi, H. M.; Ollikka, P.; Hemmila, I., *Anal. Biochem.* **2007,** *361* (1), 126.
46. Negoro, E.; Iwasaki, H.; Tai, K.; Ikegaya, S.; Takagi, K.; Kishi, S.; Yamauchi, T.; Yoshida, A.; Urasaki, Y.; Shimadzu, M.; Ueda, T., *Int. J. Infect. Diseases* **2013,** *17* (4), E271.
47. Dufva, M., *Biomol. Eng.* **2005,** *22* (5-6), 173.
48. Xu, C.; Cai, H.; Xu, Q.; He, P. G.; Fang, Y. Z., *Fresenius' J. Anal. Chem.* **2001,** *369* (5), 426
49. Cai, H.; Wang, Y. Q.; He, P. G.; Fang, Y. H., *Anal. Chim. Acta* **2002,** *469* (2), 165.
50. Harper, M. M.; Dougan, J. A.; Shand, N. C.; Graham, D.; Faulds, K., *Analyst* **2012,** *137* (9), 2063.
51. Cao, Y. W. C.; Jin, R. C.; Mirkin, C. A., *Science* **2002,** *297* (5586), 1536.
52. Dharuman, V.; Nebling, E.; Grunwald, T.; Albers, J.; Blohm, L.; Elsholz, B.; Woerl, R.; Hintsche, R., *Biosens. Bioelectron.* **2006,** *22* (5), 744.

53. Wang, S. G.; Wang, R. L.; Sellin, P. J.; Zhang, Q., *Biochem. Biophys. Res. Commun.* **2004,** *325* (4), 1433.
54. Fang, X. H.; Liu, X. J.; Schuster, S.; Tan, W. H., *J. Am. Chem. Soc.* **1999,** *121* (12), 2921.
55. Dupont-Filliard, A.; Roget, A.; Livache, T.; Billon, M., *Anal. Chim. Acta* **2001,** *449* (1-2), 45.
56. Pan, S. L.; Rothberg, L., *Langmuir* **2005,** *21* (3), 1022.
57. Healey, B. G.; Matson, R. S.; Walt, D. R., *Anal. Biochem.* **1997,** *251* (2), 270.
58. Zhao, X. J.; Tapec-Dytioco, R.; Tan, W. H., *J. Am. Chem. Soc.* **2003,** *125* (38), 11474.
59. Homola, J.; Vaisocherova, H.; Dostalek, J.; Piliarik, M., *Methods* **2005,** *37* (1), 26.
60. Isola, N. R.; Stokes, D. L.; Vo-Dinh, T., *Anal. Chem.* **1998,** *70* (7), 1352.
61. Faulds, K.; Smith, W. E.; Graham, D., *Anal. Chem.* **2004,** *76* (2), 412.
62. Stevenson, R.; Ingram, A.; Leung, H.; McMillan, D. C.; Graham, D., *Analyst* **2009,** *134* (5), 842.
63. Smith, W. E.; Dent, G., *Modern Raman Spectroscopy; A Practical Approach*. 1st ed.; John Wiley & Sons Ltd.: Chichester, 2005.
64. Ferraro, J.; Nakamoto, K., Introductory Raman Spectroscopy. Academic Press: San Diego, 1994.
65. Raman; V., C., A new radiation. Ind. J. Phys., 1928; Vol. 2, p 1.
66. Smith, W. E., *Chem. Soc. Rev.* **2008,** *37* (5), 955.
67. Dou, X. M.; Yamaguchi, Y.; Yamamoto, H.; Uenoyama, H.; Ozaki, Y., *Appl. Spectrosc.* **1996,** *50* (10), 1301.
68. Fleischmann, M.; Hendra, P. J.; McQuillan, A. J., *Chem. Phys. Lett.* **1974,** *26* (2), 163.
69. Albrecht, M. G.; Creighton, J. A., *J. Am. Chem. Soc.* **1977,** *99* (15), 5215.
70. Jeanmaire, D. L.; Vanduyne, R. P., *J. Electroanal. Chem.* **1977,** *84* (1), 1.
71. Vanduyne, R. P.; Hulteen, J. C.; Treichel, D. A., *J. Chem. Phys.* **1993,** *99* (3), 2101.
72. Jensen, T. R.; Schatz, G. C.; Van Duyne, R. P., *J. Phys. Chem. B* **1999,** *103* (13), 2394.
73. Rycenga, M.; McLellan, J. M.; Xia, Y., *Adv. Mater.* **2008,** *20* (12), 2416.
74. Rycenga, M.; McLellan, J. M.; Xia, Y., *Chem. Phys. Lett.* **2008,** *463* (1-3), 166.
75. Lal, S.; Grady, N. K.; Kundu, J.; Levin, C. S.; Lassiter, J. B.; Halas, N. J., *Chem. Soc. Rev.* **2008,** *37* (5), 898.
76. Shanmukh, S.; Jones, L.; Driskell, J.; Zhao, Y.; Dluhy, R.; Tripp, R. A., *Nano Lett.* **2006,** *6* (11), 2630.
77. Mahajan, S.; Richardson, J.; Brown, T.; Bartlett, P. N., *J. Am. Chem. Soc.* **2008,** *130* (46), 15589.
78. Corrigan, D. K.; Gale, N.; Brown, T.; Bartlett, P. N., *Angew. Chem. Int. Ed.* **2010,** *49* (34), 5917.
79. Brown, R. J. C.; Wang, J.; Tantra, R.; Yardley, R. E.; Milton, M. J. T., *Faraday Discuss.* **2006,** *132*, 201.
80. Tu, Q. A.; Eisen, J.; Chang, C., *J. Biomed. Opt.* **2010,** *15* (2), 3.
81. Ding, L. P.; Fang, Y., *Spectrochim. Acta A* **2007,** *67* (3-4), 767.

82. Faulds, K.; Smith, W. E.; Graham, D.; Lacey, R. J., *Analyst* **2002,** *127* (2), 282.
83. Rumbin, J.; Aroca, R., *Phys. Chem.* **2008,** *35*, 5412.
84. Munro, C. H.; Smith, W. E.; Garner, M.; Clarkson, J.; White, P. C., *Langmuir* **1995,** *11* (10), 3712.
85. Lee, P. C.; Meisel, D., *J. Phys. Chem.* **1982,** *86* (17), 3391.
86. Grabar, K. C.; Brown, K. R., *Anal. Chem.* **1997,** *69*, 471.
87. Turkevich, J.; Stevenson, P. C.; Hillier, J., *Discuss. Faraday Soc.* **1951,** (11), 55.
88. Leopold, N.; Lendl, B., *J. Phys. Chem.* **2003,** *107* (24), 5723.
89. Cermakova, K.; Sestak, O.; Matejka, P.; Baumruk, V.; Vlckova, B., *Coll. Czech CC* **1993,** *58* (11), 2682.
90. Heard, S. M.; Grieser, F.; Barraclough, C. G.; Sanders, J. V., *J. Colloid Interface Sci.* **1983,** *93* (2), 545.
91. Mie, G., *Annalen Der Physik* **1908,** *25* (3), 377.
92. Graham, D.; Thompson, D. G.; Smith, W. E.; Faulds, K., *Nat. Nanotechnol.* **2008,** *3* (9), 548.
93. Robson, A. F.; Hupp, T. R.; Lickiss, F.; Ball, K. L.; Faulds, K.; Graham, D., *Proc. Natl. Acad. Sci U.S.A.* **2012,** *109* (21), 8073.
94. Craig, D.; Simpson, J.; Faulds, K.; Graham, D., *Chem. Commun.* **2013,** *49* (1), 30.
95. Moskovits, M., *Rev. Mod. Phys.* **1985,** *57* (3), 783.
96. Otto, A.; Mrozek, I.; Grabhorn, H., *J. Raman Spectrosc.* **1991,** *22*, 743.
97. Cunningham, D.; Littleford, R. E.; Smith, W. E.; Lundahl, P. J.; Khan, I.; McComb, D. W.; Graham, D.; Laforest, N., *Faraday Discuss.* **2006,** *132*, 135.
98. Stacy, A. M.; Vanduyne, R. P., *Chem. Phys. Lett.* **1983,** *102* (4), 365.
99. Graham, D.; Smith, W. E.; Linacre, A. M. T.; Munro, C. H.; Watson, N. D.; White, P. C., *Anal. Chem.* **1997,** *69* (22), 4703.
100. Kim, J. H.; Chaudhary, S.; Ozkan, M., *Nanotechnology* **2007,** *18* (19), 7.
101. Faulds, K.; McKenzie, F.; Smith, W. E.; Graham, D., *Angew. Chem. Int. Ed.* **2007,** *46* (11), 1829.
102. McHugh, C. J.; Docherty, F. T.; Graham, D.; Smith, W. E., *Analyst* **2004,** *129* (1), 69.
103. Harper, M.; McKeating, K.; Faulds, K., *Phys. Chem. Chem. Phys.* **2013**.
104. Stokes, R. J.; Macaskill, A.; Lundahl, P. J.; Smith, W. E.; Faulds, K.; Graham, D., *Small* **2007,** *3*, 1593.
105. Dougan, J. A.; Faulds, K., *Analyst* **2012,** *137* (3), 545.
106. Barhoumi, A.; Halas, N. J., *J. Am. Chem. Soc.* **2010,** *132* (37), 12792.
107. Papadopoulou, E.; Bell, S. E. J., *Analyst* **2010,** *135* (12), 3034.
108. Papadopoulou, E.; Bell, S. E. J., *Angew. Chem. Int. Ed.* **2011,** *50* (39), 9058.
109. Faulds, K.; Jarvis, R.; Smith, W. E.; Graham, D.; Goodacre, R., *Analyst* **2008,** *133* (11), 1505.
110. Faulds, K.; McKenzie, F.; Graham, D., *Analyst* **2007,** *132*, 1100.
111. Fu, W. L.; Zhen, S. J.; Huang, C. Z., *Analyst* **2013,** *138* (10), 3075.

112. Zavarine, I. S.; Khaselev, O.; Zhang, Y., *J. Electrochem. Soc.* **2003,** *150* (4), C202.
113. McAnally, G.; McLaughlin, C.; Brown, R.; Robson, D. C.; Faulds, K.; Tackley, D. R.; Smith, W. E.; Graham, D., *Analyst* **2002,** *127* (6), 838.
114. Enright, A.; Fruk, L.; Grondin, A.; McHugh, C. J.; Smith, W. E.; Graham, D., *Analyst* **2004,** *129* (10), 975.
115. Faulds, K.; Stewart, L.; Smith, W. E.; Graham, D., *Talanta* **2005,** *67* (3), 667.
116. Espy, M. J.; Uhl, J. R.; Sloan, L. A.; Buckwalter, S. P.; Jones, M. F.; Vetter, E. A.; Yao, J. D. C.; Wengenack, N. L.; Rosenblatt, J. E.; Cockerill, F. R.; Smith, T. F., *Clin. Microbiol. Rev.* **2006,** *19* (3), 165.
117. Nie, S. M.; Chiu, D. T.; Zare, R. N., *Anal. Chem.* **1995,** *67* (17), 2849.
118. Li, H. T.; Ying, L. M.; Green, J. J.; Balasubramanian, S.; Klenerman, D., *Anal. Chem.* **2003,** *75* (7), 1664.
119. Faulds, K.; Barbagallo, R. P.; Keer, J. T.; Smith, W. E.; Graham, D., *Analyst* **2004,** *129* (7), 567.
120. Graham, D.; Mallinder, B. J.; Whitcombe, D.; Watson, N. D.; Smith, W. E., *Anal. Chem.* **2002,** *74* (5), 1069.
121. Faulds, K.; Fruk, L.; Robson, D. C.; Thompson, D. G.; Enright, A.; Smith, W. E.; Graham, D., *Faraday Discuss.* **2006,** *132*, 261.
122. Wabuyele, M. B.; Vo-Dinh, T., *Anal. Chem.* **2005,** *77* (23), 7810.
123. Wang, H.-N.; Vo-Dinh, T., *Nanotechnology* **2009,** *20* (6), 065101.
124. Jung, J.; Chen, L.; Lee, S.; Kim, S.; Seong, G. H.; Choo, J.; Lee, E. K.; Oh, C.-H.; Lee, S., *Anal. Bioanal. Chem.* **2007,** *387* (8), 2609.
125. MacAskill, A.; Crawford, D.; Graham, D.; Faulds, K., *Anal. Chem.* **2009,** *81* (19), 8134.
126. van Lierop, D.; Faulds, K.; Graham, D., *Anal. Chem.* **2011,** *83* (15), 5817.
127. Qian, X. M.; Zhou, X.; Nie, S. M., *J. Am. Chem. Soc.* **2008,** *130* (45), 14934.
128. Stokes, R. J.; Dougan, J. A.; Graham, D., *Chem. Commun.* **2008,** (44), 5734.
129. Vo-Dinh, T.; Houck, K.; Stokes, D. L., *Anal. Chem.* **1994,** *66* (20), 3379.
130. Mirkin, C. A.; Letsinger, R. L.; Mucic, R. C.; Storhoff, J. J., *Nature* **1996,** *382* (6592), 607.
131. Alivisatos, A. P.; Johnsson, K. P.; Peng, X. G.; Wilson, T. E.; Loweth, C. J.; Bruchez, M. P.; Schultz, P. G., *Nature* **1996,** *382* (6592), 609.
132. Nie, S. M.; Emery, S. R., *Science* **1997,** *275* (5303), 1102.
133. Perney, N. M. B.; Baumberg, J. J.; Zoorob, M. E.; Charlton, M. D. B.; Mahnkopf, S.; Netti, C. M., *Opt. Express* **2006,** *14* (2), 847.
134. Li, H. X.; Rothberg, L., *Proc. Natl. Acad. Sci. U. S. A.* **2004,** *101* (39), 14036.
135. van Lierop, D.; Faulds, K.; Graham, D., *Anal. Chem.* **2011,** *83* (15), 5817.
136. Driskell, J. D.; Tripp, R. A., *Chem. Commun.* **2010,** *46* (19), 3298.
137. Garrell, R. L., *Anal. Chem.* **1989,** *61* (6), A401.
138. Faulds, K.; Littleford, R. E.; Graham, D.; Dent, G.; Smith, W. E., *Anal. Chem.* **2004,** *76* (3), 592.

139. Creighton, J. A., *Surf. Sci.* **1983,** *124* (1), 209.
140. Gu, J.; Leszczynski, J.; Bansal, M., *Chem. Phys. Lett.* **1999,** *311* (3-4), 209.
141. Balagurumoorthy, P.; Brahmachari, S. K.; Mohanty, D.; Bansal, M.; Sasisekharan, V., *Nucleic Acids Res.* **1992,** *20* (15), 4061.
142. Kushon, S. A.; Jordan, J. P.; Seifert, J. L.; Nielsen, H.; Nielsen, P. E.; Armitage, B. A., *J. Am. Chem. Soc.* **2001,** *123* (44), 10805.
143. Jang, N. H., *Bull. Korean Chem. Soc.* **2002,** *23* (12), 1790.
144. Fiol, J. J.; Terron, A.; Moreno, V., *Inorg. Chim. Acta* **1986,** *125* (3), 159.
145. Papadopoulou, E.; Bell, S. E. J., *J. Phys. Chem.* **2011,** *115* (29), 14228.
146. Papadopoulou, E.; Bell, S. E. J., *J. Phys. Chem.* **2010,** *114* (51), 22644.
147. Demers, L. M.; Ostblom, M.; Zhang, H.; Jang, N. H.; Liedberg, B.; Mirkin, C. A., *J. Am. Chem. Soc.* **2002,** *124* (38), 11248.
148. Sautter, R. L.; Brown, W. J.; Mattman, L. H., *Infect. Control Hosp. Epidemiol.* **1988,** *9* (5), 204.
149. Davies, S.; Zadik, P. M.; Mason, C. M.; Whittaker, S. J., *Br. J. Biomed. Sci.* **2000,** *57* (4), 269.
150. Boyce, J. M., *J. Hosp. Infect.* **2001,** *48*, S9.
151. Hryniewicz, W., *Infection* **1999,** *27*, S13.
152. Francois, P.; Pittet, D.; Bento, M.; Pepey, B.; Vaudaux, P.; Lew, D.; Schrenzel, J., *J. Clin. Microbiol.* **2003,** *41* (1), 254.
153. Dougan, J. A.; MacRae, D.; Graham, D.; Faulds, K., *Chem. Commun.* **2011,** *47* (16), 4649.
154. Seidel, M.; Niessner, R., *Anal. Bioanal. Chem.* **2008,** *391* (5), 1521.
155. Stoermer, R. L.; Keating, C. D., *J. Am. Chem. Soc.* **2006,** *128* (40), 13243.
156. Sokolov, K.; Chumanov, G.; Cotton, T. M., *Anal. Chem.* **1998,** *70* (18), 3898.
157. Michaels, A. M.; Nirmal, M.; Brus, L. E., *J. Am. Chem. Soc.* **1999,** *121* (43), 9932.
158. Hildebrandt, P.; Stockburger, M., *J. Phys. Chem.* **1984,** *88* (24), 5935.
159. Pettinger, B.; Krischer, K.; Ertl, G., *Chem. Phys. Lett.* **1988,** *151* (1-2), 151.
160. Le Ru, E.; Etchegoin, P., *Principle of Surface Enhanced Raman Spectroscopy and related plasmonic effects*. 1st ed.; Elsevier: Oxford, 2009.
161. Albelda, S. M.; Sheppard, D., *Am. J. Respir. Cell Mol. Biol.* **2000,** *23* (3), 265.
162. Taton, T. A.; Lu, G.; Mirkin, C. A., *J. Am. Chem. Soc.* **2001,** *123* (21), 5164.
163. Piner, R. D.; Zhu, J.; Xu, F.; Hong, S. H.; Mirkin, C. A., *Science* **1999,** *283* (5402), 661.
164. Borst, J. W.; Visser, A. J. W. G., *Meas. Sci. Technol.* **2010,** *21* (10), 102002.
165. Abo, M.; Urano, Y.; Hanaoka, K.; Terai, T.; Komatsu, T.; Nagano, T., *J. Am. Chem. Soc.* **2011,** *133* (27), 10629.
166. Cunningham, S.; Gerlach, J. Q.; Kane, M.; Joshi, L., *Analyst* **2010,** *135* (10), 2471.
167. Wagner, M. K.; Li, F.; Li, J. J.; Li, X. F.; Le, X. C., *Anal. Bioanal. Chem.* **2010,** *397* (8), 3213.

168. Pickup, J. C.; Hussain, F.; Evans, N. D.; Rolinski, O. J.; Birch, D. J. S., *Biosenors. Bioelectron.* **2005,** *20* (12), 2555.
169. Reed, K. C.; Mann, D. A., *Nucleic Acids Res.* **1985,** *13* (20), 7207.
170. Moss, M. T.; Green, E. P.; Tizard, M. L.; Malik, Z. P.; Hermontaylor, J., *Gut* **1991,** *32* (4), 395.
171. Thompson, D. G.; Enright, A.; Faulds, K.; Smith, W. E.; Graham, D., *Analytical Chemistry* **2008,** *80* (8), 2805-2810.
172. Barrett, L.; Dougan, J. A.; Faulds, K.; Graham, D., *Nanoscale* **2011,** *3* (8), 3221.
173. Hurst, S. J.; Lytton-Jean, A. K. R.; Mirkin, C. A., *Anal. Chem.* **2006,** *78* (24), 8313.
174. Zanchet, D.; Micheel, C. M.; Parak, W. J.; Gerion, D.; Alivisatos, A. P., *Nano Lett.* **2001,** *1* (1), 32.
175. Graham, D.; Stevenson, R.; Thompson, D. G.; Barrett, L.; Dalton, C.; Faulds, K., *Faraday Discuss.* **2011,** *149*, 291.
176. Balboni, I.; Limb, C.; Tenenbaum, J. D.; Utz, P. J., *Proteomics* **2008,** *8* (17), 3443.
177. Seurynck-Servoss, S. L.; White, A. M.; Baird, C. L.; Rodland, K. D.; Zangar, R. C., *Anal. Biochem.* **2007,** *371* (1), 105.
178. Wang, J., *Nucleic Acids Res.* **2000,** *28* (16), 3011.
179. Hahn, S.; Mergenthaler, S.; Zimmermann, B.; Holzgreve, W., *Bioelectrochemistry* **2005,** *67* (2), 151.
180. Vanoss, C. J.; Good, R. J.; Chaudhury, M. K., *J. Chromatogr.* **1987,** *391* (1), 53.
181. Irvine, E. J.; Hernandez-Santana, A.; Faulds, K.; Graham, D., *Analyst* **2011,** *136* (14), 2925.

Appendix: Publications

View Article Online / Journal Homepage / Table of Contents for this issue
Dynamic Article Links

Analyst

Cite this: *Analyst*, 2012, **137**, 2063

www.rsc.org/analyst

PAPER

Detection of SERS active labelled DNA based on surface affinity to silver nanoparticles†

Mhairi M. Harper,[a] Jennifer A. Dougan,[a] Neil C. Shand,[b] Duncan Graham[a] and Karen Faulds*[a]

Received 23rd January 2012, Accepted 5th March 2012
DOI: 10.1039/c2an35112a

Developments in specific DNA detection assays have been shown to be increasingly beneficial for molecular diagnostics and biological research. Many approaches use optical spectroscopy as an assay detection method and, owing to the sensitivity and molecular specificity offered, surface enhanced Raman scattering (SERS) spectroscopy has become a competitively exploited technique. This study utilises SERS to demonstrate differences in affinity of dye labelled DNA through differences in electrostatic interactions with silver nanoparticles. Results show clear differences in the SERS intensity obtained from single stranded DNA, double stranded DNA and a free dye label and demonstrate surface attraction is driven through electrostatic charges on the nucleotides and not the SERS dye. It has been further demonstrated that, through optimisation of experimental conditions and careful consideration of sequence composition, a DNA detection method with increased sample discrimination at lower DNA concentrations can be achieved.

Introduction

DNA detection of specific sequences has become increasingly important in the diagnosis and treatment of genetic diseases and infections. Therefore, research into new DNA detection methods is continually evolving to design techniques which are highly selective and sensitive. Currently, specific DNA detection methodologies predominantly utilise the quantitative polymerase chain reaction (qPCR) and fluorescence based detection systems.[1,2] An alternative optical detection technique is surface enhanced Raman scattering (SERS) spectroscopy, which has been shown to give improved sensitivity[3] and multiplexing capabilities[4,5] due to the spectra obtained providing molecularly specific narrow spectral bands.[6]

The use of SERS to detect DNA allows selective discrimination to be achieved through the development of innovative assays. Distinctive SERS signals have been obtained from constituent DNA bases,[7,8] however, the detection of unlabelled oligonucleotides generally produces non-sequence specific SERS signals. Thus, to achieve enhanced and discriminative SERS signals from a DNA sequence, a suitable dye label containing a chromophore has to be incorporated. To achieve surface enhancement, adsorption of the DNA labelled oligonucleotide onto a roughened metal surface, generally provided by a metallic nanoparticle suspension, is needed. Colloidal suspensions of silver and gold nanoparticles are most commonly used as SERS surfaces due to their ease of preparation and surface plasmon lying within the visible wavelength region providing further signal enhancement. The nanoparticles can be readily prepared by reduction of the corresponding metal salt using a reducing agent such as citrate,[9] EDTA,[10] hydroxylamine[11] and borohydride.[12] This forms an overall net negative charge on the surface which will prevent the adsorption of DNA due to the electrostatic repulsion with the negatively charged phosphate backbone. This repulsion can be significantly reduced by the use of an aggregating agent, such as spermine hydrochloride[13] or poly-L-lysine,[14] which interacts strongly with the DNA backbone neutralising the negative charge. The facilitation of surface adsorption is essential to achieve effective SERS as increasing the distance of the analyte from the surface will result in a diminished SERS signal. The addition of an aggregating agent also reduces the stability of the colloid, allowing partially controlled formation of nanoparticle aggregates. The formation of nanoparticle clusters creates hotspots at the particle junctions which, when irradiated with a laser excitation frequency close to the absorption maximum of the label and surface plasmon of the metal, create an intense molecularly specific vibrational spectra.[6]

SERS has been established as an analytical technique for qualitative and quantitative detection of DNA.[15,16] Single stranded DNA (ssDNA) is predominantly employed within SERS detection assays due to its high surface affinity for metallic surfaces.[17,18] Partial uncoiling of the sequence facilitates exposure of the DNA bases which will strongly adsorb onto the negatively charged silver nanoparticle.[7] Consequently, the detection of dye labelled ssDNA aggregated with spermine, will result in strong

[a]*Centre for Molecular Nanometrology, WestCHEM, Department of Pure and Applied Chemistry, University of Strathclyde, 295 Cathedral St., Glasgow, G1 1XL, UK. E-mail: Karen.faulds@strath.ac.uk; Tel: +44 (0)141 548 2507*
[b]*Dstl Porton Down, Salisbury, Wiltshire, SP4 0JQ, UK*
† Electronic supplementary information (ESI) available: Fig. S1: DNA discrimination assay. See DOI: 10.1039/c2an35112a

and distinct SERS signals.[18] Highly sensitive SERS spectroscopy has been used to obtain quantitative behaviour and limits of detection of various labelled ssDNA oligonucleotides, generating distinctive SERS spectra for individual sequences.[19,20] Single stranded DNA has also been used within signal amplification assays to detect DNA through accumulation of SERS signal. The use of enzyme digestion in these assays frequently results in isolated SERS-active dyes within the sample, however when ssDNA remains attached to the dye, surface adsorption is aided and a more intense signal is observed.[21] Conversely, numerous assays, including molecular beacons[22] and scorpion probes,[23] detect target sequences through use of a specific hybridisation event, thus, the sample mixtures will contain both single and double stranded (dsDNA). One approach to discriminate between ssDNA and dsDNA is through their differing propensities to adsorb onto silver and gold nanoparticle surfaces. This observation was first reported by Li and Rothberg showing, by colorimetric detection, that single stranded DNA has a stronger affinity to gold nanoparticles than double stranded DNA.[24] SERS molecular diagnostic assays have also been used to show the potential application of specific DNA detection through differing electrostatic properties of DNA sequences.[25] Specifically designed primers also have been utilised within a SERS assay which exploits the differing affinity of DNA structures in order to detect specific oligonucleotide sequences of interest.[26] The principle of these assays is based on the strong electrostatic attraction that the constituent bases have for the nanoparticle surface, ssDNA has greater number of exposed bases, therefore an increased signal intensity is generated. The employment of a DNA discrimination methodology as a specific detection assay offers many advantages including high reproducibility, specific detection and simple application. However, the existing method contains inherent weaknesses as often the discrimination between ssDNA and dsDNA is not large, therefore a reliable conclusion may not be drawn. This also influences the concentration range over which the method is applicable and it can be limited as a result of reduced discrimination between ssDNA and dsDNA at lower concentrations.

The principle of DNA detection through differing electrostatic properties of ssDNA and dsDNA has already been demonstrated,[24,25] here we use SERS to provide a clearer understanding of the concept and illustrate improvements to significantly increase discrimination and consequently, detection at lower DNA concentrations. Furthermore, the effect that the SERS dye and the sequence composition has on surface adsorption of the oligonucleotide was investigated.

Experimental section

Colloid preparation

EDTA silver colloid was prepared by adding EDTA (0.095 g) to 2.0 L of distilled water. The solution was heated on a hotplate and prior to boiling NaOH (0.32 g) was added. At 100 °C, silver nitrate (0.088 g) was added and the solution was boiled for 15 minutes before cooling. The resulting colloid was analysed by UV-vis spectroscopy and the λ_{max} was found to be 412 nm and the full width half-height (FWHH) was measured to be 77 nm. The nanoparticles were characterised to be approximately spherical with a diameter of 46 nm and the concentration of the colloid was calculated to be 1.14×10^{-10} mol dm^{-3}. Prior to use the pH of the colloid was adjusted to 12 using 1 M NaCl. Chemicals for the preparation of silver colloid were purchased from Sigma Aldrich.

Buffers

1.65 M phosphate buffered saline (PBS) was prepared by combining 60 mM of sodium dihydrogen phosphate and 60 mM of disodium hydrogen phosphate buffer then adding 83 mL of phosphate buffer (10 mM, pH 7) and 82.5 mL of NaCl (0.3 M) made up to 500 mL.

Tris–tween buffer was prepared using 10 mM tris(hydroxymethyl) aminomethane hydrochloride (Tris–HCl), 100 mM NaCl and 0.05% Tween 20 and was made up to a volume of 100 mL. The pH of the solution was adjusted to 7.4 using 1 M NaCl.

Oligonucleotides

Oligonucleotides were purchased from ATDbio Ltd. and MWG Operon on 1 μmol and 0.01 μmol scale respectively with HPLC purification (Table 1 and 3). Single TAMRA dye was deprotected from a 3′ TAMRA CPG column from Link technologies, which had been treated with 3% trichloroacetic acid/DCM and concentrated ammonium hydroxide solution.

DNA hybridisation

All DNA hybridisations were carried out using a Minicycler PTC-150 system. An aliquot of the oligonucleotide probe and complementary sequence (500 μL, 1 μM) were added to a PCR tube and incubated in 0.3 M PBS. The temperature was raised to 95 °C for 2 minutes and slowly cooled 1 °C min^{-1} to 25 °C. This was also carried out using probe and dye with no complement sequence, excess 0.3 M PBS buffer was added to keep concentrations consistent. Dilution series were carried out for each sample by diluting in 0.3 M PBS.

SERS analysis

In a disposable cuvette DNA/dye (5 μL, X μM, where X ranges from 0.4 to 0.02 μM) was added. To this, an aqueous solution of spermine hydrochloride (20 μL, 0.1 M), PBS solution (100 μL, 1.65 M) and Tris–tween buffer (30 μL, pH 7.4) was added. Finally the mixture was diluted by addition of silver EDTA reduced colloid (395 μL, pH 12). The sample was thoroughly mixed and the SERS spectra were recorded within 1 minute of colloid addition on a Renishaw model 100 probe system with 514.5 nm laser excitation (1 × 1 s, 6 mW, 20× obj). The spectra were baseline corrected using Grams software. 5 replicate analyses of 5 replicate samples at each concentration were analysed. A dilution series was carried out to obtain the limit of detection of labelled oligonucleotide. The equation of the linear line was used to calculate the detections limits. The limit was estimated to be 3 times the standard deviation of the blank divided by the slope of the linear line.

Table 1 DNA sequence and modification information

Name	Sequence (5′–3′)	5′-Label	GC content
T20 probe	GGTTCATATAGTTATAATAA	TAMRA	20%
T20 comp	TTATTATAACTATATGAACC	—	20%

Results and discussion

Herein we demonstrate through the use of SERS, the differences in affinity of dye labelled ssDNA, dsDNA and a dye label adsorbed onto silver nanoparticles, as well as the effect that this has on the resultant SERS signal. A SERS active dye was incorporated into the DNA sequence to obtain enhanced signals, therefore, the dye label with no DNA was also analysed to investigate its role in surface adsorption. DNA detection was carried out using a synthetic oligonucleotide probe, consisting of 20 bases and a 5′ TAMRA label. A TAMRA label modification was used to identify the sequence since previous studies have shown TAMRA labelled oligonucleotides can be effectively detected by SERS.[20] A single stranded T20 probe containing a low GC content (20%) was used to evaluate the difference in electrostatic interaction of ssDNA (T20 probe), dsDNA (T20 probe and T20 comp) and a SERS-active TAMRA dye (Table 1). The modified TAMRA labelled probes were either mixed with an exact complementary sequence or excess buffer and hybridised in 0.3 M PBS, resulting in three distinct samples; ssDNA and dsDNA and single TAMRA dye which had been deprotected from a 3′ TAMRA CPG column. The DNA/dye samples were added to a cuvette and mixed with 0.1 M spermine hydrochloride to aggregate and aid adsorption of the DNA to the nanoparticles. Silver EDTA-reduced colloid was added to the sample mixture providing the metal surface for DNA adsorption. The SERS spectra were recorded within 1 minute of colloid addition using 514.5 nm laser excitation.

Characteristic TAMRA signals were obtained from both the ssDNA and dsDNA (Fig. 1) with no differences in peak position obtained between ssDNA and dsDNA spectra. However, dsDNA samples give a markedly lower intensity signal as expected. This is likely to be a result of the varying affinities which single and double stranded DNA sequences have for metal nanoparticle surfaces due to differences in structure and electrostatic properties (Fig. 2). The essential differences arise as the flexible structure of ssDNA permits strands to uncoil, exposing the bases which are electrostatically attracted to the surface. Thus, ssDNA has a high affinity for the nanoparticle surface adsorbing strongly onto the metal generating a high SERS intensity. In contrast, dsDNA forms a stable double helix structure which encloses the bases. Consequently, due to the rigid dsDNA structure, surface adsorption will be inhibited and a lower SERS signal will be obtained from the sample. The repulsion between the negatively charged DNA backbone and negatively charged metal surface is effectively eliminated through addition of excess spermine hydrochloride. The amine interacts strongly with the polyanionic backbone, efficiently neutralising the charge, indicating that surface attraction is directed through electrostatic interactions between the bases and nanoparticle surface. The presence of a fluorescence background with the omission of SERS signal from the dye molecule indicates that the TAMRA dye is not adsorbed sufficiently close enough to the metal surface to be identified by SERS. This further demonstrates that surface attraction is driven by attachment of nucleotides and not the TAMRA dye. This is in agreement with previous studies,[21,27] showing that, following enzyme digestion, that more sensitive SERS detection can be achieved through detection of TAMRA labelled DNA rather than released free dye. From these observations, DNA assays can be designed to detect the presence of specific target sequences through hybridisation and differences in SERS intensity of ssDNA and dsDNA.

Previous studies have utilised SERS to discriminate between ssDNA and dsDNA. MacAskill *et al.*, exploited SE(R)RS to ascertain the presence of target DNA oligonucleotides in a homogeneous multiplexed assay. Within the study three dyes (TAMRA, FAM and HEX) were used to show differences in affinity of ssDNA and dsDNA. Discrimination between the three dye labelled oligonucleotides were obtained, however, a fundamental understanding of DNA adsorption onto the surface was not determined. This study focuses on the concept of oligonucleotide adsorption onto silver nanoparticles through changes in SERS signals and has so far shown clear distinctions between

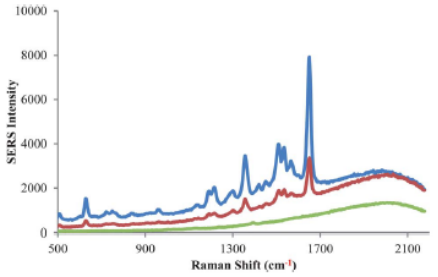

Fig. 1 SERS spectra of TAMRA labelled DNA and single dye (concentration of 3.6 nM) obtained using 514.5 nm laser excitation (1 s, 6 mW, 20× obj): blue – single stranded TAMRA labelled probe (T20); red – double stranded TAMRA labelled probe (T20 + complement); green – TAMRA dye label.

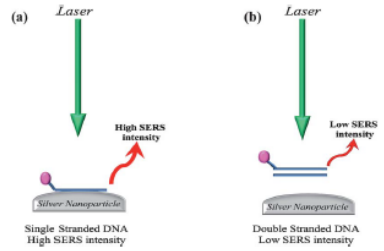

Fig. 2 DNA affinity principle: (a) single stranded DNA is strongly adsorbed onto the silver nanoparticle surface producing a high SERS intensity; (b) double stranded DNA is further from the nanoparticle surface producing low SERS intensity.

ssDNA, dsDNA and free TAMRA dye. However, this assay system can only be applied when distinct intensity differences between ssDNA and dsDNA samples are observed. Thus, the experimental conditions were optimised to obtain quantitative results with maximum discrimination between ssDNA and dsDNA sequences. Previous experimental conditions utilised within an established DNA discrimination assay,[25] were used as the basis to compare the initial experimental conditions and conditions after optimisation.

Assay optimisation

To establish the largest discrimination in SERS intensity between ssDNA and dsDNA, a study was carried out altering various experimental parameters to determine optimum conditions. Analysis of the silver EDTA colloid illustrated that increased discrimination between ssDNA and dsDNA was obtained when the pH of the final SERS mixture was increased to pH 8.3 through increasing the pH of the silver colloidal suspension (pH 12). Whereas, application of the initial experimental conditions using a final SERS mixture of pH 7, gave a lower SERS discrimination (Fig. 3(a)). The difference in observations is most likely as a result of an increased charge density on the EDTA nanoparticle surface from the ionisable surface capping layer providing increased surface attraction at higher pH. The volume of colloid used within the SERS analysis was increased from 275 μL to 395 μL (Fig. 3(b)) providing a larger accessible nanoparticle surface area for enhanced DNA adsorption and greater signal discrimination. To maintain the final concentration and obtain comparable results the volumes were kept constant through the reduction of the volume of PBS buffer added as the volume of colloid was increased. However, to ensure DNA stability within the mixture, the concentration of NaCl within the PBS buffer was increased to achieve an overall concentration of 1.65 M within the PBS buffer. Initial experimental conditions used 0.3 M PBS giving a NaCl concentration of 0.12 M within the final reaction mixture, which can facilitate DNA hybridisation, however lower NaCl concentrations will serve to decrease DNA duplex stability. The addition of an increased NaCl concentration in 1.65 M PBS provided a final reaction concentration of 0.3 M, which will facilitate DNA hybridisation with greater DNA duplex stability. Results have shown that an increased concentration of NaCl within the PBS buffer gives significantly higher ssDNA and dsDNA discrimination than using 0.3 M PBS (Fig. 3(c)). Thus, indicating that a higher concentration of salt results in higher DNA stability, aggregation and charge screening, therefore surface adsorption and signal intensity is improved.

The fully optimised conditions were applied over a range of DNA concentrations to evaluate the signal intensity against the initial conditions. Differences in SERS intensity between ssDNA and dsDNA were plotted over a range of six DNA concentrations, Fig. 4, demonstrating optimisation of the DNA discrimination method gave an overall higher SERS intensity difference over an extended concentration range. It has further been demonstrated that the degree of reproducibility is improved, whilst maintaining sequence discrimination, though implementation of the combined enhanced SERS parameters illustrated in the reduction of the error bars between Fig. 4 to Fig. 3. These observations clearly indicate the discrimination between ssDNA and dsDNA has significantly increased through method optimisation and subsequently an improved DNA discrimination detection method was obtained. The optimised SERS conditions were applied within a concentration study to determine the quantitative differences in affinity between dye labelled ssDNA, dsDNA and the dye molecule alone. Five replicates of each dilution were analysed and the average of the principle peak at 1650 cm^{-1} was plotted against concentration to produce the linear concentration responses shown in Fig. 5. It was found that significant discrimination between the ssDNA, dsDNA and dye molecule was obtained at concentrations above 0.45 nM. Quantitative responses were obtained from the ssDNA and dsDNA labelled probes, thus, the detection limits were calculated for each probe and the results agree with previous findings, since the limit of detection for the single stranded oligonucleotide is over a magnitude lower than the double stranded oligonucleotide

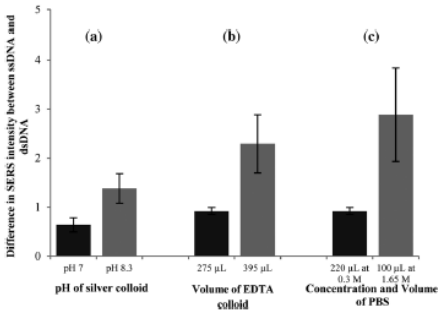

Fig. 3 Initial experimental conditions (black) and optimised experimental conditions (grey): (a) pH of EDTA silver colloid; (b) volume of EDTA colloid; (c) volume and concentration of NaCl within PBS buffer. All graphs compare the difference in SERS intensity between ssDNA and dsDNA (concentration of 3.6 nM) at 1650 cm^{-1}. Each point represents the difference between the mean of 5 replicates and the error bars represent ± one standard deviation.

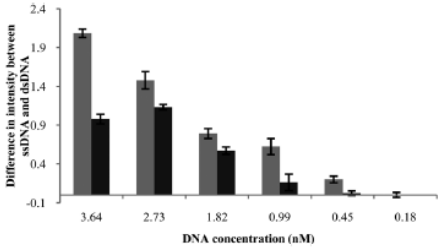

Fig. 4 Discrimination between ssDNA and dsDNA using initial experimental conditions (black) and optimised experimental conditions (grey) over a DNA concentration range. Each point represents the difference between the mean of 5 replicates and error bars represent ± one standard deviation.

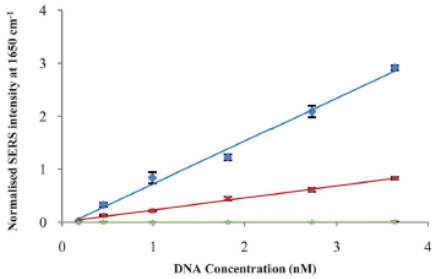

Fig. 5 Linear plot of TAMRA labelled DNA and single dye: blue – single stranded TAMRA labelled probe (T20); red – double stranded TAMRA labelled probe (T20 + complement); green – TAMRA dye label. Each point represents the mean of 5 replicates and error bars represent ± one standard deviation.

(Table 2). No SERS signal was obtained from the dye molecule under these conditions therefore the calculated signal intensity was fundamentally negligible and no limit of detection could be obtained. The results obtained demonstrate discernible difference between ssDNA, dsDNA and a single dye label by SERS.

Application of these improved DNA discrimination conditions within an established assay is vital to demonstrate the versatility for use in a practical detection system. The optimised SERS method was applied within a previously published assay concept,[25] in which the presence of a target sequence was shown through discrimination of complementary DNA (dsDNA) and non-complementary DNA (ssDNA). Utilisation of the optimised conditions within the existing assay gave a signal discrimination of 7.4 times between ssDNA and dsDNA samples at 0.9 nM, compared to the 1.4 times difference obtained at the same concentration when using original assay conditions (Fig. S1†). These results indicate that optimisation of the experimental conditions within this assay have given significantly larger discrimination between samples and the target DNA is able to be clearly detected at lower concentrations. Consequently, as a result of the larger discrimination between ssDNA and dsDNA, the presence of specific target sequences can be accurately determined at reduced concentrations with greater confidence.

Determination of effect of sequence composition

The concept of the methodology has been clearly illustrated, therefore, it was important to determine the applicability of the assay using DNA sequences of varying compositions. This study has shown, discernible differences between ssDNA and dsDNA through use of SERS spectroscopy when utilising a DNA probe

Table 2 Limits of detection (L.O.D) for ds and ss oligonucleotides

TAMRA labelled DNA probe	L.O.D (M)
Single stranded	2.88×10^{-12}
Double stranded	1.15×10^{-11}

Table 3 DNA sequences for sequence composition comparison and corresponding GC content

Name	Sequence (5′–3′)	5′-Label	GC content (%)
T50 probe	TTGGACGCGCTGGCTAATAA	TAMRA	50
T50 comp	TTATTAGCCAGCGCGTCCAA	—	50
T80 probe	TTGGACGCGCTGGCGCCGCC	TAMRA	80
T80 comp	GGCGGCGCCAGCGCGTCCAA	—	80

containing 20% GC content, however the effect of SERS discrimination on different sequences was analysed. The sequences were designed to contain increasing numbers of guanine (G) and cytosine (C) bases to determine the effect of sequence composition on surface adsorption properties of the oligonucleotide. Three synthetic oligonucleotide probes containing a 5′ TAMRA label and consisting of either 20, 50 or 80% GC content were utilised (Tables 1 and 3).

A clear distinction between each of the single stranded labelled probes was observed, with the highest signal intensity observed from probes containing 20% GC bases and the lowest signal intensity obtained from the 80% GC probe (Fig. 6(a)). In addition, higher discrimination between the ssDNA and dsDNA was also obtained from the 20% probe (Fig. 6(b)). Lower ssDNA signal intensity and structure discrimination was seen from sequences containing 50% GC bases, however significant sequence

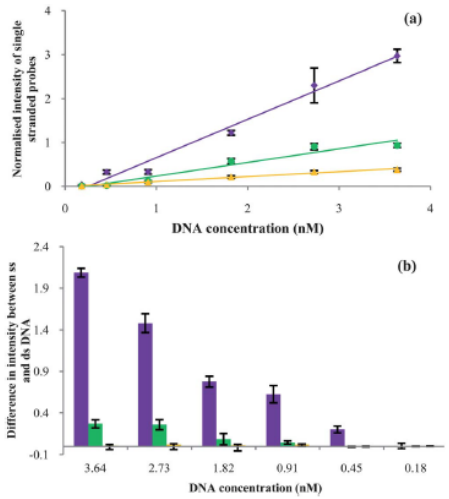

Fig. 6 20, 50 and 80% TAMRA labelled probes; (a) intensity of single stranded probes, (b) difference in intensity of single and double stranded probes; purple – 20% GC TAMRA labelled probe (T20); green – 50% GC TAMRA labelled probe (T50); yellow – 80% GC TAMRA labelled probe (T80). (a) Each point represents the mean of 5 replicates, (b) each point represents the difference between the mean of 5 replicates. Error bars represent ± one standard deviation.

discrimination was still obtained. Whereas, high GC content sequences, 80%, displayed low ssDNA signal intensities with no discrimination between single and double stranded oligonucleotides. These results suggest increased numbers of GC bases cause a reduction in electrostatic adsorption of sequences onto silver nanoparticles. Guanine rich oligonucleotides are prone to self-association, forming secondary structures, including G-tetrads or guanine-quartets, through stabilised guanine–guanine bonds.[28] This results in reduced surface affinity and SERS signals. Therefore, results indicate that the higher GC content sequences are forming secondary structure within both single and double stranded samples, impeding sequence hybridisation and surface adsorption. The probes used within this study are hetero-oligonucleotides, mimicking DNA sequences detected within molecular assays. Therefore, these results demonstrate that under these optimised SERS conditions higher discrimination between ssDNA and dsDNA is obtained for sequences which contain low GC content. These observations have a significant impact on the ability to determine the presence or absence of target sequence using this methodology within diagnostic assays. The SERS signals of constituent bases, nucleosides, nucleotides and oligonucleotide chains can vary greatly depending on structure orientation and experimental conditions.[29,30] Papadopoulou and Bell have exploited SERS to demonstrate label-free detection of a molecular beacon through sequence orientation to the nanoparticle surface.[31] This further demonstrates that SERS has become increasingly valuable in the understanding of DNA surface chemistry properties and the effect which base composition and sequence structure can have on DNA detection.

Conclusions

This study has illustrated an understanding of the principle of specific DNA detection through differences in electrostatic interactions by SERS. SERS has been effectively utilised to quantitatively discriminate between TAMRA labelled single stranded, double stranded DNA and a dye molecule on silver nanoparticles, with higher SERS intensities observed for ssDNA compared to dsDNA. It was further demonstrated that surface attraction is driven through the constituent bases and the dye contributes minimally to surface adsorption. If spermine had not been added, no SERS would have been obtained under these conditions.[17] The experimental conditions were optimised to develop a method that allows discrimination of DNA to be established with greater confidence and at lower concentrations. The composition of the base sequence has proven to be highly influential on the discrimination of target samples, with an increasing percentage of GC content within oligonucleotides found to cause a decrease in surface affinity for silver nanoparticles. A DNA detection method has been shown here, which through careful consideration of SERS conditions and target sequences, can provide a simple and selective biological assay method.

Acknowledgements

MMH and KF would like to thank Dstl for funding, KF and JAD would like to thank the EPSRC for funding (EP/F005407/1) and the Royal Society for a Wolfson research merit award to DG.

Notes and references

1 M. J. Espy, J. R. Uhl, L. A. Sloan, S. P. Buckwalter, M. F. Jones, E. A. Vetter, J. D. C. Yao, N. L. Wengenack, J. E. Rosenblatt, F. R. Cockerill and T. F. Smith, *Clin. Microbiol. Rev.*, 2006, **19**, 165.
2 R. T. Ranasinghe and T. Brown, *Chem. Commun.*, 2005, 5487–5502.
3 K. Faulds, R. P. Barbagallo, J. T. Keer, W. E. Smith and D. Graham, *Analyst*, 2004, **129**, 567–568.
4 K. Faulds, F. McKenzie, W. E. Smith and D. Graham, *Angew. Chem., Int. Ed.*, 2007, **46**, 1829–1831.
5 K. Faulds, R. Jarvis, W. E. Smith, D. Graham and R. Goodacre, *Analyst*, 2008, **133**, 1505–1512.
6 K. K. Hering, R. Moller, W. Fritzsche and J. Popp, *ChemPhysChem*, 2008, **9**, 867–872.
7 E. Papadopoulou and S. E. J. Bell, *Angew. Chem., Int. Ed.*, 2011, **50**, 9058–9061.
8 N. H. Jang, *Bull. Korean Chem. Soc.*, 2002, **23**, 1790–1800.
9 S. M. Heard, F. Grieser, C. G. Barraclough and J. V. Sanders, *J. Colloid Interface Sci.*, 1983, **93**, 545–555.
10 C. H. Munro, W. E. Smith, M. Garner, J. Clarkson and P. C. White, *Langmuir*, 1995, **11**, 3712–3720.
11 N. Leopold and B. Lendl, *J. Phys. Chem. B*, 2003, **107**, 5723–5727.
12 S. H. Chen and K. Kimura, *Langmuir*, 1999, **15**, 1075–1082.
13 D. Graham, W. E. Smith, A. M. T. Linacre, C. H. Munro, N. D. Watson and P. C. White, *Anal. Chem.*, 1997, **69**, 4703–4707.
14 D. Cunningham, R. E. Littleford, W. E. Smith, P. J. Lundahl, I. Khan, D. W. McComb, D. Graham and N. Laforest, *Faraday Discuss.*, 2006, **132**, 135–145.
15 Y. W. C. Cao, R. C. Jin and C. A. Mirkin, *Science*, 2002, **297**, 1536–1540.
16 L. R. Allain and T. Vo-Dinh, *Anal. Chim. Acta*, 2002, **469**, 149–154.
17 D. Graham, B. J. Mallinder and W. E. Smith, *Biopolymers*, 2000, **57**, 85–91.
18 K. Faulds, W. E. Smith and D. Graham, *Analyst*, 2005, **130**, 1125–1131.
19 K. Faulds, W. E. Smith and D. Graham, *Anal. Chem.*, 2004, **76**, 412–417.
20 R. J. Stokes, A. Macaskill, P. J. Lundahl, W. E. Smith, K. Faulds and D. Graham, *Small*, 2007, **3**, 1593–1601.
21 J. A. Dougan, D. MacRae, D. Graham and K. Faulds, *Chem. Commun.*, 2011, **47**, 4649–4651.
22 S. Tyagi and F. R. Kramer, *Nat. Biotechnol.*, 1996, **14**, 303–308.
23 D. Whitcombe, J. Theaker, S. P. Guy, T. Brown and S. Little, *Nat. Biotechnol.*, 1999, **17**, 804–807.
24 H. X. Li and L. Rothberg, *Proc. Natl. Acad. Sci. U. S. A.*, 2004, **101**, 14036–14039.
25 A. MacAskill, D. Crawford, D. Graham and K. Faulds, *Anal. Chem.*, 2009, **81**, 8134–8140.
26 D. van Lierop, K. Faulds and D. Graham, *Anal. Chem.*, 2011, **83**, 5817–5821.
27 D. M. Kong, Y. P. Huang, X. B. Zhang, W. H. Yang, H. X. Shen and H. F. Mi, *Anal. Chim. Acta*, 2003, **491**, 135–143.
28 K. Poon and R. B. Macgregor, *Biopolymers*, 1998, **45**, 427–434.
29 E. Papadopoulou and S. E. J. Bell, *Analyst*, 2010, **135**, 3034–3037.
30 E. Papadopoulou and S. E. J. Bell, *J. Phys. Chem. C*, 2011, **115**, 14228–14235.
31 E. Papadopoulou and S. E. J. Bell, *Chem. Commun.*, 2011, **47**, 10966–10968.

View Article Online / Journal Homepage / Table of Contents for this issue
Dynamic Article Links

ChemComm

Cite this: *Chem. Commun.*, 2012, **48**, 9412–9414

www.rsc.org/chemcomm

COMMUNICATION

Specific detection of DNA through coupling of a TaqMan assay with surface enhanced Raman scattering (SERS)†‡

Mhairi M. Harper,[a] Barry Robertson,[a] Alastair Ricketts[b] and Karen Faulds*[a]

Received 7th July 2012, Accepted 1st August 2012
DOI: 10.1039/c2cc34859d

We have combined the benefits of a TaqMan assay with surface enhanced Raman scattering (SERS), to generate a novel DNA detection method which provides increased sensitivity, with clear applications for disease identification through clinical testing. Target DNA detection limits by SERS were shown to be lower than conventional fluorescence detection and clinically relevant samples of methicillin-resistant *Staphylococcus aureus* were detected with high specificity.

Many DNA assays provide selective and sensitive detection, therefore, research is continually being progressed to develop more effective and competitive molecular diagnostic methods. The use of DNA detection by fluorescence is an established and commonly utilised technique with low detection limits routinely obtained.[1] However, previous studies have shown SERS to be more sensitive, with the potential of surpassing fluorescence detection by three orders of magnitude.[2] SERS is an accurate and molecularly specific spectroscopy technique, which has previously been utilised for DNA detection[3,4] and can offer benefits over alternative analysis such as multiple sequence detection.[5,6] In this study we have investigated an improved assay system which couples the benefits of a TaqMan assay[7] and SERS, to enhance sensitivity and specificity.

Conventional TaqMan assays have been widely used as a DNA detection method,[8–10] in which signal is generated through enzymatic probe cleavage. The probe incorporates a fluorophore and quencher connected through the complementary oligonucleotide. In this form any fluorescence emitted from the fluorophore is absorbed by the quencher.[11] The specific DNA sequence contained within the probe is complementary to a region within the target gene, and during the polymerase chain reaction (PCR) the probe will hybridise adjacent to the primer binding site. The assay then utilises the 5′ to 3′ exonuclease activity of the thermostable enzyme *Thermus aquaticus* (Taq) polymerase to simultaneously amplify the template and digest the TaqMan probe. Thus, once the probe has been hydrolytically cleaved, quenching is eliminated as a result of the increased interfluorophore distance. The accumulation of free dye label as a result of amplification of target sequence can then be monitored during the reaction through the increase in fluorescence signal. The assay has many benefits including low post-PCR manipulation, target specificity and sensitivity. However, some TaqMan probes can show poor allelic discrimination and inefficient fluorophore quenching, resulting in high background signal which will reduce the sensitivity and selectivity of the assay. Previous studies have overcome these issues through incorporation of modified probes, resulting in reduced background fluorescence.[12,13]

Herein, we have exploited the benefits of the TaqMan assay coupled with the advantages of SERS in a novel TaqSERS assay. To obtain effective SERS analysis the probe must incorporate a suitable SERS active dye and have compatibility with the surface chemistry of the enhancing substrate. Silver nanoparticle suspensions are preferred due to the simplistic preparation and beneficial optical properties. With the aid of spermine,[14] dye labelled DNA effectively adsorbs onto the negatively charged citrate surface layer of the silver nanoparticles, producing a molecularly specific vibrational spectrum. Maximum DNA surface absorption and optimal SERS was obtained through addition of excess spermine, which effectively neutralises the charge on the DNA backbone whilst also facilitating the partially controlled formation of nanoparticle clusters.[15] Optimal SERS detection within the modified TaqMan assay was achieved through redesigning the probe to contain a biotin residue at the 5′-terminus followed by a 29 base sequence complementary to a specific region of the target gene. Adjacent to the coding region, a HEG-spacer was incorporated, intended to terminate the progression of the enzyme. This was followed by 10 adenine bases terminated with a 3′-TAMRA dye, Fig. 1. The attachment of an oligonucleotide "tail" to the TAMRA dye has previously been shown to significantly enhance the SERS signal obtained.[15,16] Surface attraction has shown to be directed through the electrostatic interactions between the bases and the nanoparticle surface, producing more intense SERS signals, compared to the unattached TAMRA dye.[8] Indeed, a comparable probe without HEG-10A attachment produced no detectable SERS signals over a range of concentrations (Fig. S1, ESI‡). The TaqSERS assay was designed to contain a sequence complementary to the

[a] *Centre for Molecular Nanometrology, WestCHEM, Department of Pure and Applied Chemistry, University of Strathclyde, 295 Cathedral St, Glasgow, G1 1XL, UK. E-mail: Karen.faulds@strath.ac.uk; Tel: +44 (0)141 548 2507*
[b] *Renishaw Diagnostics Ltd, Nova Technology Park, Glasgow, G33 1AP, UK*

† This article is part of the *ChemComm* 'Emerging Investigators 2013' themed issue.

‡ Electronic supplementary information (ESI) available: Experimental procedure; colloid preparation, oligonucleotides, TaqSERS assay, SERS and fluorescence detection and gel electrophoresis. Fig. S1–S5 and Table S1. See DOI: 10.1039/c2cc34859d

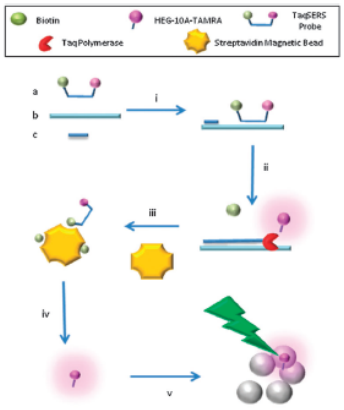

Fig. 1 TaqSERS assay; (i) hybridisation of TaqSERS probe **a**, target sequence **b** and primers **c**, (ii) Taq polymerase enzyme simultaneously elongates primers and digests probe, (iii) streptavidin coated magnetic beads are introduced to remove any undigested biotinylated probe and free biotin, (iv) magnet removes beads from system leaving TAMRA labelled DNA "tail" in supernatant, (v) dilute citrate-reduced silver nanoparticles with spermine hydrochloride (0.1 mol dm^{-3}) were added. Within 5 min the SERS spectrum was recorded using 514.5 nm laser excitation.

mecA gene sequence within the methicillin-resistant *S. Aureus* (MRSA) bacterium (Table S1, ESI‡).[17] The incorporation of the TaqSERS probe into PCR facilitates hybridisation of the complementary region of the probe and PCR primers to specific regions within the MRSA target. The sequences were specifically designed to enable the probe and primer to hybridise in close proximity. This allows the Taq polymerase enzyme to simultaneously extend the primer through deoxynucleoside triphosphate (dNTP) addition, whilst exploiting the 5′ to 3′ exonuclease activity to digest the probe. This allows amplification of the template whilst separating the biotin and SERS dye within the probe. The undigested probe was then removed from the reaction mixture through a biotin–streptavidin interaction. Streptavidin coated magnetic beads were added to the post-PCR mixture, immobilising undigested probe on the bead which was then magnetically removed from the reaction. This ensures only SERS signals were obtained from the TAMRA dye with a 10A base "tail" remaining within the supernatant mixture.

The TaqSERS assay was carried out initially incorporating a 99 base synthetic target corresponding to the methicillin-resistant mecA gene from MRSA. A non-complementary control of nonsense DNA was also amplified to determine the specificity of the assay. The nonsense sequence does not contain a region which is complementary to the mecA probe sequence, thus, no hybridisation or digestion of the probe should occur during the assay. The spectra shown in Fig. 2 demonstrates that only in the presence of MRSA target DNA are distinctive TAMRA peaks with high signal intensity observed, whereas only weak TAMRA peaks were observed from the

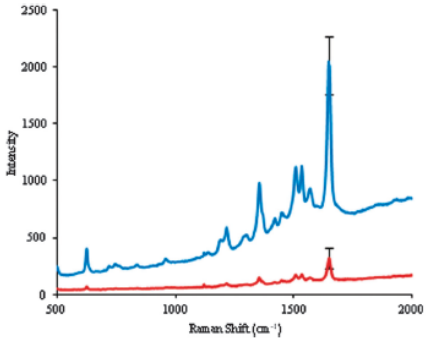

Fig. 2 SERS spectra recorded using 514.5 nm laser excitation containing blue: synthetic MRSA target and red: synthetic nonsense control.

nonsense control. A noticeable intensity difference of 6.3 was obtained from the peak at 1650 cm^{-1} between the MRSA target and nonsense control. The low nonsense signal obtained can be attributed to a small proportion of probe being digested in the absence of hybridisation to the target sequence or due to not all the probe being removed in the wash step (Fig. S2, ESI‡). However, the amount of signal detected from the control was negligible in comparison to the signal intensity obtained from the full assay.

To investigate the sensitivity of the assay, a concentration range of the 99 base synthetic MRSA template was analysed. The assay is highly dependent on PCR and as a result the limit of detection can be difficult to obtain. Since PCR is an exponential reaction, different concentrations of template may produce similar levels of DNA amplification and probe digestion through increasing the number of PCR cycles accordingly. Therefore, to enable the limit of detection of the assay to be calculated, the number of cycles was fixed. We determined that the highest template concentration, 19 pg μL^{-1}, was fully amplified within 23 PCR cycles, Fig. S3 (ESI‡). Therefore, this number of cycles was employed and enabled all the concentrations of template to begin amplification whilst maintaining the discrimination in DNA amplification between samples. The samples were analysed by SERS to establish the limits of detection, four replicates of each concentration were analysed 5 times and the average SERS intensity of the major peak height plotted against concentration, Fig. 3. A quantitative response was obtained for SERS detection, thus the detection limit was calculated (Table 1). The same samples were also analysed using fluorescence detection and the calculated limits of detection obtained are also shown in Table 1. It can be seen that through use of SERS, increased sensitivity was achieved with the detection limit obtained being an order of magnitude lower than its fluorescence counterpart. The low detection limit obtained from SERS analysis demonstrates that the assay is highly efficient and emphasises the potential which this assay has for use within clinical testing. It should also be noted that the SERS detection limits reported here are potentially lower than would be observed if a comparison had been made using a

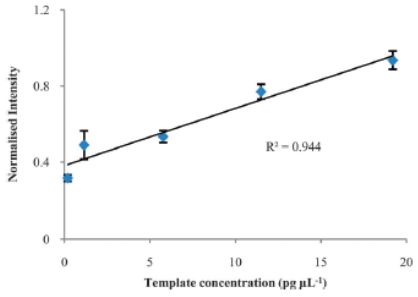

Fig. 3 Calibration curve of normalised SERS intensity at 1650 cm^{-1} against template concentration. Each point represents the mean of 4 × 5 replicates. Error bars represent ± one standard deviation.

Table 1 Limits of detection (L.O.D.) of MRSA template using different detection methods

Detection method	L.O.D. (g μL^{-1})	L.O.D. (mol dm^{-3})
SERS	6.0×10^{-14}	7×10^{-15}
Fluorescence	6.6×10^{-13}	7.5×10^{-14}

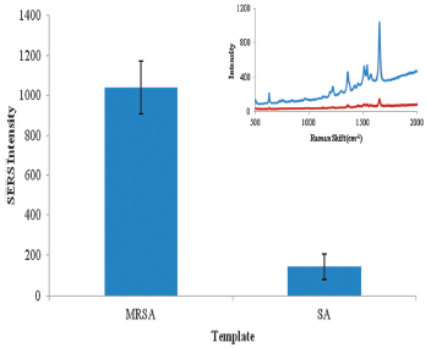

Fig. 4 SERS spectra recorded using 514.5 nm laser excitation containing blue: genomic MRSA target and red: genomic SA control. Both used template concentration of 1.2×10^{-10} g μL^{-1}.

conventional TaqMan probe. Higher background signals can be obtained within a standard TaqMan assay due to the occurrence of incomplete quenching obtained from the intact TaqMan probe. However, we have incorporated a separation step within the assay to reduce the background obtained.

To demonstrate that this assay could be used for genuine clinically relevant samples, the TaqSERS assay was carried out detecting the mecA gene within a genomic MRSA strain and a *Staphylococcus Aureus* (SA) strain employed as a control. The SA sequence does not contain the methicillin-resistant region, therefore, the mecA probe cannot hybridise and should be removed from the reaction during the streptavidin bead wash step. A clear distinction between the full MRSA assay and the SA control were obtained, Fig. 4, with a large discrimination between the sample and control observed.

This study has demonstrated that the use of SERS within a TaqMan assay has lowered the detection limits observed compared with fluorescence. The use of fluorescence detection in a conventional TaqMan assay can be limited as a result of high background signals from incomplete quenching within the probe and overlapping broad signals inhibiting multiple sequence detection. We have overcome these issues by developing a novel DNA detection method through coupling a TaqMan assay with SERS analysis, consequently enhancing the sensitivity and selectivity of the assay. Quantitative SERS responses were obtained from the TaqSERS assay showing increased sensitivity over comparable fluorescence analysis by at least an order of magnitude. Significantly distinct SERS signals were obtained from the detection of the mecA gene within a genomic MRSA strain when compared to a control strain. Incorporation of SERS analysis generates the potential for multiple target strains to be detected due to the molecularly specific narrow spectral bands obtained. These results show the applicability that the TaqSERS assay has to be utilised within biological detection.

The authors thank Dstl for funding and acknowledge Professor Duncan Graham at University of Strathclyde for helpful discussions.

Notes and references

1 M. J. Espy, J. R. Uhl, L. A. Sloan, S. P. Buckwalter, M. F. Jones, E. A. Vetter, J. D. C. Yao, N. L. Wengenack, J. E. Rosenblatt, F. R. Cockerill and T. F. Smith, *Clin. Microbiol. Rev.*, 2006, **19**(3), 165.
2 K. Faulds, R. E. Littleford, D. Graham, G. Dent and W. E. Smith, *Anal. Chem.*, 2004, **76**(3), 592.
3 D. Graham, B. J. Mallinder, D. Whitcombe, N. D. Watson and W. E. Smith, *Anal. Chem.*, 2002, **74**(5), 1069.
4 Y. W. C. Cao, R. C. Jin and C. A. Mirkin, *Science*, 2002, **297**(5586), 1536.
5 K. Faulds, F. McKenzie, W. E. Smith and D. Graham, *Angew. Chem., Int. Ed.*, 2007, **46**(11), 1829.
6 K. Faulds, R. Jarvis, W. E. Smith, D. Graham and R. Goodacre, *Analyst*, 2008, **133**(11), 1505.
7 P. M. Holland, R. D. Abramson, R. Watson and D. H. Gelfand, *Proc. Natl. Acad. Sci. U. S. A.*, 1991, **88**(16), 7276.
8 T. Morris, B. Robertson and M. Gallagher, *J. Clin. Microbiol.*, 1996, **34**(12), 2933.
9 B. Kimura, S. Kawasaki, T. Fujii, J. Kusunoki, T. Itoh and S. J. A. Flood, *J. Food Prot.*, 1999, **62**(4), 329.
10 I. Laurendeau, M. Bahuau, N. Vodovar, C. Larramendy, M. Olivi, I. Bieche, M. Vidaud and D. Vidaud, *Clin. Chem.*, 1999, **45**(7), 982.
11 R. T. Ranasinghe and T. Brown, *Chem. Commun.*, 2005, (44), 5487.
12 J. Nurmi, A. Ylikoski, T. Soukka, M. Karp and T. Lovgren, *Nucleic Acids Res.*, 2000, **28**(8), 6.
13 E. A. Lukhtanov, S. G. Lokhov, V. V. Gorn, M. A. Podyminogin and W. Mahoney, *Nucleic Acids Res.*, 2007, **35**(5), e30.
14 D. Graham, W. E. Smith, A. M. T. Linacre, C. H. Munro, N. D. Watson and P. C. White, *Anal. Chem.*, 1997, **69**(22), 4703.
15 M. M. Harper, J. A. Dougan, N. C. Shand, D. Graham and K. Faulds, *Analyst*, 2012, **137**(9), 2063.
16 J. A. Dougan, D. MacRae, D. Graham and K. Faulds, *Chem. Commun.*, 2011, **47**(16), 4649.
17 P. Francois, D. Pittet, M. Bento, B. Pepey, P. Vaudaux, D. Lew and J. Schrenzel, *J. Clin. Microbiol.*, 2003, **41**(1), 254.